SYNTHESIS OF NOVEL LIPID A ANALOGS AS POTENTIAL LIGANDS FOR TOLL-LIKE RECEPTOR 4

A thesis submitted in partial fulfillment of the requirements for the degree of Master of Science

Department of Chemistry

Lakehead University

Thunder Bay, Ontario

Jordan David Lewicky

Fall 2009

ABSTRACT

Lipid A, the glycolipid component of Gram-negative bacterial lipopolysaccharide has been shown to engage the Toll-like receptor 4 (TLR4) signalling pathway. While this signalling cascade results in cellular mediators which serve to activate the immune system and eliminate the invading organism, the associated toxicity is potentially harmful to the host. With an ever increasing molecular understanding of TLR4 mediated signalling, synthetic analogs of the natural Lipid A structure and the structure-activity relationship information they provide have emerged as a potential method of harnessing the desired immunomodulating effects from the undesired toxicity. As such, the therapeutic potential of TLR4 signalling is becoming an increasing possibility.

Two novel synthetic frameworks have been designed and synthesized to potentially mimic the natural Lipid A structure. A dimeric monosaccharide framework was obtained, however, attempts at functionalization (R = Lipid) to generate a series of analogs were generally unsuccessful due to unforeseen circumstances. A revised synthetic strategy has thereby been undertaken to allow more facile functionalization of this framework. A monosaccharide framework in which diethanolamine is employed as an acyclic scaffold replacing one of the sugar groups common to the natural disaccharide Lipid A structure has also been obtained. Functionalization (R = Lipid) has been successfully achieved, with further functionalization of this framework through the acyclic hydroxyl moiety intended. Ultimately, biological evaluation will determine the potential of these frameworks as being ligands for TLR4.

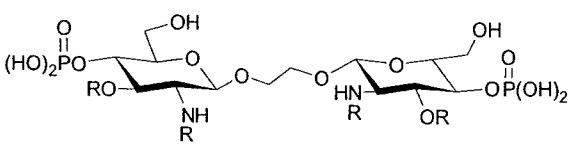

Dimeric Monosaccharide Framework

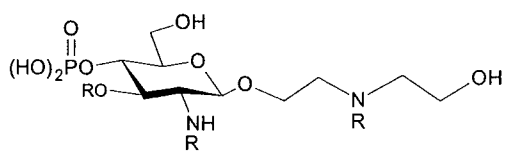

Diethanolamine Monosaccharide Framework

ACKNOWLEDGMENTS

I wish to express the utmost gratitude to my supervisor and mentor, Dr. Zi-Hua Justin Jiang, for his guidance and support throughout my M.Sc. studies. I am very grateful to Dr. Christine Gottardo, Dr. Marina Ulanova, and the rest of the faculty of the Lakehead University chemistry department. A special thanks to Ainsley Bharath, Brad Miller, and Debbie Puumala at chemistry stores for their patience and encouragement, as well as Matthew Kaskiw, the fellow graduate student in our research group for his help and friendship.

I would like to extend my appreciation to the staff of the instrumentation laboratory, especially, Mr. Keith Pringnitz and Mr. Ain Raitsakas for their technical aids on NMR, MS, and CHN combustion analysis.

A debt of gratitude is owed to Biomira Inc., for their support in the form of valuable chemical supplies.

Financial supports from Natural Sciences and Engineering Research Council (NSERC) and Ontario Graduate Scholarship (OGS) are gratefully acknowledged.

Finally, my deepest gratitude goes out to my parents, for their support, encouragement, and understanding, which have allowed me to accomplish this work.

ABBREVIATIONS

AGP	aminoalkyl glucosaminide 4-phosphate
Anal	analytical
approx	approximate
Ar	aryl
br	broad
$(BnO)_2PN(iPr)_2$	dibenzyl N,N-diisopropylphosphoramidite
calcd	calculated
$CHCl_3$	chloroform
$CNCCl_3$	trichloroacetonitrile
COSY	correlated spectroscopy
d	doublet
DBU	1,8-diazabicyclo[5.4.0]undec-7-ene
DCC	N,N'-dicyclohexylcarbodiimide
DCM	dichloromethane
dd	double doublet
DEA	diethanolamine
DIPEA	diisopropylethylamine
DMAP	4-dimethylaminopyridine
DMF	N,N-dimethylformamide
E. coli	*Escherichia coli*
ESI	electrospray ionization
Et_3N	triethylamine
EtOAc	ethyl acetate
Fmoc	9-fluorenylmethoxycarbonyl
GPI	glycosylphosphatidylinositol
h	hour
HBTU	O-(benzotriazole-1-yl)- *N,N,N',N'*-tetramethyluronium hexafluorophosphate
HOAc	acetic acid

HR	high resolution
Hz	hertz
IL-1	interleukin-1
IL-6	interleukin-6
J	coupling constant
LBP	lipopolysaccharide binding protein
LPS	lipopolysaccharide
mCD-14	membrane bound CD-14
m-CPBA	*m*-chloroperoxybenzoic acid
MeOH	methanol
mg	milligram
MHz	megahertz
min	minutes
MLA	monophosphoryl Lipid A
mol	moles
mmol	millimoles
MS	mass spectroscopy
NaH	sodium hydride
Na_2SO_4	sodium sulphate
$NaHCO_3$	sodium bicarbonate
NBS	N-bromosuccinimide
NMR	nuclear magnetic resonance
PAMP	pathogen-associated molecular pattern
PRR	pattern recognition receptor
py	pyridine
rt	room temperature
s	singlet
SAR	structure-activity relationship
sCD-14	serum soluble CD-14
SIRS	systemic inflammatory response syndrome
t	triplet

TBAF	tetrabutylammonium fluoride
TBDMS	*tert*-butyldimethylsilyl
TIR	Toll/interleukin-1
TLC	thin layer chromatography
TLR	Toll-like receptor
TMS	tetramethylsilane
TMSOTf	trimethylsilyl trifluoromethanesulfonate
TNF-α	tumour necrosis factor α
Troc	2,2,2-trichloroethoxycarbonyl

TABLE OF CONTENTS

1 INTRODUCTION & OBJECTIVES

1.1 Biological background

1.1.1 An introduction to immunity

Immunity is a biological term describing a state in which sufficient biological defences are present to avoid infection or disease. There are two separate arms of the immune system which work in concert to protect the host, and involve both specific and non-specific components. The innate immune system acts as the first line of defence, working to eliminate a wide range of pathogens irrespective of antigen specificity. This form of immunity is present in the host from birth. The adaptive immune system is comprised of components that adapt themselves to each new pathogen, and generate a so-called pathogen-specific immunity. Moreover, in adapting to a pathogen, the adaptive immune system also bestows upon the host a "memory", thus allowing for a much stronger immunological response if the pathogen is encountered again. As such, this form of defence is often referred to as acquired immunity [1].

One primary role of the innate immune system is the induction of an inflammatory response. The secretion of inflammatory cytokines serves to control the spread and eliminate much of the invading pathogen. The second, equally important role of the innate immune system is the induction of the adaptive immune system, whose action not only serves to eliminate any remaining pathogenic threat, but also to generate the ever important "pathogenic memory" [2].

1.1.2 The innate immune system

The innate immune system serves as the first line of defence against invading pathogens[1]. It uses a group of pattern recognition receptors (PRRs) to distinguish non-self pathogenic products from host molecules by recognizing unique pathogen-associated molecular patterns (PAMPs). PAMPs are conserved structural motifs that are found throughout the pathogenic world [3]. Innate host identification of pathogenic patterns or components, therefore, relies on the inability of pathogens to dramatically alter these critical components [4]. Some examples of the common PAMPs include bacterial products such as peptidoglycan [5], lipoteichoic acid [6], lipopolysaccharide (LPS) [7], and flagellin [8], as well as viral RNA [9].

1.1.3 Lipopolysaccharide (LPS) as a trigger of innate immunity

LPS is a unique glycolipid molecule ubiquitous to Gram-negative bacteria. It constitutes the outer portion of the outer membrane, a second lipid bilayer outside of the cytoplasmic membrane characteristic to this type of bacteria [10]. Pffeifer first described this material firmly bound to the cells of *Vibrio cholerae* in 1892, and given its toxicity aptly named the material endotoxin [13]. The intrinsic activity of LPS in higher animals is the stimulation of the innate immune system as observed by the induction of inflammatory cytokines such as interleukin-6 (IL-6) and tumour necrosis factor α (TNFα). LPS is, perhaps, the most effective trigger of the innate immune responses, with its potent toxicity causing high fever, tissue damage, and even death in experimental animals. A serious clinical syndrome in humans known as septic shock, which can ultimately become fatal, occurs if the LPS level remains elevated for an extended period of time [11].

LPS consists of three distinct covalently linked segments; the O-polysaccharide, core oligosaccharide, and a glycolipid (**Figure 1**). The O-polysaccharide at the distal terminal is composed of repeating oligosaccharide units, whose structure varies between bacterial species and strains, while the core oligosaccharide is comprised of more conserved structures. The glycolipid portion located at the proximal terminal, later named Lipid A, anchors the molecule to the bacterial outer membrane via hydrophobic interaction [12, 13].

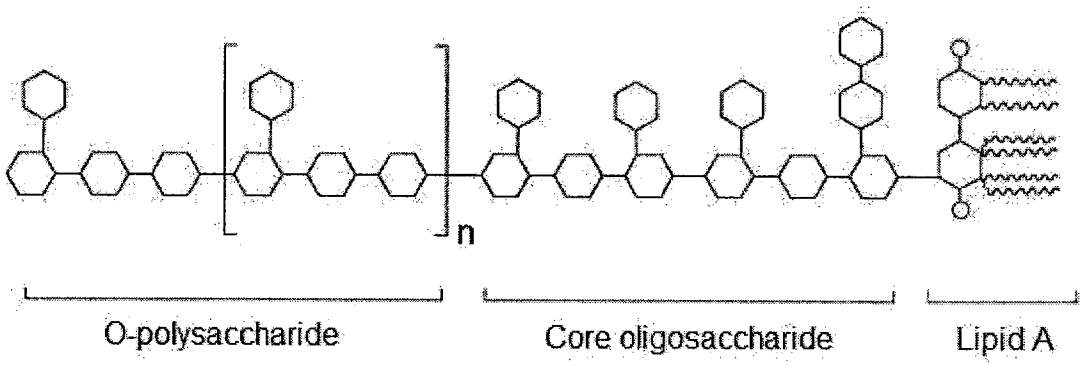

Figure 1. Schematic representation of LPS

1.1.4 Lipid A as endotoxic principle of LPS

Westphal and Lüderitz discovered that mild acid treatment of LPS allowed for the cleavage of the linkage between the core oligosaccharide and the glycolipid. This liberated glycolipid, which they named Lipid A, was shown to be solely responsible for the endotoxic activity of LPS [14]. As such, the chemical structure of Lipid A became an area of intense investigation. However, due to its amphipathic nature, extensive purification was inhibited. Therefore, the structure of the hydrophilic backbone and the presence of *O*- and *N*-linked acyl moieties were only proposed, and the exact structural details were not known [15, 16]. The first successful isolation of a single molecular species of Lipid A from the *Escherichia coli* (*E. coli*) Re mutant was reported by Imoto *et al*, and its chemical structure was elucidated by spectroscopic and chemical analysis [17] (**Figure 2**). The backbone consists of a β-(1-6) linked disaccharide of glucosamine, which is bisphosphorylated at the 1- and 4'-hyrdoxyl groups. This disaccharide backbone is common to Lipid A regardless of bacterial species or strain. However, significant variability in the number, length, and composition of the acyl lipid chains exists between bacterial species. This structural variability has been proposed as the mechanism responsible for the highly variable degree of toxicity associated with different bacterial species [18]. The *E. coli* Lipid A molecule was also synthesized by Imoto *et al* [18, 19], and shown to be identical with its natural counterpart in terms of both *in vitro* and *in vivo* activities [20].

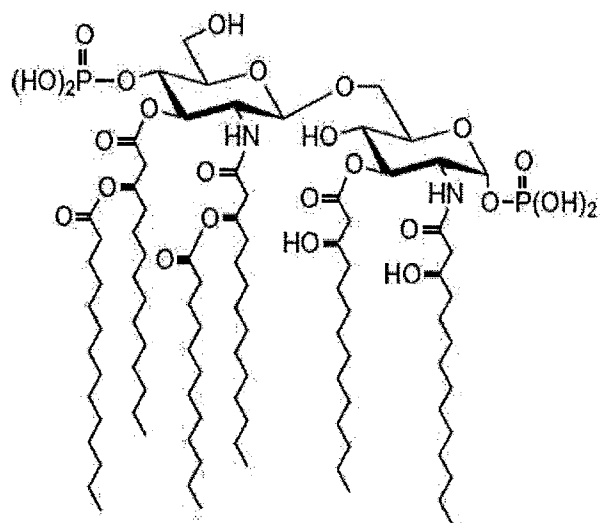

Figure 2. Lipid A isolated from *E. coli*

1.1.5 Toll-like receptors (TLRs) as innate immune system receptors

The pioneering work that led to the discovery of LPS and its glycolipid component Lipid A as the Gram-negative bacterial trigger of the innate immune response was undertaken without a clear understanding of the mechanism through which this response is generated. Only in recent years have significant advances in the understanding of the mechanisms of innate immunity evolved. The discovery of a protein named Toll in *Drosophila* brought about a revolutionary change in the understanding of innate immune receptors. Toll was discovered as a membrane bound protein which participates in the defence against fungi. A genomic search resulted in the discovery of homologous proteins in mammals which were called Toll-like receptors (TLRs) [21]. Characteristic to these receptors is a defined amino acid homology with the interleukin-1 (IL-1) receptor. The Toll/IL-1 (TIR) domain has been shown to regulate intracellular signalling pathways leading to gene expression through interaction with intracellular adaptor proteins such as MyD88, TRIF, and TRAM. These adaptor molecules are what differentially regulate the expression of the inflammatory cytokines associated with the non-specific response [22].

To date 13 mammalian members of the TLR family have been discovered, with 10-or-more distinct TLRs having been identified in humans [23]. Although all members of the TLR family share a large degree of sequence homology, growing evidence suggests specificity in their recognition and response [22]. The TLRs involved in the recognition of bacterial ligands are transmembrane proteins with leucine rich, horseshoe shaped extracellular domains that are thought to play a major role in PAMP based pathogen detection. TLR4 and TLR5 recognize LPS and bacterial flagellin respectively, while TLRs 1, 2, and 6 work cooperatively in the recognition of lipoproteins and glycolipids from Gram-positive bacteria. In contrast, the other members of the TLR family are restricted to the cytoplasm. TLRs 3, 7, and 8 are involved in the detection of viral RNA, while TLR9 is specific to the recognition of unmethylated DNA common to both bacteria and viral sources [24].

1.1.6 LPS/Lipid A induced TLR4 signalling pathway

TLR-4 has been identified as the target of Gram-negative bacterial LPS/Lipid A [22, 25]. The interaction of TLR-4 and its ligand has been, perhaps, the most studied of all mammalian TLRs, with significant effort having gone into the delineation of the precise molecular events that ultimately lead to the profound biological response generated. Several obligate accessory proteins have been discovered that are critically involved in the recognition of LPS/Lipid A. Lipopolysaccharide binding protein (LBP) found in serum, binds aggregate forms of LPS and facilitates the transfer of monomeric LPS to CD-14 [26]. CD-14 exists as both a serum soluble (sCD-14) and a glycosylphosphatidylinositol (GPI) anchored membrane protein (m-CD14) [27]. Either form of CD-14 has been shown to be responsible for the transfer of monomeric LPS to a third accessory protein, MD-2 [7]. MD-2 is a protein which lacks any intracellular domains and has been shown to bind to the extracellular domains of TLR4 [28]. The TLR4-MD-2 complex is expressed as dimers on the surface of immune cells, the presence of which is essential for the recognition of LPS/Lipid A [29]. Transfer of LPS from CD-14 to the TLR4-MD-2 receptor complex is thought to bring about a reorganization of the cytoplasmic TIR domain of TLR4, enabling the induction of two separate signalling pathways with the recruitment of adaptor molecules MyD88, Mal, TRIF, and TRAM (**Figure 3**). MyD88 dependent signalling leads to the production of inflammatory cytokines such as TNF-α, IL-6, and IL-1β, while the TRIF dependent pathway leads to the production of species such as nitric oxide, and IFN-β, one result of which is the activation of the adaptive arm of the immune system [30].

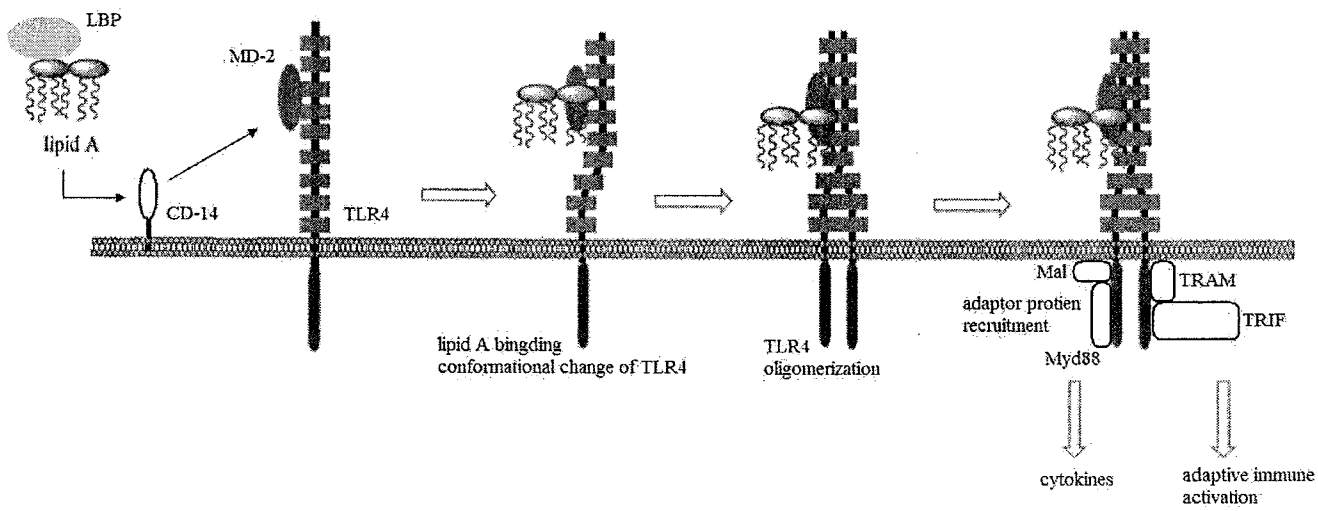

Figure 3. Schematic representation of LPS/Lipid A induced TLR4 signalling [31]

1.1.7 TLR4 signalling antagonism

Antagonism of the TLR4 signalling pathway has also been reported. Several natural antagonist Lipid A structures isolated from various bacterial sources have been noted. For example, Lipid A structures from *R. capsulatas* and *R. sphaeroides* show potent antagonism of *E. coli* Lipid A induced TLR4 activation (**Figure 4**) [32].

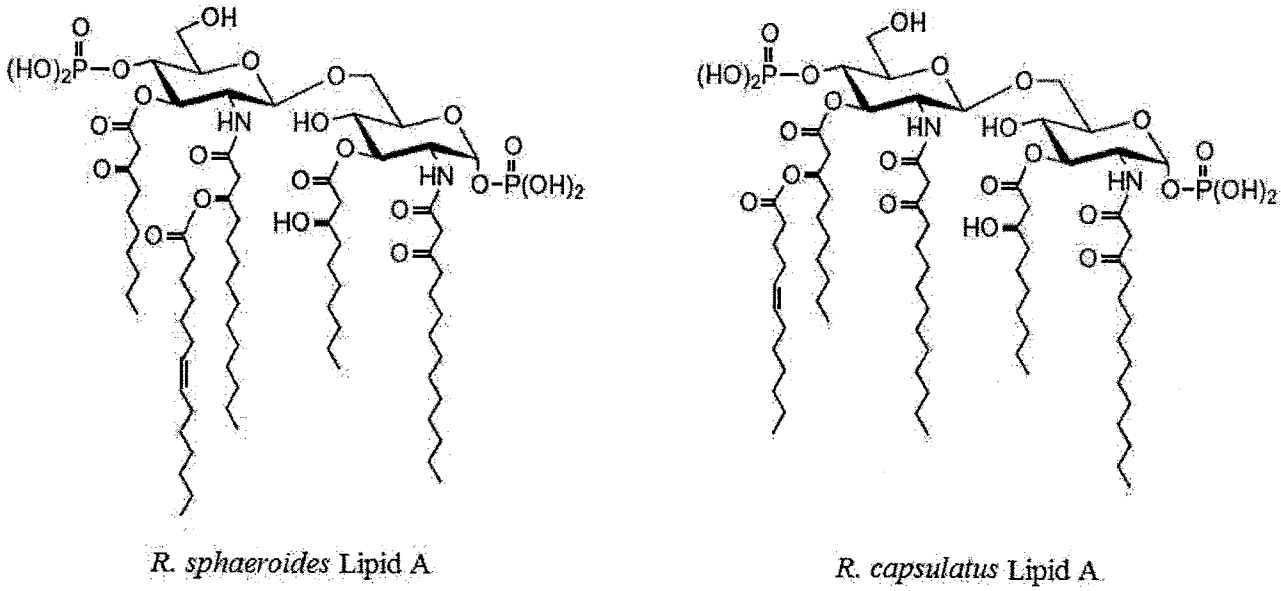

Figure 4. Natural TLR4 antagonists

Lipid IVa, a tetra-acyl biosynthetic precursor of the *E. coli* Lipid A molecule, which lacks the two β-acyloxy lipid chains was proposed and synthesized (**Figure 5**) [32, 33]. Lipid IVa was shown to have full endotoxic activity compared to *E. coli* Lipid A when tested using murine cells [34]. However, it was also shown to behave as an antagonist, inhibiting the endotoxic activity of *E. coli* Lipid A when tested using human cells [35].

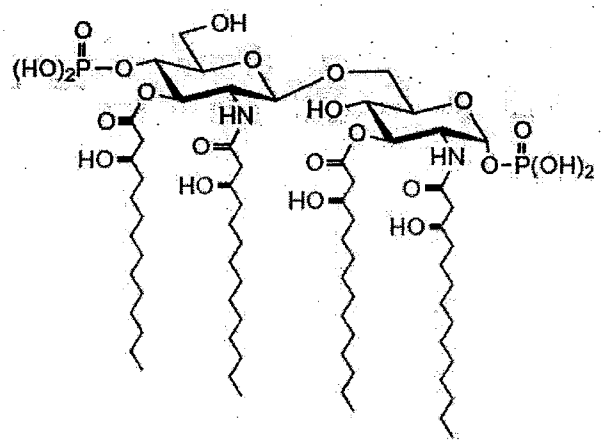

Figure 5. Biosynthetic precursor Lipid IVa

Biochemical investigations confirmed that murine MD-2 binds both Lipid A and Lipid IVa similarly, ultimately leading to TLR4 oligomerization and signalling with either ligand. The same combination of human MD-2 and TLR4 was found to effectively bind Lipid IVa, but neither a conformational change nor the oligomerization of TLR4 occurs (**Figure 6**). Furthermore, a chimeric complex of murine TLR4 and human MD-2 behaves in the same manner. It was therefore concluded that MD-2 is responsible for this species-specific recognition difference [36]. The antagonism of the TLR4 signalling cascade in the human system was viewed as a promising approach to the treatment of bacterial sepsis, a topic which is discussed in detail later.

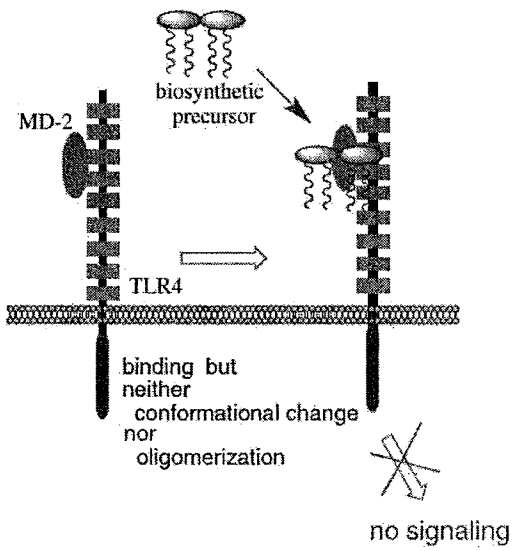

Figure 6. Schematic representation of Lipid IVa TLR4 antagonism [31]

1.1.8 MD-2

With the interesting results noted with Lipid IVa and the species specific response of MD-2 [36], a great deal of investigation has gone into the structure and function of this protein. Noteworthy is that although TLR4 has long been considered the LPS receptor, no direct evidence has been obtained showing that its Lipid A segment actually binds to the receptor. There is considerable evidence, however, that Lipid A and its biosynthetic precursor Lipid IVa bind MD-2 [37]. This has led many to hypothesize that the true ligand for TLR4 is not LPS/Lipid A, but is in fact a conformationally active form of MD-2.

Recently, the crystal structure of human MD-2 was obtained both in its native from, as well as bound to antagonist lipid IVa. A large and deep hydrophobic cavity is reported, in which all four acyl chains of the ligand are found. Moreover, the conformational change of MD-2 upon binding lipid IVa was observed to be minimal. The authors speculated that the hydrophobic cavity could not likely accommodate more than the four acyl chains found in lipid IVa, and that the additional acyl chains in agonistic Lipid A might bring about a conformational change in the MD-2-ligand complex that ultimately induces the conformational changes in TLR4 necessary for signal transduction [38]. Nonetheless, these hypotheses are only speculative, and a crystal structure of MD-2 bound to agonistic Lipid A is necessary in order to determine the exact mechanism through which this differential regulation occurs. To date, no such structure has been reported.

1.2 Manipulation of TLR4 signalling

1.2.1 Therapeutic potential of TLR4 signalling pathway

Given the far reaching impacts of the TLR4 signalling pathway, it has been targeted for its possible therapeutic potentials. Therapeutic potential has centered on three main areas: anti-sepsis treatments, vaccine adjuvants, and anti-cancer therapies [31]. With an ever increasing knowledge of the biochemical pathway of TLR4 signalling, the manipulation of this pathway for potential beneficial effects is becoming a more realistic possibility.

1.2.2 Anti-sepsis treatments

The secretory products released as a result of bacterial LPS induced TLR4 signalling serve to assist the host in eradicating, and preventing the spread of the infecting pathogen. Unfortunately, the continued presence of elevated levels of bacterial LPS in the blood, having been released from dead or dying bacteria, can lead to a biological over-reaction which results in the release of toxic levels of these cellular mediators. This reaction is referred to as the systemic inflammatory response syndrome (SIRS), and is commonly known as sepsis. Characteristic to sepsis are life-threatening responses such as tissue damage, vascular leakage, hypotension, organ dysfunction and eventual failure resulting in death [39].
The antagonistic action of Lipid IVa and various other Lipid A molecules in humans has led to theories that antagonists of the TLR4 signalling complex could potentially be used for the treatment of sepsis. The competitive inhibition of these antagonists could serve not only to treat sepsis once it has developed, thereby preventing death in the host, but also to prevent the bacterial infections that ultimately cause the condition [39].

1.2.3 Vaccine adjuvants

The goal of vaccinations is to stimulate the adaptive arm of the immune system to generate a response that ultimately bestows upon the host an "immunological memory" such that a strong immunological response can be generated upon future encounter with the pathogen. While most conventional vaccines employ dead, attenuated microbes, or microbial fragments as stimulating agents, problems associated with vaccine manufacture and the presence of contaminants have led to considerable efforts in vaccine refinement. However, with refinement and simplification of microbial vaccines, a concomitant loss in vaccine potency has resulted. This has led to the co-administering of adjuvants alongside vaccines to potentiate this weak immunogenicity [40, 41]. The term adjuvant is used to describe an immune stimulating agent that increases the response to a vaccine. Ideally, the increased immune response should exist primarily in the adaptive arm of the immune system, with innate responses minimized to prevent undesired side effects [42].

Given the strong immunological responses that result from TLR4 signalling activation, the signalling pathway has been tapped for its potential adjuvant characteristics. However, an

underlying concern is the strong inflammatory response associated with TLR4 activation. In order to serve as a successful adjuvant system, the ability to stimulate the adaptive immune system must be uncoupled from the strong cytokine response [43].

1.2.4 Anticancer treatments

Chemotherapy and radiation therapy can delay the progression of cancer, but in many cases the cancer can relapse. TLR4 agonism is a promising molecular treatment against chemotherapy and radiation relapsing cancer metastases. The potent anticancer action of microbes or microbial products has been known since the beginning of the 18th century when Deider reported that infection in cancer patients was concomitant with disease remission [44]. This antitumor effect was found by Shear *et al* to be due to LPS [45]. It is now known that stimulation of the Myd88 signalling pathway induces transitory increases in TNF-α cytokine levels. TNF-α has been shown to selectively increase the permeability of tumoral neoangiogenic vessels to cytotoxic drugs [46]. Moreover, nitric oxide derived from TLR4 stimulation participates in local tumoricidal activity against many tumor types [47, 48]. This cytotoxic effect against tumor cells was found to be associated with apoptosis [47]. Unfortunately, because of the toxicity associated with LPS, the treatment of cancer patients has been limited to the local application of only small amounts of bacterial LPS, these doses being too low to obtain any beneficial antitumor effects [49].

1.2.5 TLR4 therapeutic concerns

In order for the modulation of TLR4 signalling to be practical for immunotherapeutic purposes, certain issues need to be addressed. The most important concern is the high toxicity associated with naturally derived Lipid A based molecules. Therefore, an important issue for the design of safe immune modulators is a detailed knowledge of structure-activity relationships (SARs), which would allow the harnessing of the beneficial effects without causing toxicity. This information is difficult to obtain using isolated compounds, a direct result of the inhomogeneity encountered with natural Lipid A preparations. Natural preparations suffer from a lack of consistency in both composition and performance, even when derived from the same bacterial strain. Moreover, possible contamination with other inflammatory components is also of prime concern [50]. As such, recent work has been focused on the

preparation of single molecular species by way of chemical synthesis. Chemical synthesis not only provides single, pure molecules, but also allows for the creation of structural analogs of the natural Lipid A molecules. By modifying the natural structure, those structural details that are beneficial to desired therapeutic purposes may be separated from those details that are associated with the undesired toxicity.

1.3 Synthetic Lipid A analogs

1.3.1 Disaccharide analogs

Over the past decade, a great deal of research has gone into the synthesis of analogs of the Lipid A disaccharide structure with hope that beneficial immune modulating properties can be separated from the associated high toxicity. One notable discovery is that through the removal of the anomeric phosphate and the 3-O acyl chain of the reducing sugar in Lipid A derived from *Salmonella minnesota* RC595, a significant decrease in endotoxicity is achieved [51]. The resulting structure, known as monophosphoryl Lipid A (MLA), as well as numerous analogs of its structure have been synthesized (**Figure 7**) [52]. Certain MLA type structures have show excellent adjuvant characteristics, and has been approved for therapeutic vaccine use [52, 53].

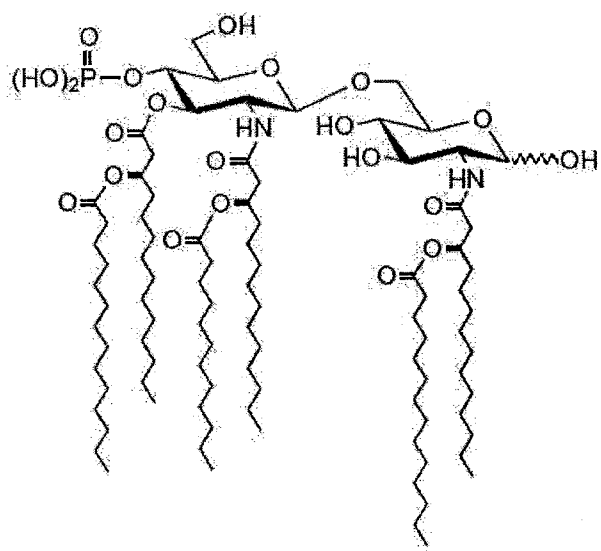

Figure 7. MLA structure derived from *Salmonella minnesota* RC595 Lipid A

Recently, Mata-Haro *et al* have reported that MLA somehow engages the TLR4-MD-2 complex differently from Lipid A molecules that possess high endotoxicity. MLA has been shown to selectively activate only the TRIF-TRAM arm of the TLR4 signalling pathway, thus only engaging the adaptive immune system (**Figure 8**). The failure of MLA to engage the Myd88-Mal pathway, which controls the expression of inflammatory cytokines, appears to account for the lack of harmful toxic effects normally associated TLR4 signalling activation. These findings have provided an empirical basis supporting the use of MLA as a vaccine adjuvant, as it shows that it is not simply weakly endotoxic [54].

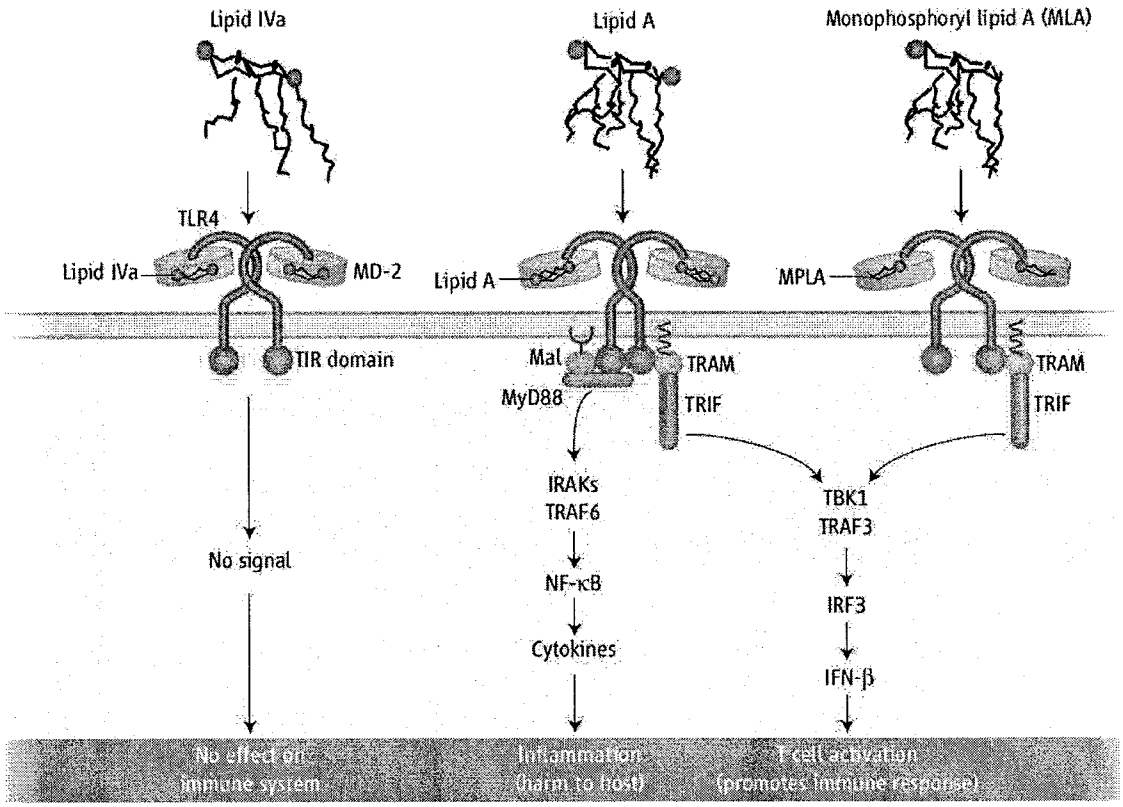

Figure 8. MLA induced TLR4 signalling compared to normal Lipid A and lipid IVa [55]

Biophysical characterization of synthetic Lipid A analogs has revealed that the molecular shape and supramolecular structures of agonistic and antagonistic compounds differ significantly. TLR4 agonists form non-lamellar aggregate structures and adopt a conical conformation, while antagonists form lamellar aggregates and adopt a cylindrical shape (**Figure 9**). The partial agonistic properties of MLA have been proposed to be a product of the molecule adopting a less conical shape than that of highly endotoxic Lipid A analogs [56, 57].

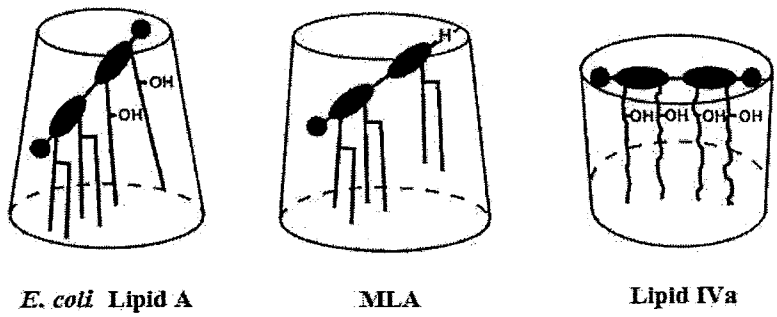

Figure 9. Molecular shape of TLR4 agonists and antagonists [56, 57]

Two highly promising TLR4 antagonists have been synthesized based on the naturally occurring antagonistic structures of *R. capsulatas* and *R. sphaeroides* Lipid A. E5531, a structural mimetic of *R. capsulatas,* is a potent endotoxin antagonist with no detectable agonistic activities (**Figure 10**) [58, 59, 60, 61]. E5564, based on *R. sphaeroides* Lipid A, has shown similar activity with a notable increase in potency and duration of effect. Currently, E5564 is in clinical trials as an anti-sepsis treatment under the name Eritoran [62, 63, 64]. The crystal structure of E5564 bound to murine TLR4-MD-2 was recently reported. Similar to the results obtained with synthetic antagonist lipid IVa [37], the four lipid chains in E5564 were noted to effectively fill the hydrophobic cavity of MD-2. Noteworthy is that no interaction between the ligand and TLR4 was observed, thus further fuelling the speculation as the mechanism through which MD-2 activates TLR4 oligomerization upon binding of agonistic ligand [65].

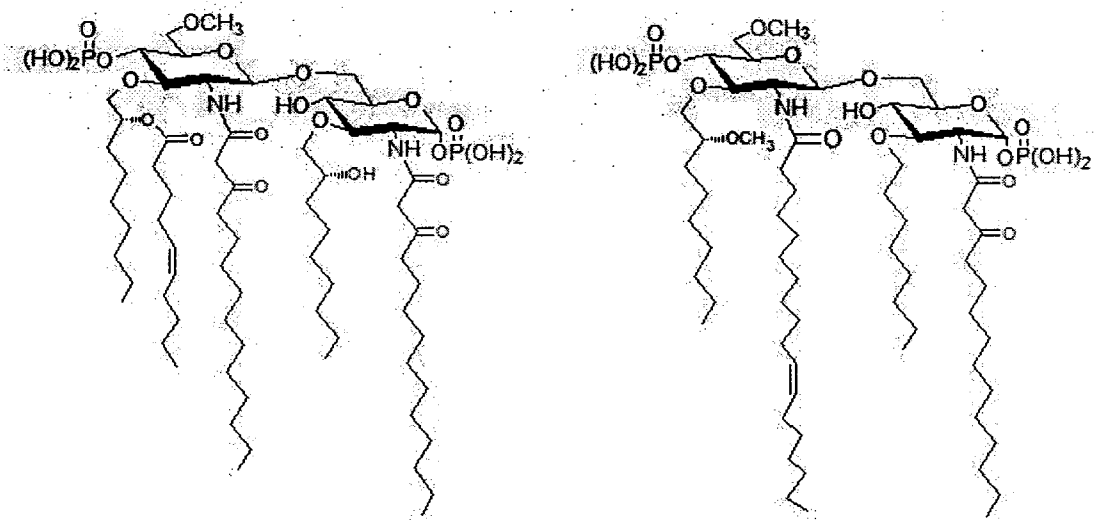

Figure 10. Synthetic disaccharide TLR4 antagonists

Perhaps one of the most notable discoveries in terms of disaccharide Lipid A analogs is the synthetic analogue OM-174 (**Figure 11**). This compound has shown significant promise as a treatment for chemotherapy and radiotherapy relapsing cancers. Its toxicity was noted to be more than 10^5 lower than that of LPS [66]. The immunostimulatory properties of OM-174 are not only being targeted for their anti-tumour effect as discussed earlier, but also for a palliative of chemotherapy induced immunodepression, which has the potential to result in fatal opportunistic infections [46].

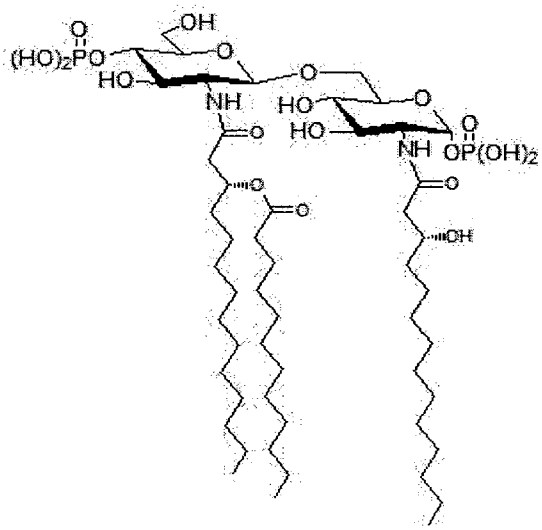

Figure 11. Synthetic anti-cancer agent OM-174

1.3.2 Monosaccharide analogs

Numerous subunit derivatives of bacterial Lipid A have also been synthesized. These molecules have typically been synthetic analogs of either the reducing or non-reducing glucosamine functionalities of Lipid A, or analogs in which one of the saccharide units has been replaced with an acyclic scaffold. These subunit analogs provide a structural motif more amenable than more complex disaccharide versions to the systematic SAR investigations needed to separate the toxic properties from the beneficial immunostimulatory effects. Synthetic analogs of either the reducing or non-reducing glucosamine moieties of Lipid A which contain up to five lipid chains typically exhibit very low biological activities. Moreover, monosaccharide analogs of the reducing glucosamine often exhibit TLR4 antagonist characteristics. However, certain monosaccharide derivatives, mainly of the non-reducing subunit which possess three lipid chains show an elevated level of immunostimulatory power, yet low toxicity in comparison to natural Lipid A [42]. GLA-60 has shown the best adjuvant properties among various non-reducing subunit analogs (**Figure 12**) [67]. Biophysical characterization of GLA-60 shows that it forms mainly unilamellar aggregates and adopts a slightly conical shape, which is consistent with its reduced toxicity [68].

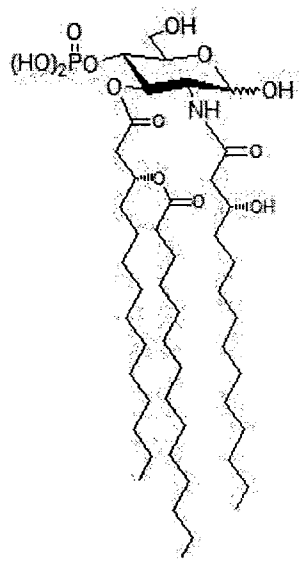

GLA-60

Figure 12. Monosaccharide Lipid A analogs

A novel class of monosaccharide Lipid A mimetics known as aminoalkyl glucosaminide 4-phosphates (AGPs), in which the reducing sugar has been replaced with an N-acyl aglycon unit, have shown significant promise as both TLR4 agonists and antagonists (**Figure 13**). Adjuvant potential showed a profound dependence on both lipid chain and aglycon chain length, as well as on the nature of the aglycon α-substituent. The highest levels of immunostimulatory activity are noted when the secondary lipid chains (R_1, R_2, R_3) are 10 to 12 carbons in length, the aglycon is 2-carbons long (n = 1), and the aglycon α-substituent is a carboxyl group, as exemplified by CRX-527 (**Figure 13**). Immunostimulatory activity is abolished in TLR4 antagonist CRX-526, in which the length of the secondary acyl groups has been reduced to 6-carbons [70]. Biophysical characterization of CRX-527 shows that the individual molecules adopt a conical shape and form non-lamellar aggregate structures in solution, which is consistent with its agonistic activity. In contrast, antagonist CRX-526 has been reported to form the lamellar aggregates characteristic to antagonistic molecules [27]. RC-529, in which the α-carboxyl moiety has been eliminated shows an even greater activity to toxicity profile, and has been investigated for uses as a pediatric vaccine adjuvant, an area where toxicity must be further minimized [53].

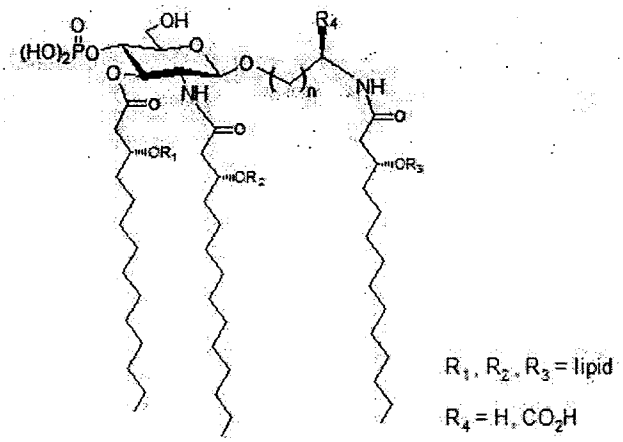

AGP generic structure

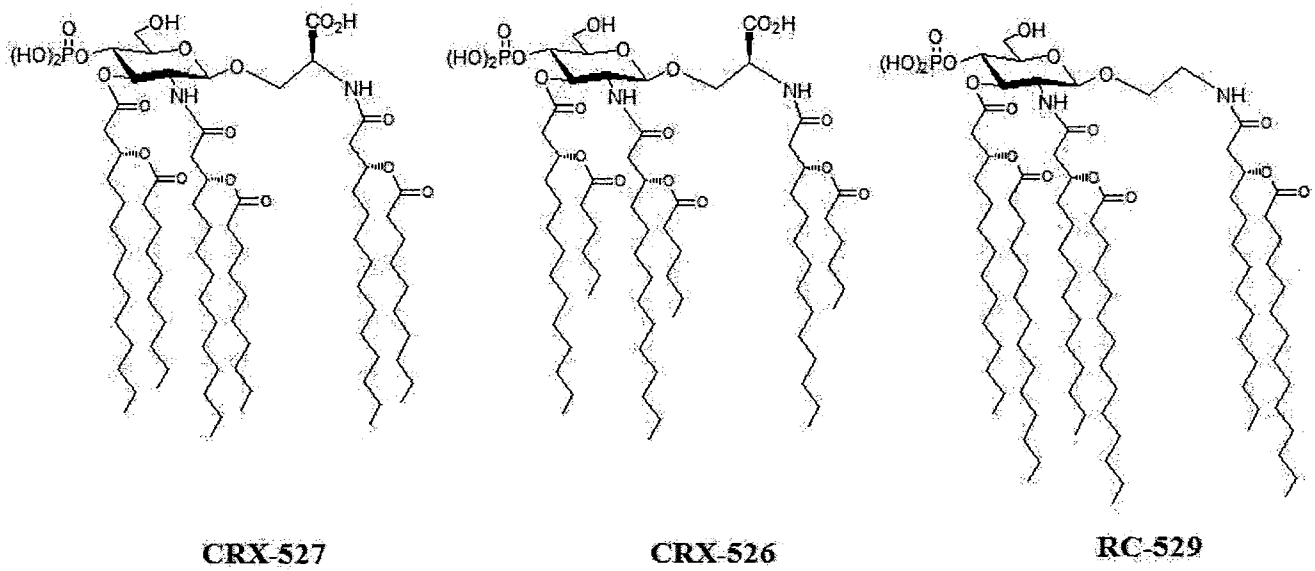

CRX-527 **CRX-526** **RC-529**

Figure 13. AGP class Lipid A mimetics

As further testament to the AGP approach of adjuvant design using synthetic monosaccharide derivatives of Lipid A, a set of analogs possessing an N-acylated pentaerythritol aglycon unit were synthesized (**Figure 14**). These compounds were noted to exhibit a biological activity similar to that of natural Lipid A, inducing the secretion of high levels of inflammatory cytokines. In a totally synthetic liposomal vaccine system these analogs were noted to exhibit strong immunostimulatory adjuvant properties [71].

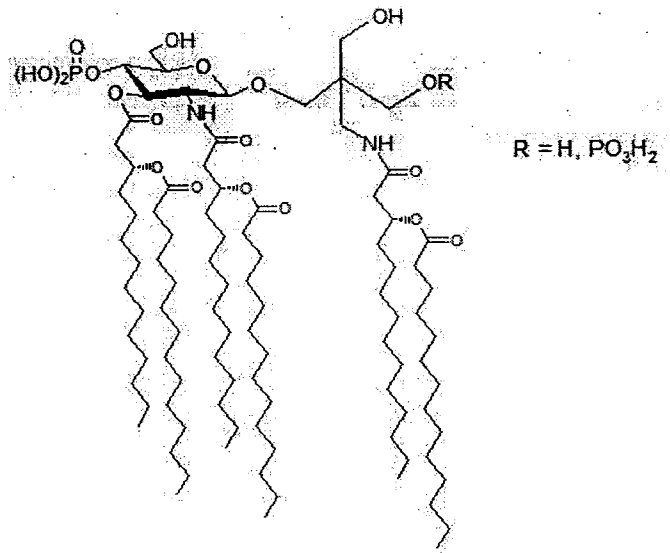

Figure 14. Pentaerythritol based monosaccharide Lipid A analogs

1.4 Objectives of thesis project

The synthetic Lipid A analogs reported to date have been a significant feat, and have provided a wealth of information in the way of SARs. However, the full picture as to the characteristics of the Lipid A structure that are responsible for the desired immunomodulatory properties in comparison to those that impart the undesired levels of toxicity is not fully understood. In order for the full therapeutic potential of the TLR4 signalling pathway to be harnessed, a clearer understanding of the activity to toxicity relationship must be achieved.

The goal of the present study is the synthesis of novel analogs of the Lipid A structure. Biological testing will determine the viability of these analogs as being ligands for TLR4. The ultimate desire is a synthetic Lipid A analog with a far better activity to toxicity relationship profile.

2 RESULTS & DISCUSSION

2.1 Dimeric monosaccharide Lipid A analogs

2.1.1 Design

Previously reported syntheses of disaccharide Lipid A analogs have involved the separate synthesis of both the reducing, and non-reducing monosaccharide moieties which are ultimately coupled to form the β-1→6 glycosidic linkage natural to the Lipid A molecule. Throughout these syntheses, a commonly encountered issue has been the loss of the chemically labile anomeric phosphate functionality [42]. Although this strategy has proven successful and numerous analogs have been synthesized, the lengthy and laborious nature involving the use of sensitive glycolipid molecules are significant drawbacks.

Herein, a synthetically unique dimeric monosaccharide backbone is being proposed as an alternative to the archetypical β-1→6 linked disaccharide structure (**Figure 15**). Envisioned are two identical glucosamine sugar moieties linked together through an ethylene glycol spacer, the choice of which has been made in attempts to mimic the overall length of the naturally occurring β-1→6 glycosidic linkage. One proposed advantage of this novel dimeric monosaccharide backbone is that it employs a simplified synthetic strategy, in which only the preparation of one monosaccharide unit is required. In addition, neither the monosaccharide units nor the final dimeric backbone contain an anomeric phosphate functionality, a characteristic which is proposed to increase the overall stability of the molecules, and aid in their synthesis.

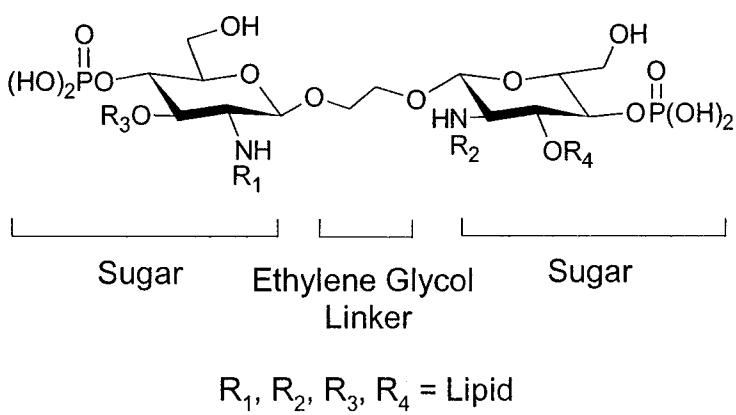

Figure 15. Novel dimeric monosaccharide structural backbone

Intended to be synthesized are three different dimeric monosaccharide analogs of the canonical Lipid A structure to initially determine the viability of this novel structural backbone (**Figure 16**). Proposed analog **I** lacks any 3-*O*-acyl lipid moieties, while analogs **II** and **III** differ in both the number and substitution pattern of the 3-*O* β-hydroxy lipid groups. SAR investigations have shown the lipid chain length is directly correlated to the activity of Lipid A analogs. A minimum length of 10 carbons seems necessary for activity, while increasing the chain length past 16 carbons adds little beneficial effect [42]. As such, the lipid chain length of the proposed analogs has been kept at a consistent 14 carbon length for these initial investigations.

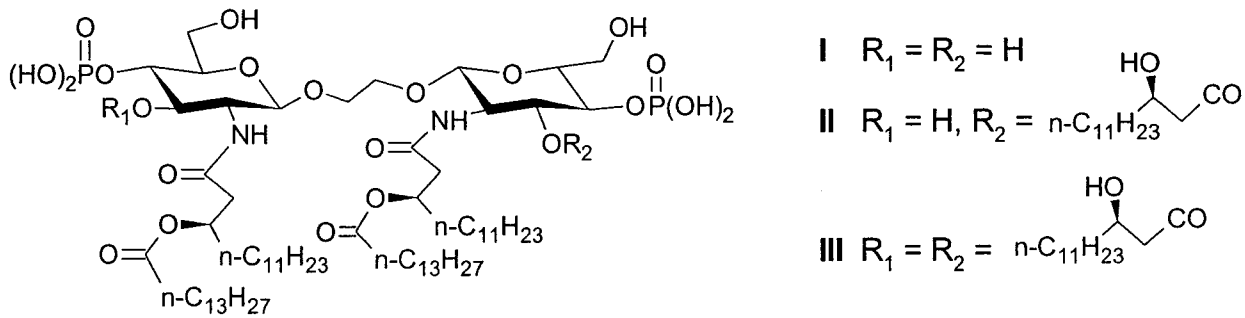

Figure 16. Proposed dimeric monosaccharide Lipid A analogs

2.1.2 Retrosynthetic analysis

Beginning with desired analog **III**, C-6 and phosphate hydroxyl moieties were first chosen to be globally protected with the benzyl (Bn) group, such that final global deprotection via hydrogenolysis was possible (**Scheme 1**). Separating the lipid moieties from the dimeric monosaccharide backbone yielded dilipid acid **I**, and protected β-OH monolipid acid **3**. Suitable protection of the nucelophilic β-hydroxyl moiety was necessary to prevent its participation in undesired reactions. As such, the 2,2,2-trichloroethoxycarbonyl (Troc) was employed such that selective deprotection of the β-OH was attainable at a desired point in the synthetic process. The nucelophilic 3-OH and 2-NH_2 functionalities that resulted from lipid cleavage were protected with the 9-fluorenylmethoxycarbonol (Fmoc) and Troc protecting groups respectively. These protecting groups were chosen for two primary purposes. The first is that they allow for selective deprotection, and ultimately the selective incorporation of acyl

lipid moieties. Moreover, the N-Troc protecting group was chosen for its proven stereoselective β-glycoside directing capability by virtue of neighbouring group participation [43, 71, 72]. Cleavage of both glycosidic linkages in the structural backbone yielded trichloroacetimidate glycosyl donor **9**, and ethylene glycol as the glycosyl acceptor. Further deconstruction of donor **9** results in readily accessible glucosamine derivative **4** [73] as the starting point of the dimeric monosaccharide backbone synthesis.

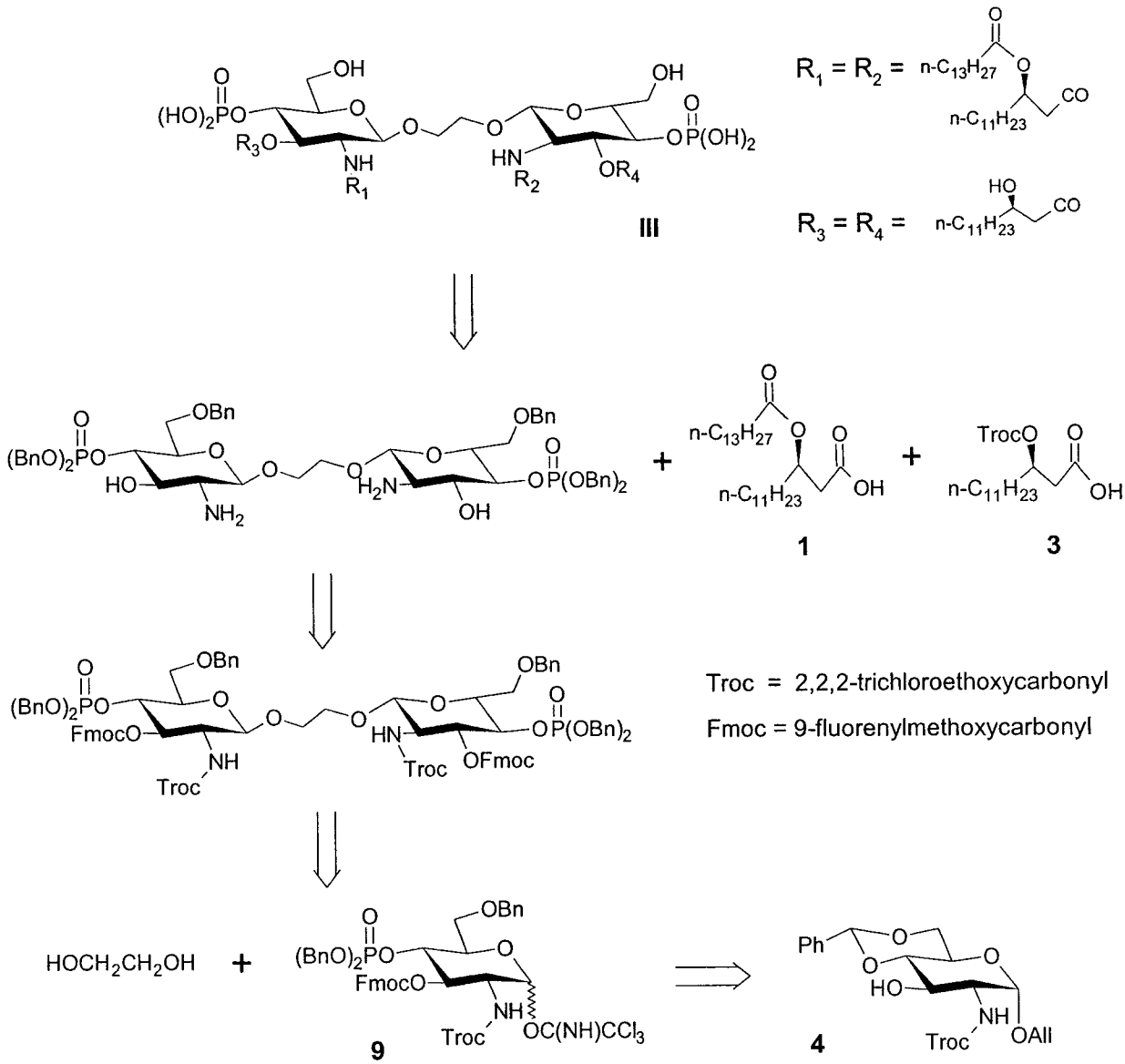

Scheme 1. Retrosynthetic analysis of proposed dimeric monosaccharide Lipid A analog **III**

2.1.3 Lipid acid syntheses

Retrosynthetic analysis (**Scheme 1**) indicated the need for both dilipid acid **1** and Troc protected β-OH monolipid acid **3**. Dilipid acid **1** was supplied as a gift from Biomira Inc., and was synthesized according to known literature procedures [74]. Protected monolipid acid **2** was synthesized from 3-(R)-hydroxypenta-1-decene[75], which was also generously supplied by Biomira Inc. The β-OH was first protected as its Troc ester via reaction with Troc-Cl in pyridine to give **2** in a 93% yield (**Scheme 2**). Permanganate oxidation of the alkene functionality in **2** followed, yielding protected monolipid acid **3** in 88% yield.

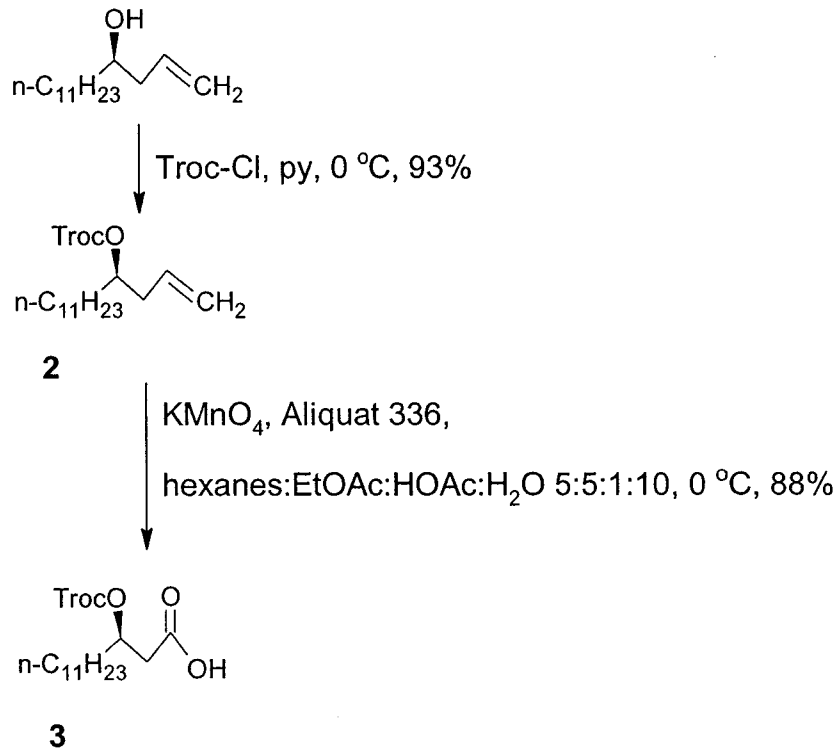

Scheme 2. Synthesis of protected β-OH monolipid acid **3**.

2.1.4 Synthesis of starting sugar 4

According to known literature procedures [19, 73] the amine moiety in glucosamine hydrochloride was first protected with the installation of the desired N-Troc functionality (**Scheme 3**). The anomeric allylic group was next installed via Fischer glycosylation with allyl alcohol. Finally, the 4-OH and 6-OH groups were protected via the installation of the 4,6-O-benzylidene group to yield **1** in 31% yield overall for the three steps.

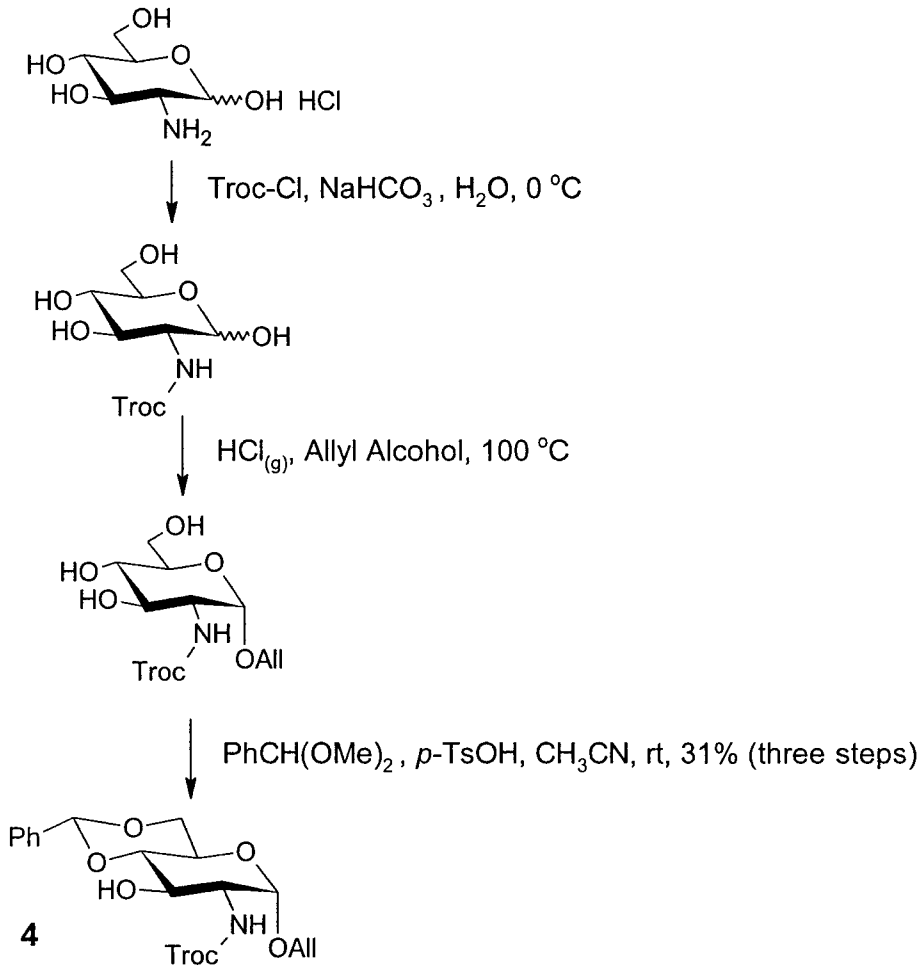

Scheme 3. Synthesis of glucosamine derivative **4**

2.1.5 Synthesis of trichloroacetimidate glycosyl donor 9

Synthesis began with the protection of the 3-OH in **4** with the desired Fmoc functionality. Reaction of **4** with 9-fluorenylmethoxychloroformate in pyridine gave **5** in 89% yield (**Scheme 4**). Installation at the 3-OH was confirmed by ^{1}H NMR data, specifically the downfield shift of H-3 from δ 3.91 ppm to δ 5.21-5.26 ppm. Regioselective opening of the benzylidene ring with sodium cyanoborohydride and ethereal HCl produced the 4-OH **6** in 85% yield. Protection of said 4-OH followed via phosphitylation with N,N-diisopropylphosphoramidite in the presence of 5-phenyltetrazole, and *in-situ* oxidation with *m*-chloroperoxybenzoic acid (m-CPBA) to yield dibenzyl phosphotriester **7** in 79% overall yield. ^{1}H NMR data of **7** (δ 4.71, ddd, *J* 9.5, 9.5, 9.0 Hz, H-4) confirmed the desired regioselectivity in the ring opening of **5**. Removal of the allyl group at the anomeric position was achieved by a two step procedure in which the allylic double bond was first isomerized using [bis(methyldiphenylphosphine)](1,5-cyclooctadiene) iridium(I) hexafluorophosphate, and then hydrolyzed using N-bromosuccinimide (NBS) to provide anomeric hydroxyl **8** in 79% overall yield. Conversion of **8** to the donor trichloroacetimidate **9** was effected in 1 h by treatment with trichloroacetonitrile and catalytic sodium hydride. The α-isomer (^{1}H NMR δ 6.43, d, *J* 4.0 Hz, H-1) was isolated in 81% yield. Longer reaction times in this reaction led to decreasing yield as additional spots on TLC were observed. This transformation is usually achieved with the use of 1,8-diazabicyclo[5.4.0]undec-7-ene (DBU) as catalytic base, however if employed, the 3-*O*-Fmoc functionality would also have been cleaved.

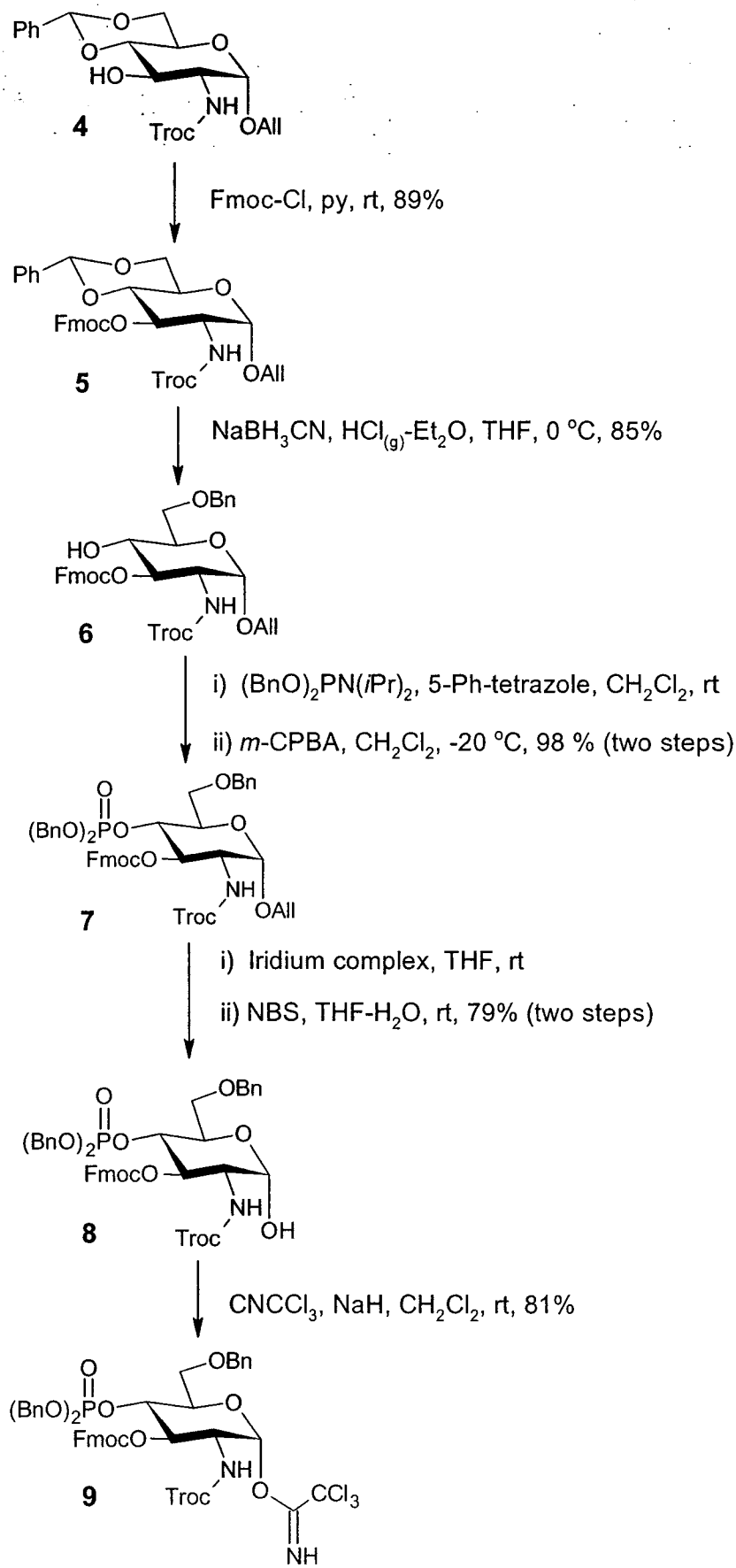

Scheme 3. Synthesis of trichloroacetimidate glycosyl donor **9**.

2.1.6 First attempts at direct synthesis of dimeric monosaccharide backbone

Direct coupling of two units of trichloroacetimidate glycosyl donor **9** with ethylene glycol to obtain the desired disaccharide backbone was envisioned to proceed through a successive di-glycosylation pathway. A Lewis acid catalyzed glycosylation reaction between donor **9** and the ethylene glycol first would proceed to give monosaccharide intermediate **10**, which would further react with remaining imidate to yield the desired dimeric monosaccharide **11** (**Scheme 4**).

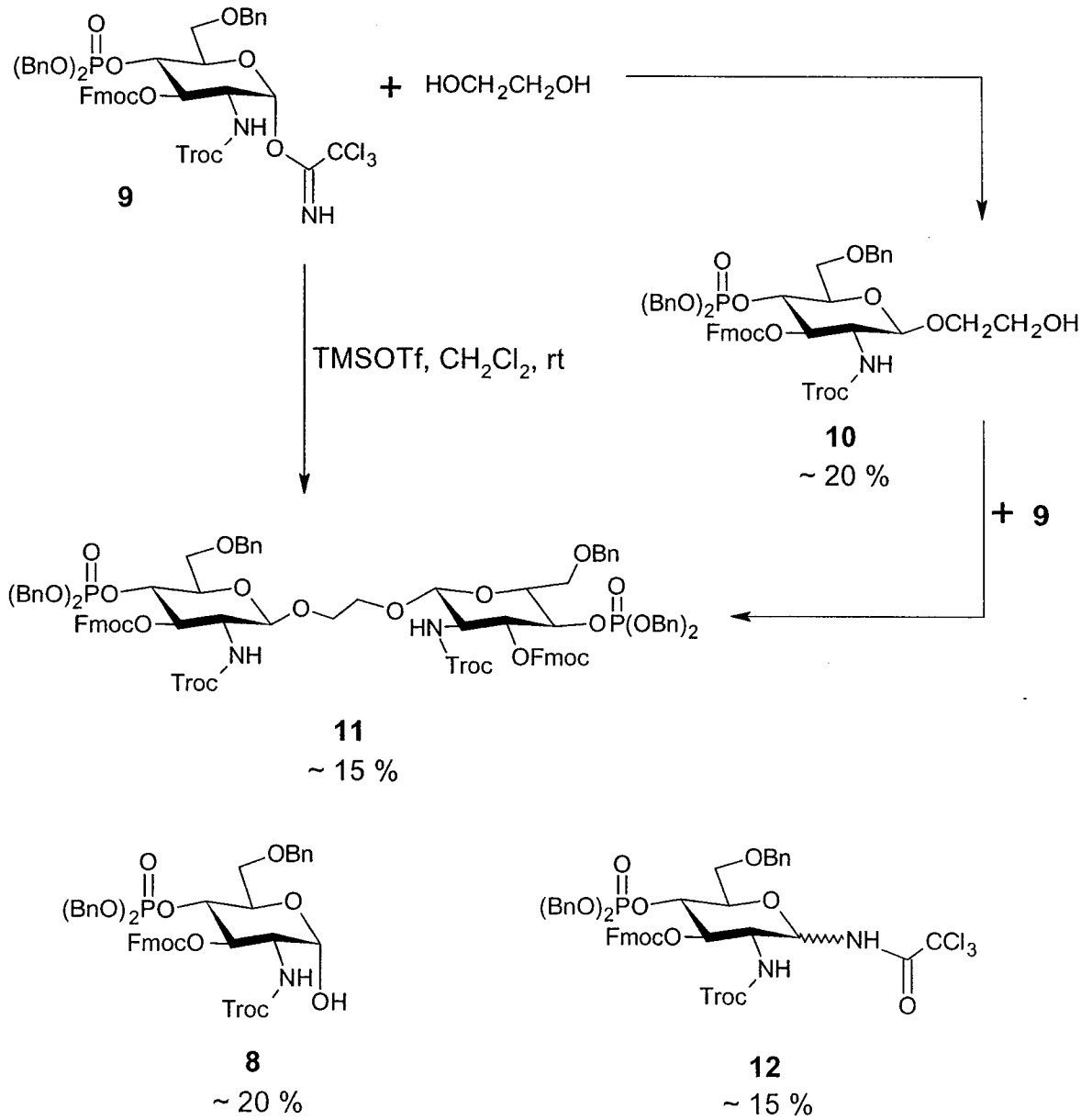

Scheme 4. Initial attempt at direct one step formation of dimeric monosaccharide **11**

Initial attempts at carrying out the direct synthesis of the dimeric monosaccharide backbone utilized slightly more than 2 equivalents of imidate **9** to 1 equivalent of ethylene glycol (**Scheme 4**). Numerous products were formed in roughly equal amounts, as visualized by TLC, and several attempts were made at their isolation and characterization. However, significant difficulties in chromatographic separation were encountered, and thus no analytically pure samples for structure confirmation purposes were obtained. Crude spectroscopic data provided evidence of the formation of monosaccharide intermediate **10** and desired dimeric monosaccharide **11** in 20 and 15% approximate yields respectively. Furthermore, the crude spectroscopic data also indicated the formation of imidate by-product **12** in 15% approximate yield. This by-product is known to result in glycosylation reactions when there is an absence of, or a pronounced lack of reactivity in the glycosyl acceptor. Finally, TLC comparison with known anomeric hydroxyl **8** also provided evidence of its formation in approximately 20% yield. These unexpected results dictated that a re-evaluation of the potential for a direct one step coupling be made.

2.1.7 Synthesis of monosaccharide intermediate 10

Given the confidence in the initial glycosylation reaction to yield monosaccharide intermediate **10**, the question was posed as to whether or not the second glycosylation to yield the desired dimeric monosaccharide structure could occur? Or, was there some force, be it sterics, electronics, or any other effect, that was interfering in the formation of the dimeric monosaccharide, and ultimately causing the formation of the undesired side products (**Scheme 4**)? To investigate this, a linear synthetic pathway was developed in which the monosaccharide intermediate **10** was specifically targeted, from which further glycosylation reactions could be investigated. This pathway involved protecting one of the hydroxyl moieties in the ethylene glycol, such that its glycosylation with imidate **9** and subsequent deprotection should yield only the desired monosaccharide **10**. Thus, ethylene glycol was converted to mono-silyl ether **13** in a 70% yield through reaction with *tert*-butyldimtheylsilychloride (TBDMS-Cl) and imidazole in N,N-dimethylformamide (DMF) (**Scheme 5**). The glycosylation of **13** with imidate **9** under promotion by the catalyst trimethylsilyl trifluoromethanesulfonate (TMSOTf) in dichloromethane (DCM) gave protected monosaccharide **14** in 81% yield. ^{1}H NMR data of **14** (δ 4.76, d, J = 8.0 Hz, H-1) confirmed the desired β-glycoside linkage.

Removal of the silyl ether protecting group via tetrabutylammonium fluoride (TBAF) in an acetic acid (HOAc) acidified tetrahydrofuran (THF) solution at 0 °C gave monosaccharide **10** in 73% yield. Lower than expected yields were attributed to the potential basic cleavage of the Fmoc functionality by TBAF, which is substantiated by TLC evidence of an additional compound, although no analytically pure sample was obtained.

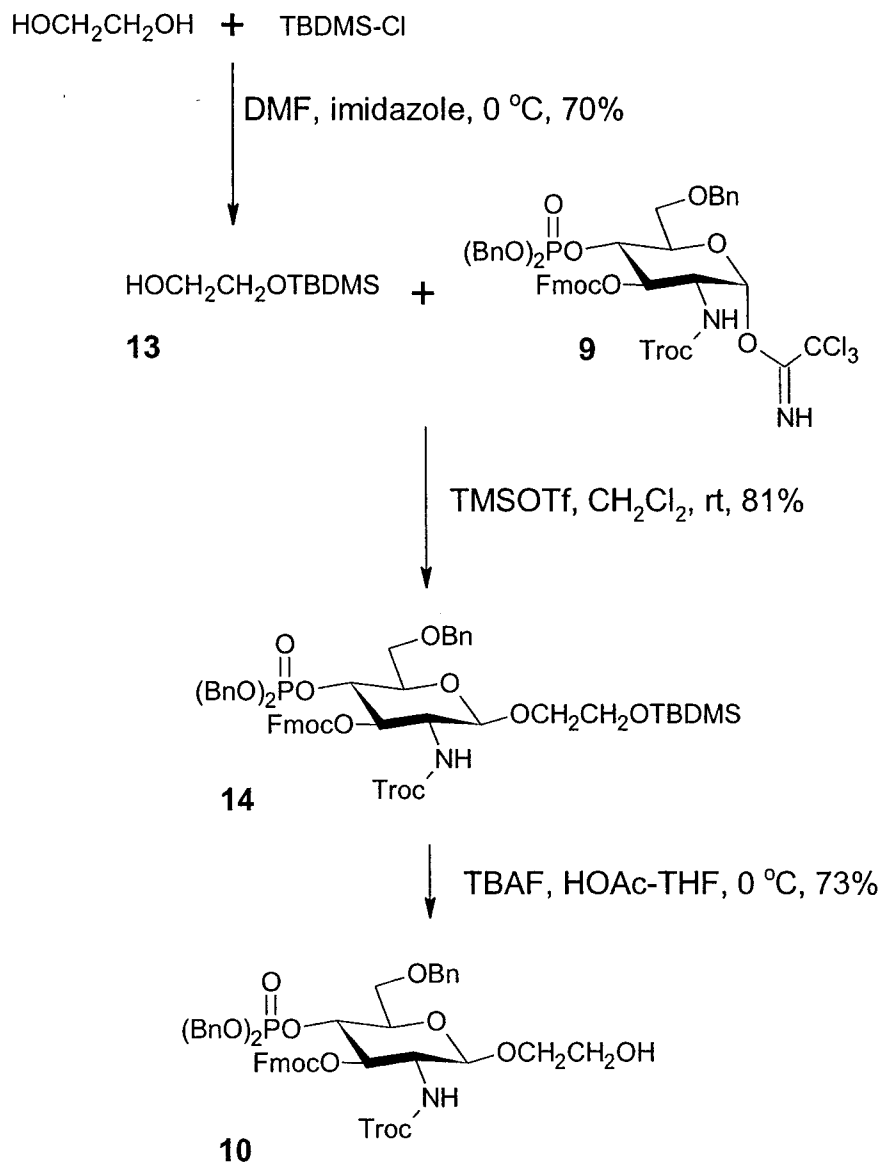

Scheme 5. Synthesis of monosaccharide intermediate **10**.

2.1.8. Glycosylation of monosaccharide 10

TLC comparison of confirmed monosaccharide **10** with the previously attempted direct syntheses of the dimeric monosaccharide backbone (**Scheme 4**) confirmed its formation. This further fuelled the question being posed as to whether or not the second glycosylation reaction could occur. To investigate this, a TMSOTf promoted glycosylation reaction between **10** and trichloroacetimidate **9** was attempted (**Scheme 6**). Interestingly, the desired dimeric monosaccharide **11** was formed with ease in an 83% yield. The symmetry of **11**, as indicated by ^{1}H NMR data confirmed the newly formed β-glycosidic bond. TLC comparison of the now confirmed dimeric monosaccharide **11** with the previous attempts at its direct synthesis (**Scheme 4**) confirmed its formation, albeit in significantly less than expected yields.

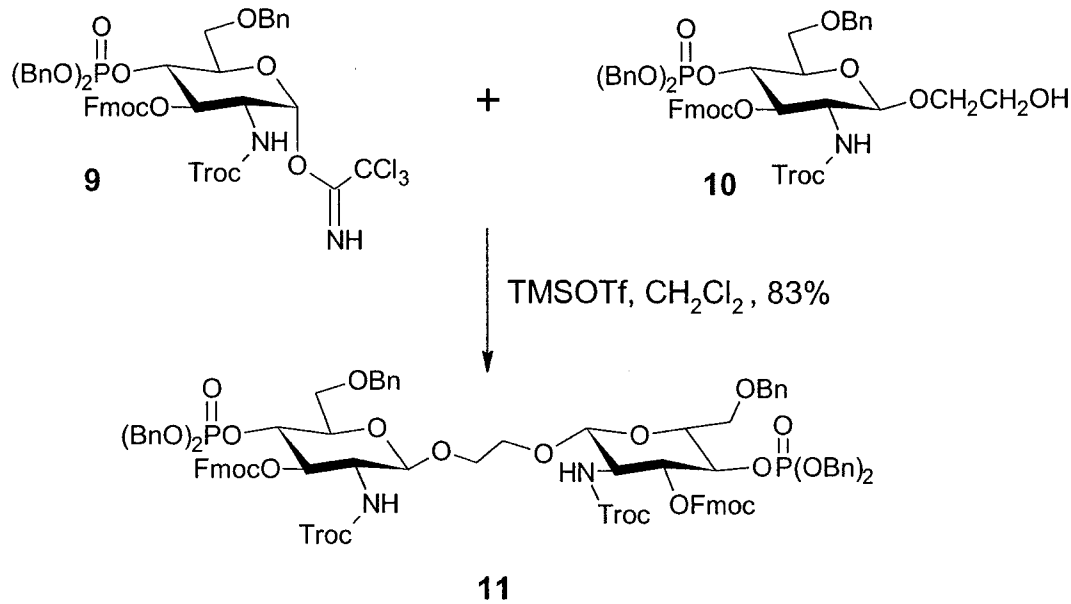

Scheme 6. Glycosylation of monosaccharide **10**

With the success in the linear synthesis of dimeric monosaccharide **11** from monosaccharide intermediate **10**, the notion of an interfering force hindering the formation of **11** was abolished. Moreover, of most importance is that a proof of concept of the originally proposed direct synthetic strategy was achieved. However, the question remained as to what was preventing

this now proven reaction from occurring when attempted in a direct, one-pot synthetic attempt (**Scheme 4**).

2.1.9 A return to direct synthesis of dimeric monosaccharide backbone

Interestingly, by pure chance it was discovered during the synthesis of monosaccharide **10** that the ethylene glycol had a very poor solubility in the DCM solvent employed for the glycosylation reactions. This solubility problem was found to be alleviated with the addition of THF. Therefore, the direct synthesis of dimeric monosaccharide **11** was attempted yet again using mixtures of varying compositions of DCM and THF as the solvent. All of these reactions showed significant production of the desired product. Moreover, all reactions showed evidence of remaining monosaccharide **10**. The yield was maximized at 74 % in an equivolume mixture of the two solvents, with monosaccharide **10** being isolated in an 11 % yield (**Scheme 7**).

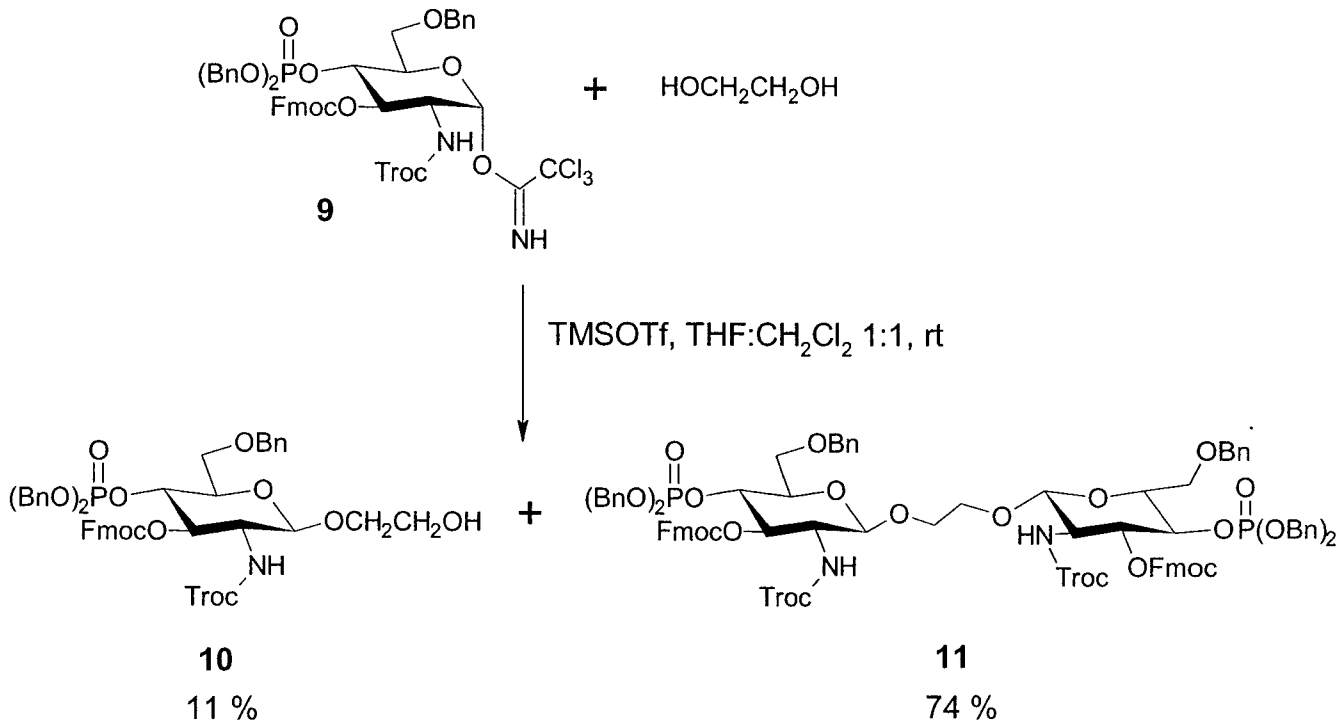

Scheme 7. Direct synthesis of dimeric monosaccharide **11**

The fact that monosaccharide **10** still remains in the reaction mixture indicates that the second glycosylation to form **11** is the rate limiting step in these direct synthesis reactions. Furthermore, it is also evident that optimum reaction conditions for this direct one step coupling have not been found, and thus require further investigation.

2.1.10 Amide lipid installation

With success in synthesizing the dimeric monosaccharide **11** by both a one step direct, and sequential linear method, focus shifted to the installation of lipid functionalities and the creation of analogs of the Lipid A molecule. The N-Troc protecting group was removed via treatment with zinc in a THF/HOAc 4:1 mixture to provide di-amine **15** as the main intermediate for subsequent amide bond syntheses (**Scheme 8**). Given the instability associated with free amines [42], **15** was used in its crude form and not subjected to any purification, and as such, spectroscopic data was not obtained. Coupling of di-amine **15** with dilipid acid **1** [74] promoted by N,N'-dicyclohexylcarbodiimide (DCC) afforded the dilipid amide **16** in a 65% overall yield. ^{1}H NMR data of **16** (δ 6.60, d, J = 5.0 Hz, NH) confirmed the formation of the desired amide bond. The lower than expected yield was attributed to the decomposition of the relatively instable free amine, as additional spots on TLC were observed. However, no analytically pure samples were obtained from these additional spots.

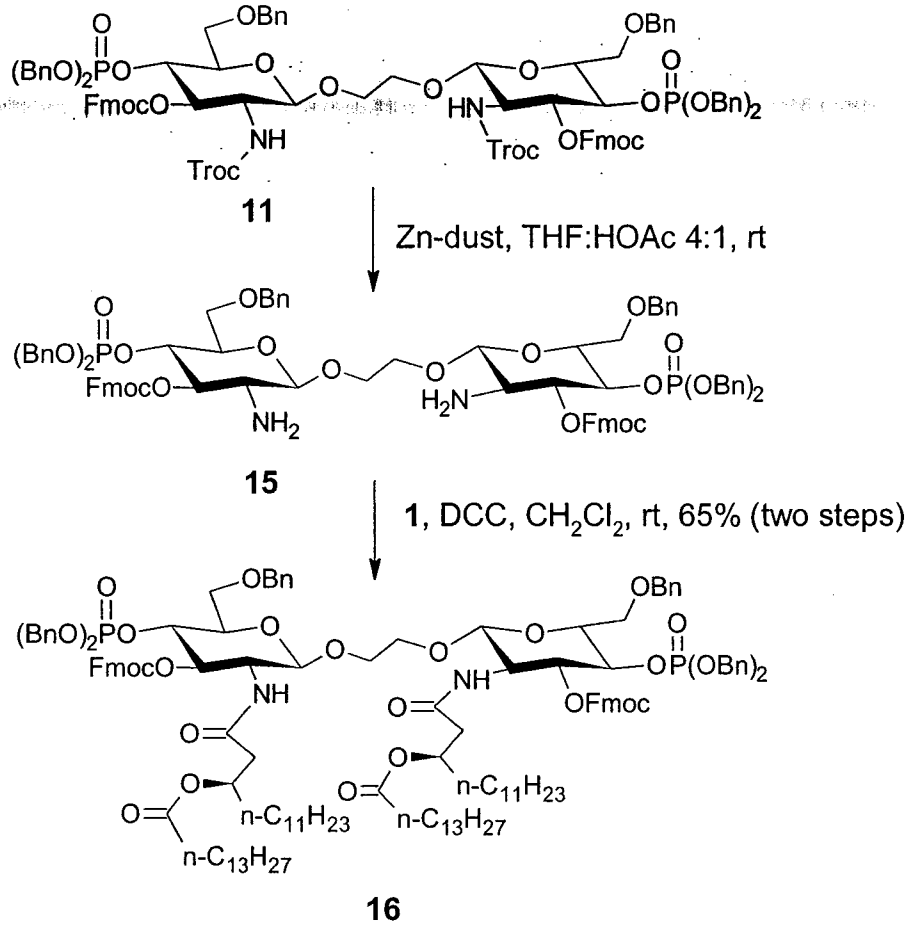

Scheme 8. Synthesis of dilipid amide **16**

2.1.11 Cleavage of the Fmoc protection group

With the successful installation of the amide dilipid functionality in **16**, deprotection of the 3-OH moiety via cleavage of the Fmoc protecting group was to follow. The initial attempt involved subjecting **16** to a DBU catalyzed deprotection in THF. What at first glance on TLC appeared to be a successful one spot to one spot conversion, was complicated by preliminary spectroscopic data. The ^{1}H NMR spectrum (not shown) was significantly more complicated than originally anticipated, and upon closer examination, indicated the presence of multiple unique sugar containing species. Further TLC investigations confirmed these findings in showing that what in some systems appeared as a single spot, actually appeared as three different, yet significantly close spots in other systems. Attempts at chromatographic

separation were made, however the compounds remained as an inseparable mixture. Migration of the chemically labile 4-dibenzylphosphotriester was proposed, with the formation of a three product mixture envisioned as a result of an incomplete migration (**Scheme 9**). It was therefore proposed that the three compounds resulting from the cleavage of the Fmoc functionality were the 3,3'-diphosphate (**18**) in which both phosphates have migrated, the 4,3' / 3,4'-diphosphate (**19**) in which only one phosphate has migrated, and finally the desired 4,4'-diposphate (**17**) in which phosphate migration has not occurred.

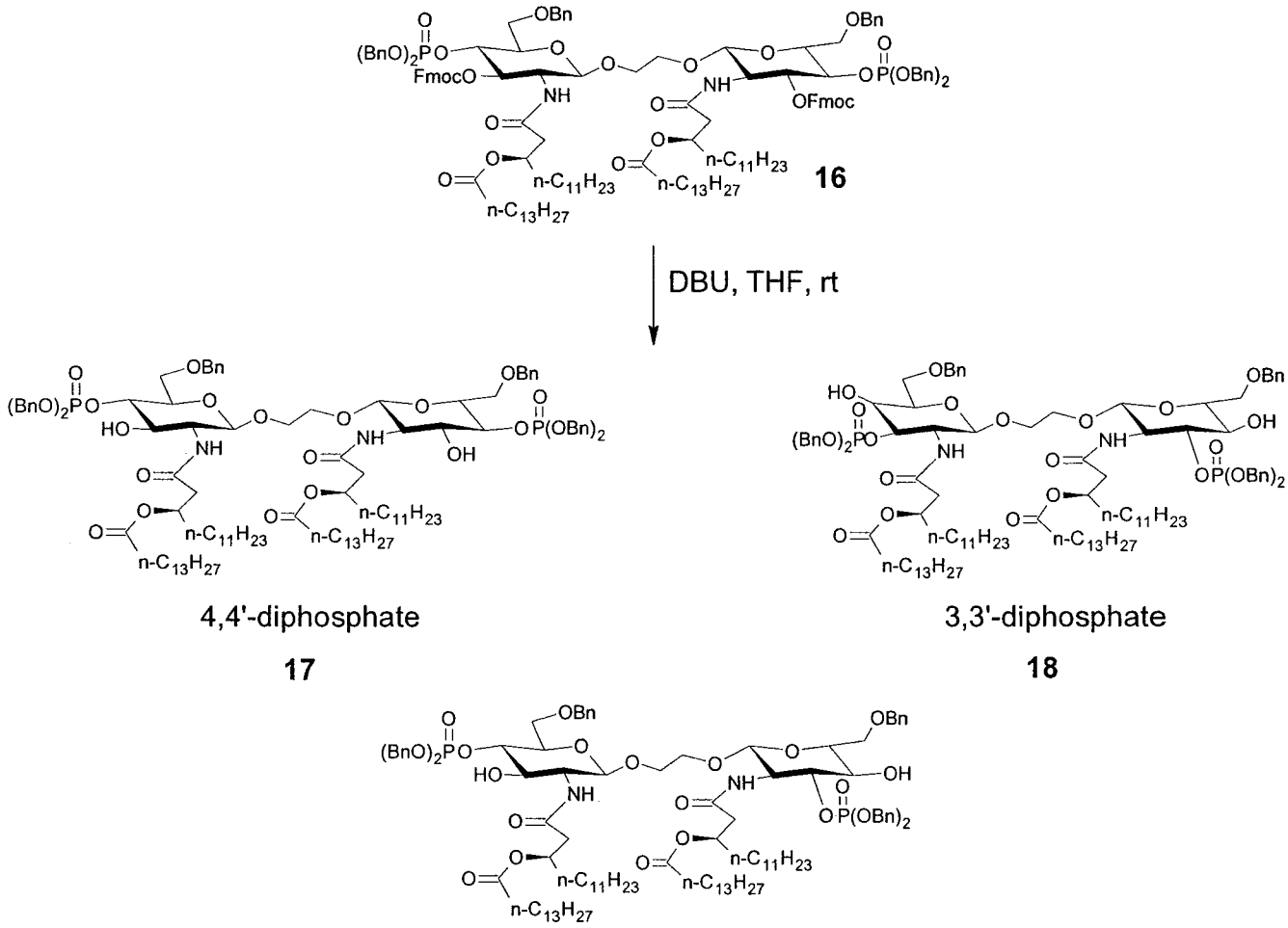

Scheme 9. Cleavage of the 3-O Fmoc protecting group

^{1}H NMR data for the mixture was in support of this proposal. Examination of the amide proton region indicated the presence of two doublets, and one peak resembling a triplet (**Figure 17**). The two doublets were thought to correspond to the symmetric 4,4' and 3,3'-diphosphate species, while the triplet was thought to be a product of the overlapping signals from the two different amide protons in the asymmetric 4,3' / 3,4'-diphosphate.

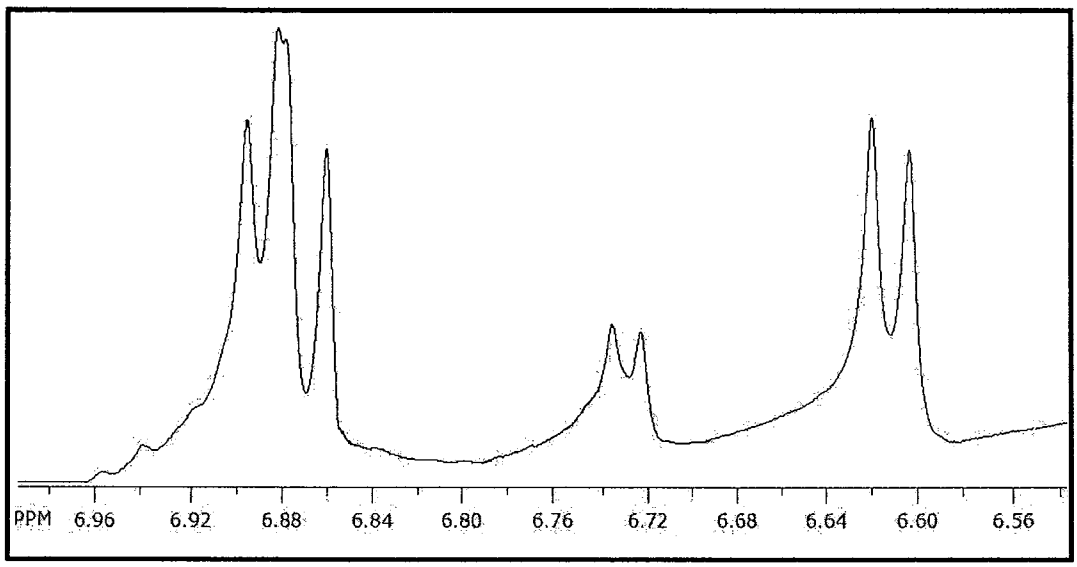

Figure 17. ^{1}H NMR amide region expansion

Examination of the mechanism by which the Fmoc functionality is cleaved provided insight as to the undesired migration of the 4-dibenzylphosphotriester moiety (**Scheme 10**). The base catalyzed cleavage to form the desired 3-OH product is shown mechanistically (**Scheme, Path A**). However, it appears that a nucelophilic attack on the protected 4-dibenzylphosphotriester is also possible during this cleavage given its spatial proximity to the 3-O position of the sugar, which ultimately results in the undesired migration of the phosphate group (**Scheme 10, Path B**).

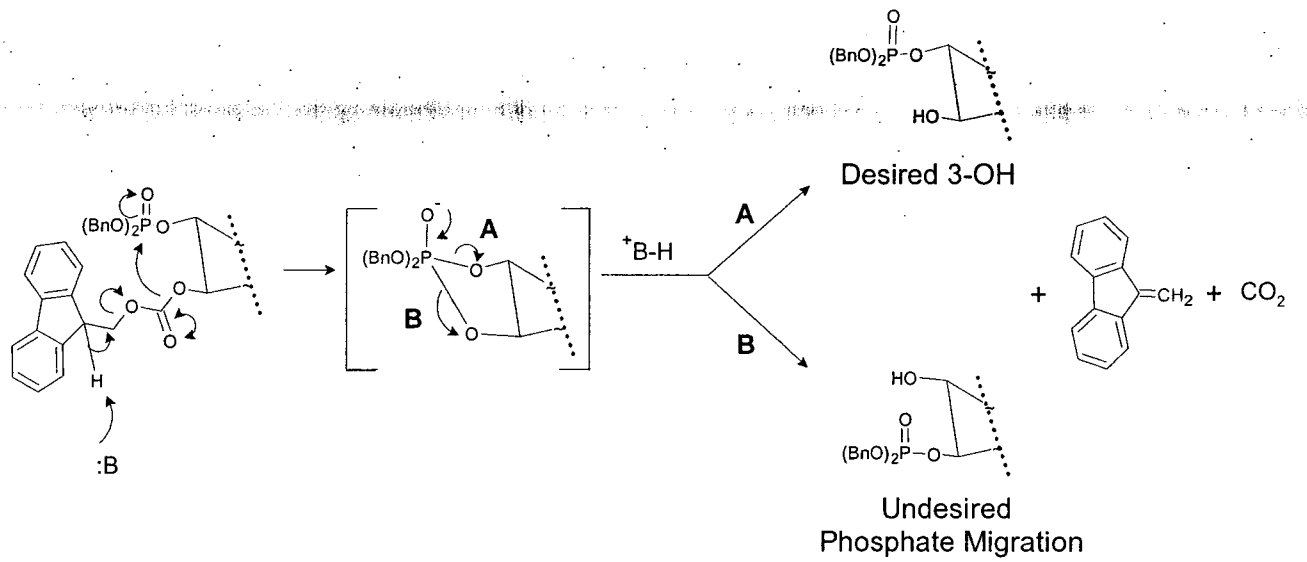

Scheme 10. Base catalyzed Fmoc cleavage and potential phosphate migration

In attempts to circumvent the potential phosphate migration, the deprotection of **16** was attempted further, now with the inclusion of protic solvent MeOH (**Scheme 11**). The inclusion of MeOH was thought to have the potential to increase the propensity of the reaction to go to the desired 3-OH product. The developing oxide ion at the 3-position maybe protonated by the MeOH before it attacks the 4-phosphotriester group, thus preventing the undesired migration. Furthermore, a different base, specifically TBAF, was also tried with hopes that these reaction conditions would hinder the migration of the phosphate. Unfortunately however, similar results were obtained for each of these conditions. Given the close structural similarity of the three products obtained, further attempts at chromatographic separation were abandoned.

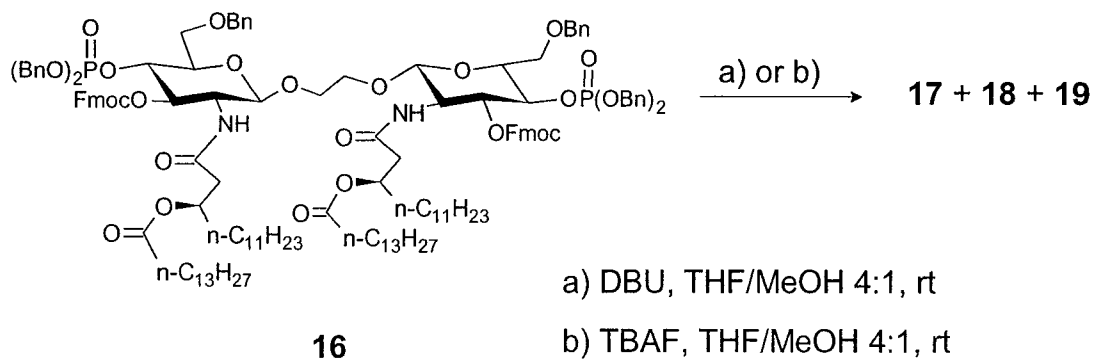

Scheme 11. Alternate attempts at Fmoc cleavage

2.1.12 Global deprotection of dilipid amide 16

With the undesired, and unexpected results obtained in the attempted deprotection of the 3-O-Fmoc group (**Scheme 9**), a re-evaluation as to the attainability of the proposed series of dimeric monosaccharide Lipid A analogs (**Figure 16**) was necessary. However, proposed analog **I** was still viewed as attainable, and could be easily accessed through the global deprotection of dilipid amide **16**. As such, **16** was subjected to a global deprotection via Palladium catalyzed hydrogenolysis (**Scheme 13**). Literature reports suggested that removal of the Fmoc protecting group through hydrogenolysis could be achieved [76], however preliminary TLC evidence of the hydrogenolysis indicated that this was not occurring. Therefore, the resulting product after workup was further subjected to a piperidine treatment in $CHCl_3$ to afford **20** in a 65% overall yield. Given the amphipathic nature of **20** and its tendency to form aggregates in solution, spectroscopic data has yet to be successfully obtained. However, high resolution electrospray mass spectrometry results have confirmed its identity.

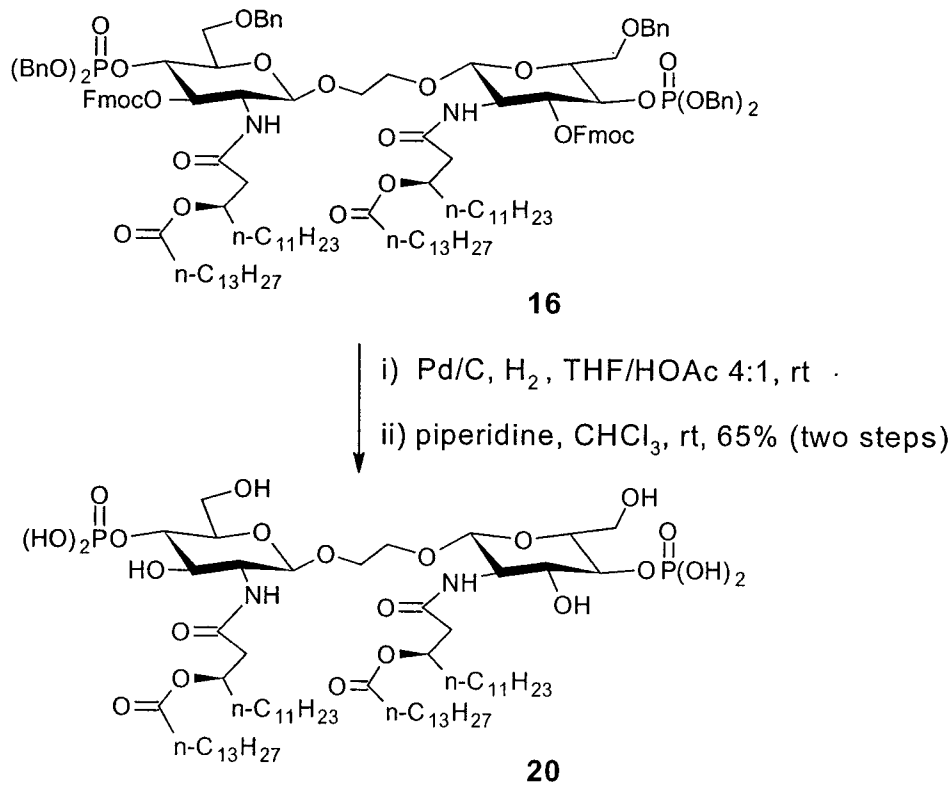

Scheme 13. Global deprotection of dilipid amide **16**

2.1.13 Re-evaluation of proposed Lipid A analogs

Contemplating the results of the initial attempts at obtaining the free 3-OH, the general consensus was that further attempts to selectively remove the Fmoc protecting group would only be an exercise in futility. In order to successfully install lipids at this position, a new synthetic strategy would have to be employed. This strategy would involve the formation of the 3-O lipid esters before the installation of the phosphate moiety, and ultimately before the formation of the dimeric monosaccharide backbone. Given the laborious nature of investigating this proposed strategy, as well as time limitations, the incorporation of lipid functionalities at the 3-OH position of the disaccharide backbone was temporarily abandoned. However, the fact that there have been several biologically active synthetic Lipid A analogs reported in which only N-acylation was present, the most notable of which is OM-174 [46, 66], dictated that novel analogs with solely N-acylation be designed and synthesized for biological testing alongside previously obtained analog **20** (**Scheme 13**).

Although now limited by the presence of the 3-O-Fmoc protecting group, two new analogs were envisioned which could employ the current dimeric monosaccharide framework. Said analogs would involve varying the degree and pattern of acylation present at the N position. Newly proposed analog **IV** (**Figure 18**) would introduce asymmetry in the pattern of *N*-acylation, and was proposed to directly mimic the structure of OM-174 [46, 66]. Analog **V** was proposed to examine the effect of an increase in the degree of acylation, and would involve the incorporation of a novel trilipid acid moiety.

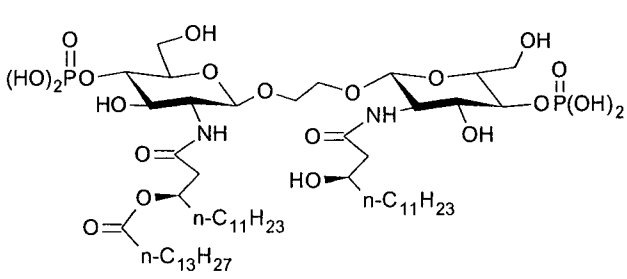

IV

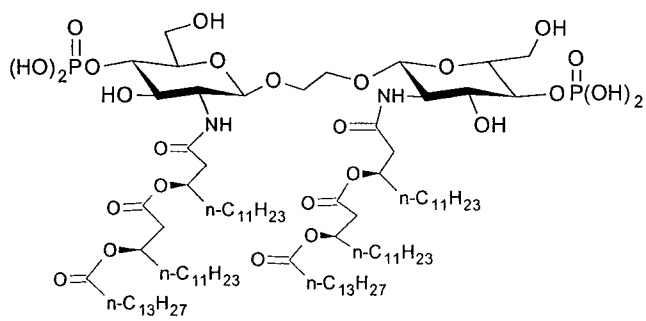

V

Figure 18. Revised dimeric monosaccharide Lipid A analogs

2.1.14 Attempted synthesis of proposed analog IV

Newly proposed Lipid A analog **IV** (**Figure 18**) was envisioned to be readily attainable through first the acylation of di-amine **15** with Troc protected β-OH monolipid acid **3**. Selective deprotection of the β-OH functionality, followed by its controlled reaction with the appropriate lipid acyl chloride would yield **IV**. As such, di-amine **15** was first coupled with monolipid acid **3** under DCC promotion to form **21** in 53% yield (**Scheme 14**). Lower than ideal yields were again contributed to the general instability of the amine as indicated by the formation of additional spots on TLC, although no analytically pure samples from these spots were obtained. Subsequent deprotection of the β-OH via treatment with zinc in a THF/HOAc 4:1 mixture to provide **22** in an 82% yield.

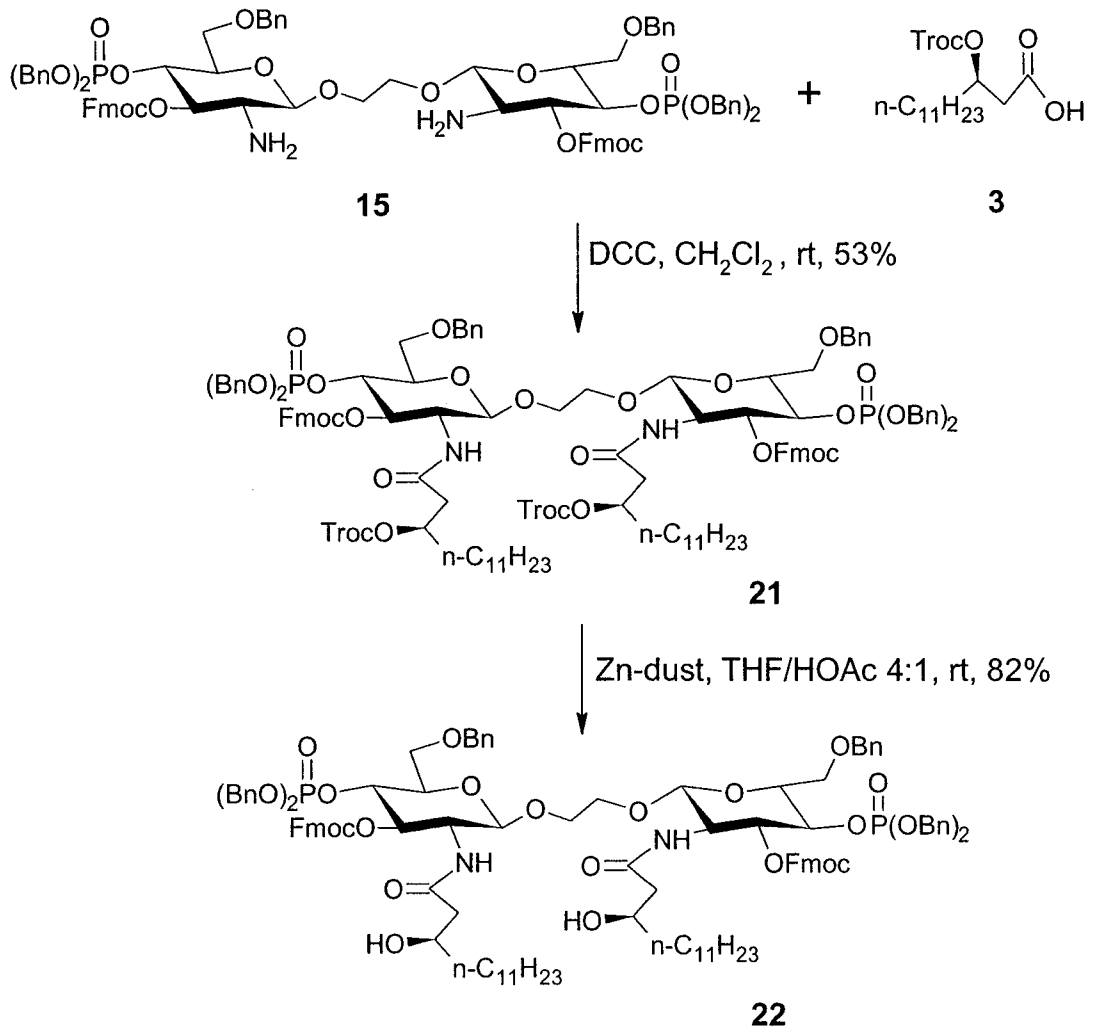

Scheme 14. Synthesis of β-OH amide **22**

The controlled reaction of the β-OH in **22** with tetradecanoyl chloride in attempts to selectively incorporate only one secondary lipid chain was next attempted in a variety of conditions (**Scheme 15**). However, there was a significant lack of reactivity noted for **22**, both with the inclusion of catalytic DMAP, and an increased temperature

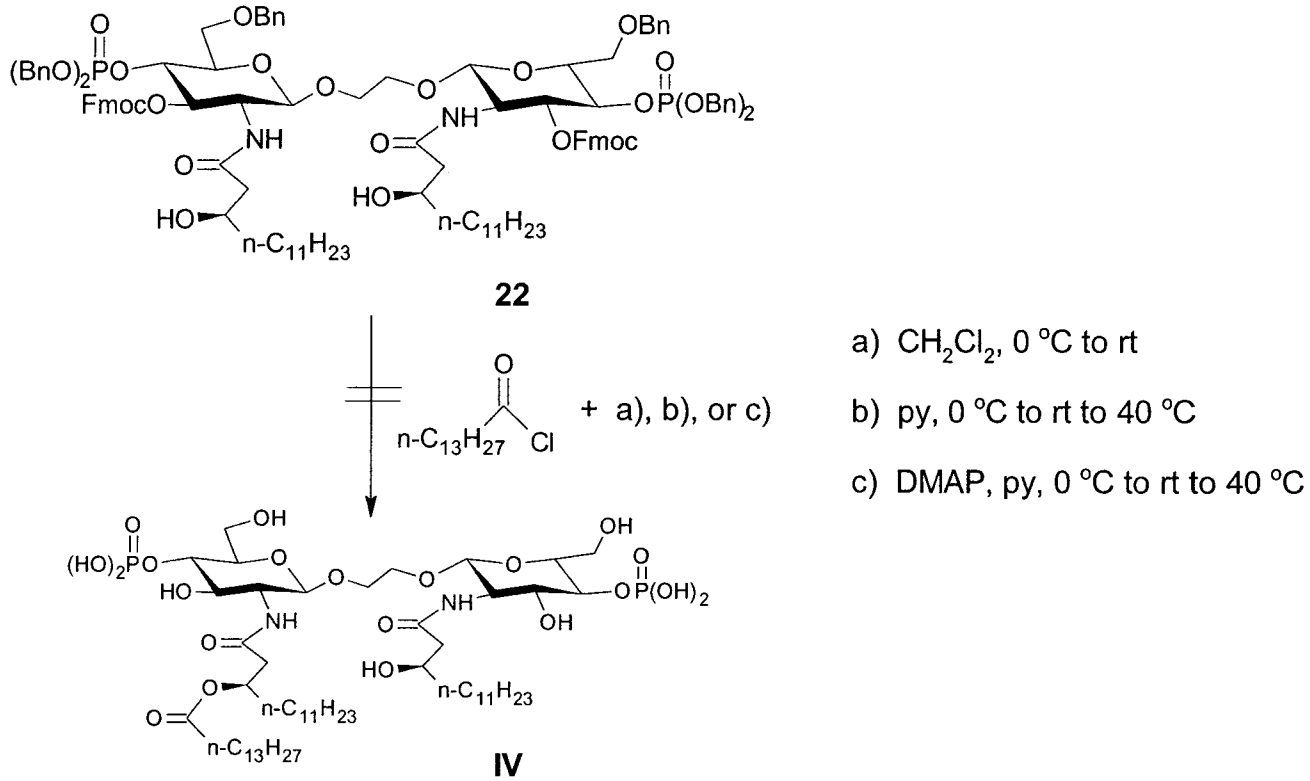

Scheme 15. Attempted acylation of β-OH functionality

Given the unpredicted lack of reactivity noted for **22**, possible sources of interference were evaluated. Examining the structure of **22**, a possible situation in which intramolecular hydrogen binding between the β-hydroxyl and the amide NH proton forming a pseudo-six member ring was envisioned (**Figure 19, A**). One significant resonance structure of this structure was envisioned to be the one in which there is a C=N bond formed between the carbonyl C and the amide N (**Figure 19, B**). In said structure, the NH proton would be expected to experience a significant positive character. Moreover, the β-OH would experience an overall decrease in electron density through induction to the positively charged N, thus potentially decreasing its nucelophilicity. Supporting this theory was ^1H

NMR data, in which a significant downfield shift (≈ 0.5 ppm) of the amide NH proton was noted upon the deprotection of **21** into **22** (**Scheme 14**). Further investigation is necessary to determine the extent of said interactio, and if it can be disrupted such that the true nucelophilicity of the β-OH can be obtained.

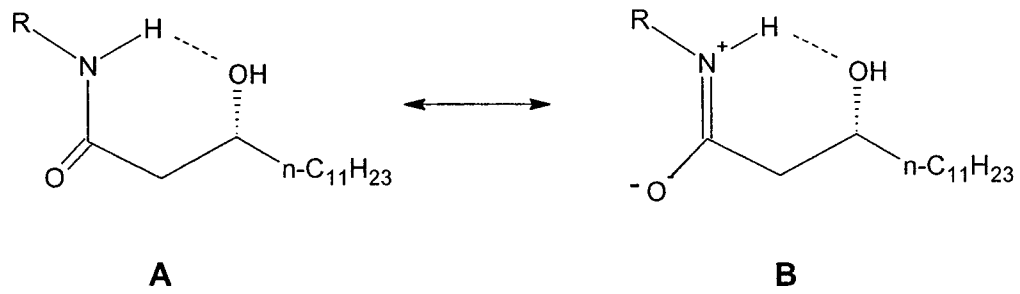

A **B**

Figure 19. Proposed intramolecular hydrogen bonding in **22**

2.1.15 Attempted synthesis of proposed trilipid amide analogue V

Proposed trilipid amide analogue **V** (**Figure 18**) required that a trilipid acid be synthesized for its eventual incorporation into the desired amide bond. This species was seen as resulting from the coupling of dilipid acid **1**[74] and 3-(R)-hydroxypenta-1-decene[75], followed by an appropriate oxidation to yield the acid moiety. As such, the two lipid species were first coupled via a DCC promoted reaction using catalytic DMAP in CH_2Cl_2. Unexpectedly, three products were obtained as a virtually inseparable mixture (**Scheme 16**). The identity of compounds **22** and **24** were confirmed both by comparison to known reference compounds, as well as GC coupled mass spectroscopic results. The small amount of pure **25** isolated allowed for spectroscopic data to be obtained confirming its identity.

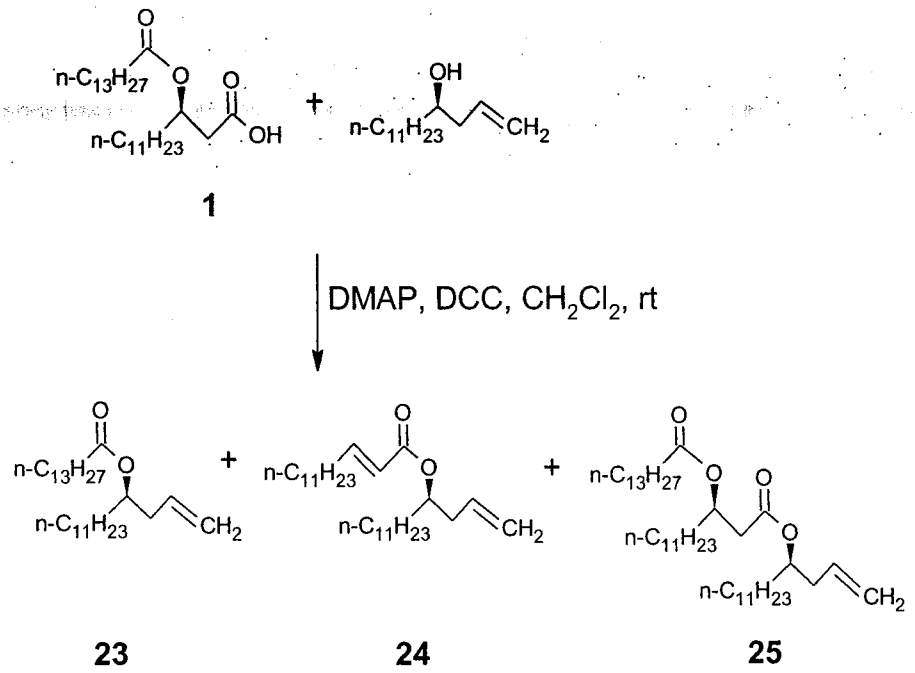

Scheme 16. Attempted synthesis of trilipid acid

These unexpected results were rationalized by examining the mechanism through which this Steglich type esterification proceeds (**Scheme 17**). Dilipid acid **1** first nucleophilically attacks the DCC forming species **26**. Literature evidence suggests that **26** is susceptible to attack by further dilipid acid to form anhydride species **27** [74]. Base catalyzed elimination of an α-proton results in the formation of **28** and **29**, which upon coupling to the 3-(R)-hydroxypenta-1-decene ultimately form the undesired compounds. Whether this elimination is occurring from species **26** or **27** is not entirely understood at this time. As to the identity of the base which causes said elimination, evidence suggests that this was in fact DMAP. Several similar attempts at the coupling were performed in effort to minimize the degree of said elimination. Varying amounts of the DMAP catalyst were tested, with higher DMAP levels leading to an increased presence of the undesired eliminated products, as visualized qualitatively by TLC.

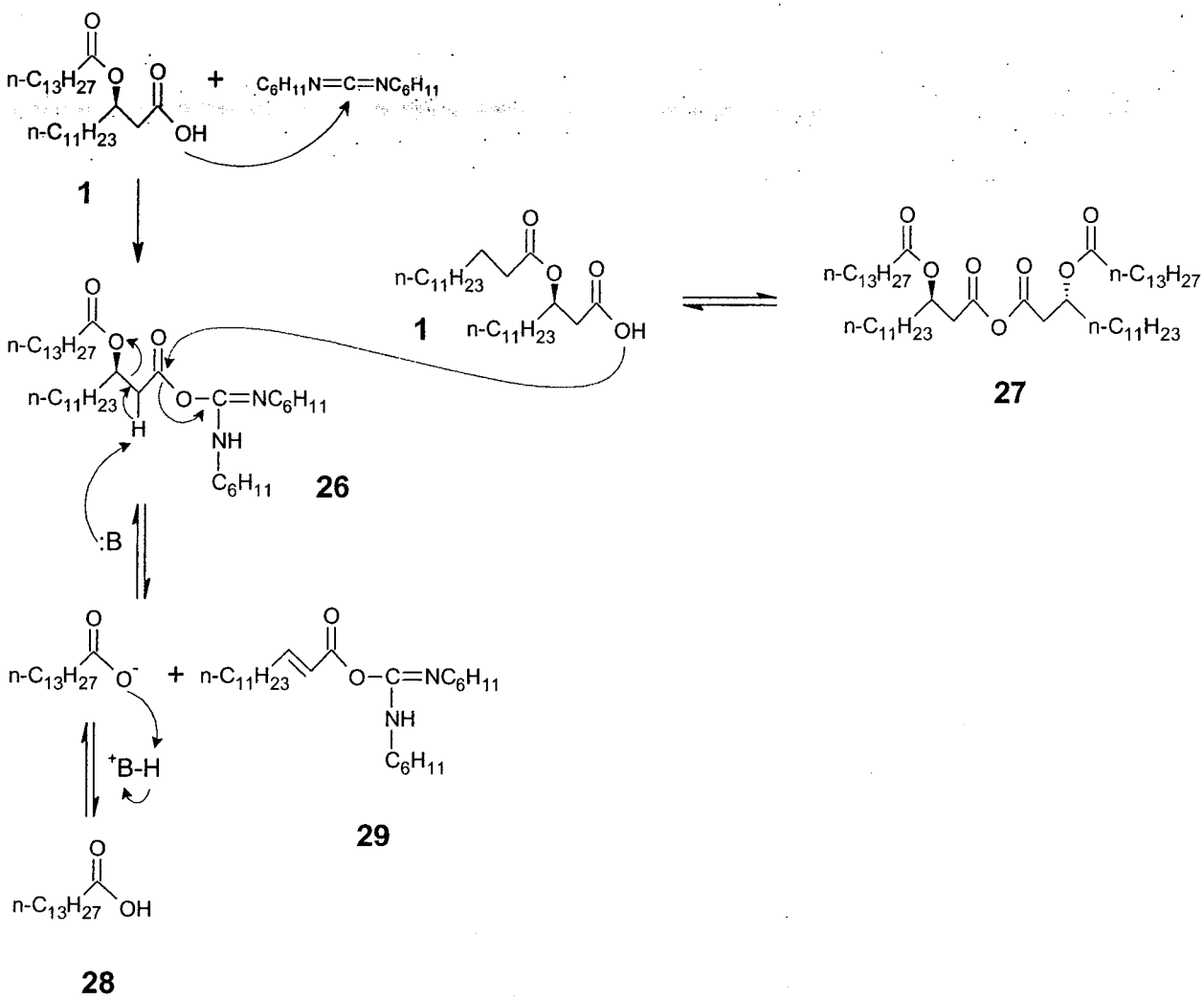

Scheme 17. Mechanism of base catalyzed lipid elimination

The inseparable three compound mixture was subjected to a $KMnO_4$ oxidation, and upon purification an inseparable mixture of dilipid acid **1** and desired trilipid acid **30** was obtained (**Scheme 18**). In effort to allow for chromatographic separation, the inseparable mixture of dilipid and trilipid acids (**1** & **30**) was subjected to phenacylation via a triethylamine (Et_3N) catalyzed reaction with 2-bromoacetophenone in EtOAc. Trilipid phenacyl ester **31** was successfully separated and obtained in pure form. Deprotection with zinc in HOAc, finally afforded pure trilipid acid **30** in a 24% overall yield.

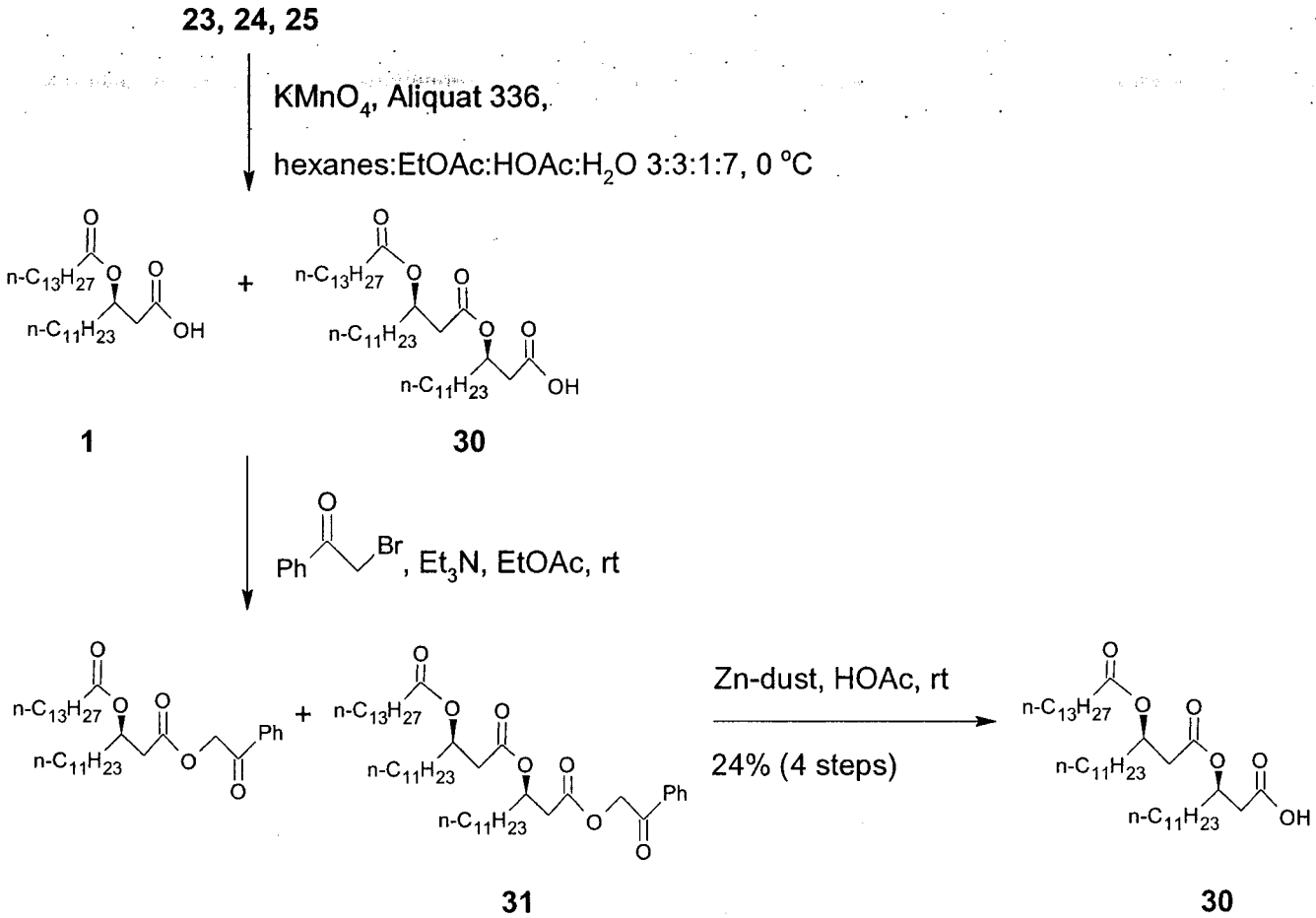

Scheme 18. Synthesis of trilipid acid **32**

In the Initial attempts at coupling trilipid acid **30** with di-amine **15** (**Scheme 19**) to form proposed analog **V**, numerous closely related products were noted as visualized by TLC, and thus have resulted in significant difficulties in chromatographic separation. As such, no analytically pure sample of the coupled product has been obtained as of yet. A possible explanation of these unexpected results lies in the increased overall size of trilipid acid **30** compared to those lipid acids with which successful couplings have been performed. A situation was envisioned in which steric hindrance due to the increased size of **30** ultimately would result in a decreased rate of coupling. Given the general instability of di-amine **15** in solution, the propensity of this basic moiety to cause cleavage of the 3-O-Fmoc protecting group, or migration of the chemically labile 4-dibenzyl phosphotriester would be increased with a decreased rate of amide bond formation. As such, the potential for a multitude of

chemically similar products would exist. Unfortunately, due to a lack of material and time constraints, further attempts at the coupling have been abandoned.

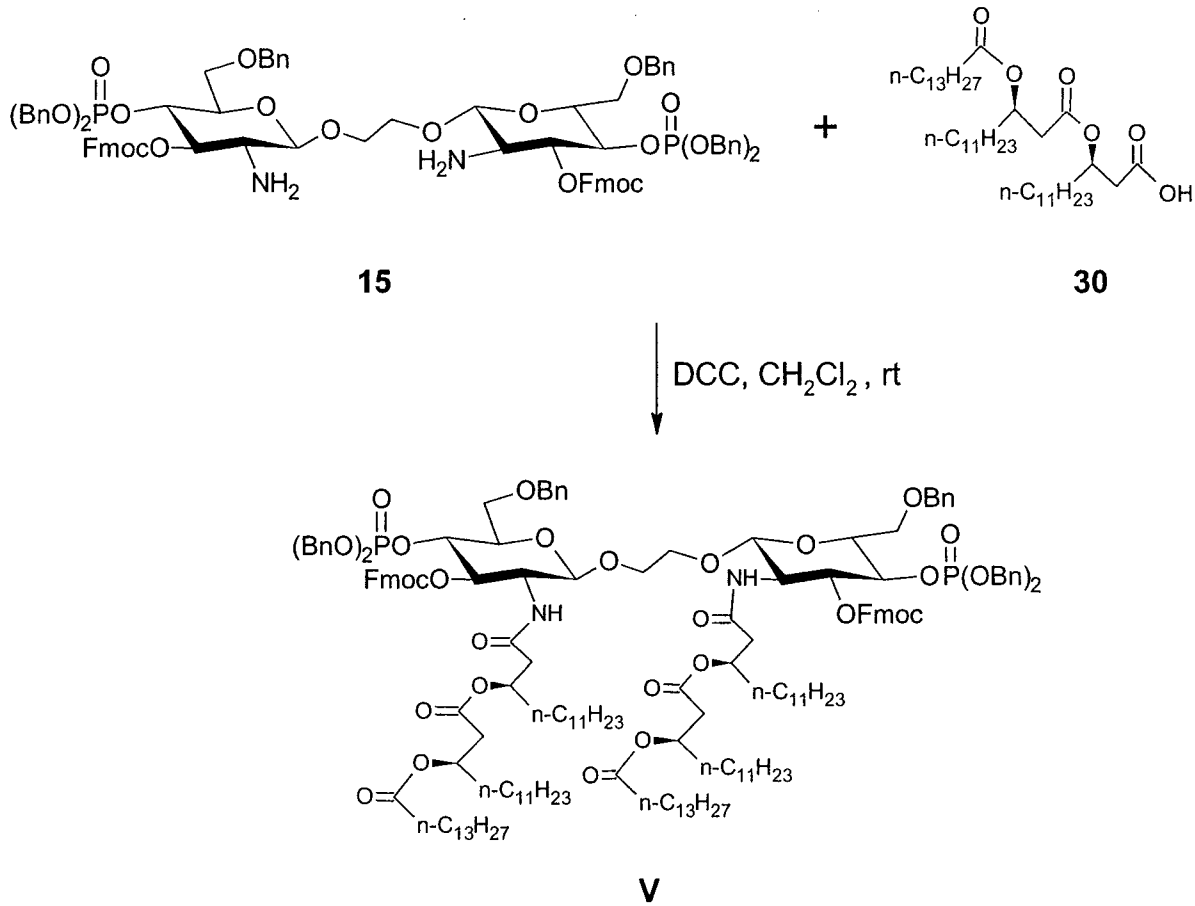

Scheme 19. Attempted synthesis of proposed analog **V**

2.1.16 Revised synthetic pathway

Given the problems encountered with phosphate migration, and the general lack of success in the synthesis of the revised series of proposed dimeric monosaccharide Lipid A analogs, a new synthetic pathway has been undertaken with the help of colleagues in the lab in which the intent is to synthesize analogs of the dimeric monosaccharide backbone with acylation present at the 3-O position. This pathway involves the formation of the 3-O lipid esters before the installation of the 4-O phosphate moiety, and ultimately before the formation of the dimeric monosaccharide backbone. Therefore, according to known

literature procedures [71], glucosamine derivative **4** [19, 73] has been coupled with dilipid acid **1**, and ultimately converted into trichloroacetimidate donor **32** (**Scheme 20**). In a similar manner to the synthesis of **11** (**Scheme 7**), it is intended that donor **32** be coupled with ethylene glycol to obtain the desired dimeric monosaccharide framework, from which analogs of the Lipid A structure can be obtained.

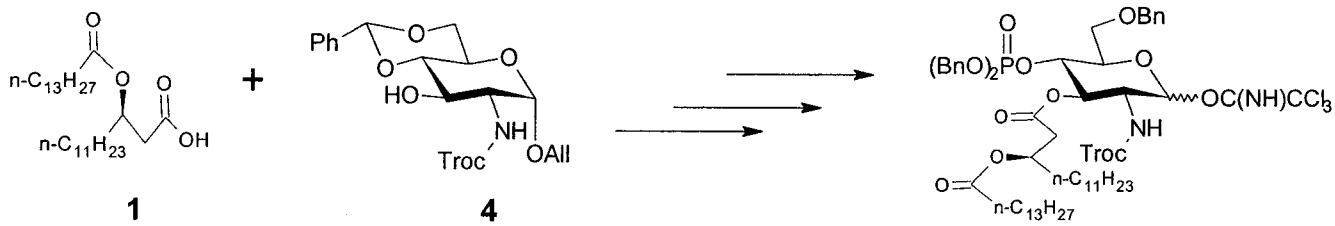

Scheme 20. Synthesis of trichloroacetimidate donor **32**

2.2 Diethanolamine based monosaccharide Lipid A analogs

2.2.1 Design

During the redesign of the dimeric monosaccharide Lipid A analog synthesis, and the ultimate synthesis of trichloroacetimidate donor **32**, a novel series of monosaccharide Lipid A analogs were envisioned. Similar in premise to the AGP class of Lipid A analogs (**Figure 13**), proposed monosaccharide analogs **VI** and **VII** have one of the saccharide units of the natural disaccharide Lipid A backbone replaced by a diethanolamine (DEA) based acyclic scaffold (**Figure 20**). One proposed advantage of this novel monosaccharide framework over the AGP class structural framework is that it offers an additional chemical scaffold upon which further functionalization can occur, thereby offering the potential for further novel Lipid A mimetics. Analogs **VI** and **VII** are intended to be synthesized for initial investigations into the viability of this framework at interacting with the TLR4 signalling complex.

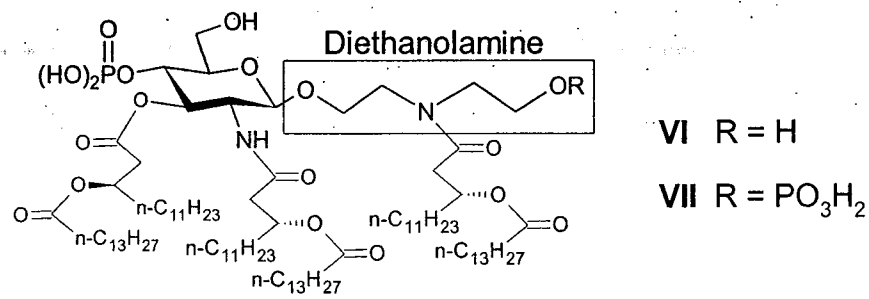

Figure 20. Proposed diethanolamine based monosaccharide Lipid A analogs

2.2.2 Retrosynthetic analysis

Beginning with desired analog **VII**, C-6 and phosphate hydroxyl moieties were again chosen to be globally protected with the benzyl (Bn) group, such that final global deprotection via hydrogenolysis was possible (**Scheme 21**). Eliminating the sugar amide lipid functionality, transforming the phosphotriester moiety of the acyclic scaffold into its parent hydroxyl, and finally the cleavage of the glycosidic bond ultimately yielded trichloroacetimidate donor **32** and diethanolamine derived amide acceptor **33**. The use of the N-Troc protecting paradigm in **32** was again employed for its proven stereoselective β-glycoside directing capability by virtue of neighbouring group participation [43, 71, 72].

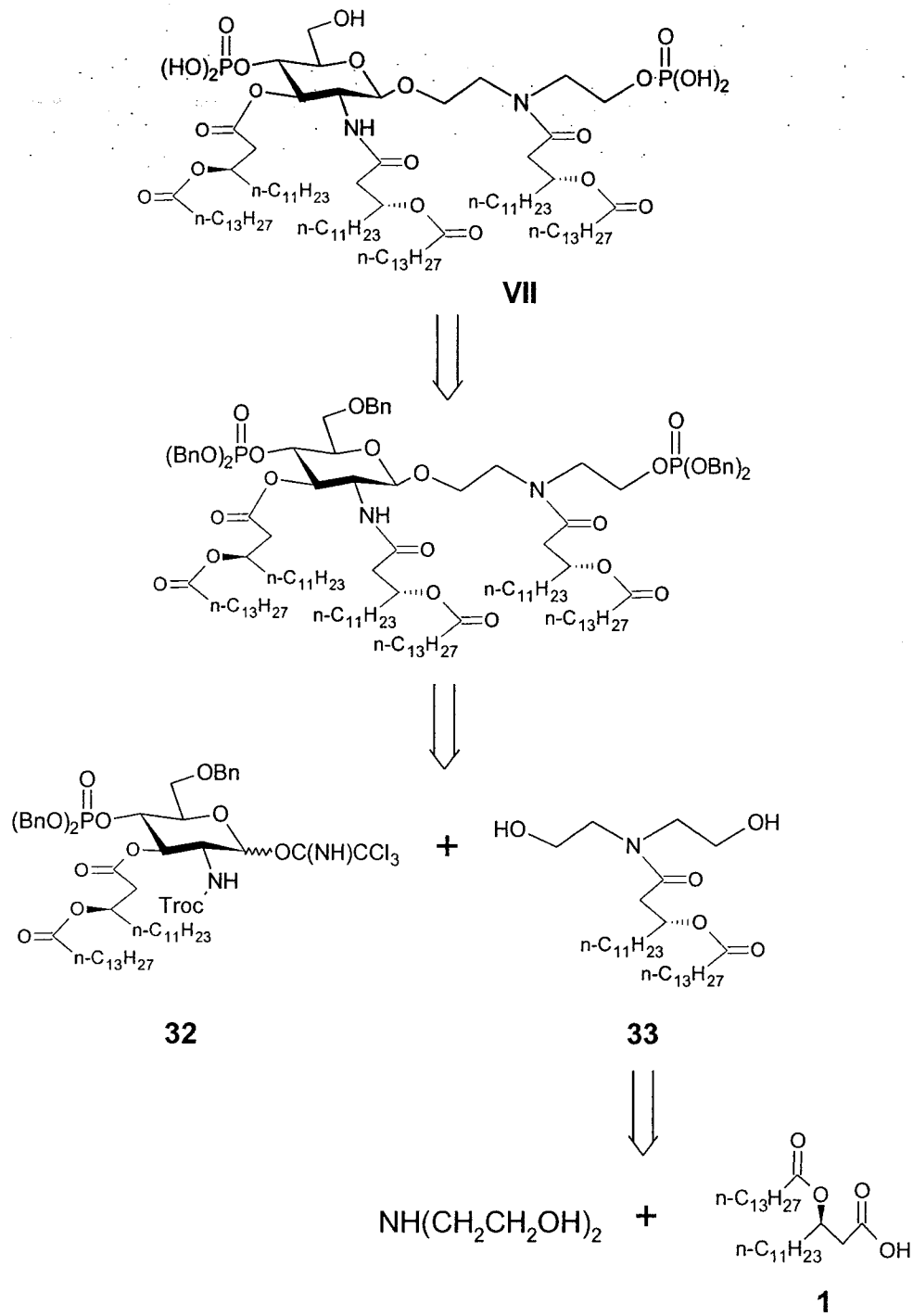

Scheme 21. Retrosynthesis of proposed monosaccharide Lipid A analogue **VII**

2.2.3 Synthesis of amide acceptor 33

Initial attempts at the synthesis of amide acceptor **33** involved the coupling of dilipid acid **1** with DEA under DCC promotion in THF, the results of which was an inseparable mixture of at least two compounds. Crude spectroscopic results for the mixture (not shown) were indicative of a similar elimination process as that encountered in the synthesis of trilipid acid **30** (**Schemes 16, 17**). These unexpected results were partly attributed to a poor solubility of DEA in the THF solvent. Successful coupling of **1** and DEA was brought about through the use of peptide coupling reagent *O*-(benzotriazol-1-yl)-*N,N,N',N'*-tetramethyluronium hexafluorophosphate (HBTU) and N'N-diisopropyl ethylamine (DIPEA) in DMF, for a 68% yield of amide **33** (**Scheme 22**).

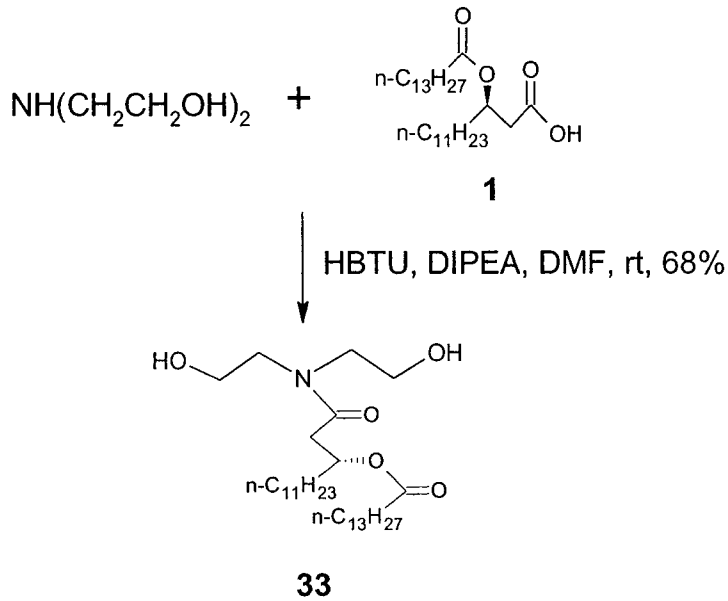

Scheme 22. Synthesis of acceptor amide **33**

2.2.4 Glycosylation to form monosaccharide framework

With the successful synthesis of amide acceptor **33**, glycosylation with imidate donor **32** was to follow. As such, a TMSOTf promoted glycosylation reaction between **33** and trichloroacetimidate **32** was attempted (**Scheme 23**). Given the secondary amide nature of acceptor **33**, the desired β-glycoside **34**, as indicated by ^{1}H NMR data of **34** (δ 4.78, d,

0.4H, *J* 8.0 Hz, H-1B), was isolated in a 53 % yield as two rotational isomers in an approximate 3:2 ratio. A second significant product was also isolated from the reaction in approximately 15% yield. An analytically pure sample of the compound has yet to be obtained, however, preliminary spectroscopic data indicates its identity as being the di-glycosylated product **35**.

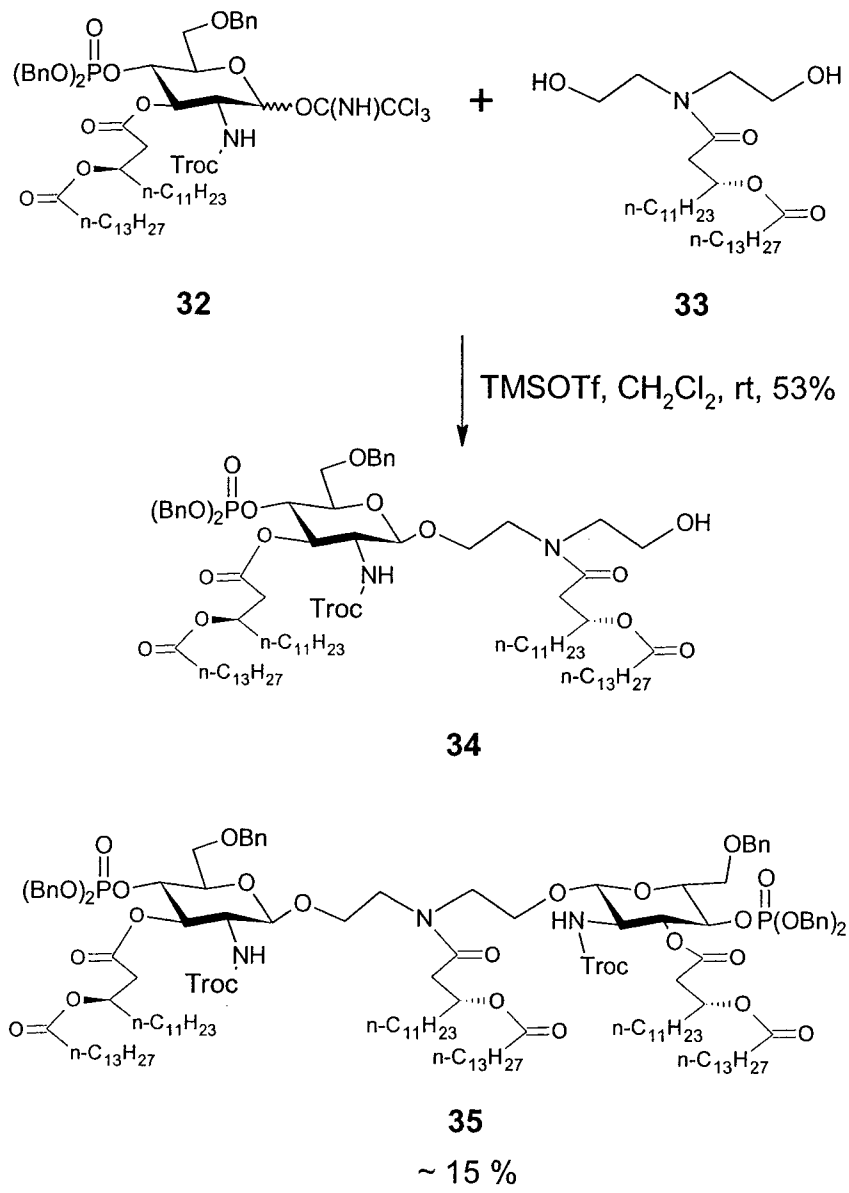

Scheme 23. Synthesis of DEA based monosaccharide framework

2.2.5 Installation of sugar amide linkage

The N-Troc protecting in glycoside **34** was cleaved to form amine **36** via treatment with zinc dust in a 4:1 THF/HOAc acid mixture (**Scheme 24**). Complete consumption of **34** was not achieved within a 3 hr reaction time, with approximately 10-15% remaining. Initially, the stability of free amine **36** was questioned, and as such, this compound was used in its crude form and not subjected to chromatographic purification. DCC promoted coupling of **36** with dilipid acid **1** in DCM gave the desired amide **37** in a 43% overall yield, again as mixture of two rotational isomers with an approximately 3:2 relative ratio. Free amine **36** was also recovered in 21%. Given the surprising stability of free amine **36** in solution, spectroscopic data was obtained thus allowing for conformation of its structure.

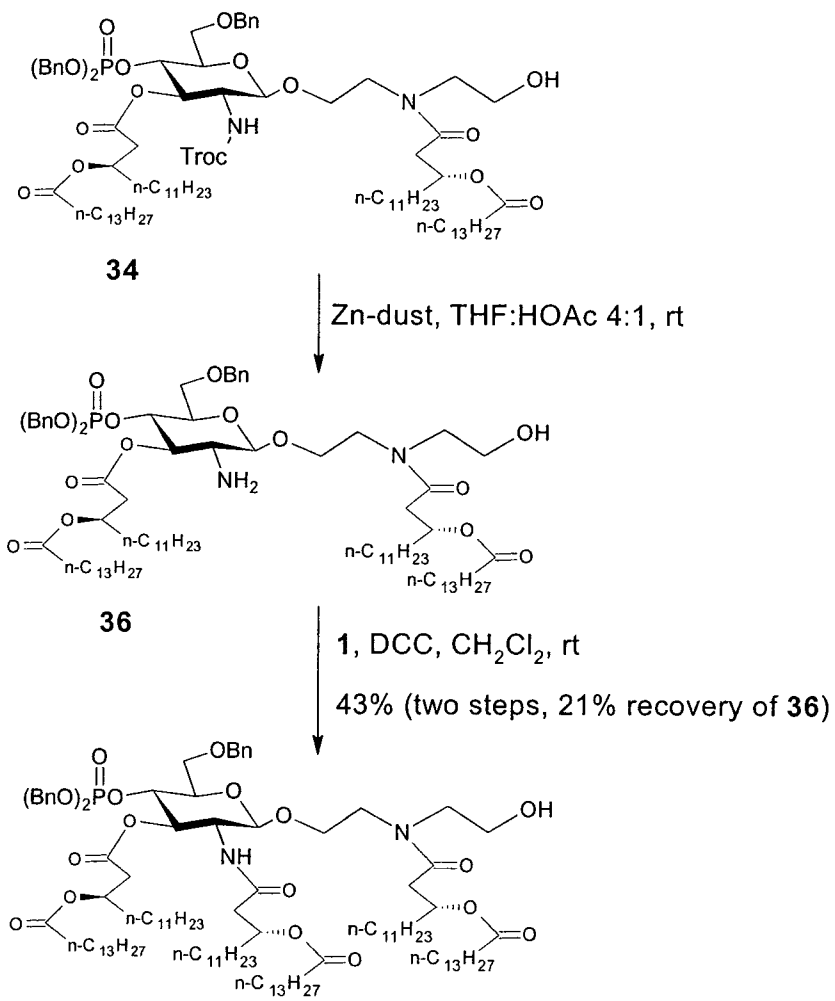

Scheme 24. Installation of sugar lipid amide functionality

2.2.6 Global deprotection of 37 to form proposed analog VI

With the successful isolation of the desired monosaccharide framework in **37**, proposed Lipid A analog **VI** (**Figure 20**) could be obtained through global deprotection of the remaining benzyl protecting groups. Therefore, **37** was subjected to a Palladium catalyzed hydrogenation to ultimately yield desired **38** in a 30% yield (**Scheme 25**). Given the amphipathic nature of **38**, and its tendency to form aggregates in solution, spectroscopic data has yet to be successfully obtained. The compound has been submitted for high resolution electrospray mass spectrometry analysis to confirm its identity.

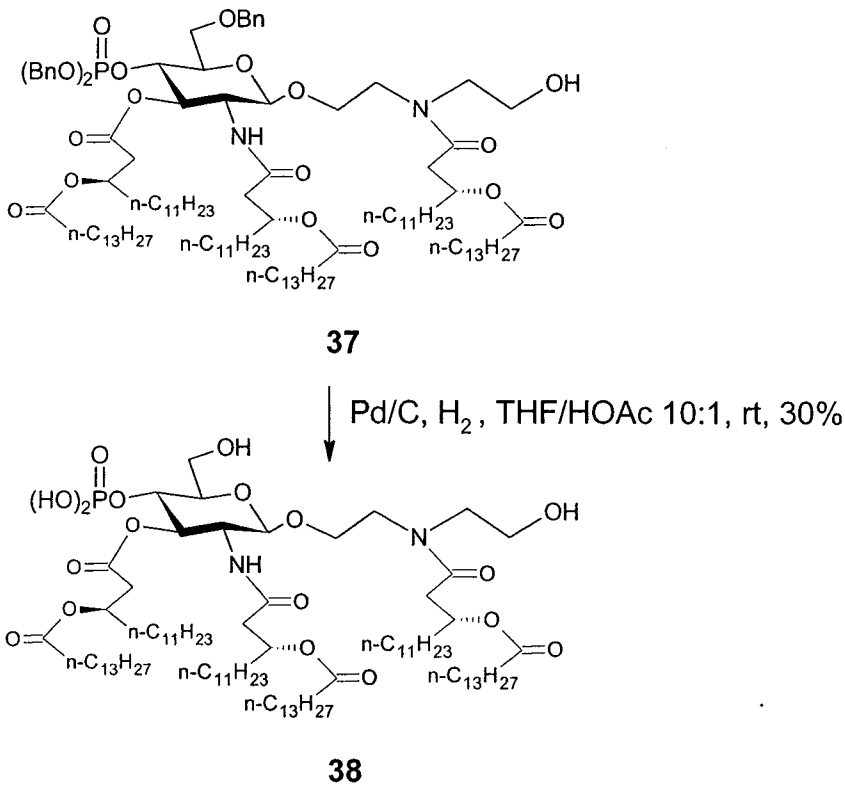

Scheme 25. Global deprotection of **37**

2.3 Future Work

2.3.1 Synthesis of proposed Analog VII

The synthesis of proposed monosaccharide Lipid A analog **VII** (**Figure 20**) is intended. Installation of the desired dibenzyl phosphotriester functionality on the DEA based acyclic

scaffold in **37** will yield **39** (**Scheme 26**). Upon successful isolation of **39**, its global deprotection via hydrogenolysis will thereby yield proposed analog **VII**.

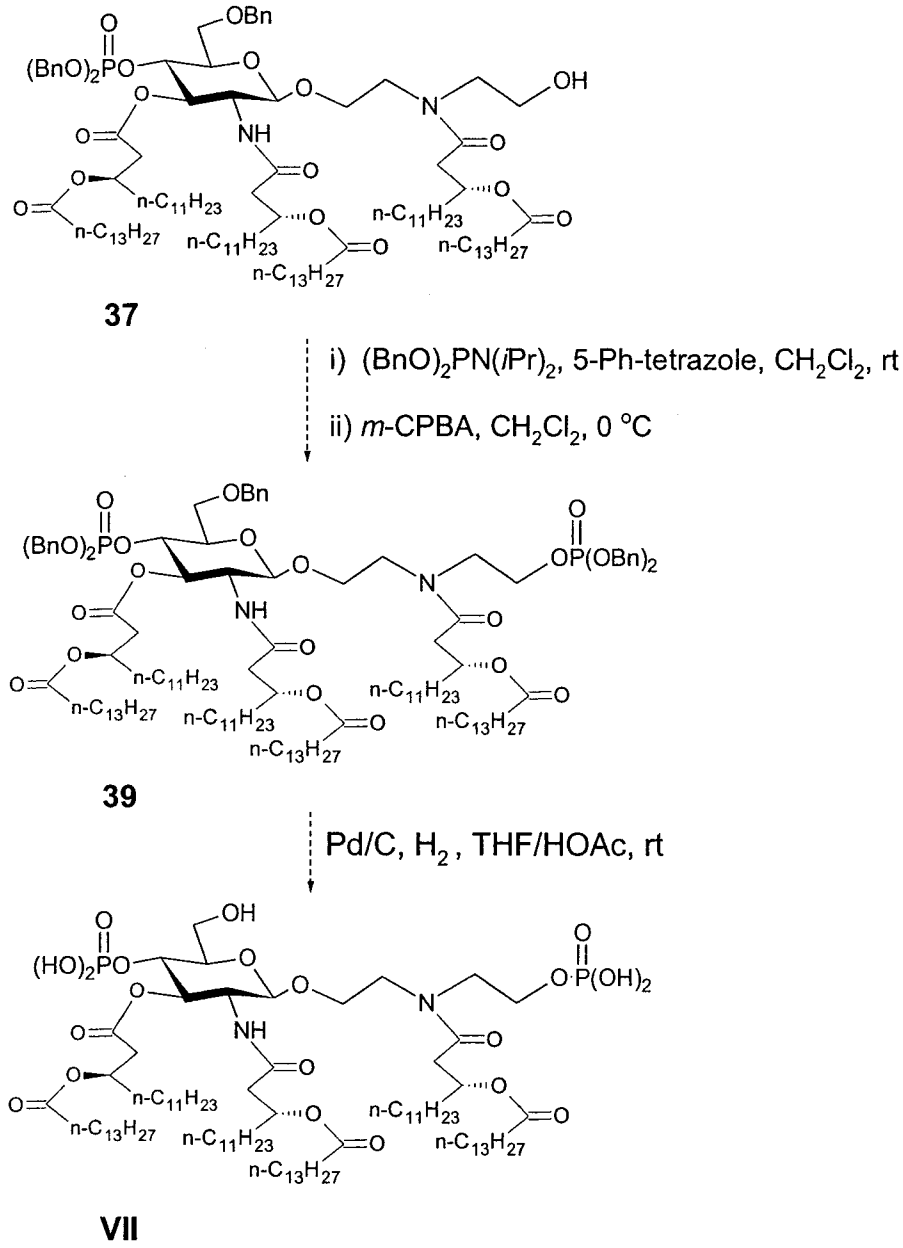

Scheme 26. Proposed synthetic route to monosaccharide Lipid A analog **VII**

2.3.2 Revised synthesis of dimeric monosaccharide Lipid A analogs

As noted earlier, a revised synthetic pathway has been designed and undertaken, the intent of which is the synthesis of dimeric monosaccharide Lipid A analogs with 3-*O* acylation. In a similar fashion as to the synthesis of **11** (**Scheme 7**), it is intended that the dimeric monosaccharide framework **40** be synthesized from donor imidate **32** (**Scheme 20**) and ethylene glycol (**Scheme 27**). Upon successful isolation of **40**, amine deprotection and subsequent acylation, followed by global deprotection will yield a series of Lipid A analogs with desired acylation patterns.

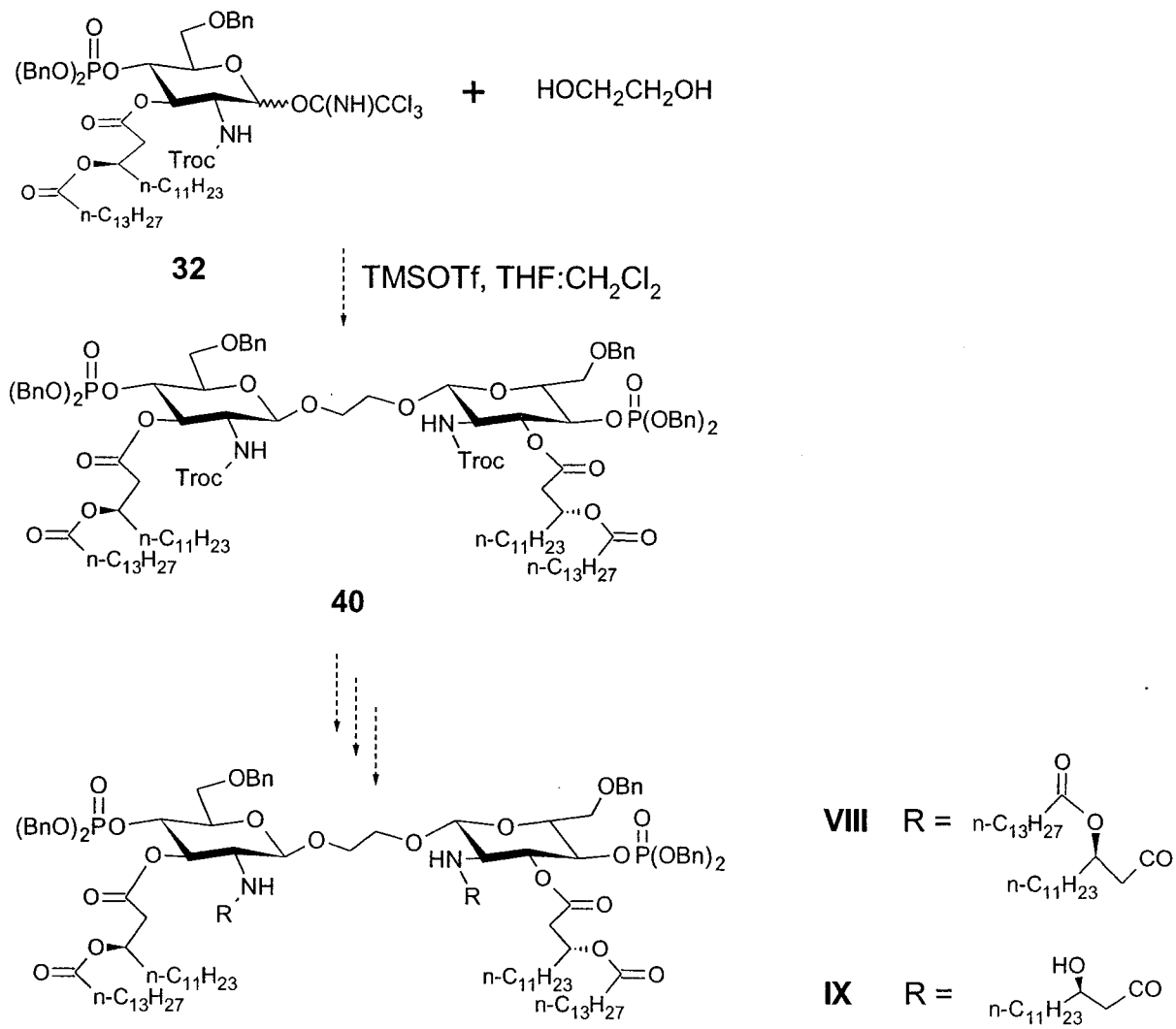

Scheme 27. Revised synthetic route to dimeric monosaccharide Lipid A analogs

2.3.3 Biological Evaluation

Successfully synthesized Lipid A analogs will be evaluated both for their potential to stimulate, as well as to inhibit the TLR4 signalling pathway. Human monocytes and murine macrophages will be exposed to each analog, and the enzyme-linked immunosorbent assay (ELISA) technique will be employed to measure the cytokine responses generated. Specific cytokines to be measured include TNF-α, IL-6, and IL-8. These results will allow for an evaluation as to the potential of these novel frameworks as being synthetic mimics of the natural Lipid A structure.

3 CONCLUSION

Lipopolysaccharide (LPS) has been discovered as the immunostimulatory pattern of Gram-negative bacteria. The active component of LPS is the glycolipid portion known as Lipid A, the likes of which has been shown to stimulate the TLR4 signalling pathway. Given the broad downstream implications of TLR4 signalling, the receptor has been the target of significant investigation for its potential therapeutic uses. A large amount of this investigation has centered on the delineation of the precise molecular events that occur upon TLR4 activation by LPS/Lipid A. With an ever increasing understanding of these events, a great deal of effort has thereby gone into the creation of synthetic analogs of the Lipid A structure. The ultimate goal of these synthetic analogs is the harnessing of the beneficial immunostimulatory properties from the undesired, and potentially fatal toxic effects. These analogs provide an increasing knowledge in the form of structure-activity relationships, such that the potential therapeutic targeting of the TLR4 signalling pathway is becoming a more realistic possibility. Two novel synthetic frameworks designed to mimic the structure of natural Lipid A have thus been synthesized for their evaluation as potential ligands of TLR4.

A dimeric monosaccharide framework has been synthesized, in which two identical sugar units are linked through an ethylene glycol spacer. This framework is thought to offer advantages in terms of both chemical stability and ease of synthesis. The use of the N-Troc protection paradigm in imidate donor **9** yielded the desired β-glycosidic linkages in **11**. Deprotection and installation of the desired acylation pattern at the N position proceeded as proposed. However, deprotection of the 3-*O*-Fmoc protecting group ultimately resulted in the undesired migration of the chemically labile 4-dibenzylphosphotriester moiety. Incorporation of acylation at the 3-*O* position was thereby abandoned, and focus shifted to varying the acylation pattern at the N position. Attempts to incorporate both asymmetry, and an increase in the degree of N-acylation were both generally unsuccessful. Consequently, a revised synthetic approach for the synthesis of dimeric monosaccharide Lipid A analogs with both *N*- and *O*-acylation has thus been undertaken.

A monosaccharide framework has also been synthesized, in which a diethanolamine (DEA) based acyclic scaffold is intended to mimic the second sugar common to the natural Lipid A

disaccharide structure. One advantage this framework is thought to offer over previously reported monosaccharide analogs is that it allows for further functionalization, and thus the potential for further SAR data. DEA was successfully converted to lipid amide **33**, which upon glycosylation with imidate donor **32** afforded the desired monosaccharide framework. The use of the N-Troc protecting paradigm in **32** again afforded the desired β-glycosidic linkage. The desired acylation pattern has been installed at the N position, and one finalized analog of this framework already obtained. Future work will include the synthesis of other analogs and their biological evaluation.

4 EXPERIMENTAL

4.1 General Methods

All air and moisture sensitive reactions were performed under nitrogen atmosphere. All commercial reagents were used as supplied. Pyridine was distilled over potassium hydroxide, dichloromethane was distilled over calcium hydride, and methanol was distilled from magnesium turnings and a catalytic amount of iodine. Anhydrous *N,N*-dimethylformamide (DMF) was purchased from Aldrich. ACS grade solvents were purchased from Fisher and used for chromatography without distillation. TLC was performed on Silica Gel 60Å F_{254} (thickness 250 μm) purchased from Silicycle Inc., Canada, with detection by fluorescence (254 nm) and by dipping into 15% H_2SO_4 solution and/or Mostaine reagent [ammonium molybdate ($(NH_4)_6Mo_7O_{24}\cdot 4H_2O$, 20 g) and cerium (IV) sulfate ($Ce(SO_4)_2$, 0.4 g) in 10% H_2SO_4 solution (400 ml)] followed by charring at ~120 °C. Flash column chromatography was performed on Silica Gel 60 (40-63 μm) also purchased from Silicycle Inc., Canada. ^1H and ^{13}C NMR spectra were recorded on a Varian Unity Inova 500 MHz spectrometer. Tetramethylsilane (TMS, δ 0.00 ppm) or solvent peaks were used as internal standards for ^1H and ^{13}C NMR spectra. The chemical shifts were given in ppm and coupling constants in Hz indicated to a resolution of ± 0.5 Hz. Multiplicity of proton signals is indicated as follows: s (singlet), d (doublet), dd (double doublet), t (triplet), q (quartet), m (multiplet), and br (broad). For spectroscopic assignments, primary acyl chains are designated with L, secondary acyl chains are designated L', and tertiary acyl chains are denoted L". For those compounds which exist as a mixture of two rotational isomers, the designation of A or B will be used to distinguish between the two where possible. Optical rotations were measured with a Perkin Elmer 343 Polarimeter at 22 °C. High resolution electrospray (HR-ESI) mass spectra were measured on the Applied Biosystems Mariner Biospectrometry

Workstation at the University of Alberta, Canada. Elemental analyses were carried out on a CEC (SCP) 240-XA Analyzer instrument by Lakehead University Instrumentation Laboratory (LUIL).

4.2 Synthetic Procedures and Structure Characteristics

3-(R)-(2,2,2-trichloroethoxycarbonyloxy)-penta-1-decene **(2)**:

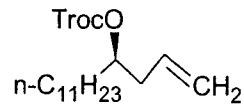

To a solution of 3-(R)-hydroxypenta-1-decene [75] (3.78 g, 16.70 mmol) in dry pyridine (25 mL) cooled to 0°C (ice water bath), Troc-Cl (3.70 mL, 25.1 mmol) was added. The mixture was stirred at the reduced temperature for 2 h before being quenched via the addition of water (20 mL). The resulting mixture was diluted with EtOAc (100 mL) and washed successively with a cold HCl solution (6 M, 30 mL), cold water (50 mL), and a saturated sodium bicarbonate solution (50 mL). The organic phase was dried over Na_2SO_4, concentrated, and purified by flash column chromatography to give **2** (6.18 g, 93%) as a colorless syrup. R_f 0.23 (hexane/EtOAc, 100:1.5); $[\alpha]_D^{22}$ + 14.5 (*c* 1.0, $CHCl_3$); ^1H NMR (500 MHz, $CDCl_3$): δ 0.88 (t, 3H, *J* 7.0 Hz, CH_3, lipid), 1.21-1.36 (br m, 20H, 10 x CH_2, lipid), 1.60-1.67 (m, 2H, H-4_L), 2.38-2.41 (m, 2H, $OC\underline{H}_2CH=CH_2$), 4.75-4.85 (m, 3H, H-3_L, $OCH_2CH=C\underline{H}_2$), 5.08-5.14 (m, 2H, Troc-Ha, Troc-Hb), 5.72-5.81 (m, 1H, $OCH_2C\underline{H}=CH_2$); ^{13}C NMR (125 MHz, $CDCl_3$): δ 14.37 ($\underline{C}H_3$, lipid), 22.93 ($\underline{C}H_2$, lipid), 25.40 ($\underline{C}H_2$, lipid), 29.58 ($\underline{C}H_2$, lipid), 29.71 ($\underline{C}H_2$, lipid), 29.77 ($\underline{C}H_2$, lipid), 29.86 ($\underline{C}H_2$, lipid), 32.15 ($\underline{C}H_2$, lipid), 33.78 ($\underline{C}H_2$, lipid), 38.79 ($\underline{C}H_2$, lipid), 76.80 (Troc-$\underline{C}H_2$), 79.75 ($O\underline{C}H_2CH=CH_2$), 94.69 (Troc-CCl_3), 118.58 ($OCH_2CH=\underline{C}H_2$), 133.19 ($OCH_2\underline{C}H=CH_2$), 154.12 (C=O); Anal. Calcd for $C_{18}H_{31}Cl_3O_3$: C, 53.81; H, 7.78. Found: C, 53.79; H, 7.39.

3-(R)-(2,2,2-trichloroethoxycarbonyloxy)-tetradecanoic acid **(3)**:

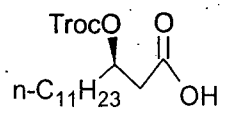

To a mixture of **2** (4.56 g, 11.34 mmol) and Aliquat 336 (0.10 mL) in hexanes (50 mL), EtOAc (50 mL), and acetic acid (10 mL) cooled to 0 °C (ice water bath), an aqueous $KMnO_4$ solution (6.35 g, 39.71 mmol in 100 mL) was added. The reaction was stirred vigorously at the reduced temperature for 2 h before the successive addition of sodium sulphite (12.6 g, 99.97 mmol), and concentrated HCl (15 mL). The organic phase was separated, and the aqueous phase extracted with EtOAc (3 x 150 mL). The combined organic phase was washed with a saturated sodium chloride solution (60 mL), dried with Na_2SO_4 and concentrated. Flash column chromatography (hexane/EtOAc, 5:1) on the residue yielded **3** (4.21 g, 88%) as a colorless syrup. R_f 0.20 (hexane/EtOAc, 5:1); $[\alpha]_D^{22}$ 0.0 (*c* 1.0, $CHCl_3$); ^1H NMR (500 MHz, $CDCl_3$): δ 0.88 (t, 3H, *J* 7.0 Hz, CH_3, lipid), 1.17-1.38 (br m, 18 H, 9 x CH_2, lipid), 1.63-1.74 (m, 2H, H-4_L) 2.65 (dd, 1H, *J* 16.5, 5.0 Hz, H-2_{La}), 2.76 (dd, 1H, *J* 16.5, 8.0 Hz, H-2_{Lb}), 4.76-4.83 (m, 2H, Troc-Ha, Troc-Hb), 5.13-5.21 (m, 1H, H-3_L); ^{13}C NMR (125 MHz, $CDCl_3$): δ 14.36 ($\underline{C}H_3$, lipid), 22.93 ($\underline{C}H_2$, lipid), 25.14 ($\underline{C}H_2$, lipid), 29.48 ($\underline{C}H_2$, lipid), 29.57 ($\underline{C}H_2$, lipid), 29.66 ($\underline{C}H_2$, lipid), 29.73 ($\underline{C}H_2$, lipid), 29.84 ($\underline{C}H_2$, lipid), 32.14 ($\underline{C}H_2$, lipid), 34.16 ($\underline{C}H_2$, lipid), 38.91 ($\underline{C}H_2$, lipid), 75.92 (C-3_L), 76.91 (Troc-$\underline{C}H_2$), 94.77 (Troc-$\underline{C}Cl_3$), 153.79 (C=O), 176.50 (C=O); Anal. Calcd for $C_{17}H_{29}Cl_3O_5$: C, 48.64; H, 6.96 Found: C, 48.98; H, 6.67.

Allyl 4,6-O-benzylidene-2-deoxy-2-(2,2,2-trichloroethoxycarbonylamino)-α-D-glucopyranoside **(4)**:

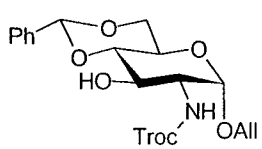

According to literature procedures [19, 73], glucosamine hydrochloride (37.00 g, 171.60 mmol) was first reacted with 2,2,2-trichloroethyl chloroformate (Troc-Cl, 35.50 mL, 257.40 mmol) and sodium bicarbonate (37.50 g, 446.20 mmol) in water (500 mL). The white solid formed was filtered out of the reaction mixture and recrystallized from refluxing ethanol. The resulting white solid (25.67 g) was then added to a suspension of $HCl_{(g)}$ in allyl alcohol (3.5 g in 120 mL) and stirred at 100 °C for 40 min. The resulting residue (≈ 40 g) after concentration of the reaction mixture *in vacuo* was then mixed with benzaldehyde dimethylacetal (23 mL, 153.98 mmol) and *p*-toluenesulfonic acid monohydrate (1.95 g, 10.27 mmol) in acetonitrile (180 mL). After stirring at room temperature for 4 h, the reaction was quenched via the addition of triethylamine (30 mL) and concentrated. Purification of the residue via repeated flash chromatography (hexane/EtOAc, 3:1) yielded **4** (26.12 g, 31% over three steps).

Allyl 4,6-O-benzylidene-2-deoxy-3-O-(9-fluorenylmethoxycarbonyl)-2-(2,2,2-trichloroethoxycarbonylamino)-α-D-glucopyranoside **(5)**:

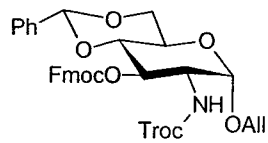

To a cooled solution (ice water bath) of **4** (8.05g, 16.68 mmol) and DMAP (204 mg, 1.67 mmol) in pyridine (35 mL), 9-fluorenylmethoxychloroformate (6.50 g, 25.00 mmol) was added. After stirring at room temperature for 4 h, the reaction was quenched with MeOH. Pyridine was removed *in vacuo* via co-distillation with toluene (3 x 15 mL). The residue was dissolved in EtOAc (800 mL), and washed with cold water (300 mL). The organic layer was dried over Na_2SO_4, and concentrated under vacuum. The residue was subjected to flash column chromatography (hexane/EtOAc, 3:1) to give pure **5** (10.46 g, 89%) as a white solid. R_f 0.31 (hexane/EtOAc, 3.5:1); $[\alpha]_D^{22}$ + 44.7 (*c* 1.0, $CHCl_3$); ^1H NMR (500 MHz, $CDCl_3$): δ 3.79-3.85 (m, 2H, H-6a, H-6b), 3.95-4.04 (m, 2H,

H-4, H-5), 4.17-4.25 (m, 3H, H-2, Fmoc-C<u>H</u>, OCH<u>H</u>CH=CH_2), 4.30-4.35 (m, 3H, Fmoc-C<u>H_2</u>, OC<u>H</u>HCH=CH_2), 4.53 (d, 1H, *J* 12.0 Hz, Troc-Ha), 4.64 (d, 1H, *J* 12.0 Hz, Troc-Hb), 4.96 (d, 1H, *J* 3.5 Hz, H-1), 5.21-5.26 (m, 2H, NH, H-3), 5.31 (d, 1H, *J* 17.0 Hz, OCH_2CH=CH<u>H</u>), 5.43 (d, 1H, *J* 10.0 Hz, OCH_2CH=C<u>H</u>H), 5.57 (s, 1H, Ph-C<u>H</u>), 5.85-5.93 (m, 1H,OCH_2C<u>H</u>=CH_2), 7.18-7.75 (m, 13H, Ar-<u>H</u>); ^{13}C NMR (125 MHz, $CDCl_3$): δ 46.65 (Fmoc-<u>C</u>H), 54.90 (C-2), 63.24 (C-5), 68.96 (C-6), 69.02 (O<u>C</u>H_2CH=CH_2), 70.69 (Fmoc-<u>C</u>H_2), 74.42 (C-3), 74.77 (Troc-<u>C</u>H_2), 79.13 (C-4), 95.45 (Troc-<u>C</u>Cl_3), 97.27 (C-1), 101.86 (Ph-<u>C</u>H), 118.93 (OCH_2CH=<u>C</u>H_2), 120.25 (<u>C</u>H-Ar), 125.37 (<u>C</u>H-Ar), 125.44 (<u>C</u>H-Ar), 126.41 (<u>C</u>H-Ar), 127.42 (<u>C</u>H-Ar), 128.10 (<u>C</u>H-Ar), 128.45 (<u>C</u>H-Ar), 129.35 (<u>C</u>H-Ar), 133.16 (OCH_2<u>C</u>H=CH_2), 137.03 (<u>C</u>-Ar), 141.39 (<u>C</u>-Ar), 141.42 (<u>C</u>-Ar), 143.32 (<u>C</u>-Ar), 143.42 (<u>C</u>-Ar), 154.49 (C=O), 155.37 (C=O); Anal. Calcd for $C_{34}H_{32}Cl_3NO_9$: C, 57.93; H, 4.58; N, 1.99. Found: C, 57.81; H, 4.52; N, 1.73.

Allyl 6-O-benzyl-2-deoxy-3-O-(9-fluorenylmethoxycarbonyl)-2-(2,2,2-trichloroethoxycarbonylamino)-α-D-glucopyranoside **(6)**:

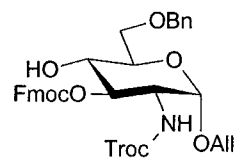

A solution of **5** (7.43 g, 10.54 mmol) in dry THF (50 mL) and molecular sieves (4 Å, 5 g) was stirred at room temperature under nitrogen for 20 min. Sodium cyanoborohydride (6.65 g, 105.40 mmol) was added and the mixture was cooled to 0°C, followed by the drop wise addition of dry ethereal-$HCl_{(g)}$ until no gas was evolved. The mixture was poured into a saturated sodium bicarbonate solution (100 mL) and the solids were filtered out before the removal of THF *in vacuo*. The resulting solution was extracted with EtOAc (3 x 200 mL), and the combined organic phase was washed with a saturated sodium chloride solution (150 mL), dried over Na_2SO_4, and concentrated *in*

vacuo. The resulting residue was purified by flash chromatography (hexane/EtOAc, 3.5:1 → 2:1) to give **6** as a white solid (6.34 g, 85 %). R_f 0.34 (hexane/EtOAc, 2.5:1), $[\alpha]_D^{22}$ + 55.4 (*c* 1.0, $CHCl_3$); ^1H NMR (500 MHz, $CDCl_3$): δ 2.76 (br s, 1H, OH), 3.33 (dd, 1H, *J* 10.0, 4.0 Hz, H-6b), 3.80-3.87 (m, 2H, H-5, H-6a), 3.92 (dd, 1H, *J* 10.0, 10.0 Hz, H-4), 4.01 (dd, 1H, *J* 12.8, 6.5 Hz, Fmoc-CHH), 4.09 (ddd, 1H, *J* 10.0, 10.0, 3.5 Hz, H-2), 4.18-4.26 (m, 2H, Fmoc-CH, Fmoc-CHH), 4.35-4.42 (m, 2H, $OCH_2CH=CH_2$), 4.56-4.66 (m, 4H, Troc-Ha, Troc-Hb, Ph-CH_2), 4.93 (d, 1H, *J* 3.0 Hz, H-1), 5.02 (dd, 1H, *J* 10.0, 10.0 Hz, H-3), 5.21-5.36 (m, 3H, NH, $OCH_2CH=CH_2$), 5.86-5.92 (m, 1H, $OCH_2CH=CH_2$), 7.30-7.77 (m, 13H, Ar-H); ^{13}C NMR (125 MHz, $CDCl_3$): δ 46.47 (Fmoc-CH), 53.80 (C-2), 68.48 (Fmoc-CH_2), 69.43 (C-6), 69.89 (C-5), 70.24 (C-4), 70.43 ($OCH_2CH=CH_2$), 73.64 (Ph-CH_2), 74.46 (Troc-CH_2), 77.83 (C-3), 95.24 (Troc-CCl_3), 96.34 (C-1), 118.34 ($OCH_2CH=CH_2$), 120.01 (CH-Ar), 125.18 (CH-Ar), 127.19 (CH-Ar), 127.64 (CH-Ar), 127.84 (CH-Ar), 127.87 (CH-Ar), 128.44 (CH-Ar), 133.09 ($OCH_2CH=CH_2$), 137.58 (C-Ar), 141.19 (C-Ar), 143.05 (C-Ar), 143.17 (C-Ar), 154.20 (C=O), 155.74 (C=O); Anal. Calcd for $C_{34}H_{34}Cl_3NO_9$: C, 57.76; H, 4.85; N, 1.98. Found: C, 57.52; H, 4.73; N, 2.01.

Allyl 6-O-benzyl-2-deoxy-4-O-(di-O-benzylphosphono)-3-O-(9-fluorenylmethoxycarbonyl)-2-(2,2,2-trichloroethoxycarbonylamino)-α-D-glucopyranoside **(7)**:

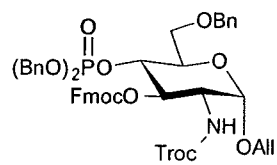

To **6** (6.34 g, 8.96 mmol) in dry dichloromethane (50 mL), 5-phenyltetrazole (2.30 g, 15.69 mmol) and dibenzyl N,N-diisopropylphosphoramidite (5.2 mL, 15.69 mmol) were added and stirred at room temperature for 1 h. The mixture was then cooled to -20 °C, *m*-chloroperbenzoic acid (4.03 g, 77%, 17.92 mmol) was added and the mixture was stirred at the reduced temperature for

1h. The reaction was poured into a saturated sodium bicarbonate solution (100 mL) and extracted with dichloromethane (3 x 100 mL). The combined organic phase was washed with a saturated sodium chloride solution (100 mL), dried over Na_2SO_4, and concentrated *in vacuo*. Repeated flash column chromatography on the residue (hexane/EtOAc, 2:1) afforded **7** (8.53 g, 98 % over two steps) as a white solid. R_f 0.24 (hexane/EtOAc, 2.5:1); $[\alpha]_D^{22}$ + 59.4 (*c* 1.0, $CHCl_3$); ^1H NMR (500 MHz, $CDCl_3$): δ 3.71-3.77 (m, 2H, H-6a, H-6b), 3.94-3.97 (m, 2H, $OC\underline{H}_2CH=CH_2$), 4.01-4.08 (m, 2H, H-5, Fmoc-CH$\underline{H}$), 4.14-4.23 (m, 2H, H-2, Fmoc-C$\underline{H}$), 4.28 (dd, 1H, *J* 9.8, 7.5 Hz, Fmoc-C$\underline{H}$H), 4.44-4.60 (m, 4H, Troc-Ha, Troc-Hb, Ph-$C\underline{H}_2$), 4.71 (ddd, 1H, *J* 9.5, 9.5, 9.0 Hz, H-4), 4.88-4.98 (m, 5H, H-1, $(PhC\underline{H}_2O)_2P$), 5.22-5.43 (m, 4H, NH, H-3, $OCH_2CH=C\underline{H}_2$), 5.85-5.93 (m, 1H, $OCH_2C\underline{H}=CH_2$), 7.19-7.77 (m, 13H, Ar-$\underline{H}$); ^{13}C NMR (125 MHz, $CDCl_3$): δ 46.48 (Fmoc-$\underline{C}$H), 54.24 (C-2), 68.17 (C-6), 68.88 (Fmoc-$\underline{C}H_2$), 69.70 (d, *J* 5.5 Hz, $(Ph\underline{C}H_2O)P$), 69.78 (d, *J* 5.5 Hz, $(Ph\underline{C}H_2O)P$), 70.10 (C-5), 70.66 ($O\underline{C}H_2CH=CH_2$), 73.54 (C-4), 73.60 ($Ph\underline{C}H_2$), 74.72 (Troc-$\underline{C}H_2$), 76.13 (C-3), 95.36 (Troc-$\underline{C}Cl_3$), 96.28 (C-1), 118.78 ($OCH_2CH=\underline{C}H_2$), 120.13 (CH-Ar), 125.35 (CH-Ar), 125.43 (CH-Ar), 127.22 (CH-Ar), 127.29 (CH-Ar), 127.67 (CH-Ar), 127.69 (CH-Ar), 127.93 (CH-Ar), 128.00 (CH-Ar), 128.39 (CH-Ar), 128.45 (CH-Ar), 128.54 (CH-Ar), 128.59 (CH-Ar), 133.04 ($OCH_2\underline{C}H=CH_2$), 135.62 (dd, *J* 7.25, 7.25 Hz, C-Ar), 137.99 (C-Ar), 141.22 (C-Ar), 141.26 (C-Ar), 143.20 (C-Ar), 143.23 (C-Ar), 154.25 (C=O), 155.34 (C=O); Anal. Calcd for $C_{48}H_{47}Cl_3NO_{12}P$: C, 59.61; H, 4.90; N, 1.45. Found: C, 59.86; H, 5.07; N, 1.56.

6-O-benzyl2-deoxy-4-O-(di-O-benzylphosphono)-3-O-(9-fluorenylmethoxycarbonyl)-2-(2,2,2-trichloroethoxycarbonylamino)-α-D-glucopyranoside **(8)**:

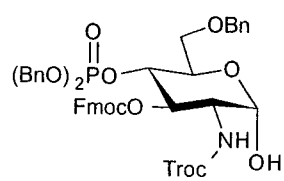

Into a suspension of [bis(methyldiphenylphosphine)](1,5-cyclooctadiene) iridium(I) hexafluorophosphate (338 mg, 0.40 mmol), in dry THF (10 mL) hydrogen gas is bubbled until a yellowish solution is formed (about 5 min). This solution was then added to a solution of **7** (8.25 g, 8.53 mmol) in dry THF (40 mL), and the mixture is stirred at room temperature for 2h. Water (3 mL) and freshly recrystallized N-bromosuccinimide (2.36 g, 12.80 mmol) were added and the reaction was stirred for a further 1h. The residue obtained after solvent removal was dissolved in EtOAc (200 mL) and washed with a saturated sodium bicarbonate solution (2 x 50 mL). The combined organic phase was dried over Na_2SO_4, concentrated, and purified by repeated flash column chromatography (hexane/EtOAc, 3:2) to afford white solid **8** (6.45 g, 79%) as purely the α isomer. R_f 0.22 (hexane/EtOAc, 3:2); $[\alpha]_D^{22}$ + 36.3 (*c* 1.0, $CHCl_3$); ^1H NMR (500 MHz, $CDCl_3$): δ 3.62-3.77 (m, 3H, H-6a, H-6b, OH), 3.95 (dd, 1H, *J* 10.3, 8.5 Hz, Fmoc-CHH), 4.04-4.12 (m, 2H, H-2, Fmoc-CH), 4.21 (dd, 1H, *J* 9.0, 6.5 Hz, H-5), 4.28 (dd, 1H, *J* 10.3, 7.5 Hz, Fmoc-CHH), 4.43-4.60 (m, 5H, Troc-Ha, Troc-Hb, H-4, Ph-CH_2), 4.86-4.98 (m, 4H, $(PhCH_2O)_2P$), 5.23-5.28 (m, 2H, H-1, H-3), 5.42 (d, 1H, *J* 9.5 Hz, NH), 7.18-7.77 (m, 13H, Ar-H); ^{13}C NMR (125 MHz, $CDCl_3$); δ 46.51 (Fmoc-CH), 54.54 (C-2), 68.74 (C-6), 69.50 (C-5), 69.62 (d, *J* 5.5 Hz, $(PhCH_2O)P$), 69.85 (d, *J* 5.5 Hz, $(PhCH_2O)P$), 70.70 (Fmoc-CH_2), 73.69 (Ph-CH_2), 74.06 (C-4), 74.76 (Troc-CH_2), 75.89 (C-3), 91.66 (C-1), 95.39 (Troc-CCl_3), 120.17 (CH-Ar), 125.50 (CH-Ar), 125.64 (CH-Ar), 127.37 (CH-Ar), 127.44 (CH-Ar), 127.85 (CH-Ar), 128.08 (CH-Ar), 128.12 (CH-Ar), 128.62 (CH-Ar), 128.70 (CH-Ar), 128.76 (CH-Ar), 135.67 (dd, *J* 7.25, 7.25 Hz, C-Ar), 137.61 (C-Ar), 141.37 (C-Ar), 141.40 (C-Ar), 143.32 (C-Ar), 143.38 (C-Ar), 154.33 (C=O), 155.33 (C=O); Anal. Calcd for $C_{45}H_{43}Cl_3NO_{12}P$: C, 58.29; H, 4.67; N, 1.51. Found: C, 58.67; H, 4.92; N, 1.42.

6-O-benzyl-2-deoxy-4-O-(di-O-benzylphosphono)-3-O-(9-fluorenlymethoxycarbonyl)-2-(2,2,2-trichloroethoxycarbonylamino)-α-D-glucopyranosyl trichloroacetimidate **(9)**:

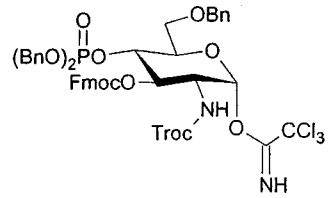

To a solution of **9** (5.95 g, 6.42 mmol) in dry dichloromethane (10 mL), trichloroacetonitrile (3.22 mL, 32.1 mmol) and sodium hydride (23 mg, 0.22 mmol) were added successively. The mixture was stirred at room temperature for 1 h upon which the solvent was removed *in vacuo*, followed by co-distillation with EtOAc (2 x 20 mL). The residue was purified by flash column chromatography (hexane/EtOAc, 2.5:1 with 0.5% Et_3N) to afford **9** (5.57 g, 81%) as a white fluffy solid. R_f 0.29 (hexane/EtOAc, 3:1); $[\alpha]_D^{22}$ + 41.4 (*c* 1.0, $CHCl_3$); ^1H NMR (500 MHz, $CDCl_3$): δ 3.71-3.77 (m, 2H, H-6a, H-6b), 3.99-4.11 (m, 3H, Fmoc-CHH, Fmoc-CH, H-2), 4.31-4.37 (m, 2H, Fmoc-CHH, H-5), 4.46-4.66 (m, 5H, Troc-Ha, Troc-Hb, H-4, Ph-CH_2), 4.86-5.01 (m, 4H, $(PhCH_2O)_2P$), 5.29-5.33 (m, 2H, NH, H-3), 6.43 (d, 1H, *J* 4.0 Hz, H-1), 7.18-7.74 (m, 13H, Ar-H), 8.75 (s, 1H, NH); ^{13}C NMR (125 MHz, $CDCl_3$); δ 46.26 (Fmoc-CH), 54.23 (C-2), 67.60 (C-6), 69.80 (d, *J* 5.5 Hx, $(PhCH_2O)P$), 69.99 (d, *J* 5.5 Hz, $(PhCH_2O)P$), 70.93 (Fmoc-CH_2), 72.63 (C-5), 72.69 (C-4), 73.69 (Ph-CH_2), 74.84 (Troc-CH_2), 75.32 (C-3), 90.76 (CCl_3 imidate), 94.82 (C-1), 95.3 (Troc-CCl_3), 120.26 (CH-Ar), 125.40 (CH-Ar), 125.53 (CH-Ar), 127.44 (CH-Ar), 127.85 (CH-Ar), 127.91 (CH-Ar), 128.19 (CH-Ar), 128.56 (CH-Ar), 128.69 (CH-Ar), 128.77 (CH-Ar), 135.71 (dd, *J* 7.25, 7.25 Hz, C-Ar), 138.03 (C-Ar), 141.44 (C-Ar), 143.20 (C-Ar), 143.22 (C-Ar), 154.25 (C=O), 155.67 (C=O), 160.61 (C=NH); Anal. Calcd for $C_{47}H_{43}Cl_6N_2O_{12}P$: C, 52.68; H, 4.04; N, 2.61. Found: C, 52.79; H, 4.21; N, 2.46.

1-[6-O-benzyl-2-deoxy-4-(di-O-benzylphosphono)-3-O-(9-fluorenylmethoxycarbonyl)-2-(2,2,2-trichloroethoxycarbonylamino)-β-D-glucopyranosyl]-2-hydroxyethane **(10)**:

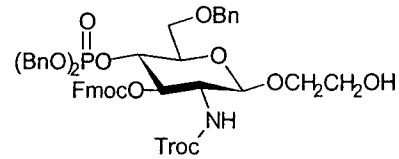

To a mixture of **14** (165 mg, 0.15 mmol) and glacial acetic acid (0.86 mL, 15.20 mmol) in dry THF (3 mL) cooled to 0 °C (ice water bath), a tetrabutylammonium fluoride solution (1 M in THF, 0.19 mL, 0.19 mmol) was added. The mixture was stirred at 0 °C for 4 h, and at room temperature for a further 4 h, upon which the solvent was removed *in vacuo*. The residue was dissolved in dichloromethane (50 mL) and washed with a saturated sodium bicarbonate solution (25 mL). The organic phase was dried over Na_2SO_4, concentrated, and purified via flash column chromatography (hexane/EtOAc, 1:1.25) to afford **10** (108 mg, 73%) as a white solid. R_f 0.26 (hexane/EtOAc, 1:1.25); $[\alpha]_D^{22}$ + 15.2 (*c* 1.0, $CHCl_3$); ^{1}H NMR (500 MHz, $CDCl_3$): δ 3.11 (br s, 1H, OH), 3.65-3.86 (m, 8H, H-6a, H-6b, H-2, H-5, OCH_2CH_2OH, OCH_2CH_2OH), 4.01 (dd, 1H, *J* 9.5, 7.5 Hz, Fmoc-CHH), 4.11 (dd, 1H, *J* 7.5, 7.5 Hz, Fmoc-CH), 4.33 (dd, 1H, *J* 7.5, 7.5 Hz, Fmoc-CHH), 4.47-4.65 (m, 5H, Troc-Ha, Troc-Hb, H-4, Ph-CH_2), 4.76 (d, 1H, *J* 8.0 Hz, H-1), 4.91-4.95 (m, 4H, $(PhCH_2O)_2P$), 5.29 (dd, 1H, *J* 10.0, 10.0 Hz, H-3), 5.61 (d, 1H, *J* 8.0 Hz, NH), 7.15-7.74 (m, 23H, Ar-H); ^{13}C NMR (125 MHz, $CDCl_3$); δ 46.58 (Fmoc-CH), 56.83 (C-2), 68.66 (2C, OCH_2CH_2OH, OCH_2CH_2OH), 69.81 (d, *J* 5.5 Hz, $(PhCH_2O)P$), 69.92 (d, *J* 5.5 Hz, $(PhCH_2O)P$), 70.75 (Fmoc-CH_2), 73.58 (C-6), 73.75 (Troc-CH_2), 74.05 (2C, C-4, C-5), 74.67 (Ph-CH_2), 76.75 (C-3), 95.53 (Troc-CCl_3), 101.46 (C-1), 120.24 (CH-Ar), 125.41 (CH-Ar), 125.53 (CH-Ar), 127.39 (CH-Ar), 127.45 (CH-Ar), 127.87 (CH-Ar), 128.00 (CH-Ar), 128.12 (CH-Ar), 128.20 (CH-Ar), 128.64 (CH-Ar), 128.74 (CH-Ar), 128.81 (CH-Ar), 128.85 (CH-Ar), 135 .64 (dd, *J* 7.25, 7.25 Hz, C-Ar), 137.84 (C-Ar), 141.44 (C-Ar), 143.35 (C-Ar), 154.40 (C=O), 155.25 (C=O); Anal. Calcd for

$C_{47}H_{47}Cl_3NO_{13}P$: C, 58.12; H, 4.88; N, 1.44. Found: C, 58.27; H, 4.97; N, 1.52; HRESI-MS (*m/z*) Calcd for $C_{47}H_{47}Cl_3NO_{13}PNa$ $[M + Na]^+$: 992.1751, found: 992.1743.

1,2-di-[6-O-benzyl-2-deoxy-4-O-(di-O-benzylphosphono)-3-O-(9-fluorenylmethoxycarbonyl)-2-(2,2,2-trichloroethoxycarbonylamino)-β-D-glucopyranosyl]-ethane **(11)**:

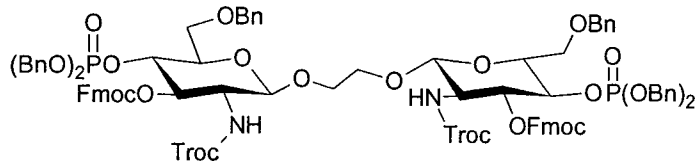

Method 1: A solution of **10** (121 mg, 0.13 mmol) and **9** (180 mg, 0.17 mmol) in dry dichloromethane (3 mL) and molecular sieves (4 Å, 2.0 g) was stirred under nitrogen at room temperature for 20 min. A solution of TMSOTf (0.01 M in dichloromethane, 0.25 mL) was added drop wise. The mixture was stirred at room temperature for 45 min before a saturated sodium bicarbonate solution (10 mL) is added to quench the reaction. Solids were filtered out before the mixture was extracted with dichloromethane (3 x 25 mL). The combined organic phase was dried over Na_2SO_4, concentrated, and purified via flash column chromatography (hexane/EtOAc, 1.25:1) to yield **11** (195 mg, 83%) as a white fluffy solid.

Method 2: In a similar way as described above, a solution of **9** (400 mg, 0.37 mmol), ethylene glycol (11 mg, 0.18 mmol), and molecular sieves (4 Å, 2.0 g) in dry dichloromethane (1.5 mL) and dry THF (1.5 mL) was stirred under nitrogen at room temperature for 20 min. A solution of TMSOTf (0.01 M in dry dichloromethane, 70 µL) was added drop wise, and the mixture stirred at room temperature for 20 min. The reaction was quenched by the addition of a saturated sodium bicarbonate solution (10 mL), before being filtered and extracted with dichloromethane (3 x 25 mL). The combined organic phase was dried over Na_2SO_4, concentrated, and purified via flash column chromatography (hexane/EtOAc, 3:2) to yield **11** (248 mg, 74%) as a fluffy

white solid. R_f 0.35 (hexane/EtOAc, 1:1), $[\alpha]_D^{22}$ + 5.5 (*c* 1.0, $CHCl_3$); ^1H NMR (500 MHz, $CDCl_3$): δ 3.61-3.69 (m, 3H, H-6a, H-6b, H-5), 3.78-3.83 (m, 2H, H-2, (OCHHCHHO)/2), 3.91-3.94 (m, 2H, Fmoc-CHH, (OCHHCHHO)/2), 4.05 (dd, 1H, *J* 7.5, 7.5 Hz, Fmoc-CH), 4.26 (dd, 1H, *J* 7.5, 7.5 Hz, Fmoc-CHH), 4.46-4.75 (m, 6H, Troc-Ha, Troc-Hb, Ph-CH_2, H-4, H-1), 4.88-4.96 (m, 4H, $(PhCH_2O)_2P$), 5.13-5.16 (dd, 1H, *J* 10.0, 10.0 Hz, H-3), 5.67 (d, 1H, *J* 7.5 Hz, NH), 7.14-7.72 (m, 23H, Ar-H); ^{13}C NMR (125 MHz, $CDCl_3$); δ 46.53 (Fmoc-CH), 56.73 (C-2), 68.59 (C-6), 69.11 (OCH_2CH_2O)/2), 69.77 (d, *J* 5.5 Hz, $(PhCH_2O)P$), 69.83 (d, *J* 5.5 Hz, $(PhCH_2O)P$), 70.70 (Fmoc-CH_2), 73.63 (Troc-CH_2), 73.93 (C-4), 74.14 (C-5), 74.63 (Ph-CH_2), 77.33 (C-3), 95.74 (Troc-CCl_3), 100.97 (C-1), 120.17 (CH-Ar), 125.49 (CH-Ar), 125.61 (CH-Ar), 127.38 (CH-Ar), 127.43 (CH-Ar), 127.82 (CH-Ar), 127.87 (CH-Ar), 128.08 (CH-Ar), 128.14 (CH-Ar), 128.60 (CH-Ar), 128.70 (CH-Ar), 128.75 (CH-Ar), 135.70 (dd, *J* 7.25, 7.25 Hz, C-Ar), 138.12 (C-Ar), 141.40 (C-Ar), 141.43 (C-Ar), 143.37 (C-Ar), 154.73 (C=O), 155.25 (C=O); Anal. Calcd for $C_{92}H_{88}Cl_6N_2O_{24}P_2$: C, 58.76; H, 4.72; N, 1.49. Found: C, 58.52; H, 4.65; N, 1.52; HRESI-MS (*m/z)* Calcd for $C_{92}H_{88}Cl_6N_2O_{24}P_2Na$ $[M + Na]^+$: 1899.3210, found: 1899.3232.

2-hydroxy-1-tertbutyldimethylsilyloxy-ethane **(13)**:

$HOCH_2CH_2OTBDMS$

A mixture of ethylene glycol (3.82 mL, 68.4 mmol) and imidazole (1.45 g, 21.27 mmol) in dry N,N-dimethylformamide (8 mL) was cooled to 0 °C (ice water bath) and *tert*-butyldimethylsilylchloride (2.57 g, 17.01 mmol) was added. The mixture was stirred at the reduced temperature for 4 h before being quenched via the addition of cold water (200 mL). The mixture was extracted with EtOAc (3 x 200 mL), with the combined organic layers dried over Na_2SO_4 and concentrated. The residue was purified by flash column chromatography (hexane/EtOAc, 15:1) to give **13** (2.1 g, 70%) as a colorless

syrup. R_f 0.25 (hexane/EtOAc, 9:1); $[\alpha]_D^{22}$ 0.0 (*c* 1.0, $CHCl_3$); ^1H NMR (500 MHz, $CDCl_3$): δ 0.21 (s, 6H, $Si(C\underline{H}_3)_2$), 0.82 (s, 9H, $SiC(C\underline{H}_3)_3$), 1.99 (t, 1H, *J* 6.0 Hz, OH), 3.55-3.63 (m, 4H, $HOC\underline{H}_2CH_2OTBDMS$, $HOCH_2C\underline{H}_2OTBDMS$); ^{13}C NMR (125 MHz, $CDCl_3$); δ -5.16 ($Si(\underline{C}H_3)_2$), 18.52 ($Si\underline{C}(CH_3)_3$), 26.08 ($SiC(\underline{C}H_3)_3$), 63.85 ($HO\underline{C}H_2CH_2OTBDMS$), 64.34 ($OCH_2\underline{C}H_2OTBDMS$); Anal. Calcd for $C_8H_{20}O_2Si$: C, 58.64; H, 11.43. Found: C, 58.62; H, 11.40.

1-[6-O-benzyl-2-deoxy-4-O-(di-O-benzylphosphono)-3-O-(9-fluorenylmethoxycarbonyl)-2-(2,2,2-trichloroethoxycarbonylamino)-β-D-glucopyranosyloxy]-2-tertbutldimethylsilyloxyethane **(14)**:

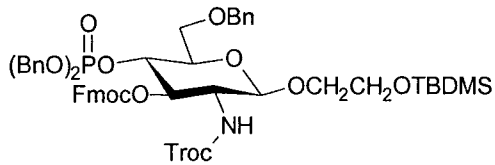

A solution of **9** (240 mg, 0.22 mmol), and **13** (124 mg, 0.70 mmol) in dry dichloromethane (4 mL) and molecular sieves (4 Å, 2.0 g) was stirred under nitrogen for 30 min at room temperature. A solution of TMSOTf (0.01 M in dichloromethane, 0.56 mL) is added drop wise in about 3 min. The mixture is stirred at room temperature for 1 h before a saturated sodium bicarbonate solution (10 mL) is added to quench the reaction. Solids were filtered out before the mixture was extracted with dichloromethane (3 x 25 mL). The combined organic phase was dried over Na_2SO_4, concentrated, and purified via flash column chromatography (hexane/acetone, 3.75:1) to yield **14** (196 mg, 81%) as a colorless syrup. R_f 0.28 (hexane/EtOAc, 2.5:1); $[\alpha]_D^{22}$ + 12.9 (*c* 1.0, $CHCl_3$); ^1H NMR (500 MHz, $CDCl_3$): δ 0.06 (s, 6H, $Si(C\underline{H}_3)_2$), 0.89 (s, 9H, $SiC(C\underline{H}_3)_3$), 3.65-3.83 (m, 7H, H-6a, H-5, H-2, $OC\underline{H}_2CH_2OTBDMS$, $OCH_2C\underline{H}_2OTBDMS$), 3.89 (dd, 1H, J = 10.0, 5.0 Hz, H-6b), 3.97 (dd, 1H, *J* 9.5, 7.5 Hz, Fmoc-CH$\underline{H}$), 4.07 (dd, 1H, *J* 7.5, 7.5 Hz, Fmoc-C$\underline{H}$), 4.28 (dd, 1H, *J* 7.5, 7.5 Hz, Fmoc-C$\underline{H}$H), 4.47-4.60 (m, 5H, Troc-Ha, Troc-Hb, H-4, Ph-$C\underline{H}_2$), 4.76 (d, 1H, *J* 8.0 Hz, H-1), 4.89-4.95 (m, 4H, $(PhC\underline{H}_2O)_2P$), 5.22 (dd, 1H, *J* 10.0, 10.0 Hz, H-3), 5.31 (d, 1H, *J* 7.0 Hz, NH), 7.16-7.71 (m, 23H, Ar-H); ^{13}C

NMR (125 MHz, $CDCl_3$); δ -5.09 (Si($\underline{C}H_3$)), -5.03 (Si($\underline{C}H_3$)), 18.55 (Si$\underline{C}(CH_3)_3$), 26.16 (SiC($\underline{C}H_3)_3$), 46.63 (Fmoc-$\underline{C}$H), 56.80 (C-2), 62.89 ($OCH_2\underline{C}H_2$OTBDMS), 68.74 ($O\underline{C}H_2CH_2$OTBDMS), 69.78 (d, *J* 5.5 Hz, (Ph$\underline{C}H_2$O)P), 69.85 (d, *J* 5.5 Hz, (Ph$\underline{C}H_2$O)P), 70.65 (Fmoc-$\underline{C}H_2$), 71.26 (C-6), 73.74 (Troc-$\underline{C}H_2$), 73.98 (C-5), 74.50 (C-4), 74.70, Ph-$\underline{C}H_2$), 77.19 (C-3), 95.55 (Troc-$\underline{C}Cl_3$), 100.92 (C-1), 120.20 ($\underline{C}$H-Ar), 120.49 ($\underline{C}$H-Ar), 125.58 ($\underline{C}$H-Ar), 127.39 ($\underline{C}$H-Ar), 127.47 ($\underline{C}$H-Ar), 127.83 ($\underline{C}$H-Ar), 127.87 ($\underline{C}$H-Ar), 128.10 ($\underline{C}$H-Ar), 128.14 ($\underline{C}$H-Ar), 128.57 ($\underline{C}$H-Ar), 128.70 ($\underline{C}$H-Ar), 128.75 ($\underline{C}$H-Ar), 135.80 (dd, *J* 7.25, 7.25 Hz, $\underline{C}$-Ar), 138.23 ($\underline{C}$-Ar), 141.40 ($\underline{C}$-Ar), 141.47 ($\underline{C}$-Ar), 143.42 ($\underline{C}$-Ar), 154.27 (C=O), 155.17 (C=O); Anal. Calcd for $C_{53}H_{61}Cl_3NO_{13}PSi$: C, 58.64; H, 5.66; N, 1.29. Found: C, 58.27; H, 5.36; N, 1.28.

1,2-di-[6-O-benzyl-2-deoxy-4-O-(di-O-benzylphosphono)-3-O-(9-fluorenylmethoxycarbonyl)-2-amino-β-D-glucopyranosyl]-ethane **(15)**:

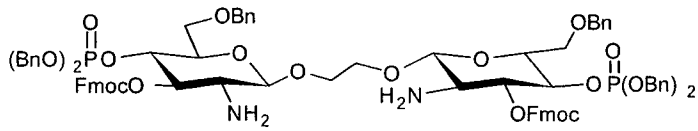

To a solution of **11** (1.2 g, 0.64 mmol) in dry THF (8 mL) and acetic acid (2 mL), zinc powder (1.0 g) was added. The mixture was stirred at room temperature for 30 min and then filtered. The solid was washed with acetic acid (30 mL) and the filtrate concentrated *in vacuo*. The residue was dissolved in dichloromethane (150 mL) and washed with a saturated sodium bicarbonate solution (75 mL). After separating the organic layer, the aqueous phase was extracted with dichloromethane (2 x 75 mL). The combined organic phase was dried with Na_2SO_4 and concentrated to obtain the di-amine **15** (1.1 g) as a white fluffy solid, which was used directly in the subsequent coupling reactions.

1,2-di-[6-O-benzyl-2-deoxy-4-O-(di-O-benzylphosphono)-3-O-(9-fluorenylmethoxycarbonyl)-2-((R)-3-tetradecanoyloxytetradecanamido)-β-D-glucopyranosyl]-ethane **(16)**:

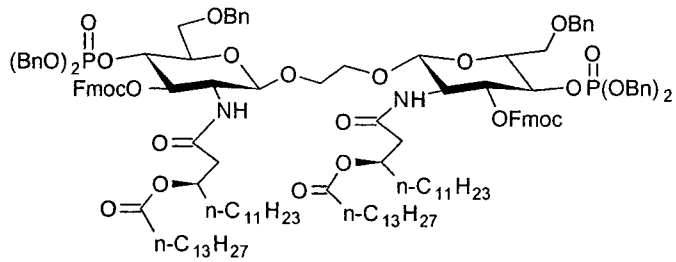

A mixture of the di-amine **15** (1.1 g), dilipid acid **1** [74] (870 mg, 1.91 mmol), and DCC (760 mg, 3.83 mmol) in dry dichloromethane (5 mL) was stirred at room temperature for 20 h. Water (0.10 mL) was added and the reaction mixture was stirred for a further 20 min. The solid was then filtered through a sintered glass funnel with a bed of Na_2SO_4. The filtrate was concentrated and the residue purified by repeated flash column chromatography (hexane/acetone, 3:1) to afford **16** (997 mg, 65 % over two steps) as a colorless syrup. R_f 0.26 (hexane/acetone, 3:1); $[\alpha]_D^{22}$ + 5.9 (*c* 1.0, $CHCl_3$); ^{1}H NMR (500 MHz, $CDCl_3$): δ 0.86-0.89 (m, 6H, 2 x CH_3, lipid), 1.08-1.36 (br m, 38H, 19 x CH_2, lipid), 1.50-1.60 (m, 4H, H-4_L, H-$3_{L'}$), 2.21-2.25 (m, 2H, H-$2_{L'}$), 2.32 (dd, 1H, *J* 14.5, 6.5 Hz, H-2_{La}), 2.44 (dd, 1H, *J* 14.5, 6.5 Hz, H-2_{Lb}), 3.66-3.89 (m, 6H, H-6a, H-6b, H-2, H-5, (OC$\underline{H}_2$C$\underline{H}_2$O)/2), 3.95 (dd, 1H, *J* 10.0, 8.0 Hz, Fmoc-CH$\underline{H}$), 4.10 (dd, 1H, J = 8.0, 8.0 Hz, Fmoc-C$\underline{H}$), 4.28 (dd, 1H, *J* 10.0, 8.0 Hz, Fmoc-C$\underline{H}$H), 4.45-4.62 (m, 3H, Ph-C$\underline{H}_2$, H-4), 4.84-4.97 (m, 5H, H-1, (PhC$\underline{H}_2$O)$_2$P), 5.07 (m, 1H, H-3_L), 5.32 (dd, 1H, *J* 9.5, 9.5 Hz, H-3), 6.60 (d, 1H, *J* 5.0 Hz, NH), 7.13-7.72 (m, 23H, Ar-H); ^{13}C NMR (125 MHz, $CDCl_3$); δ 14.34 ($\underline{C}H_3$, lipid), 22.89 ($\underline{C}H_2$, lipid), 25.16 ($\underline{C}H_2$, lipid), 25.23 ($\underline{C}H_2$, lipid), 25.46 ($\underline{C}H_2$, lipid), 25.81 ($\underline{C}H_2$, lipid), 29.44 ($\underline{C}H_2$, lipid), 29.57 ($\underline{C}H_2$, lipid), 29.66 ($\underline{C}H_2$, lipid), 29.77 ($\underline{C}H_2$, lipid), 29.83 ($\underline{C}H_2$, lipid), 29.87 ($\underline{C}H_2$, lipid), 29.90 ($\underline{C}H_2$, lipid), 29.91 ($\underline{C}H_2$, lipid), 32.12 ($\underline{C}H_2$, lipid), 34.14 ($\underline{C}H_2$, lipid), 34.21 ($\underline{C}H_2$, lipid), 34.71 ($\underline{C}H_2$, lipid), 41.63 (C-2_L), 46.60 (Fmoc-$\underline{C}$H), 55.28 (C-2), 68.76 (C-6), 69.00 ((OC$\underline{H}_2$C$\underline{H}_2$O)/2), 69.65 (d, *J* 5.5 Hz, (PhC$\underline{H}_2$O)P), 69.73 (d, *J* 5.5 Hz,

(Ph$\underline{C}H_2$O)P), 70.52 (Fmoc-$\underline{C}H_2$), 71.40 (C-3$_L$), 73.55 (Ph-$\underline{C}H_2$), 74.08 (C-4), 74.15 (C-5), 77.12 (C-3), 100.52 (C-1), 120.04($\underline{C}$H-Ar), 120.06 ($\underline{C}$H-Ar), 125.51 ($\underline{C}$H-Ar), 125.67 ($\underline{C}$H-Ar), 127.38 ($\underline{C}$H-Ar), 127.76 ($\underline{C}$H-Ar), 127.80 ($\underline{C}$H-Ar), 127.89 ($\underline{C}$H-Ar), 127.97 ($\underline{C}$H-Ar), 128.06 ($\underline{C}$H-Ar), 128.11 ($\underline{C}$H-Ar), 128.51 ($\underline{C}$H-Ar), 128.52 ($\underline{C}$H-Ar), 128.61 ($\underline{C}$H-Ar), 128.65 ($\underline{C}$H-Ar), 128.68 ($\underline{C}$H-Ar), 135.76 (dd, *J* 7.25, 7.25 Hz, $\underline{C}$-Ar), 138.19 ($\underline{C}$-Ar), 141.35 ($\underline{C}$-Ar), 141.37 ($\underline{C}$-Ar), 143.45 ($\underline{C}$-Ar), 143.52 ($\underline{C}$-Ar), 155.05 (C=O), 170.47 (C=O), 174.00 (C=O); HRESI-MS (*m/z*) Calcd for $C_{142}H_{190}N_2O_{26}P_2Na$ $[M + Na]^+$: 2424.2931, found: 2424.2980 and 1223.6429 $[M + 2 Na]^{2+}$.

1,2-di-[2-deoxy-4-O-phosphono-2-((R)-3 tetradecanoyloxytetradecan-amido)-β-D-glucopyranosyl]-ethane **(20)**:

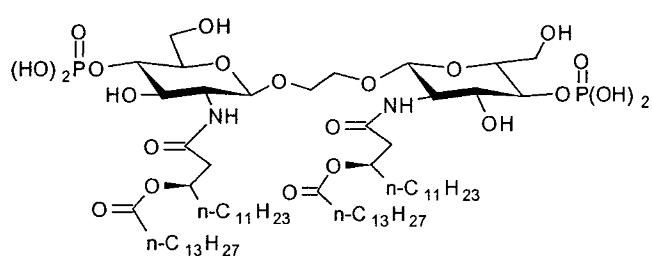

To a solution of **16** (60 mg, 0.03 mmol) in THF-HOAc (4:1, 10 ml) was added palladium on charcoal (5%, 20 mg). The mixture was stirred at room temperature under hydrogen atmosphere for 24 h. The mixture was filtered through a celite pad and the filtrate concentrated *in vacuo*. The resulting residue was dissolved in $CHCl_3$ (2 mL), piperide (30 µL, 0.30 mmol) was added, and the mixture was stirred at rt for 2 h before being concentrated. The residue was dissolved in DCM (50 mL) and washed with cold HCl (1M, 25 mL). The organic layer was washed with a saturated sodium bicarbonate solution (10 mL), dried over Na_2SO_4 and concentrated. The remainder was washed with cold EtOAc (3 x 1.5 mL) and then residual solvent removed *in vacuo*. The product was freeze dried from a dioxane-$CHCl_3$ mixture (95:5) to afford **20** (27 mg, 65%) as white solid. R_f 0.47 ($CHCl_3$/MeOH/H_2O/NH_4OH, 50:15:4:2); HRESI-MS (*m/z*) Calcd for $C_{70}H_{134}N_2O_{22}P_2$ $[M-2H]^{-2}$: 707.4379,

found: 707.4373.

1,2-di-[6-O-benzyl-2-deoxy-4-O-(di-O-benzylphosphono)-3-O-(9-fluorenylmethoxycarbonyl)-2-((R)-3-(2,2,2-trichloroethoxycarbonyloxy)-tetradecanamido)-β-D-glucopyranosyl]-ethane **(21)**:

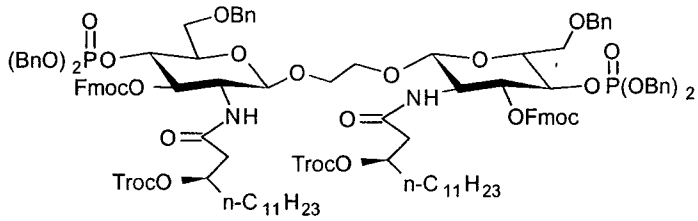

Di-amine **15** (155 mg) was combined with **3** (115 mg, 0.30 mmol) and DCC (124 mg, 0.60 mmol) in dry dichloromethane (3 mL), and stirred at room temperature for 20 h. Water (0.10 mL) was added and the reaction stirred for an additional 20 min before being filtered through a sintered glass funnel with a bed of Na_2SO_4. The filtrate was concentrated and the residue purified by flash column chromatography (hexane/acetone, 2:1) to obtain **21** (123 mg, 53% over two steps) as a colorless syrup. R_f 0.30 (hexane/acetone, 2:1); $[\alpha]_D^{22}$ + 8.5 (*c* 1.0, $CHCl_3$); ^1H NMR (500 MHz, $CDCl_3$): δ 0.87 (t, 3H, *J* 7.5 Hz, CH_3, lipid), 1.08-1.32 (br m, 18H, 9 x CH_2, lipid), 1.51-1.60 (m, 2H, H-4_L), 2.37 (dd, 1H, *J* 15.0, 5.5 Hz, H-2_{La}), 2.51 (dd, 1H, *J* 15.0, 7.5 Hz, H-2_{Lb}), 3.66-3.71 (m, 3H, H-5, (OC$\underline{H}_2$C$\underline{H}_2$O)/2), 3.78-3.86 (m, 3H, H-2, H-6a, H-6b), 3.96 (dd, 1H, *J* 10.0, 7.5 Hz, Fmoc-CH$\underline{H}$), 4.09 (dd, 1H, *J* 7.5, 7.5 Hz, Fmoc-C$\underline{H}$), 4.30 (dd, 1H, *J* 10.0, 7.5 Hz, Fmoc-C$\underline{H}$H), 4.44-4.61 (m, 4H, Troc-Ha, Troc-Hb, H-4, Ph-CH$\underline{H}$), 4.78-4.96 (m, 6H, H-1, Ph-C$\underline{H}$H, (PhC$\underline{H}_2$O)$_2$P), 5.08-5.15 (m, 1H, H-3_L), 5.31 (dd, 1H, *J* 10.0, 10.0 Hz, H-3), 6.47 (d, 1H, *J* 8.0 Hz, NH), 7.15-7.72 (m, 23H, Ar-H); ^{13}C NMR (125 MHz, $CDCl_3$); δ 14.37 ($\underline{C}H_3$, lipid), 22.92 ($\underline{C}H_2$, lipid), 25.29 ($\underline{C}H_2$, lipid), 29.58 ($\underline{C}H_2$, lipid), 29.78 ($\underline{C}H_2$, lipid), 29.86 ($\underline{C}H_2$, lipid), 29.88 ($\underline{C}H_2$, lipid), 32.14 ($\underline{C}H_2$, lipid), 34.24 (C-4_L), 41.22 (C-2_L), 46.40 (Fmoc-$\underline{C}$H), 55.42 (C-2), 68.77 ((O$\underline{C}H_2\underline{C}H_2$O)/2), 69.12 (C-6), 69.67 (d, *J* 5.5 Hz, (Ph$\underline{C}H_2$O)P), 69.74 (d, *J* 5.5 Hz, (Ph$\underline{C}H_2$O)P), 70.59 (Fmoc-$\underline{C}H_2$), 73.62 (Troc-$\underline{C}H_2$), 74.18 (C-4), 74.20 (C-5), 76.84 (Ph-$\underline{C}H_2$), 77.09 (2C, C-3, C-3_L),

94.89 (Troc-$\underline{C}Cl_3$), 100.54 (C-1), 120.11 ($\underline{C}$H-Ar), 125.30 ($\underline{C}$H-Ar), 127.42 ($\underline{C}$H-Ar), 127.78 ($\underline{C}$H-Ar), 127.82 ($\underline{C}$H-Ar), 127.84 ($\underline{C}$H-Ar), 127.87 ($\underline{C}$H-Ar), 128.06 ($\underline{C}$H-Ar), 128.10 ($\underline{C}$H-Ar), 128.13 ($\underline{C}$H-Ar), 128.36 ($\underline{C}$H-Ar), 128.52 ($\underline{C}$H-Ar), 135.74 (dd, *J* 7.25, 7.25 Hz, $\underline{C}$-Ar), 138.15 ($\underline{C}$-Ar), 141.39 ($\underline{C}$-Ar), 143.37 ($\underline{C}$-Ar), 143.51 ($\underline{C}$-Ar), 153.77 (C=O), 155.17 (C=O), 170.08 (C=O); HRESI-MS (*m/z*) Calcd for $C_{120}H_{140}Cl_6N_2O_{28}P_2Na$ $[M + Na]^+$: 2351.6160, found: 2351.7104.

1,2-di-[6-O-benzyl-2-deoxy-4-O-(di-O-benzylphosphono)-3-O-(9-fluorenylmethoxycarbonyl)-2-((R)-3-hydroxytetradecanamido)-β-D-glucopyranosyl]-ethane **(22)**:

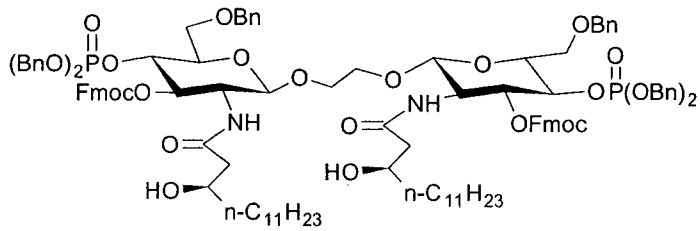

To a solution of **21** (110 mg, 0.05 mmol) in dry THF (4 mL) and acetic acid (1 mL), zinc powder (250 mg) was added. The mixture was stirred at room temperature for 30 min and then filtered. The solid was washed with acetic acid (30 mL) and the filtrate concentrated *in vacuo*. The residue was dissolved in dichloromethane (100 mL) and washed with a saturated sodium bicarbonate solution (50 mL). After separating the organic layer, the aqueous phase was extracted with dichloromethane (2 x 50 mL). The combined organic phase was dried with Na_2SO_4, concentrated and purified by flash column chromatography (hexane/acetone, 2:1) to obtain **22** (76 mg, 82%) as a colorless syrup. R_f 0.23 (hexane/acetone, 2:1); $[\alpha]_D^{22}$ – 6.9 (*c* 1.0, $CHCl_3$); ^1H NMR (500 MHz, $CDCl_3$): δ 0.87 (t, 3H, *J* 7.0 Hz, CH_3, lipid), 1.12-1.26 (br m, 18H, 9 x CH_2, lipid), 1.37-1.39 (m, 2H, H-4_L), 2.08-2.24 (m, 2H, H-2_{La}, H-2_{Lb}), 3.38 (br s, 1H, OH), 3.67 (d, 2H, *J* 9.0 Hz, (O$\underline{C}H_2\underline{C}H_2$O)/2), 3.78 (dd, 1H, *J*

16.5, 9.0 Hz, H-5), 3.90-4.03 (m, 5H, H-6a, H-6b, H-2, H-3_L, Fmoc-CHH), 4.08 (dd, 1H, *J* 7.5, 7.5 Hz, Fmoc-CH), 4.24 (dd, 1H, *J* 7.5, 7.5 Hz, Fmoc-CHH), 4.40-4.54 (m, 2H, Ph-CH_2), 4.60 (ddd, 1H, *J* 9.0, 9.0, 9.0 Hz, H-4), 4.72 (d, 1H, *J* 8.0 Hz, H-1), 4.90-4.99 (m, 4H, $(PhCH_2O)_2P$), 5.21 (dd, 1H, *J* 9.5, 9.0 Hz, H-3), 6.94 (d, 1H, *J* 9.5 Hz, NH), 7.17-7.72 (m, 23H, Ar-H); ^{13}C NMR (125 MHz, $CDCl_3$); δ 14.37 (CH_3, lipid), 22.93 (CH_2, lipid), 25.83 (CH_2, lipid), 29.48 (CH_2, lipid), 29.60 (CH_2, lipid), 29.78 (CH_2, lipid), 29.88 (CH_2, lipid), 29.91 (CH_2, lipid), 32.15 (CH_2, lipid), 37.24 (C-4_L), 44.10 (C-2_L), 46.53 (Fmoc-CH), 54.67 (C-2), 68.41 ($(OCH_2CH_2O)/2$), 68.62 (C-6), 69.11 (C-3_L), 69.73 (d, *J* 5.5, $(PhCH_2O)P$), 69.81 (d, *J* 5.5 Hz, $(PhCH_2O)P$), 70.69 (Fmoc-CH_2), 73.65 (Ph-CH_2), 74.10 (C-4), 74.31 (C-5), 77.52 (C-3), 100.32 (C-1), 120.14 (CH-Ar), 125.54 (CH-Ar), 125.57 (CH-Ar), 127.42 (CH-Ar), 127.84 (CH-Ar), 127.86 (CH-Ar), 128.04 (CH-Ar), 128.07 (CH-Ar), 128.12 (CH-Ar), 128.58 (CH-Ar), 128.61 (CH-Ar), 128.70 (CH-Ar), 128.75 (CH-Ar), 135.73 (dd, *J* 7.25, 7.25 Hz, C-Ar), 138.16 (C-Ar), 141.38 (C-Ar), 141.39 (C-Ar), 143.24 (C-Ar), 143.54 (C-Ar), 155.36 (C=O), 172.82 (C=O); HRESI-MS (*m/z*) Calcd for $C_{114}H_{138}N_2O_{24}P_2Na$ $[M + Na]^+$: 2003.8076, found: 2003.8957 and 1013.4443 $[M + 2\ Na]^{2+}$.

3-(R)-[3-((R)-tetradecanoyloxy)-tetradecanoyloxy]-penta-1-decene **(25)**:

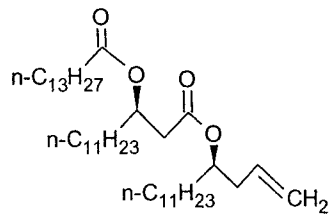

A mixture of dilipid acid **1** [74] (664 mg, 1.46 mmol), 3-(R)-hydroxypenta-1-decene [75] (330 mg, 1.46 mmol), dimethylaminopyridine (9 mg, 0.07 mmol), and DCC (904 mg, 4.38 mmol) in dry dichloromethane (2.5 mL) was stirred at room temperature for 2 h. Water (0.25 mL) was added to the reaction, and the

mixture stirred for an additional 20 min. The solid was then filtered through a sintered glass funnel with a bed of Na_2SO_4, and the filtrate concentrated. Purification of the residue was attempted via repeated flash chromatography (hexane/EtOAc, 100:2), giving only small amounts of pure **25** (< 10 mg) as a colorless syrup. The remainder (663 mg) was used directly in the subsequent oxidation reaction. R_f 0.23 (hexane/EtOAc, 100:1.5); ^{1}H NMR (500 MHz, $CDCl_3$): δ 0.88 (t, 9H, *J* 7.0 Hz, 3 x CH_3, lipid), 1.22-1.32 (br m, 58H, 29 x CH_2, lipid), 1.48-1.62 (m, 4H, H-4_L, H-$4_{L'}$), 2.24-2.38 (m, 4H, H-$2_{L''}$, $OC\underline{H}_2CH=CH_2$), 2.51 (dd, 1H, *J* 15.5, 5.5 Hz, H-$2_{L'a}$), 2.58 (dd, 1H, *J* 5.0, 7.5 Hz, H-$2_{L'b}$), 4.88-4.94 (m, 1H, H-3_L), 5.03-5.09 (m, 2H, $OCH_2CH=C\underline{H}_2$), 5.18-5.23 (m, 1H, H-$3_{L'}$), 5.69-5.78 (m, 1H, $OCH_2C\underline{H}=CH_2$); ^{13}C NMR (125 MHz, $CDCl_3$): δ 14.38 (CH_3, lipid), 22.94 ($\underline{C}H_2$, lipid), 25.26 ($\underline{C}H_2$, lipid), 25.54 ($\underline{C}H_2$, lipid), 25.52 ($\underline{C}H_2$, lipid), 29.43 ($\underline{C}H_2$, lipid), 29.57 ($\underline{C}H_2$, lipid), 29.61 ($\underline{C}H_2$, lipid), 29.65 ($\underline{C}H_2$, lipid), 29.73 ($\underline{C}H_2$, lipid), 29.76 ($\underline{C}H_2$, lipid), 29.80 ($\underline{C}H_2$, lipid), 29.81 ($\underline{C}H_2$, lipid), 29.86 ($\underline{C}H_2$, lipid), 29.89 ($\underline{C}H_2$, lipid), 29.91 ($\underline{C}H_2$, lipid), 29.94 ($\underline{C}H_2$, lipid), 32.17 ($\underline{C}H_2$, lipid), 33.76 ($\underline{C}H_2$, lipid), 34.16 ($\underline{C}H_2$, lipid), 34.77 ($\underline{C}H_2$, lipid), 38.77 ($O\underline{C}H_2CH=CH_2$), 39.68 (C-$2_{L'}$), 70.60 (C-$3_{L'}$), 73.94 (C-3_L), 117.87 ($OCH_2CH=\underline{C}H_2$), 133.97 ($OCH_2\underline{C}H=CH_2$), 170.35 (C=O), 173.36 (C=O).

3-(R)-[3-((R)-tetradecanoyloxy)-tetradecanoyloxy]-tetradecanoic acid **(30)**:

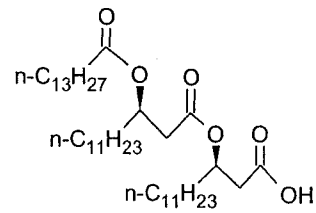

To a solution of **31** (275 mg) in acetic acid (7 mL), zinc powder (500 mg) was added. The mixture was stirred at room temperature for 2 h and then filtered. The solid was washed with EtOAc (20 mL), and concentrated. Flash column

chromatography (hexane/EtOAc, 6:1 → 3:1 with 1% acetic acid) on the residue yielded **30** (210 mg, 96%) as a white solid. R_f 0.42 (hexane/acetone, 3.5:1); $[\alpha]_D^{22}$ + 1.3 (*c* 1.0, $CHCl_3$); ^1H NMR (500 MHz, $CDCl_3$): δ 0.81 (t, 9H, *J* 6.5 Hz, 3 x CH_3 lipid), 1.11-1.32 (br m, 56H, 28 x CH_2 lipid), 1.48-1.58 (m, 6H, H-4_L, H-$4_{L'}$, H-$4_{L''}$), 2.19 (t, 2H, *J* 7.5 Hz, H-$2_{L''}$), 2.43-2.59 (m, 4H, H-2_L, H-$2_{L'}$) 5.09-5.19 (m, 2H, H-3_L, H-$3_{L'}$); ^{13}C NMR (125 MHz, $CDCl_3$): δ 14.35 (CH_3 lipid), 22.93 ($\underline{C}H_2$, lipid), 25.23 ($\underline{C}H_2$, lipid), 25.32 ($\underline{C}H_2$, lipid), 25.35 ($\underline{C}H_2$, lipid), 29.42 ($\underline{C}H_2$, lipid), 29.57 ($\underline{C}H_2$, lipid), 29.60 ($\underline{C}H_2$, lipid), 29.63 ($\underline{C}H_2$, lipid), 29.76 ($\underline{C}H_2$, lipid), 29.81 ($\underline{C}H_2$, lipid), 29.83 ($\underline{C}H_2$, lipid), 29.89 ($\underline{C}H_2$, lipid), 29.90 ($\underline{C}H_2$, lipid), 29.92 ($\underline{C}H_2$, lipid), 29.94 ($\underline{C}H_2$, lipid), 32.16 ($\underline{C}H_2$, lipid), 34.10 ($\underline{C}H_2$, lipid), 34.17 ($\underline{C}H_2$, lipid), 34.70 (C-$2_{L''}$), 39.39 (2C, C-2_L, C-$2_{L'}$), 70.48 (C-$3_{L'}$), 70.78 (C-3_L), 170.03 (C=O), 173.40 (C=O), 173.43 (C=O); Anal. Calcd for $C_{36}H_{68}O_6$: C, 72.44; H, 11.48. Found: C, 72.19; H, 11.38.

Phenacyl 3-(R)-[3-((R)-tetradecanoyloxy)-tetradecanoyloxy]-tetradecanoate **(31)**:

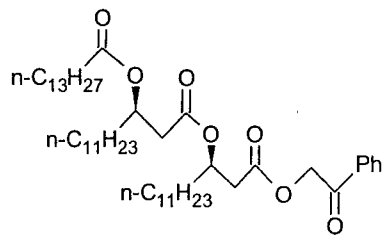

In a similar manner used for the preparation of **3**, a mixture of **18** (663 mg) and Aliquat 336 (0.10 mL) in hexanes (30 mL), EtOAc (30 mL) and acetic acid (10 mL) was oxidized by an aqueous mixture of KMnO4 (450 mg, 2.81 mmol in 70 mL). The resulting residue (683 mg) was then mixed with 2-bromoacetophenone (280 mg, 1.404 mmol) and triethyl amine (0.26 mL, 1.87 mmol) in EtOAc (5 mL). The mixture was stirred at room temperature for 2h, after which solids were removed by filtration. The filtrate was concentrated and purified by repeated flash column chromatography (hexane/CH_2Cl_2/EtOAc, 200:100:6) to yield **31** (313 mg) as a white solid. R_f

0.40 (hexane/acetone, 7:1); $[\alpha]_D^{22}$ + 2.9 (*c* 1.0, $CHCl_3$); ^1H NMR (500 MHz, $CDCl_3$): δ 0.88 (t, 9H, *J* 6.5 Hz, 3 x CH_3 lipid), 1.19-1.38 (br m, 56H, 28 x CH_2 lipid), 1.54-1.68 (m, 6H, H-4_L, H-$4_{L'}$, H-$4_{L''}$), 2.26 (t, 2H, *J* 7.5 Hz, H-$2_{L''}$), 2.55-2.65 (m, 2H, H-$2_{L'}$), 2.70-2.80 (m, 2H, H-2_L), 5.21-5.26 (m, 1H, H-$3_{L'}$), 5.28-5.37 (m, 3H, H-3_L, $C\underline{H}_2C(O)Ph$), 7.48 (dd, 2H, *J* 8.0, 7.5 Hz, *m*-H-Ar), 7.61 (t, 1H, *J* 7.5 Hz, *p*-H-Ar), 7.90 (d, 2H, *J* 8.0 Hz, *o*-H-Ar); ^{13}C NMR (125 MHz, $CDCl_3$): δ 14.35 (CH_3, lipid), 22.91 ($\underline{C}H_2$, lipid), 25.22 ($\underline{C}H_2$, lipid), 25.35 ($\underline{C}H_2$, lipid), 29.41 ($\underline{C}H_2$, lipid), 29.55 ($\underline{C}H_2$, lipid), 29.59 ($\underline{C}H_2$, lipid), 29.65 ($\underline{C}H_2$, lipid), 29.74 ($\underline{C}H_2$, lipid), 29.76 ($\underline{C}H_2$, lipid), 29.79 ($\underline{C}H_2$, lipid), 29.82 ($\underline{C}H_2$, lipid), 29.86 ($\underline{C}H_2$, lipid), 29.88 ($\underline{C}H_2$, lipid), 29.92 ($\underline{C}H_2$, lipid), 32.15 ($\underline{C}H_2$, lipid), 34.15 ($\underline{C}H_2$, lipid), 34.19 ($\underline{C}H_2$, lipid), 34.71 (C-$2_{L''}$), 38.99 (C-$2_{L'}$), 39.39 (C-2_L), 66.34 ($\underline{C}H_2C(O)Ph$), 70.49 (C-$3_{L'}$), 70.98 (C-3_L), 127.96 (*o*-CH-Ar), 129.06 (*m*-CH-Ar), 134.09 (*p*-CH-Ar), 134.45 (C-Ar), 170.01 (C=O), 170.10 (C=O), 173.32 (C=O), 191.86 (C=O); Anal. Calcd for $C_{44}H_{74}O_7$: C, 73.91; H, 10.43. Found: C, 73.75; H, 10.31.

6-O-benzyl-2-deoxy-4-O-(di-O-benzylphosphono)-3-O-((R)-tetradecanoyloxytetradecanoyl)-2-(2,2,2-trichloroethoxycarbonylamino)-α-D-glucopyranosyl trichloroacetimidate **(32)**:

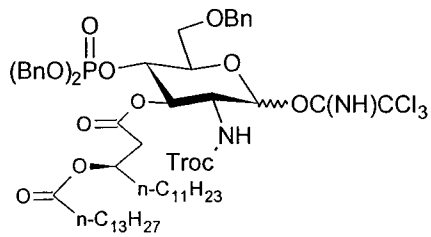

According to known literature procedures [71], glucosamine derivative **4** (1.40 g, 2.91 mmol) and dilipid acid **1** (1.10 g, 2.42 mmol) were coupled under promotion of DCC (748 mg, 3.63 mmol) and DMAP (30 mg, 0.24 mmol) in dry dichloromethane (15 ml). The resulting product after workup and purification (2.2 g, quantitative, 2.42 mmol) was combined with sodium cyanoborohydride (1.52 g, 24.2 mmol) in THF (25 mL), followed by the drop-wise addition of dry

ethereal-$HCl_{(g)}$ at 0 °C till no gas was evolved. Similar to the synthesis of **7**, the product resulting after basic workup and purification (1.85 g, 83%, 2.01 mmol) was next mixed with 5-phenyltetrazole (880 mg, 6.03 mmol) and dibenzyl N,N-diisopropylphosphoramidite (1.35 mL, 4.02 mmol) in dry dichloromethane (20 mL) before being oxidized at 0 °C via *m*-chloroperbenzoic acid (1.98 g, 77%, 8.04 mmol). In a similar manner to the synthesis of **8,** the subsequent product after basic workup and purification (2.10 g, 90%, 1.80 mmol) was reacted with the activated iridium complex (76 mg, 0.09 mmol) in THF (15 mL), before being combined with water (1 mL) and freshly recrystallized NBS (481 mg, 2.70 mmol). The resulting product (1.75 g, 87%) after workup and purification was divided, and a portion (1.00 g, 0.88 mmol) was finally converted to **32** (960 mg, 85%) through reaction with trichloroacetonitrile (0.44 mL, 4.38 mmol) and cesium carbonate (429 mg, 1.32 mmol).

N,N-di-(2-hydroxyethyl)-3-(R)-tetradecanoyloxytetradecanamide (**33**):

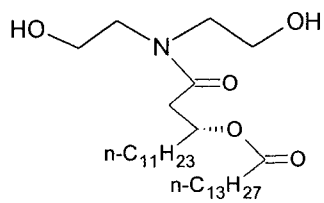

To a solution of DEA (73 mg, 0.665 mmol) in DMF (3 mL), dilipid acid 1 (302 mg, 0.665 mmol), HBTU (262 mg, 0.698 mmol), and DIPEA (0.24 mL, 1.40 mmol) were added. The mixture was stirred at room temperature for 16 h. The mixture was then concentrated, dissolved in water (30 mL), and extracted with EtOAc (3 x 30 mL). The combined organic layers were dried over Na_2SO_4, concentrated, and purified by flash column chromatography (hexane/EtOAc/MeOH, 1:1:0.125) to afford pure **33** (242 mg, 68%) as white solid. R_f 0.28 (hexane/EtOAc/MeOH, 1:1:0.1); $[\alpha]_D^{22}$ - 3.7 (*c* 1.0, $CHCl_3$); ^1H NMR (500 MHz, $CDCl_3$): δ 0.84 (t, 6H, *J* 7.0 Hz, 2 x CH_3 lipid), 1.16-1.33 (br m,

38H, 19 x CH_2 lipid), 1.51-1.62 (m, 4H, H-4L, H-$3_{L'}$), 2.23 (t, 2H, *J* 7.5 Hz, H-$2_{L'}$), 2,56 (dd, 1H, *J* 15.0, 7.5 Hz, H-2_{La}), 2.68 (dd, *J* 15.0, 7.5 Hz, H-2_{Lb}), 3.39-3.57 (m, 4H, $HOCH_2C\underline{H_2}NC\underline{H_2}CH_2OH$), 3.72-3.78 (m, 4H, $HOC\underline{H_2}CH_2NCH_2C\underline{H_2}OH$), 4.04-4.36 (br, 2H, OH x 2), 5.16-5.21 (m, 1H, H-3_L); ^{13}C NMR (125 MHz, $CDCl_3$): δ 14.11 (CH_3, lipid), 22.67 ($\underline{C}H_2$, lipid), 24.96 ($\underline{C}H_2$, lipid), 25.33 ($\underline{C}H_2$, lipid), 29.15 ($\underline{C}H_2$, lipid), 29.30 ($\underline{C}H_2$, lipid), 29.35 ($\underline{C}H_2$, lipid), 29.41 ($\underline{C}H_2$, lipid), 29.51 ($\underline{C}H_2$, lipid), 29.54 ($\underline{C}H_2$, lipid), 29.57 ($\underline{C}H_2$, lipid), 29.63 ($\underline{C}H_2$, lipid), 29.65 ($\underline{C}H_2$, lipid), 29.68 ($\underline{C}H_2$, lipid), 31.91 ($\underline{C}H_2$, lipid), 34.49 (C-$2_{L'}$), 38.76 (C-2_L), 50.29 ($HOCH_2\underline{C}H_2NCH_2CH_2OH$), 52.39 ($HOCH_2CH_2N\underline{C}H_2CH_2OH$), 60.44 ($HO\underline{C}H_2CH_2NCH_2CH_2OH$), 60.74 ($HOCH_2CH_2NCH_2\underline{C}H_2OH$), 71.40 (C-$3_L$).

2-[N-(2-hydroxyethyl)-(R)-3-tetradecanoyloxytetradecanamido]-ethan-1-yl 6-O-benzyl-2-deoxy-4-O-(di-O-benzylphosphono)-3-O-[(R)-3-tetradecanoyloxytetradecanoyl]-2-(2,2,2-trichloroethoxycarbonylamino)-β-D-glucopyranoside (**34**):

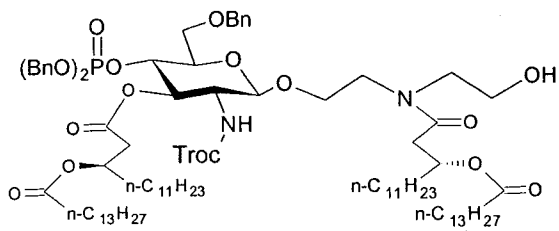

A solution of **32** (460 mg, 0.36 mmol), and **33** (194 mg, 0.0.36 mmol) in dry dichloromethane (4 mL) and molecular sieves (4 Å, 2.0 g) was stirred under nitrogen for 30 min at room temperature. A solution of TMSOTf (0.01 M in dichloromethane, 0.80 mL) is added drop wise in about 3 min. The mixture is stirred at room temperature for 1 h before a saturated sodium bicarbonate solution (10 mL) is added to quench the reaction. Solids were filtered out before the mixture was extracted with dichloromethane (3 x 25 mL). The combined organic phase was dried over Na_2SO_4, concentrated, and purified via repeated flash column chromatography (hexane/EtOAc, 3:4 to yield **34**

(314 mg, 53%) as a colorless liquid. R_f 0.40 (hexane/EtOAc, 3:4); $[\alpha]_D^{22}$ - 1.6 (*c* 1.0, $CHCl_3$); ^1H NMR (500 MHz, $CDCl_3$): δ 0.89 (t, 12H, *J* 7.0 Hz, 4 x CH_3 lipid), 1.20-1.37 (br m, 76H, 38 x CH_2 lipid), 1.46-1.81 (br m, 8H H-4_L x 2, H-3_L x 2), 2.20-2.31 (m, 4H, H-2_L x 2), 2.38-2.54 (m, 4H, H-2_L x 2), 3.25-3.40 (m, 1.2H, H-2B, H-6b), 3.42-3.52 (m, 1.8H, H-2A, H-2a), 3.56-3.84 (m, 10H, H-5, OH, ROC$\underline{H_2}$C$\underline{H_2}$NC$\underline{H_2}$C$\underline{H_2}$OH), 4.38-4.57 (m, 3H, Troc-Ha, Troc-Hb, H-4), 4.64-4.73 (m, 2H, PhC$\underline{H_2}$), 4.78 (d, 0.4H, *J* 8.0 Hz, H-1B), 4.85-4.92 (m, 4.6H, H-1A, PhC$\underline{H_2}$O)$_2$P), 5.08-5.21 (m, 2H, H-3_L x 2), 5.35 (dd, 0.4H, *J* 10.0, 10.0 Hz, H-3B), 5.54 (dd, 0.6H, *J* 9.5, 9.5 Hz, H-3A), 5.76 (d, 0.4H, *J* 8.0 Hz, NH-B), 6.24 (d, 0.6H, *J* 7.0 Hz, NH-A), 7.27-7.32 (m, 15H, Ar-H); ^{13}C NMR (125 MHz, $CDCl_3$): δ 14.34 (CH_3, lipid), 22.90 ($\underline{C}H_2$, lipid), 25,19 ($\underline{C}H_2$, lipid), 25.23 ($\underline{C}H_2$, lipid), 25.30 ($\underline{C}H_2$, lipid), 25.56 ($\underline{C}H_2$, lipid), 25.77 ($\underline{C}H_2$, lipid), 29.38 ($\underline{C}H_2$, lipid), 29.42 ($\underline{C}H_2$, lipid), 29.53 ($\underline{C}H_2$, lipid), 29.57 ($\underline{C}H_2$, lipid), 29.66 ($\underline{C}H_2$, lipid), 29.75 ($\underline{C}H_2$, lipid), 29.78 ($\underline{C}H_2$, lipid), 29.79 ($\underline{C}H_2$, lipid), 29.82 ($\underline{C}H_2$, lipid), 29.87 ($\underline{C}H_2$, lipid), 29.90 ($\underline{C}H_2$, lipid), 32.13 ($\underline{C}H_2$, lipid), 34.26 ($\underline{C}H_2$, lipid), 34.51 ($\underline{C}H_2$, lipid), 34.62 ($\underline{C}H_2$, lipid), 34.64 ($\underline{C}H_2$, lipid), 34.74 ($\underline{C}H_2$, lipid), 34.79 ($\underline{C}H_2$, lipid), 34.84 ($\underline{C}H_2$, lipid), 38.70 (($\underline{C}H_2$, lipid), 39.38 ($\underline{C}H_2$, lipid), 39.61 ($\underline{C}H_2$, lipid), 47.84 & 49.54 (ROCH$_2\underline{C}$H$_2$N$\underline{C}$H$_2$CH$_2$OH), 50.84 & 52.20 (C-6), 56.75 (C-2), 60.35 & 61.60 (ROCH$_2\underline{C}$H$_2$N$\underline{C}$H$_2$CH$_2$OH), 68.12 & 68.36 (RO$\underline{C}$H$_2$CH$_2$NCH$_2\underline{C}$H$_2$OH), 68.64 & 68.97 (RO$\underline{C}$H$_2$CH$_2$NCH$_2\underline{C}$H$_2$OH), 69.85-69.97 (m, (Ph$\underline{C}$H$_2$O)$_2$P), 70.24 (C-3_L), 70.27 (C-3_L), 71.70 (C-3_L), 71.91 & 72.52 (C-3), 72.15 (C-3_L), 73.63 (Troc-$\underline{C}$H$_2$), 73.90 & 73.94 (C-4), 74.21 & 74.25 (C-5), 74.52 & 74.67 (Ph$\underline{C}$H$_2$), 95.17 (Troc-$\underline{C}$Cl$_3$), 100.44 & 100.87 (C-1), 127.64 ($\underline{C}$H-Ar), 127.98 ($\underline{C}$H-Ar), 128.08 ($\underline{C}$H-Ar), 128.34 ($\underline{C}$H-Ar), 128.56 ($\underline{C}$H-Ar), 128.57 ($\underline{C}$H-Ar), 128.62 ($\underline{C}$H-Ar), 135.64 ($\underline{C}$-Ar), 135.68 ($\underline{C}$-Ar), 135.70 ($\underline{C}$-Ar), 137.99 ($\underline{C}$-Ar), 138.06 ($\underline{C}$-Ar), 154.54 ($\underline{C}$=O Troc), 170.25 (C=O), 170.50 (C=O), 171.18 (C=O), 171.95 (C=O), 173.65 (C=O) 173.80 (C=O) 174.28 (C=O).

2-[N-(2-hydroxyethyl)-(R)-3-tetradecanoyloxytetradecanamido]-ethan-1-yl 6-O-benzyl-2-deoxy-4-O-(di-O-benzylphosphono)-3-O-[(R)-3-tetradecanoyloxytetradecanoyl]-2-amino-β-D-glucopyranoside (**36**):

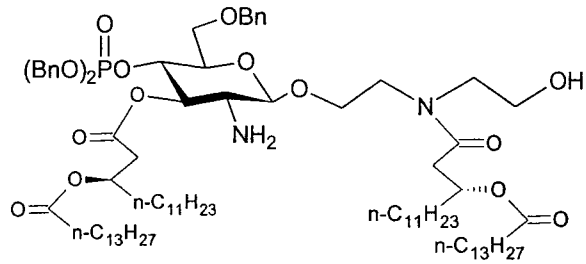

To a solution of **34** (300 mg, 0.18 mmol) in dry THF (4 mL) and acetic acid (1 mL), zinc powder (500 mg) was added. The mixture was stirred at room temperature for 3 h and then filtered. The solid was washed with acetic acid (30 mL) and the filtrate concentrated *in vacuo*. The residue was dissolved in dichloromethane (100 mL) and washed with a saturated sodium bicarbonate solution (20 mL). After separating the organic layer, the aqueous phase was extracted with dichloromethane (2 x 75 mL). The combined organic phase was dried with Na_2SO_4 and concentrated to obtain the free amine **36** (274 mg) as a colorless liquid, which was used directly in the subsequent coupling reaction. The purified portion of **36** (47 mg) recovered from the synthesis of **37** was subjected to spectroscopic analysis, and its structure confirmed. R_f 0.26 (CH_2Cl_2/MeOH, 100:4); $[\alpha]_D^{22}$ - 1.1 (*c* 1.0, $CHCl_3$); ^{1}H NMR (500 MHz, $CDCl_3$): δ 0.88 (t, 12H, *J* 7.0 Hz, 4 x CH_3 lipid), 1.20-1.35 (br m, 76H, 38 x CH_2 lipid), 1.41-1.74 (br m, 8H H-4_L x 2, H-$3_{L'}$ x 2), 2.20-2.31 (m, 4H, H-$2_{L'}$ x 2), 2.38-2.78 (m, 7H, H-2, NH_2, H-2_L x 2), 3.35-3.91 (m, 12 H, H-5, H-6a, H-6b OH, ROC$\underline{H_2}$C$\underline{H_2}$NC$\underline{H_2}$C$\underline{H_2}$OH), 4.31 (d, 0.4H, *J* 8.0 Hz, H-1B), 4.34-4.50 (m, 3.6H, H-1A, H-4, PhC$\underline{H_2}$), 4.85-4.94 (m, 4H, PhC$\underline{H_2}$O)$_2$P), 5.04-5.23 (m, 3H, H-3, H-3_L x 2), 7.27-7.36 (m, 15H, Ar-H); ^{13}C NMR (125 MHz, $CDCl_3$): δ 14.35 (CH_3, lipid), 22.92 ($\underline{C}H_2$, lipid), 25.13 ($\underline{C}H_2$, lipid), 25.17 ($\underline{C}H_2$, lipid), 25.21 ($\underline{C}H_2$, lipid), 25.24 ($\underline{C}H_2$, lipid), 25.36 ($\underline{C}H_2$, lipid), 25.62 ($\underline{C}H_2$, lipid), 25.67 ($\underline{C}H_2$, lipid), 29.36 ($\underline{C}H_2$, lipid), 29.41 ($\underline{C}H_2$, lipid), 29.42 ($\underline{C}H_2$, lipid), 29.53 ($\underline{C}H_2$, lipid), 29.55 ($\underline{C}H_2$, lipid), 29.59 ($\underline{C}H_2$, lipid), 29.63 ($\underline{C}H_2$, lipid), 29.67 ($\underline{C}H_2$,

lipid), 29.75 ($\underline{C}H_2$, lipid), 29.81 ($\underline{C}H_2$, lipid), 29.87 ($\underline{C}H_2$, lipid), 29.89 ($\underline{C}H_2$, lipid), 29.90 ($\underline{C}H_2$, lipid), 29.93 ($\underline{C}H_2$, lipid), 32.15 ($\underline{C}H_2$, lipid), 34.56 ($\underline{C}H_2$, lipid), 34.60 ($\underline{C}H_2$, lipid), 34.77 ($\underline{C}H_2$, lipid), 34.82 ($\underline{C}H_2$, lipid), 38.79 (C-$2_{L'}$), 39.23 (C-$2_{L'}$), 40.01 (C-$2_{L'}$), 40.06 (C-$2_{L'}$), 45.69 (C-2_L), 48.34 (C-2_L), 49.44 (C-2_L), 49.86 (C-2_L), 51.33 & 52.69 (C-6), 60.03 & 60.98 ($ROCH_2\underline{C}H_2N\underline{C}H_2CH_2OH$), 61.40 & 62.24 (C-2), 62.43 & 62.49 ($ROCH_2\underline{C}H_2N\underline{C}H_2CH_2OH$), 67.95 & 68.14 ($RO\underline{C}H_2CH_2NCH_2\underline{C}H_2OH$), 68.56 & 68.76 ($RO\underline{C}H_2CH_2NCH_2\underline{C}H_2OH$), 69.79-69.96 (m, $(Ph\underline{C}H_2O)_2P$), 70.34 (C-3_L), 70.38 (C-3_L), 71.33 (C-3_L), 71.52 (C-3_L), 73.58 & 73.62 ($Ph\underline{C}H_2$), 74.01 & 74.06 (C-5), 74.20 & 74.23 (C-3), 74.59 & 74.66 (C-4), 102.04 & 104.06 (C-1), 127.83 ($\underline{C}H$-Ar), 127.86 ($\underline{C}H$-Ar), 128.23 ($\underline{C}H$-Ar), 128.27 ($\underline{C}H$-Ar), 128.32 ($\underline{C}H$-Ar), 128.39 ($\underline{C}H$-Ar), 128.56 ($\underline{C}H$-Ar), 128.80 ($\underline{C}H$-Ar), 128.85 ($\underline{C}H$-Ar), 128.89 ($\underline{C}H$-Ar), 135.41-135.71 (m, $\underline{C}$-Ar), 138.12 ($\underline{C}$-Ar), 170.83 (C=O), 171.16 (C=O), 171.29 (C=O), 171.59 (C=O), 173.68 (C=O), 173.71 (C=O), 173.73 (C=O), 173.99 (C=O).

2-[N-(2-hydroxyethyl)-(R)-3-tetradecanoyloxytetradecanamido]-ethan-1-yl 6-O-benzyl-2-deoxy-4-O-(di-O-benzylphosphono)-3-O-[(R)-3-tetradecanoyloxytetradecanoyl]-2-[(R)-3-tetradecanoyloxytetradecanamido]-β-D-glucopyranoside (**37**):

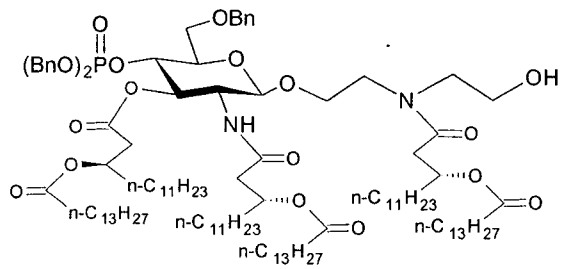

Free amine **36** (274 mg, 0.18 mmol) and dilipid acid **1** (83 mg, 0.18 mmol) were combined with DCC (75 mg, 0.36 mmol) in dry dichloromethane (3 mL), and the mixture stirred at room temperature for 36 h. Water (0.30 mL) was added to the reaction, and the mixture stirred for an additional 2 h. The solid

was then filtered through a sintered glass funnel with a bed of Na_2SO_4, and the filtrate concentrated. The residue was purified by repeated flash column chromatography (hexane/EtOAc, 2:3, and hexane/acetone, 3:1) to afford **37** (150 mg, 43%) as colorless liquid. Unreacted amine **36** (52 mg, 21%) was also recovered. R_f 0.26 (CH_2Cl_2/MeOH, 100:4); $[\alpha]_D^{22}$ - 1.1 (*c* 1.0, $CHCl_3$); ^1H NMR (500 MHz, $CDCl_3$): δ δ 0.89 (t, 18H, *J* 7.0 Hz, 4 x CH_3 lipid), 1.21-1.39 (br m, 104H, 57 x CH_2 lipid), 1.48-1.72 (br m, 12H H-4_L x 3, H-$3_{L'}$ x 3), 2.18-2.29 (m, 6H, H-$2_{L'}$ x 3), 2.46-2.76 (m, 7H, H-2, H-2_L x 3), 3.41-3.93 (m, 12 H, H-5, H-6a, H-6b OH, ROC$\underline{H_2}$C$\underline{H_2}$NC$\underline{H_2}$C$\underline{H_2}$OH), 4.29 (d, 0.4H, *J* 8.0 Hz, H-1B), 4.34-4.51 (m, 3.6H, H-1A, H-4, PhC$\underline{H_2}$), 4.87-4.93 (m, 4H, PhC$\underline{H_2}$O)$_2$P), 5.03-5.23 (m, 4H, H-3, H-3_L x 3), 7.27-7.36 (m, 15H, Ar-H); ^{13}C NMR (125 MHz, $CDCl_3$): δ 14.37 (CH_3, lipid), 22.93 ($\underline{C}H_2$, lipid), 25.19 ($\underline{C}H_2$, lipid), 25.21 ($\underline{C}H_2$, lipid), 25.23 ($\underline{C}H_2$, lipid), 25.26 ($\underline{C}H_2$, lipid), 25.29 ($\underline{C}H_2$, lipid), 25.35 ($\underline{C}H_2$, lipid), 25.39 ($\underline{C}H_2$, lipid), 25.62 ($\underline{C}H_2$, lipid), 25.70 ($\underline{C}H_2$, lipid), 26.41 ($\underline{C}H_2$, lipid), 26.49 ($\underline{C}H_2$, lipid), 26.75 ($\underline{C}H_2$, lipid), 26.87 ($\underline{C}H_2$, lipid), 29.41 ($\underline{C}H_2$, lipid), 29.43 ($\underline{C}H_2$, lipid), 29.57 ($\underline{C}H_2$, lipid), 29.61 ($\underline{C}H_2$, lipid), 29.70 ($\underline{C}H_2$, lipid), 29.71 ($\underline{C}H_2$, lipid), 29.78 ($\underline{C}H_2$, lipid), 29.79 ($\underline{C}H_2$, lipid), 29.83 ($\underline{C}H_2$, lipid), 29.90 ($\underline{C}H_2$, lipid), 29.92 ($\underline{C}H_2$, lipid), 29.94 ($\underline{C}H_2$, lipid), 32.16 ($\underline{C}H_2$, lipid), 34.35 ($\underline{C}H_2$, lipid), 34.49 ($\underline{C}H_2$, lipid), 34.61 ($\underline{C}H_2$, lipid), 34.62 ($\underline{C}H_2$, lipid), 34.68 ($\underline{C}H_2$, lipid), 34.73 ($\underline{C}H_2$, lipid), 34.79 ($\underline{C}H_2$, lipid), 38.84 (C-$2_{L'}$), 39.12 (C-$2_{L'}$), 39.44 (C-$2_{L'}$), 39.66 (C-$2_{L'}$), 39.81 (C-$2_{L'}$), 45.23 (C-2_L), 46.32 (C-2_L), 48.25 (C-2_L), 48.31 (C-2_L), 49.69 (C-2_L), 50.83 & 52.61 (C-6), 59.92 & 61.39 (ROC$\underline{H_2}$C$\underline{H_2}$NC$\underline{H_2}$C$\underline{H_2}$OH), 61.65 & 62.10 (C-2), 64.64 & 64.67 (ROC$\underline{H_2}$C$\underline{H_2}$NC$\underline{H_2}$C$\underline{H_2}$OH), 68.00 & 68.21 (ROC$\underline{H_2}$C$\underline{H_2}$NC$\underline{H_2}$C$\underline{H_2}$OH), 68.58 & 68.95 (ROC$\underline{H_2}$C$\underline{H_2}$NC$\underline{H_2}$C$\underline{H_2}$OH), 69.78-69.88 (m, (PhC$\underline{H_2}$O)$_2$P), 70.07 (C-3_L), 70.21 (C-3_L), 70.45 (C-3_L), 71.38 (C-3_L), 73.45 (C-3_L), 73.62 (PhC$\underline{H_2}$), 73.91 & 73.95 (C-5), 74.14 & 74.20 (C-3), 74.49 & 74.52 (C-4), 102.96 & 104.45 (C-1), 127.83 ($\underline{C}$H-Ar), 127.86 ($\underline{C}$H-Ar), 127.88 ($\underline{C}$H-Ar), 127.91 ($\underline{C}$H-Ar), 128.22 ($\underline{C}$H-Ar), 128.26 ($\underline{C}$H-Ar), 128.32 ($\underline{C}$H-Ar), 128.38 ($\underline{C}$H-Ar), 128.55 ($\underline{C}$H-Ar), 128.58 ($\underline{C}$H-Ar), 128.79 ($\underline{C}$H-Ar), 128.80 ($\underline{C}$H-Ar), 128.81 ($\underline{C}$H-Ar), 128.87

(CH-Ar), 135.65-135.84 (m, C-Ar), 138.09 (C-Ar), 138.11 (C-Ar), 170.71 (C=O), 170.73 (C=O), 170.76 (C=O), 170.99 (C=O), 171.13 (C=O), 171.50 (C=O), 173.39 (C=O), 173.42 (C=O), 173.54 (C=O), 173.90 (C=O).

2-[N-(2-hydroxyethyl)-(R)-3-tetradecanoyloxytetradecanamido]-ethan-1-yl 2-deoxy-4-O-phosphono-3-O-[(R)-3-tetradecanoyloxytetradecanoyl]-2-[(R)-3-tetradecanoyloxytetradecanamido]-β-D-glucopyranoside (**38**):

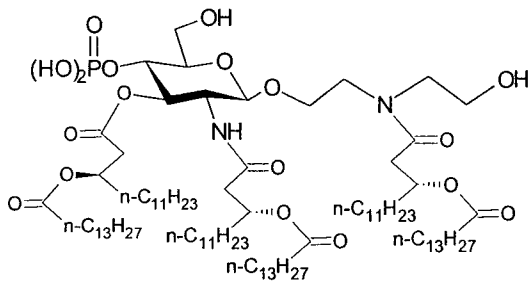

To a solution of **37** (15 mg, 0.01 mmol) in THF-HOAc (10:1, 20 ml) was added palladium on charcoal (5%, 20 mg). The mixture was stirred at room temperature under hydrogen atmosphere for 48 h. The mixture was filtered, the solid washed with THF-HOAc (10:1, 20 ml), and the filtrate concentrated. The residue was purified by flash column chromatography ($CHCl_3$/MeOH, 9:1 → $CHCl_3$/MeOH/H_2O, 3:1:0.1), and the product freeze dried from *tert*-butanol to afford **38** (5 mg, 30%) as a white solid.

5 REFERENCES

1) Schijns, V.E.J.C. *Crit. Rev. Immunol.* **2001**, *21*, 75.

2) Berzofsky, J.A.; Ahlers, J.D.; Belyakov, I.M. *Nat. Rev. Immunol.* **2001**, *1*, 209.

3) Ulevitch, R.J; Tobias, P.S. **1995**. *Annu. Rev. Immunol. 13*, 437.

4) Medzhitov, R.; Janeway, C.A. *Science* **2002**, *296*, 298.

5) Opitz, B; Schroder, N.W.J.; Spreitzer, I; Michelsen, K.S.; Kirschning, C.J.; Hallatschek, W; Zahringer, U; Hartung, T; Gobel, U.B.; Schumann, R.R. *J. Biol.Chem.* **2001**, *276*, 22041.

6) Schwander, R; Dziarski, R; Wesche, H; Rothe, M; Kirschning, C.J. *J. Biol. Chem.* **1999**, *224*, 17406.

7) Poltorak, A; He, X.L.; Smirnova, I; Liu, M.Y.; Van Huffel, C; Du, X; Birdwell, D; Alejos, E; Silva, M; Galanos, C; Freudenberg, M; Ricciardi-Castagnoli, P; Layton, B; Beutler, B. *Science*. **1998**, *282*, 2085.

8) Diebold, S.S.; Kaisho, T; Hemmi, H; Akira, S; Soussa, C.R.E. *Science*. **2004**, *303*, 1529.

9) Hayashi, F; Smith, K.D.; Ozinsky, A; Hawn, T.R.; Yi, E.C.; Goodlett, D.R.; Eng, J.K.; Akira, S; Underhill, D.M.; Aderem A. *Nature*. **2001**, *410*, 1099.

10) Raetz, C.R.H.; Whitfield, C. *Annu. Rev. Biochem.* **2002**, *71*, 635.

11) Janeway, C.A.; Medzhitov, R. *Annu. Rev. Immunol.* **2002**, *20*, 197.

12) Pffeifer, R. *Hygiene*. **1892**, *11*, 393.

13) Morrison, D; Ryan, J. Bacterial Endotoxic Lipopolysaccharide, Molecular Biochemical and Cellular Biology, Vol. I; CRC Press: Boca Raton, FL, **1992**.

14) Westphal, U; Lüderitz, O. *Z. Naturforsch.* **1952**, **7**, 548.

15) Hase, S; Rietschel, E.T. *Eur. J. Biochem.* **1976**, *63*, 101.

16) Gmainer, J; Westphal, U; Lüderitz, O. *Eur J. Biochem.* **1969**, *7*, 270.

17) Imoto, M; Kusumoto, S; Shiba, T; Naoki, H; Iwashita, T; Rietschel, E.T.; Wollenweber, H.W.Z; Galanos, C; Lüderitz, O. *Tetrahedron Lett.* **1983**, *24*, 4017.

18) Imoto, M; Yoshimura, H; Sakaguchi, N; Kusumoto, S; Shiba, T. *Tetrahedron Lett.* **1985**, *26*, 1545.

19) Imoto, M; Yoshimura, H; Sakaguchi, N; Kusumoto, S; Shiba, T; Shimamoto, T. *Bull. Chem. Soc. Jpn.* **1987**, *60*, 2205.

20) Galanos, C; Lüderitz, O; Rietschel, E.T.; Westphal, O; Brade, H; Brade, L; Freudenberg, M; Schade, U; Imoto, M; Yoshimura, H; Kusumoto, S; Shiba T. *Eur. J. Biochem.* **1985**, *148*, 1.

21) Lemaitre, B; Nicolas, E; Michauf, L; Reichart, J.M.; Hoffman, J.A. *Cell.* **1996**, *86*, 973.

22) Akira, S; Takeda, K. *Nat. Rev. Immunol.* **2004**, *4*, 499.

23) Rock, F.L.; Hardiman, G; Timas, J.C.; Kastelein, R.A.; Bazan, J.F. *Proc. Natl. Acad. Sci. U.S.A.* **1998**, *95*, 588.

24) Iwasaki, A; Medzhitov R. *Nat. Immunol.* **2004**, *5*, 987.

25) Lien, E; Means, T.K.; Heine, H; Yoshimura, A; Kusumoto, S; Fukase, K; Fenton, M.J.; Oikawa, M; Qureshi, N; Monks, B; Finberg, R.W.; Ingalls, R.R.; Golebock, D.T. *J. Clin Invest.* **2000**, *105*, 497.

26) Yu, B; Wright, S.D. *J. Biol. Chem.* **1996**, *271*, 4100.

27) Pugin, J; Ulevitch, R.J.; Tobias, P.S. *J. Exp. Med.* **1993**, *178*, 2193.

28) Shimazu, R; Akashi, S; Ogata, Y; Nagai, Y; Fukudome, K; Miyake, K; Kimoto, M. *J. Exp. Med.* **1999**, *189*, 1777.

29) Akashi, S; Saitoh, S; Wakabayashi, Y; Kikuchi, T; Takamura, N; Nogai, Y; Kusumoto, Y; Fukase, K; Kusumoto, S; Adachi, Y; Kosugi, A; Miyake, K. *J. Exp. Med.* **2003**, *198*, 1035.

30) O'Neill, L.A.J.; Bowie, A.G. *Nat. Rev. Immunol.* **2007**, *7*, 353.

31) Kusumoto, S; Fukase, K. *The Chemical Record.* **2006**, *6*, 333.

32) Imoto, M; Yoshimura, H; Yamamoto, M; Shimamotu, T; Kusumoto, S; Shiba, T. *Tetrahedron Lett.* **1984**, *25*, 2667.

33) Imoto, M; Yoshimura, H; Yamamoto, M; Shimamotu, T; Kusumoto, S; Shiba, T. *Bull. Chem. Soc. Jpn.* **1983**, *60*, 2197.

34) Galanos, C; Lehmann, V; Lüderitz, O; Rietschel, E.T; Westphal, O; Brade, H; Brade, L; Freudenberg, M.A.; Hansen-Hagge, T; Lüderitz, T; McKenzie, G; Schade, U; Stritmatter, W; Tanamoto, K; Zähringer, U; Imoto, M; Yoshimura, H; Yamamoto, M; Shimamtoto, T; Kusumoto, S; Shiba T. *Eur. J. Biochem.* **1984**, *140*, 221.

35) Loppnow, H; Brade, L; Brade, H; Reitschel, E.T.; Kusumoto, S; Shiba, T; Flad, H.D. *Eur. J. Immunol.* **1986**, *16*, 1263.

36) Saitoh, S; Akashi, S; Yamada, T; Tanimura, N; Kobayashi, M; Konno, K; Fukase, K; Kusumoto, S; Nagai, Y; Kusumoto, Y; Kosugi, A; Miyake, K. *Int. Immunol.* **2004**, *16*, 961.

37) Visintin, A; Halmen, K.A.; Latz, E; Monks, B.G.; Golenbock, D.T. *J. Immunol.* **2005**, *175*, 6465.

38) Ohto, U; Fukase, K; Miyake, K; Satow, Y. *Science*. **2007**, *316*, 1632.

39) Hawkins, L.D.; Christ, W.J.; Rossignol, D.P. Curr. Top. Med. Chem. **2004**, *4*, 1147.

40) Arnon, R; van Regenmortel, M.H.V. *FASEB J.* **1992**, *7*, 277.

41) Johnson, A.G. *Clin. Microbiol. Rev.* **1994**, *7*, 277.

42) Johsnon, D.A. *Curr. Top. Med. Chem.* **2008**, *8*, 64.

43) Jiang, Z.-H.; Koganty, R.R. *Curr. Top. Med. Chem.* **2003**, *10*, 1423.

44) Wiemann, B; Starnes, C.O. *Pharmacol. Ther.* **1994**, *64*, 529.

45) Shear, M.J.; Turner, F.C. *J. Natl. Cancer Inst.* **1943**, *4*, 81.

46) Garay, R.P.; Patrice, V; Bauer, J; Normier, G; Bardou, M; Jeannin, J.-F.; Chiavaroli, C. *Eur. J. Pharm.* **2007**, *563*, 1.

47) Umansky, V; Schirrmacher, V. *Adv. Cancer Res.* **2001**, *82*, 107.

48) Lechner, M; Lirk, P; Rieder, J. *Semin. Cancer Biol.* **2005**, *15*, 277.

49) Dobrovolskaia, M.A.; Vogel, S.N. *Microbes Infect.* **2002**, *4*, 903.

50) Persing, D.H; Coler, R.N.; Lacy, M.J.; Johnson, D.A.; Baldridge, J.R.; Hershberg, R.M., Reed, S.G. *Trends in Microbiology*. **2002**, *10*, 32.

51) Qureshi, N; Mascagni, P; Ribi, E; Takayama, K. *J. Biol. Chem.* **1985**, 260, 5271.

52) Jiang, Z.-H.; Budzynski, W.A.; Qiu, D; Yalamati, D; Koganty, R.R. *Carbohydr. Res.* **2007**, *342*, 784.

53) Evans, J.T.; Cluff, C.W.; Johnson, D.A.; Lacy, M.J.; Persing, D.H.; Baldridge, J.R. *Expert Rev. Vaccines.* **2003**, *2,* 219.

54) Mata-Haro, V; Cekic, C; Martin, M; Chilton, P.M.; Casella, C.R.; Mitchell, T.C. *Science.* **2007**, *316*, 1628.

55) Fitzgerald, K.A; Golenbock, D.T. *Science.* **2007**, *316*, 1574.

56) Seydel, U; Oikawa, M; Fukase, K; Kusumoto, S; Brandenburg, K. *Eur. J. Biochem.* **2000**, *267*, 3032.

57) Schromm, A.B.; Brandernburg, K; Loppnow, H; Moran, A.P.; Koch, M.H.J.; Rietschel, E.T.; Seydel, U. *Eur. J. Biochem.* **2000**, *267*, 2008.

58) Christ, W.J.; Asano, O; Robidoux, A.L.C.; Perez, M; Wang, Y.A.; Dubuc, G.R.; Gavin, W.E.; Hawkins, L.D.; Mcguiness, P.D.; Mullarkey, M.A.; Lewis, M.D.; Kishi, Y; Kawata, T; Bristol, J.R.; Rose, J.R.; Rossignol, D.P.; Kobayashi, S; Hishinuma, L; Kimura, A; Askawa, N; Katayama, K; Yamatsu, I. *Science.* **1995**, 268, 80.

59) Christ, W.J.; Asano, O; Robidoux, A.L.C.; Perez, M; Wang, Y.A.; Dubuc, G.R.; Gavin, W.E.; Hawkins, L.D.; Mcguiness, P.D.; Mullarkey, M.A.; Lewis, M.D.; Kishi, Y; Kawata, T; Bristol, J.R.; Rose, J.R.; Rossignol, D.P.; Kobayashi, S; Hishinuma, L; Kimura, A; Askawa, N; Katayama, K; Yamatsu, I. *Prog. Clin. Biol. Res.* **1995**, *392*, 499.

60) Kawata, T; Bristol, J.R.; Rossignol, D.P.; Rose, J.R.; Kobayashi, S; Yokohama, H; Ishibashi, A; Christ, W.J.; Katayama, K; Yamatsu, I; Kishi, Y. *Br. J. Pharmacol.* **1999**, *127*, 853.

61) Bunnel, E; Lynn, M; Habet, K; Neumann, A; Perdomo, C.A.; Friedhoff, L.T.; Rogers, S.L.; Parillo, J.E. *Crit. Care Med.* **2000**, *28*, 2713.

62) Qureshi, N; Honovich, J.P.; Hara, H; Cotter, R.J.; Takayama, K. *J. Biol. Chem.* **1998**, *263*, 5502.

63) Salimath, P.V.; Weckesser, J; Strittmatter, W; Mayer, H. *Eur. J. Biochem.* **1983**, *136*, 195.

64) Kalatshov, I.A.; Doroshenko, V; Cotter, R.J.; Takayama, K; Qureshi, N. *Anal. Chem.* **1997**, *69*, 2317.

65) Kim, H.M.; Park, B.S.; Kim, J.I.; Kim, S.E.; Lee, J; Oh, S.C.; Enkhbayar, P; Matsushima, N; Lee, H; Yoo, O.J.; Lee, J.O. *Cell.* **2007**, *130*, 906.

66) Brandenburg, K; Lindner, B.B.; Schromm, A; Koch, M.H.J.; Bauer, J; Merkli, A; Zbaeren, C; Davies, J.G.; Seydel, U. *Eur. J. Biochem.* **2000**, *267*, 3370.

67) Matsuura, M; Kiso, M; Hasegawa, A. *Infect. Immun.* **1999**, *67*, 6286.

68) Brandenburg, K; Matsuura, M; Kiso, M; Hasegawa, A; Nishimura, C; De Clercq, E. *J. Gen. Virol.* **1992**, *74*, 1399.

69) Johnson, D.A.; Sowell, C.G; Johnson, C.L.; Livesay, M.T.; Keegan, D.S.; Rhodes, M.J.; Ulrich, J.T.; Ward, J.R.; Cantrell, J.L.; Brookshie, V.G. *Bioorg. Med. Chem. Lett.* **1999**, *9*, 2273.

70) Funatogawa, K; Matsuura, M; Nakano, M; Kiso, M; Hasegawa, A. *Cells. Infect. Immun.* **1998**, *66*, 5792.

71) Jiang, Z.-H; Budzynski, W.A.; Skeels, L.N.; Krantz, M.J.; Koganty, R.R. *Tetrahedron.* **2002**, *58*, 8833.

72) Jiang, Z.-H.; Bach, M.V.; Budzynski, W.A.; Krantz, M.J.; Koganty, R.R.; Longnecker, B.M. *Biorg. Med. Chem. Lett.* **2002**, *12*, 2193.

73) Schüle, G; Ziegler, T. *Liebigs. Ann.* **1996**, 1599.

74) Kiso, M; Tanaka, S; Fujita, M; Fujishima, Y; Ogawa, Y; Hasagawa, A. *Carbohydr. Res.* **1987**, *162*, 247.

75) Hanessian, S; Tehim, A; Chen, P. *J. Org. Chem.* **1995**, *58*, 7768.

76) Maegawa, T; Fujiwara, Y; Ikawa, T; Hisashi, H; Monguchi, Y; Sajiki, H. *Amino Acids.* **2009**, *36*, 493.

6 APPENDIX

Spectroscopic Data of Corresponding Compounds

TrocO
n-C11H23
2
CH2
7
6
5
4
3
2
1
0
PPM

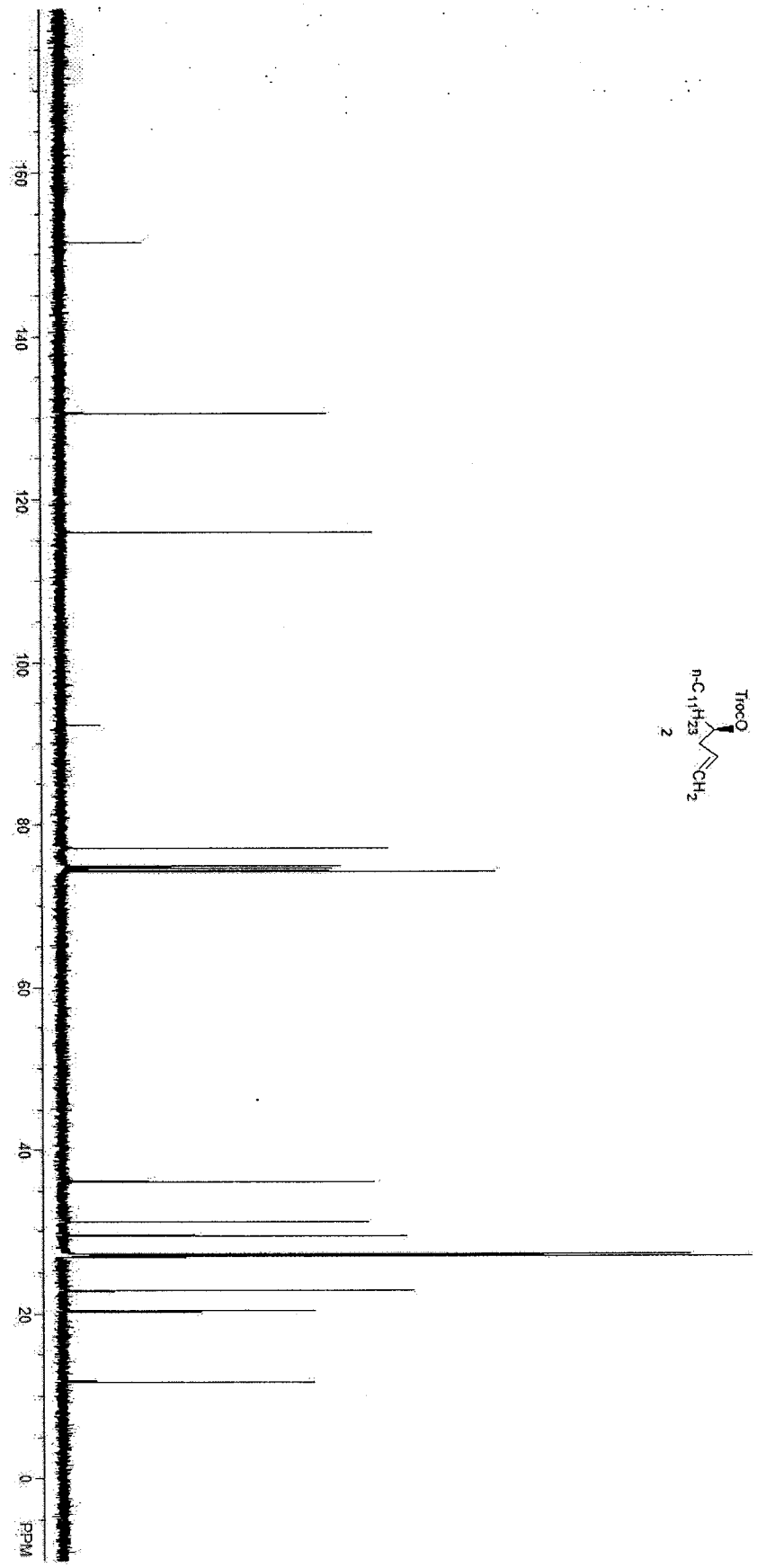
TrocO
n-C11H23
CH2
2
160
140
120
100
80
60
40
20
0
PPM

TrocO O
n-C11H23
OH
3
7
6
5
4
3
2
1
0
PPM

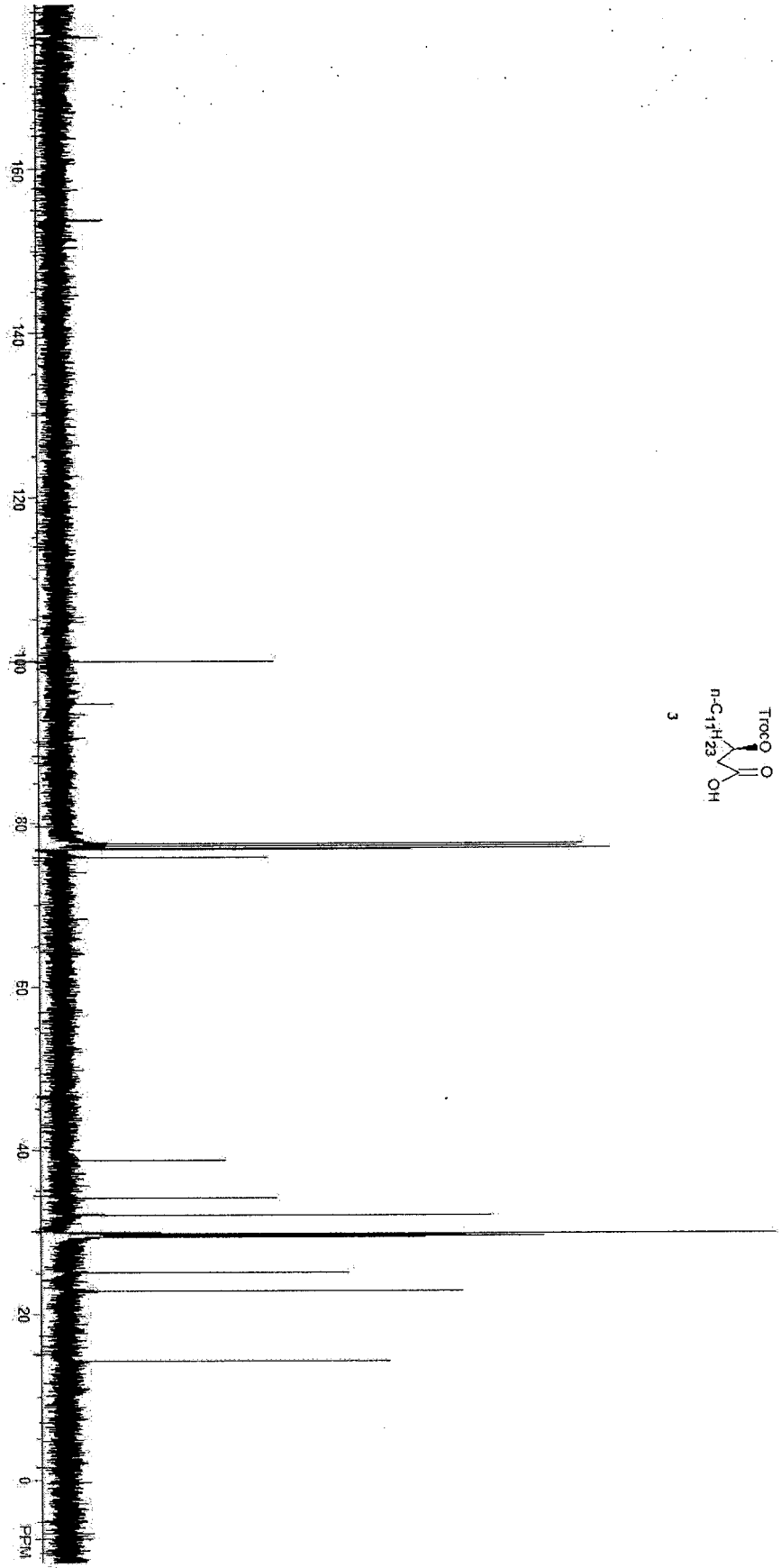
TrocO
O
n-C11H23
OH
3
160
140
120
100
80
60
40
20
0
PPM

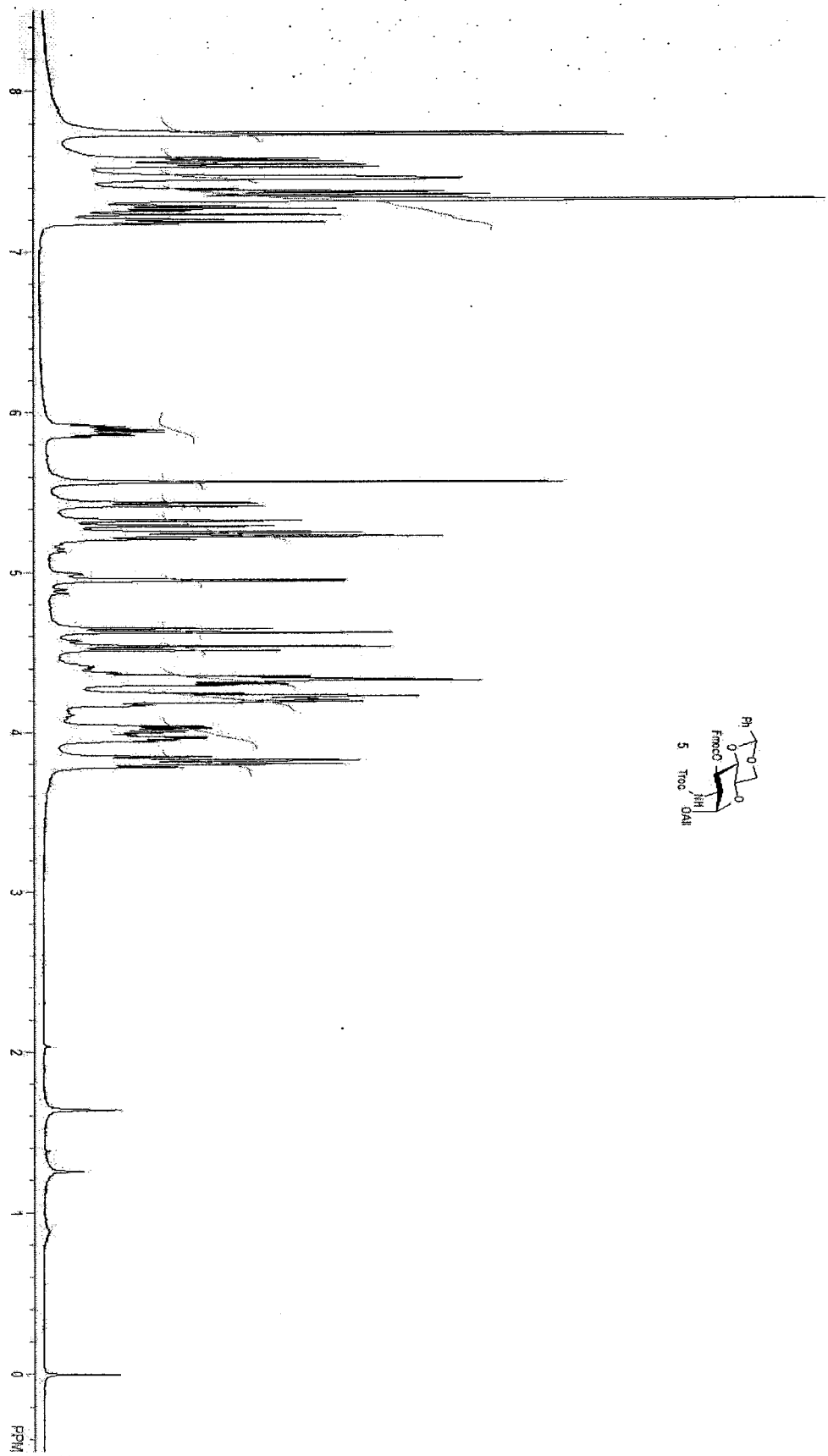
8
7
6
5
4
3
2
1
0
PPM
Ph
O
FmocO
5
Troc
NH
OAll

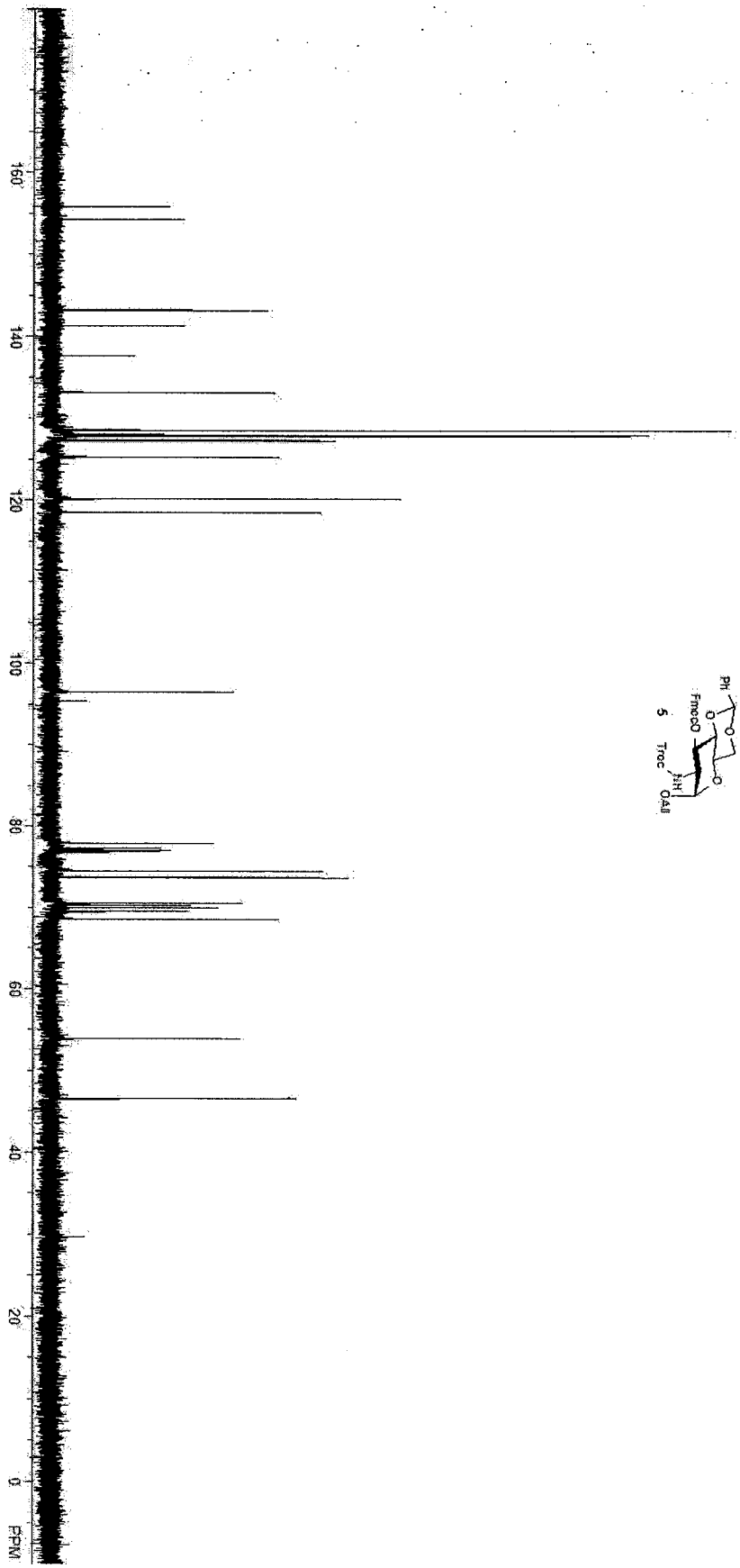
160
140
120
100
80
60
40
20
0
PPM
Ph
FmocO
5
Troc
NH
O-All

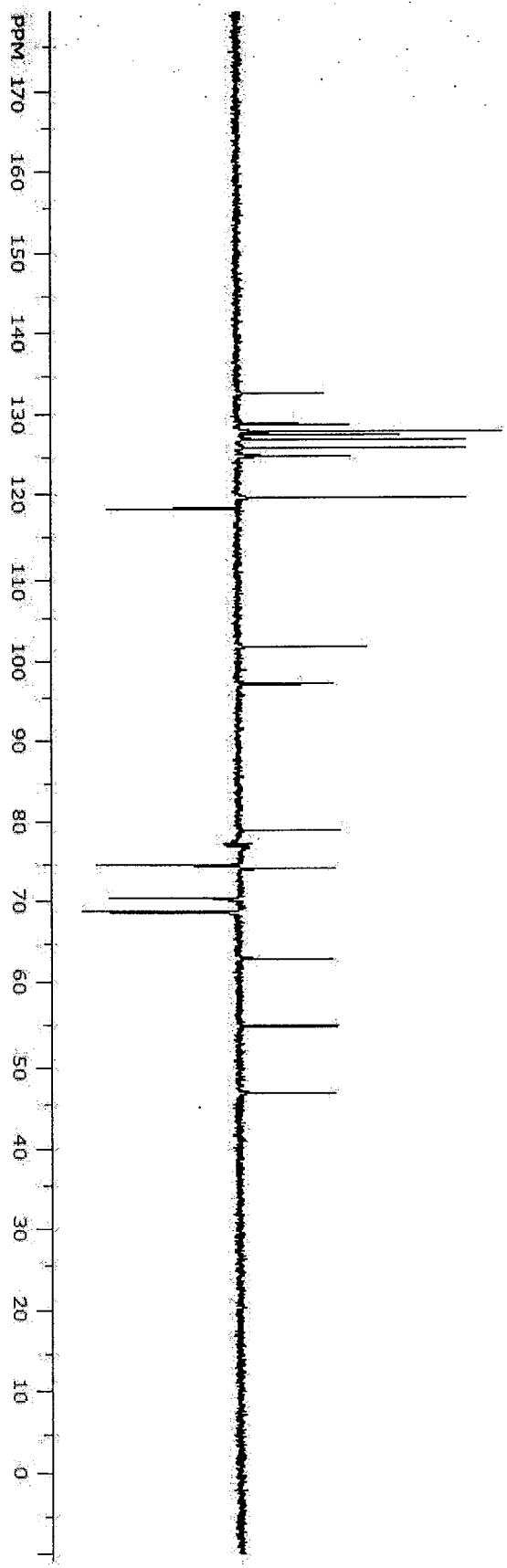
PPM
170
160
150
140
130
120
110
100
90
80
70
60
50
40
30
20
10
0

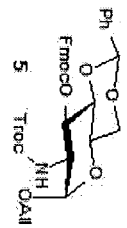
Ph
O
O
FmocO
O
5
Troc
NH
OAll

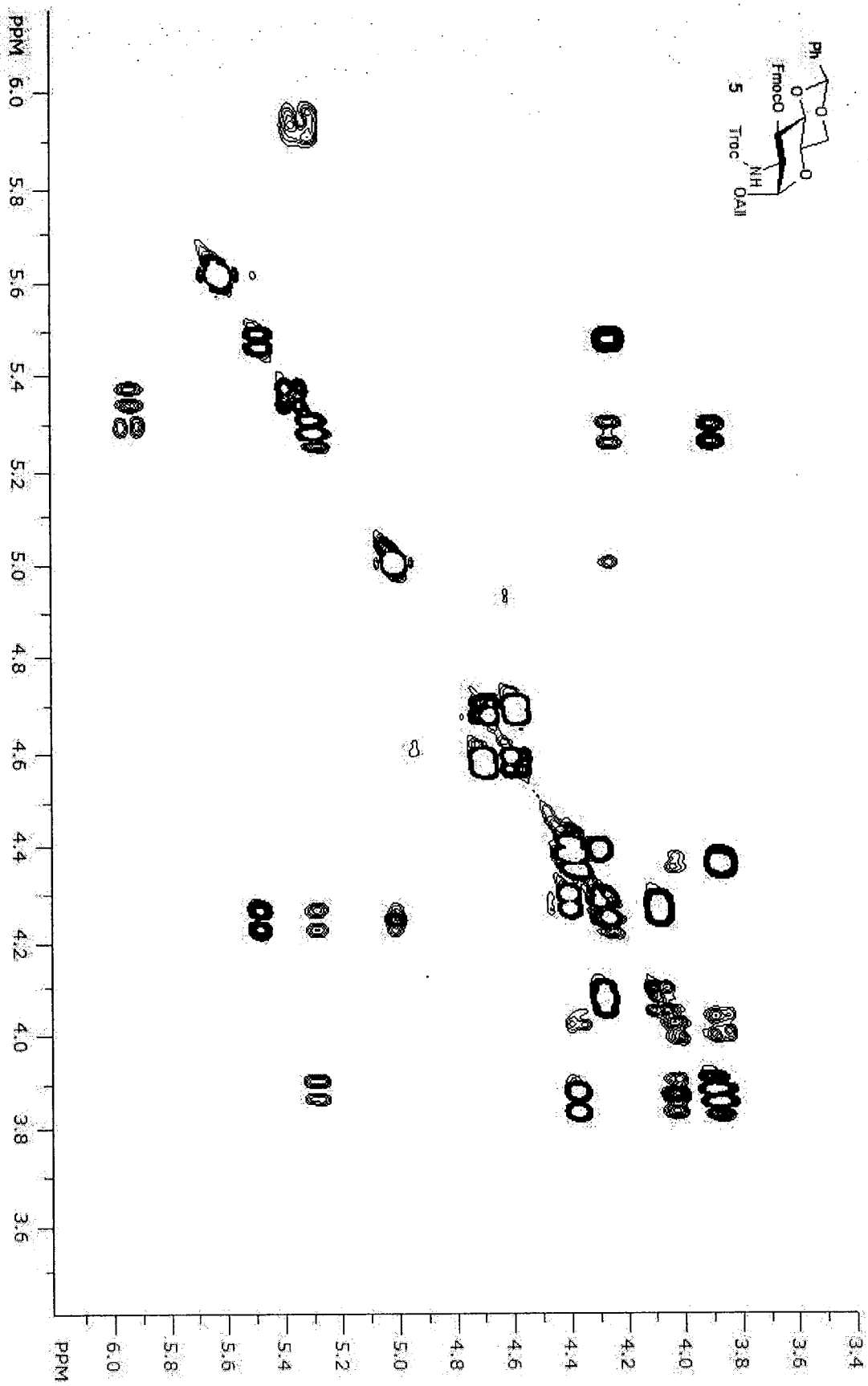
Ph
O
FmocO
O
O
5
Troc
NH
OAll
PPM
6.0
5.8
5.6
5.4
5.2
5.0
4.8
4.6
4.4
4.2
4.0
3.8
3.6
3.4

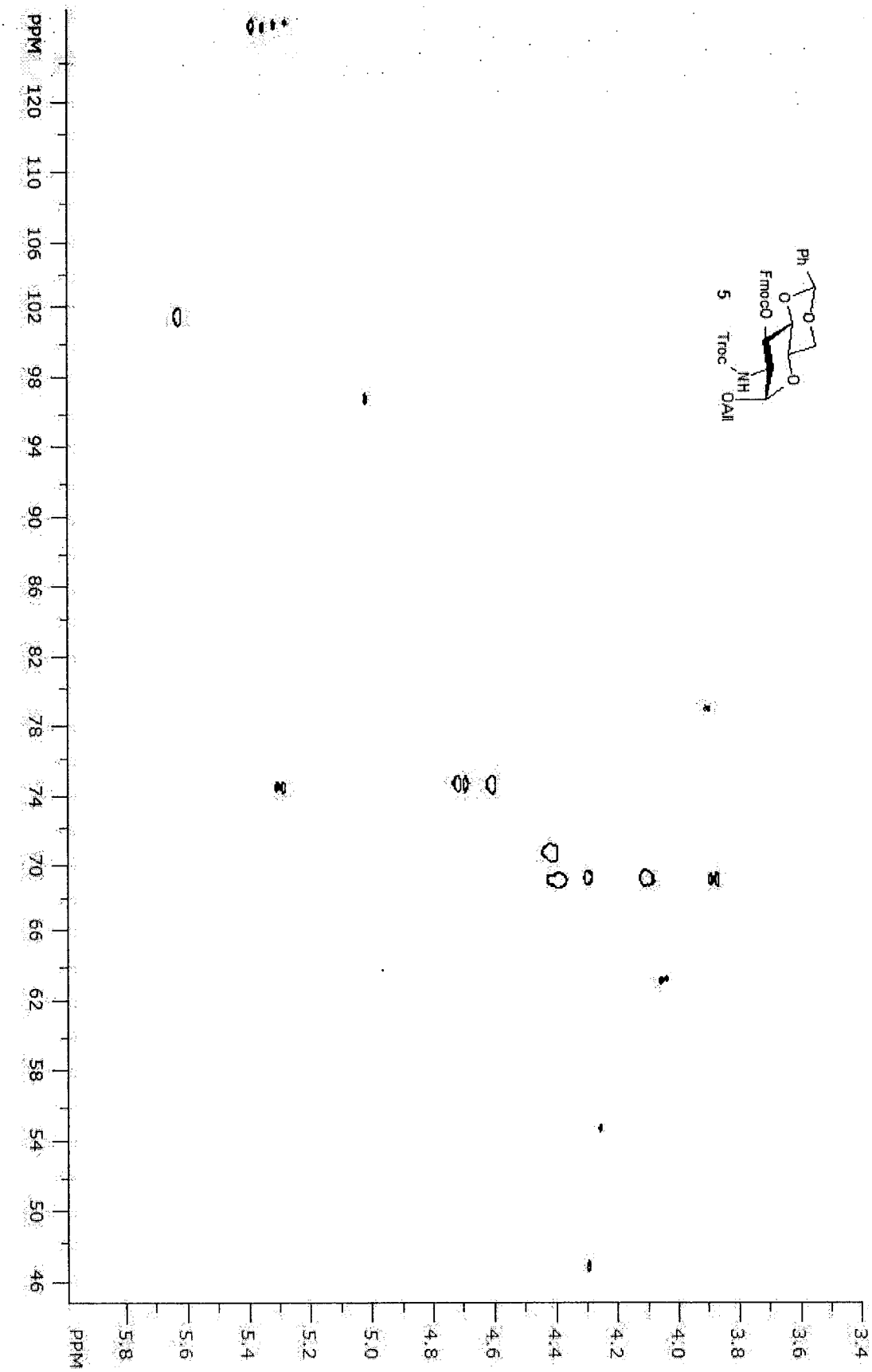
PPM
120
110
106
102
98
94
90
86
82
78
74
70
66
62
58
54
50
46
PPM
5.8
5.6
5.4
5.2
5.0
4.8
4.6
4.4
4.2
4.0
3.8
3.6
3.4
Ph
O
O
FmocO
O
5
Troc
NH
OAll

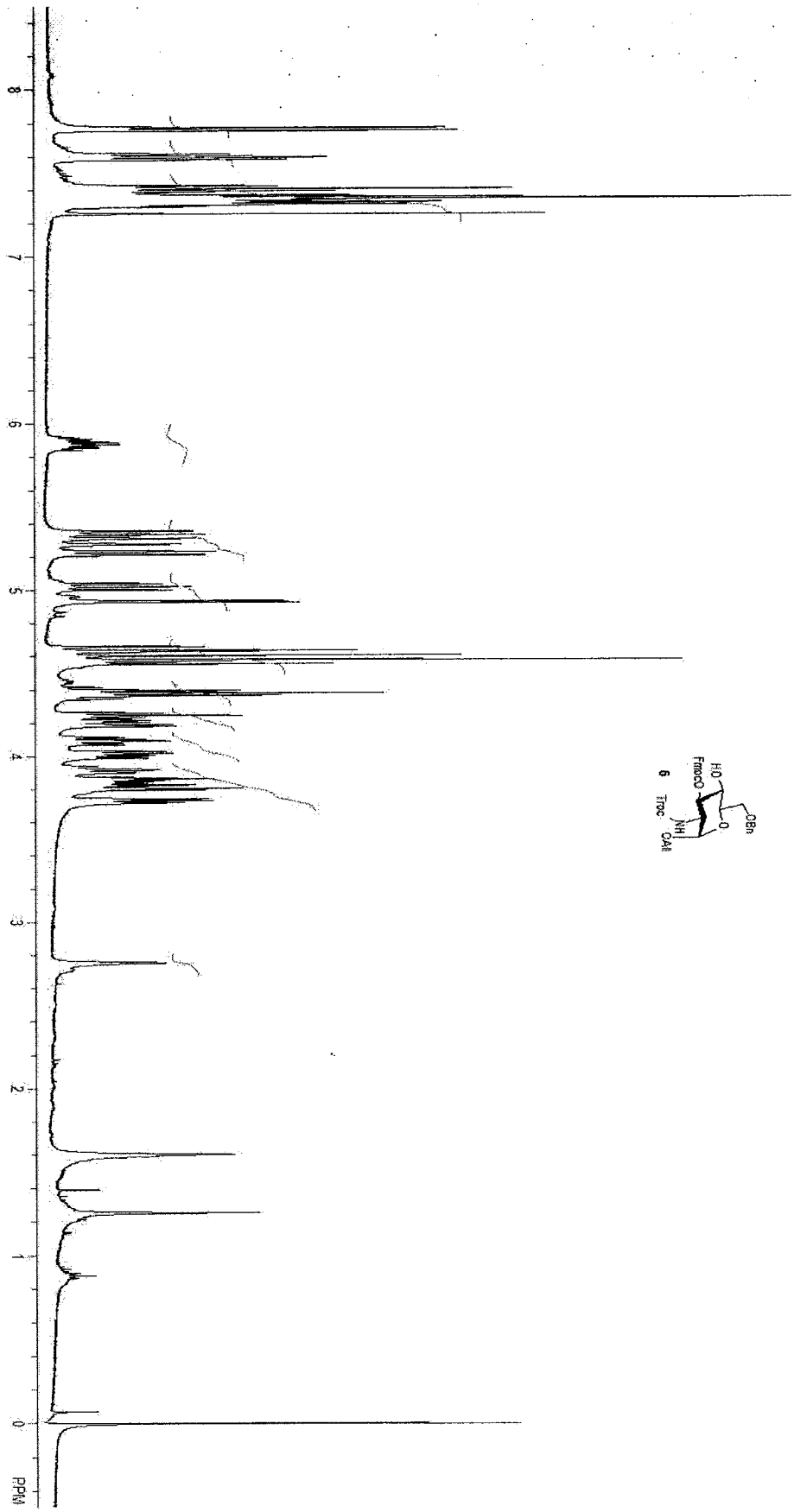
8
7
6
5
4
3
2
1
0
PPM
HO
FmocO
O
OBn
NH
CAM
TFAc

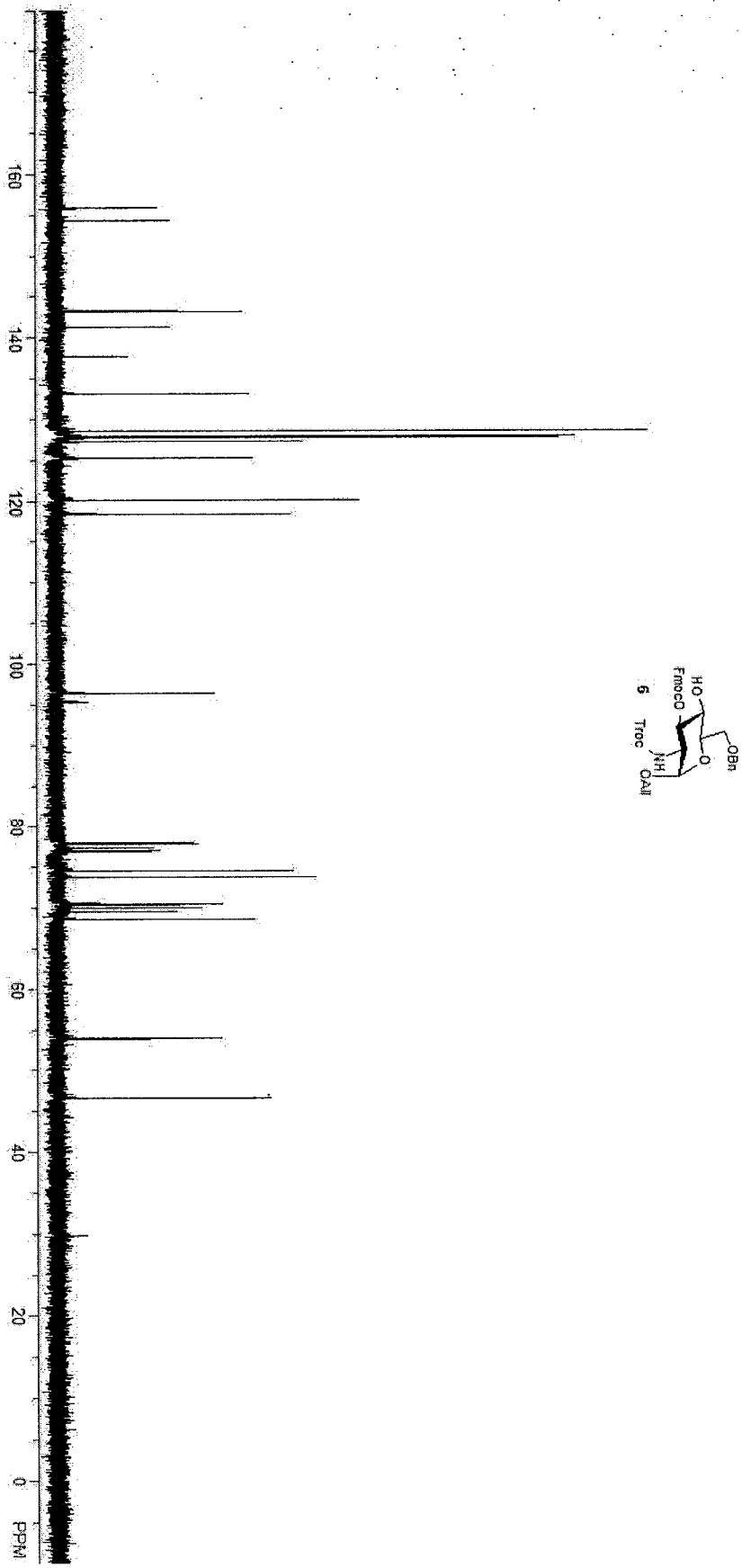
160
140
120
100
80
60
40
20
0
PPM
HO
FmocO
6
Troc
NH
O
OBn
OAll

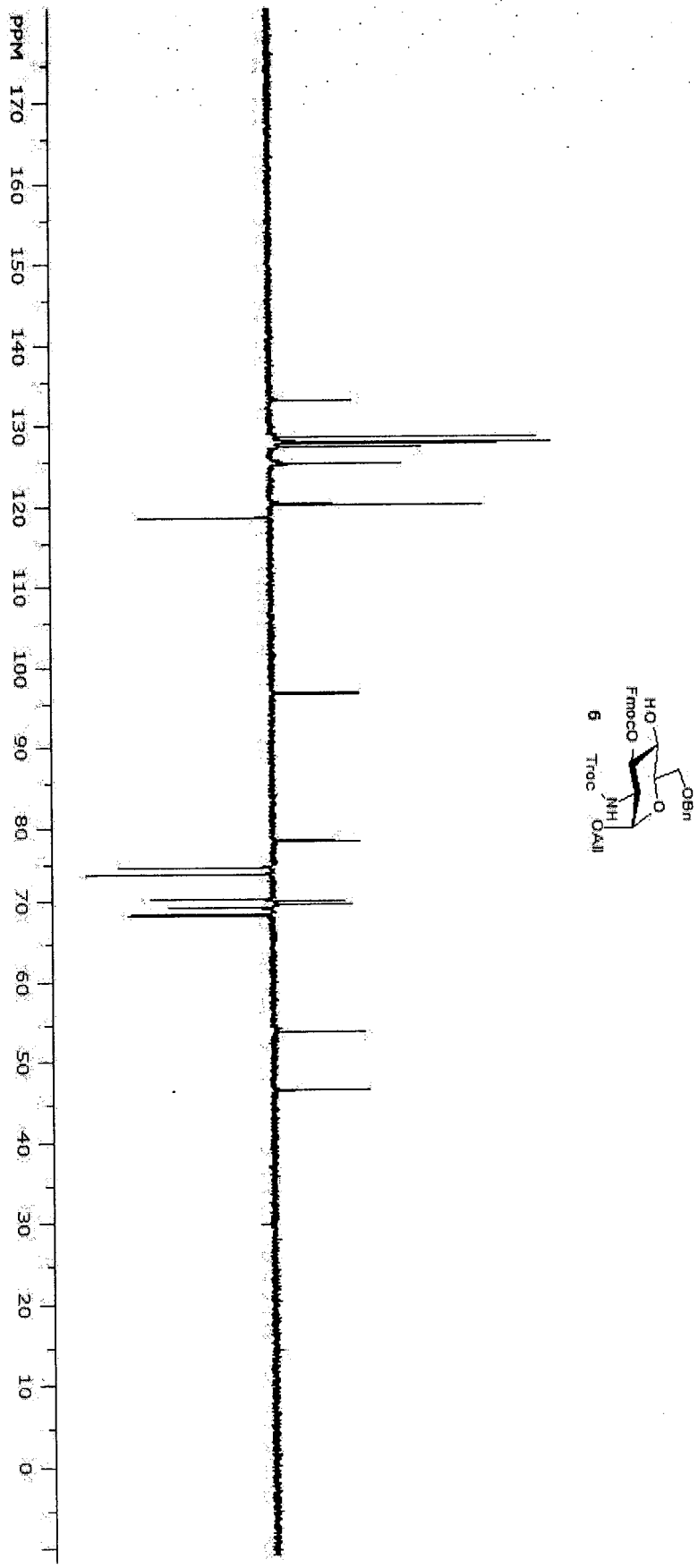
PPM
170
160
150
140
130
120
110
100
90
80
70
60
50
40
30
20
10
0
HO
FmocO
6
Troc
NH
OAll
O
OBn

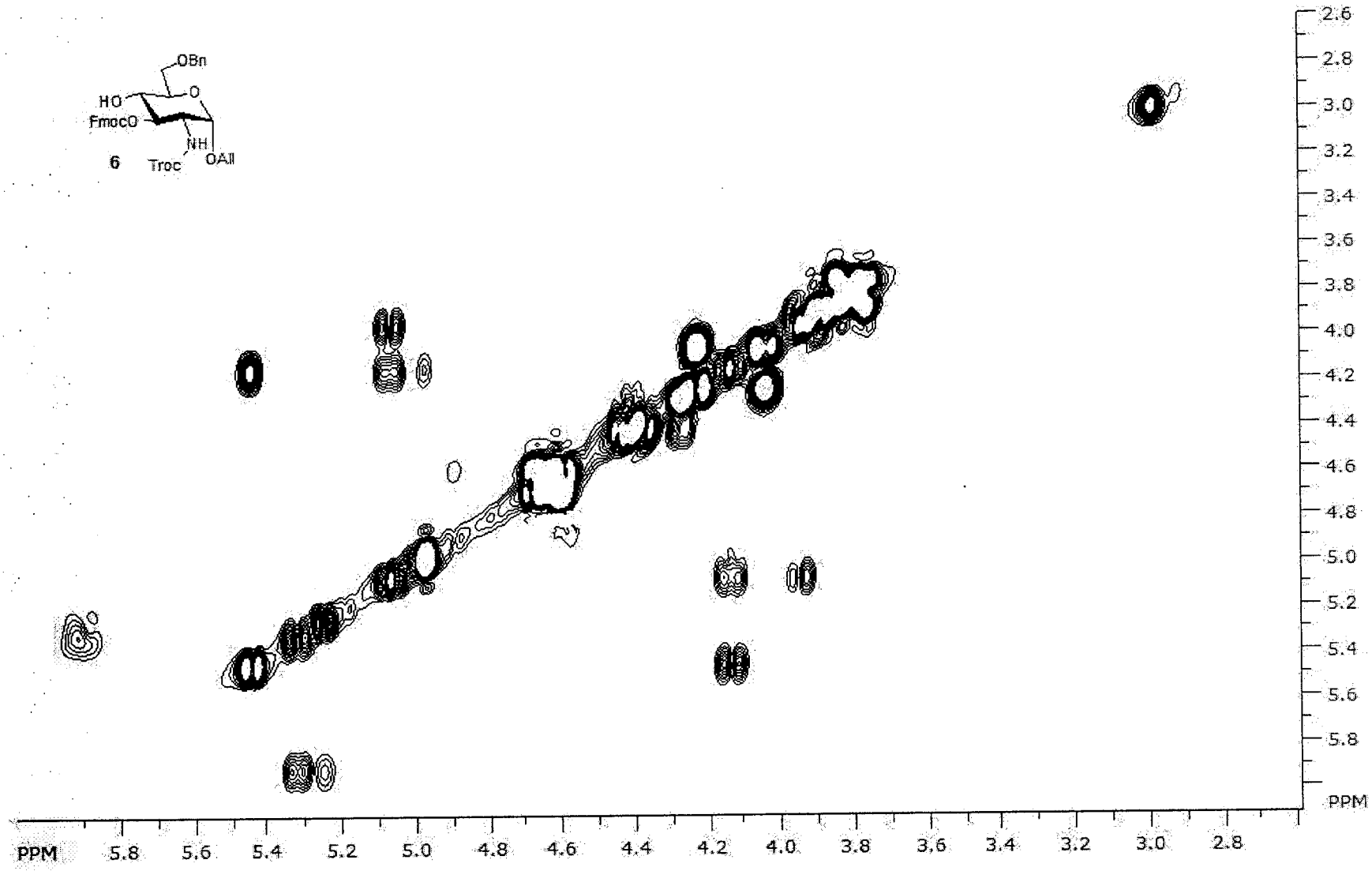
OBn
HO
O
FmocO
NH
6
Troc
OAll
2.6
2.8
3.0
3.2
3.4
3.6
3.8
4.0
4.2
4.4
4.6
4.8
5.0
5.2
5.4
5.6
5.8
PPM
PPM
5.8
5.6
5.4
5.2
5.0
4.8
4.6
4.4
4.2
4.0
3.8
3.6
3.4
3.2
3.0
2.8

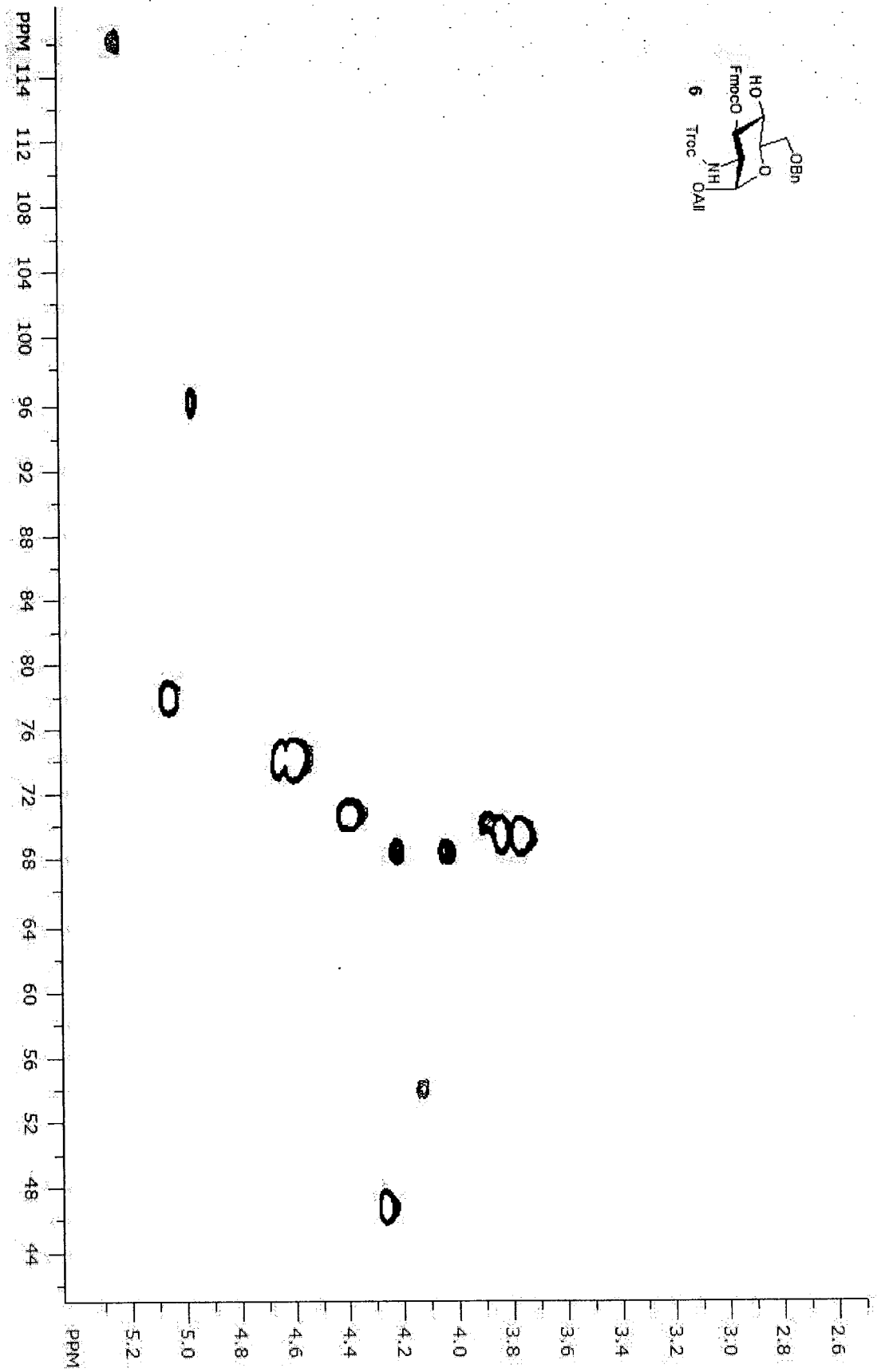
HO
FmocO
OBn
O
NH
Troc
OAll
6
PPM 114
112
108
104
100
96
92
88
84
80
76
72
68
64
60
56
52
48
44
PPM
5.2
5.0
4.8
4.6
4.4
4.2
4.0
3.8
3.6
3.4
3.2
3.0
2.8
2.6

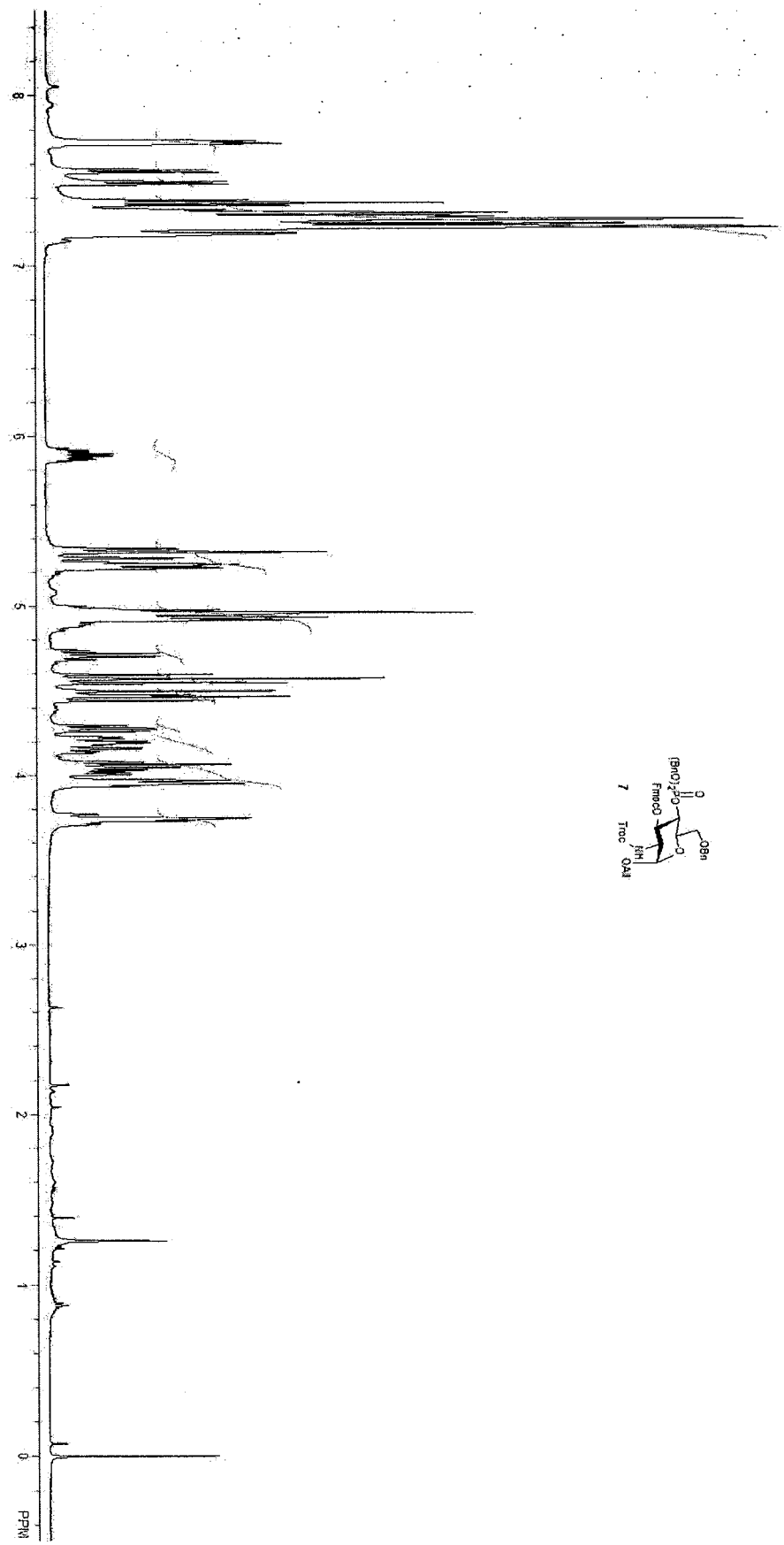
8
7
6
5
4
3
2
1
0
PPM
(BnO)2PO
FmocO
OBn
Troc
NH
OAll

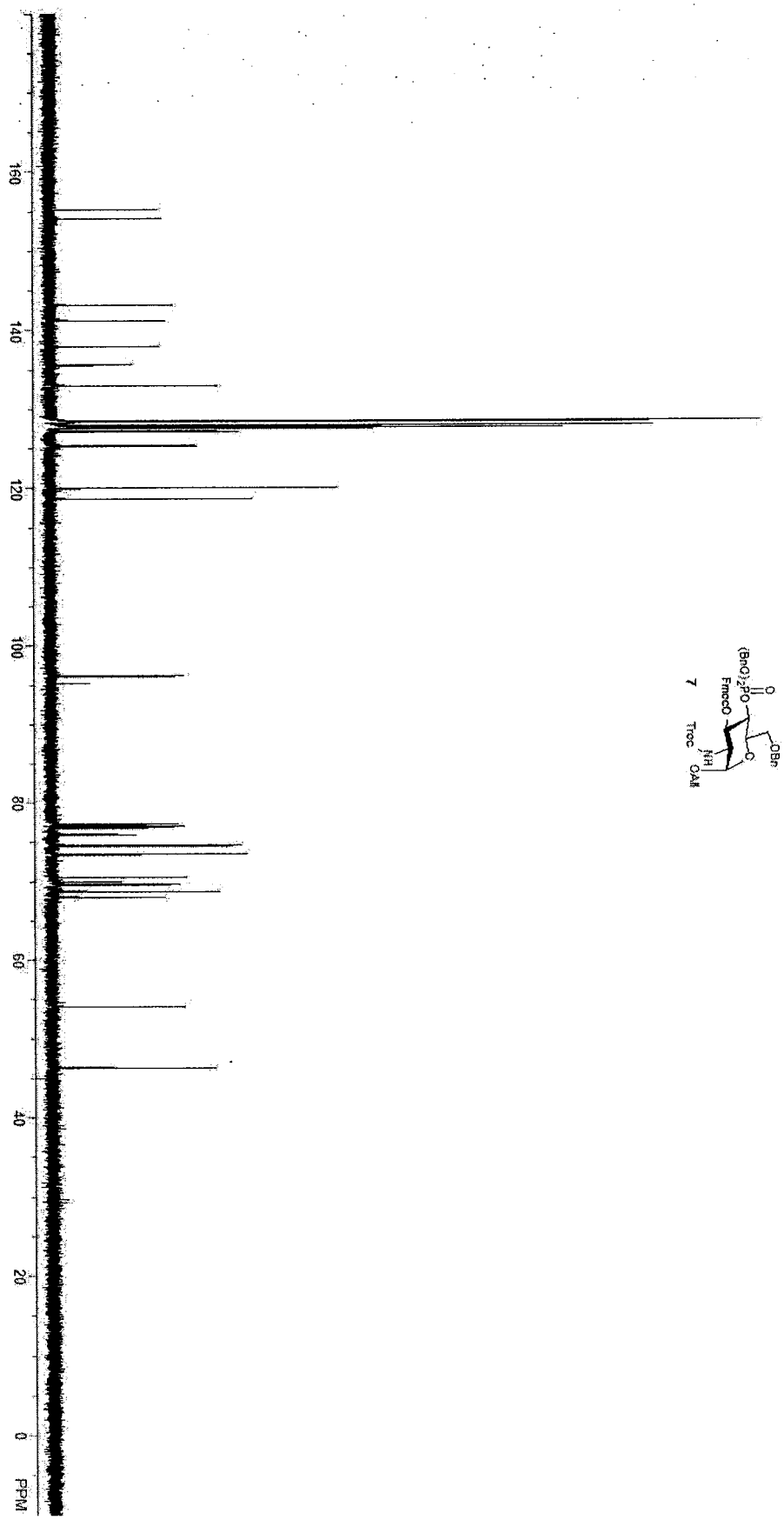
160
140
120
100
80
60
40
20
0
PPM
(BnO)2PO
FmocO
Troc
NH
OAll
OBn
7

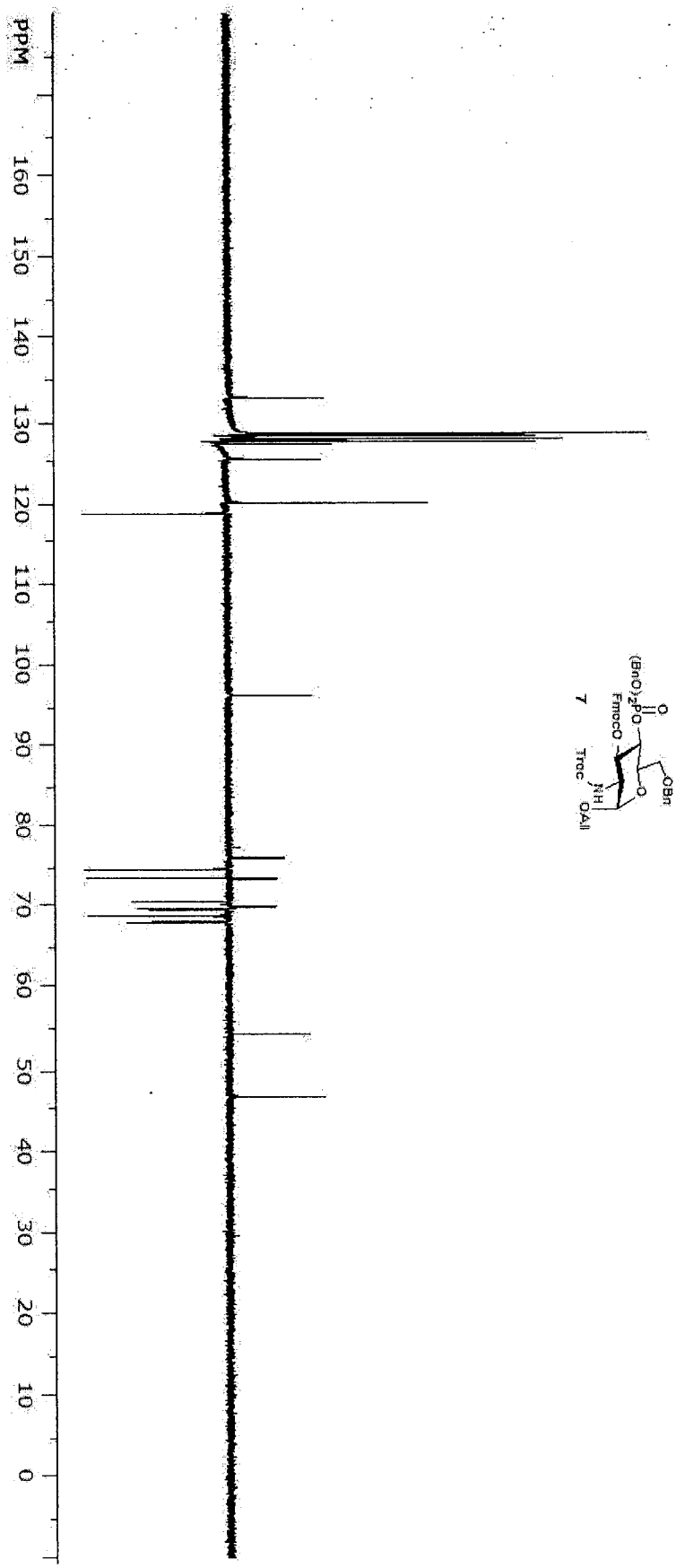
PPM
160
150
140
130
120
110
100
90
80
70
60
50
40
30
20
10
0
7
(BnO)2PO
FmocO
Troc
NH
OAll
OBn

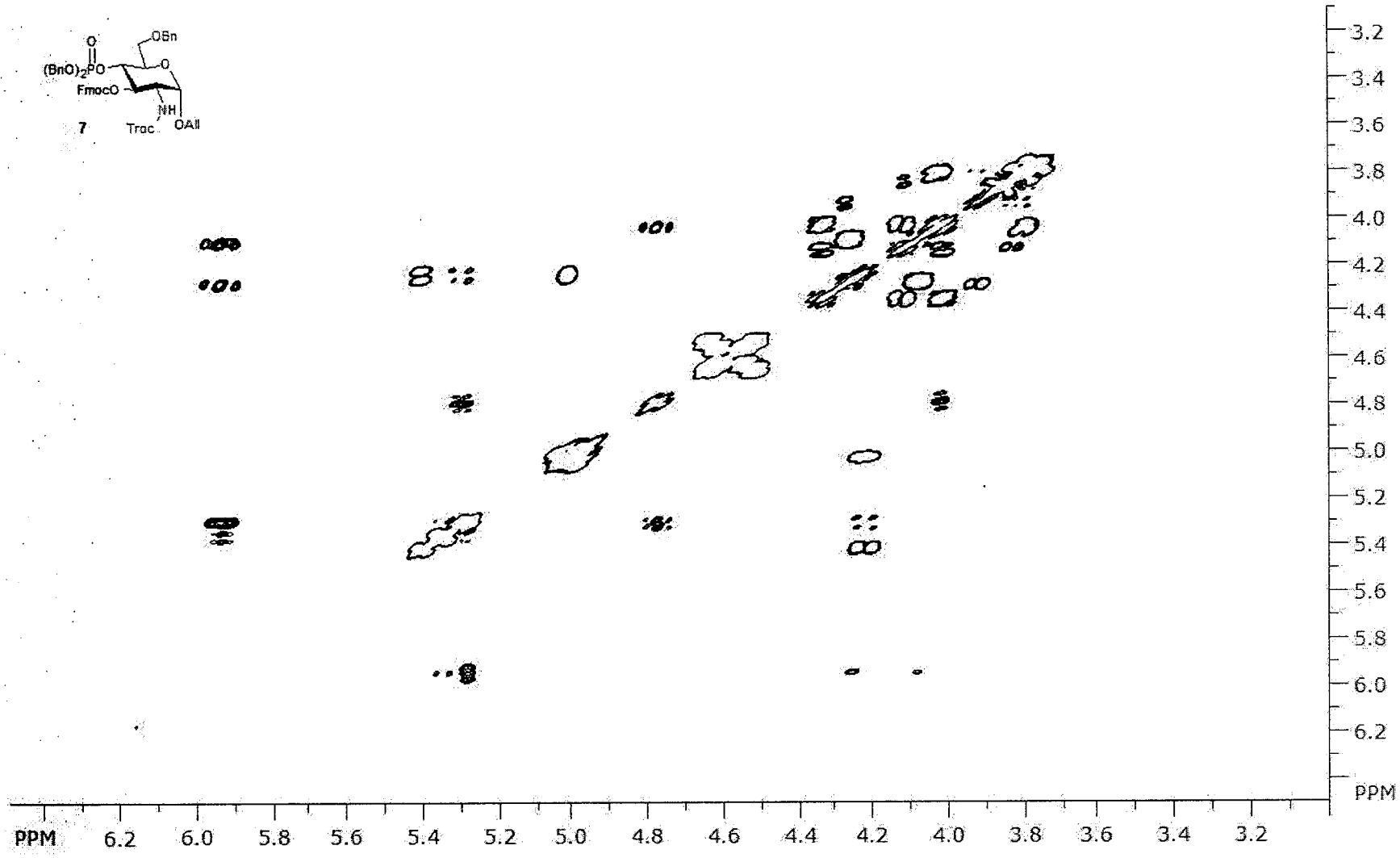
OBn
O
(BnO)2PO
O
FmocO
NH
Troc
OAll
7
PPM
6.2
6.0
5.8
5.6
5.4
5.2
5.0
4.8
4.6
4.4
4.2
4.0
3.8
3.6
3.4
3.2

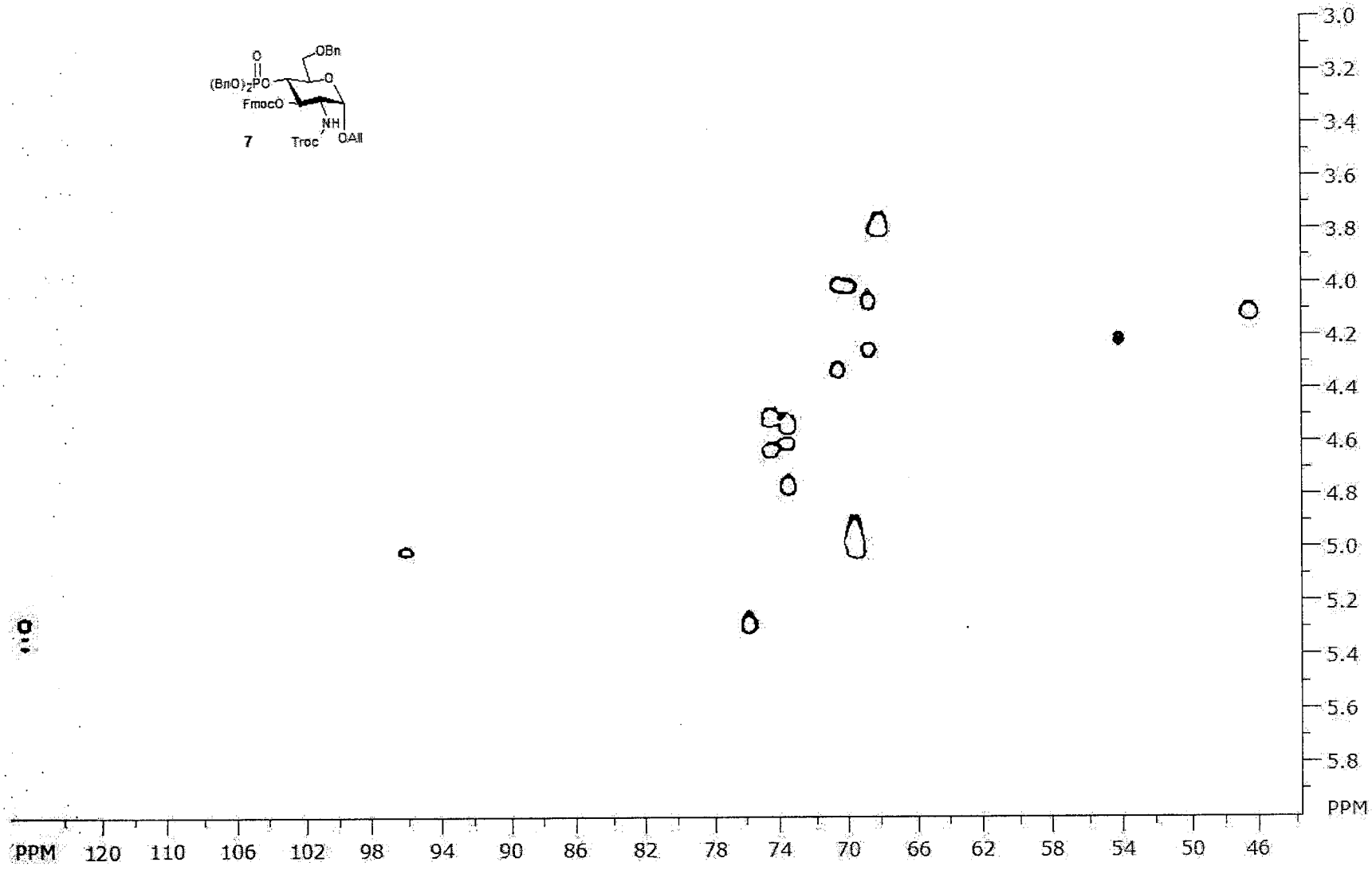
OBn
O
(BnO)2PO
FmocO
NH
Troc
OAll
7
3.0
3.2
3.4
3.6
3.8
4.0
4.2
4.4
4.6
4.8
5.0
5.2
5.4
5.6
5.8
PPM
PPM
120
110
106
102
98
94
90
86
82
78
74
70
66
62
58
54
50
46

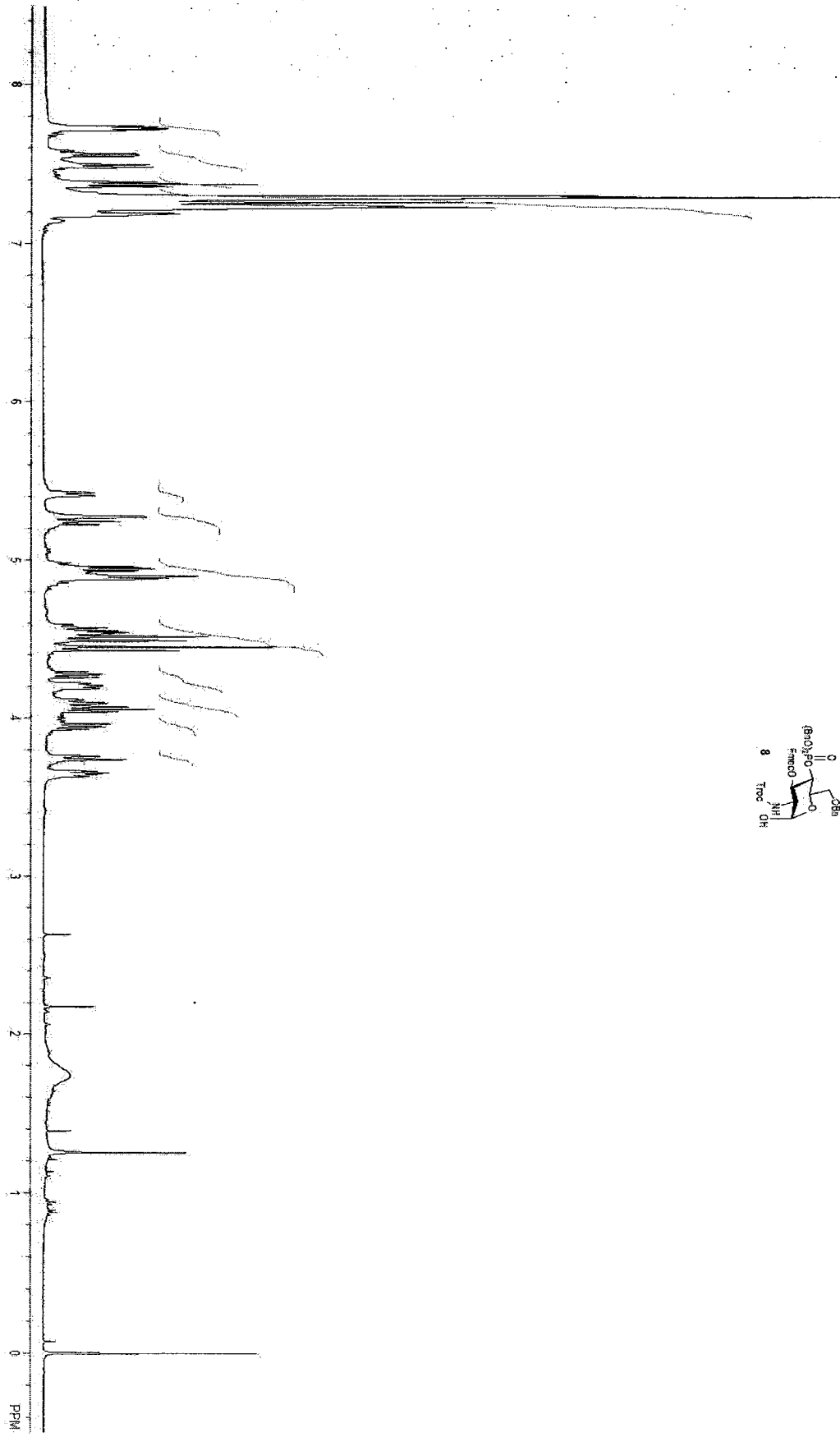
8
7
6
5
4
3
2
1
0
PPM

8
(BnO)2PO
FmocO
O
NH
Troc
OH
OBn

160
140
120
100
80
60
40
20
0
PPM

8
(BnO)2PO
FmocO
Troc
HN
HO
OBn

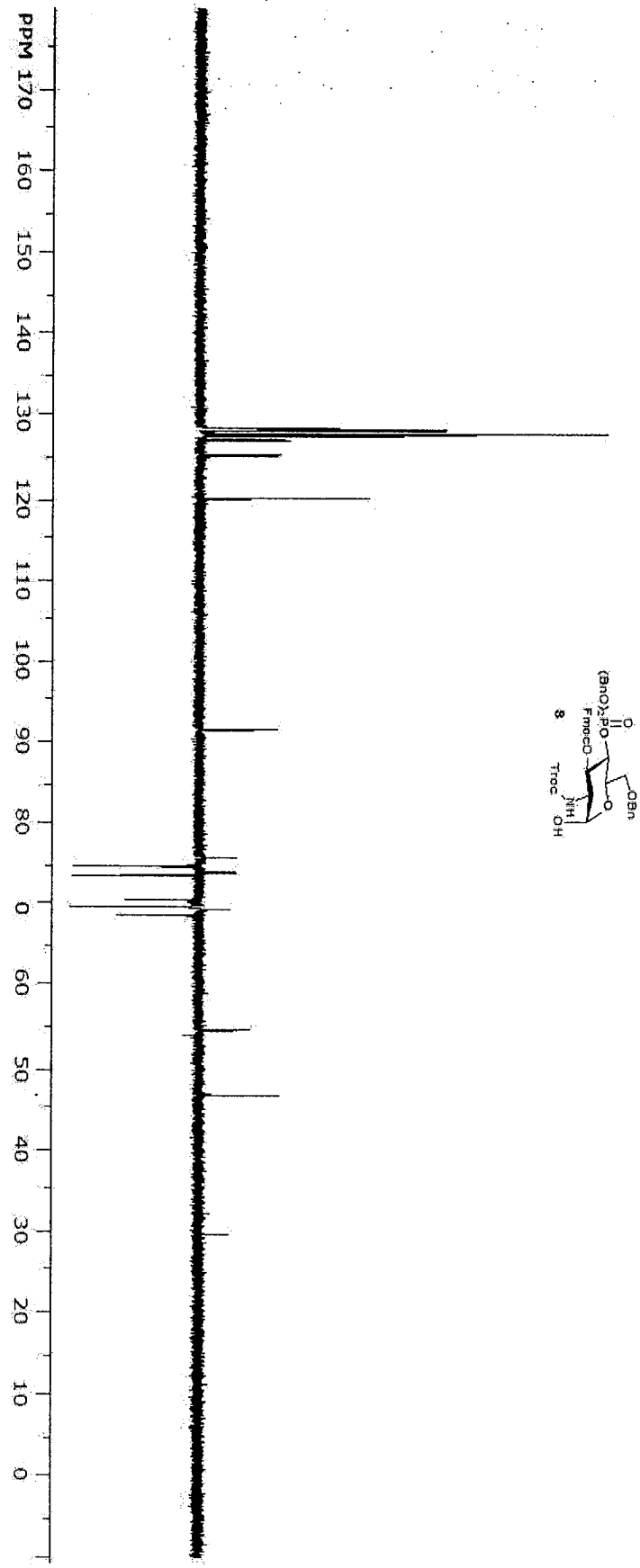
PPM 170
160
150
140
130
120
110
100
90
80
0
60
50
40
30
20
10
0
8
(BnO)2PO
FmocO
Troc
NH
OH
O
OBn

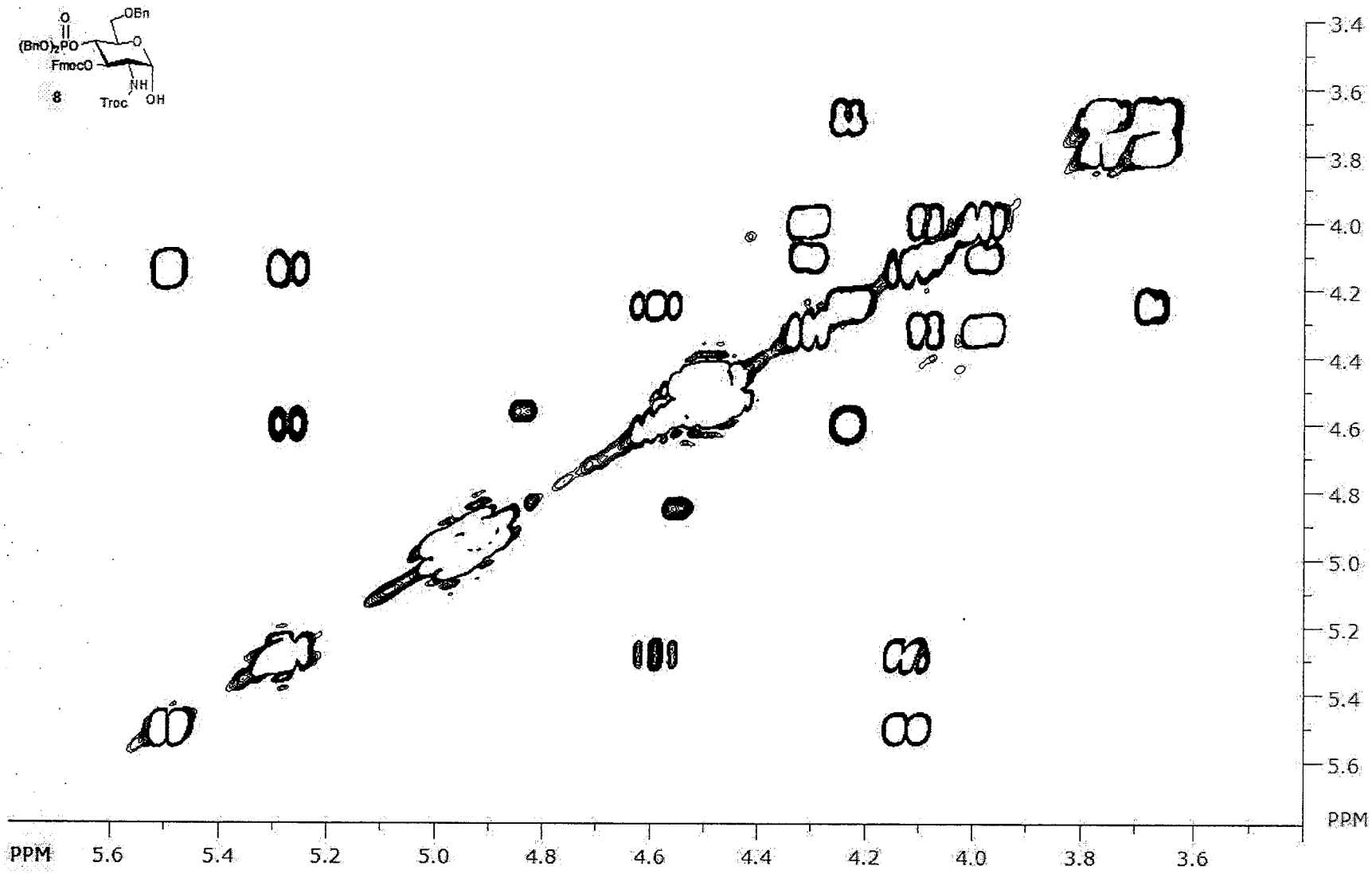
OBn
O
(BnO)2PO
FmocO
NH
Troc
OH
8
PPM
5.6
5.4
5.2
5.0
4.8
4.6
4.4
4.2
4.0
3.8
3.6
3.4

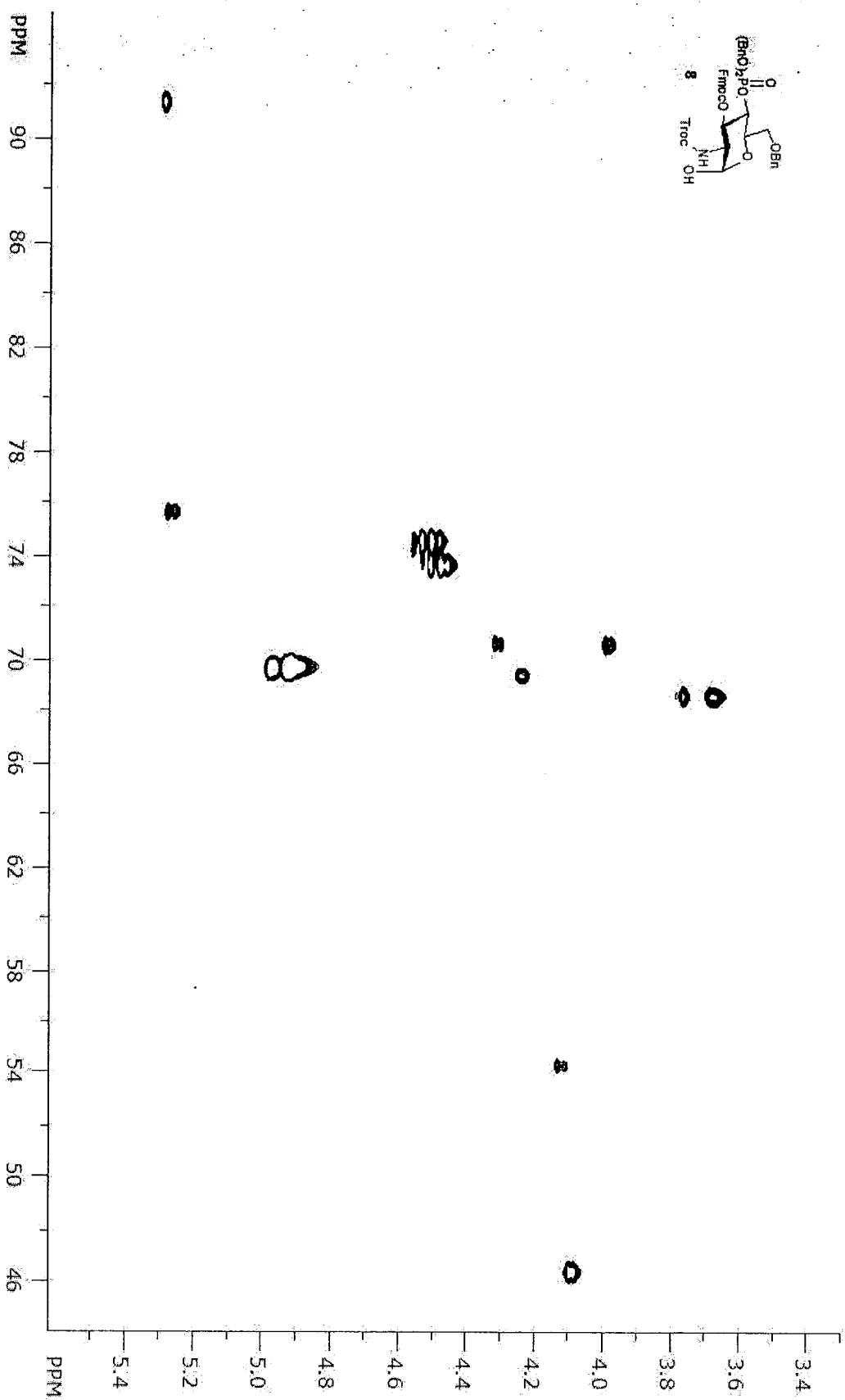
PPM
90
86
82
78
74
70
66
62
58
54
50
46
PPM
5.4
5.2
5.0
4.8
4.6
4.4
4.2
4.0
3.8
3.6
3.4
8
(BnO)2PO
FmocO
Troc
NH
O
OH
OBn

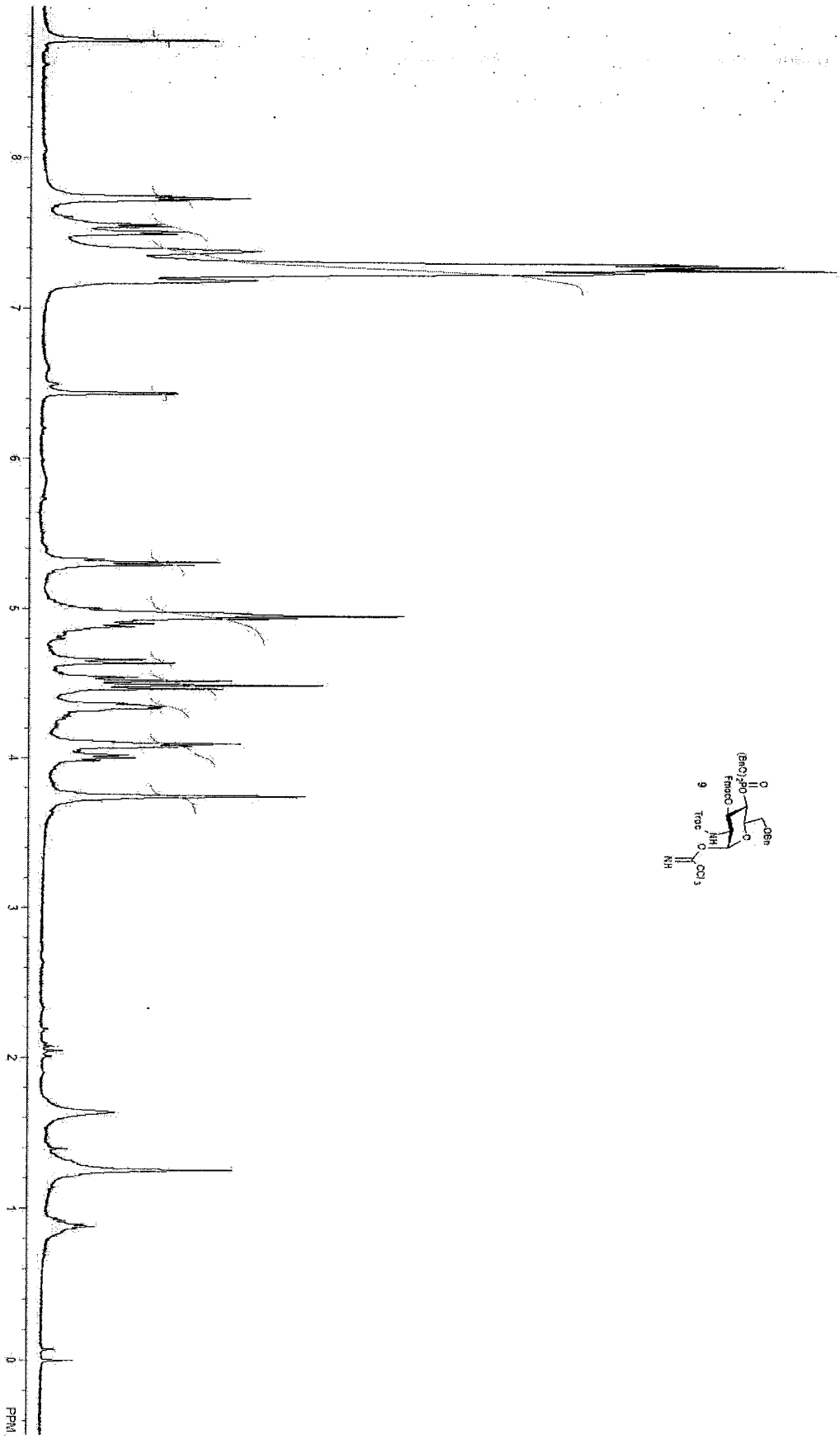
PPM
8
7
6
5
4
3
2
1
0
(BnO)2PO
FmocO
Troc
NH
OBn
NH
CCl3

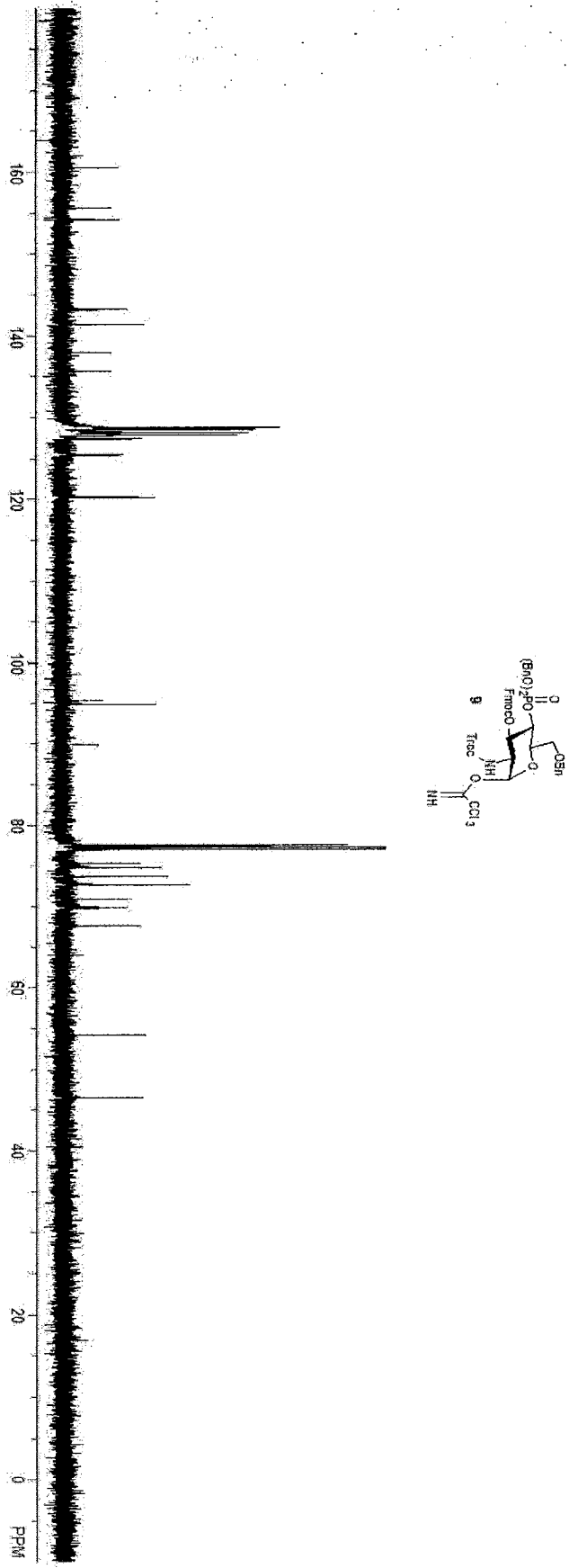
160
140
120
100
80
60
40
20
0
PPM
(BnO)2PO
FmocO
Troc
NH
NH
CCl3
OBn

PPM 170
160
150
140
130
120
110
100
90
80
70
60
50
40
30
20
10
0
(BnO)2PO
FmocO
9
Troc
NH
O
NH
CCl3
OBn
O

PPM
8
7
6
5
4
3
2
1
0

10
(BnO)2PO
MeO
Troc
NH
OBn
OCH2CH2OH

160
140
120
100
80
60
40
20
0
PPM

(BnO)2PO
FmocO
Troc
NH
OBn
OCH2CH2OH

10

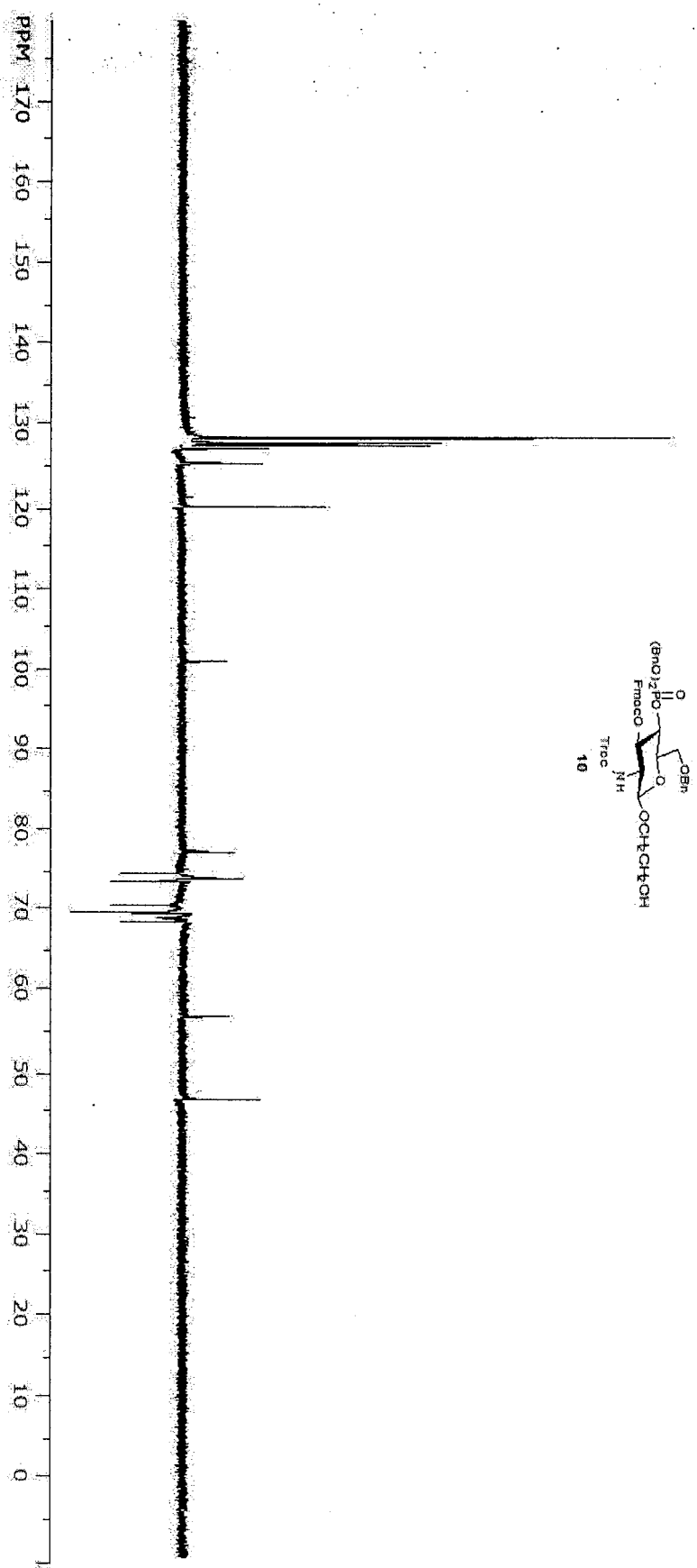
PPM
170
160
150
140
130
120
110
100
90
80
70
60
50
40
30
20
10
0
(BnO)2PO
FmocO
Troc
NH
OBn
OCH2CH2OH
16

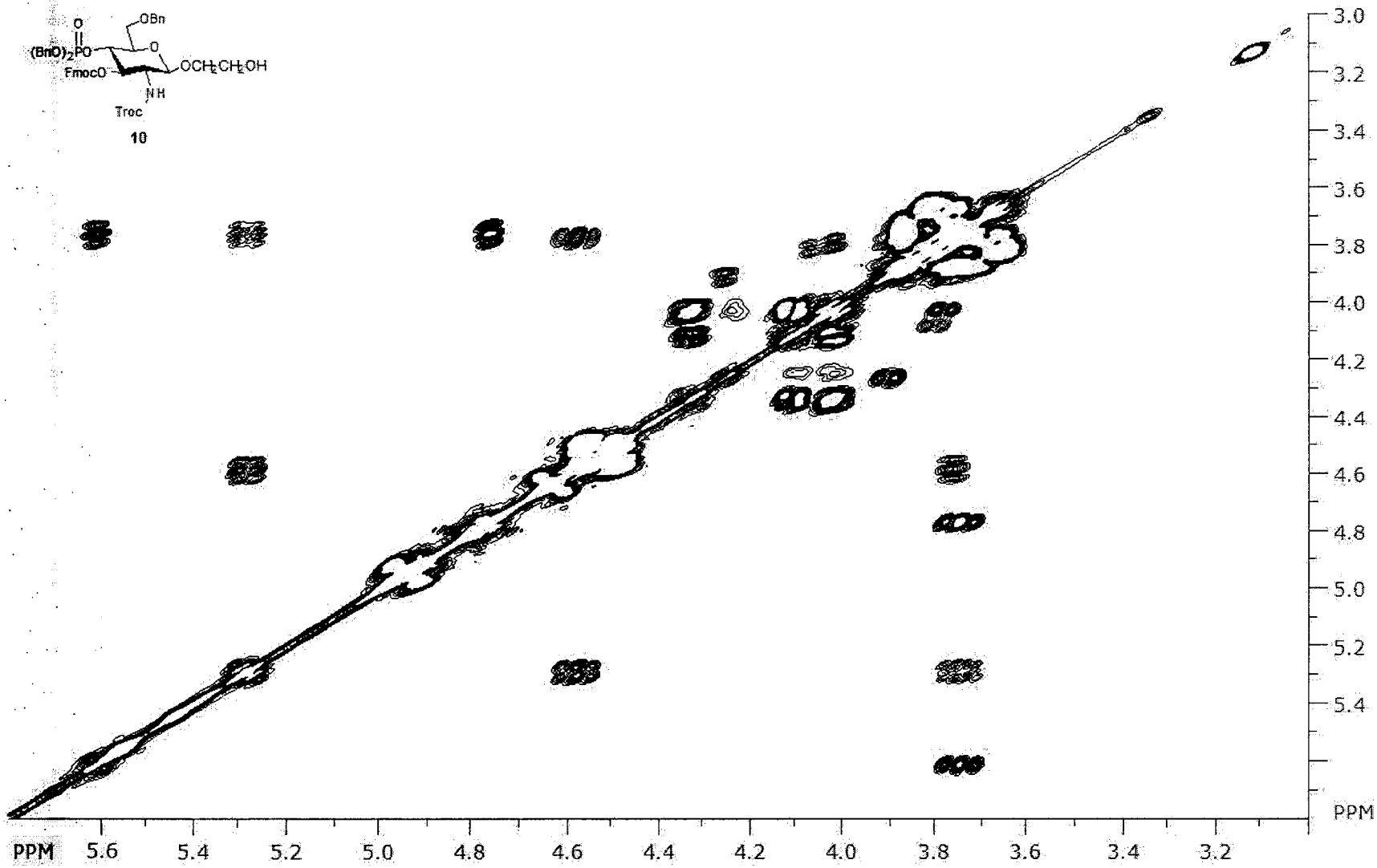
OBn
O
(BnO)2PO
O
OCH2CH2OH
FmocO
NH
Troc
10
3.0
3.2
3.4
3.6
3.8
4.0
4.2
4.4
4.6
4.8
5.0
5.2
5.4
PPM
PPM
5.6
5.4
5.2
5.0
4.8
4.6
4.4
4.2
4.0
3.8
3.6
3.4
3.2

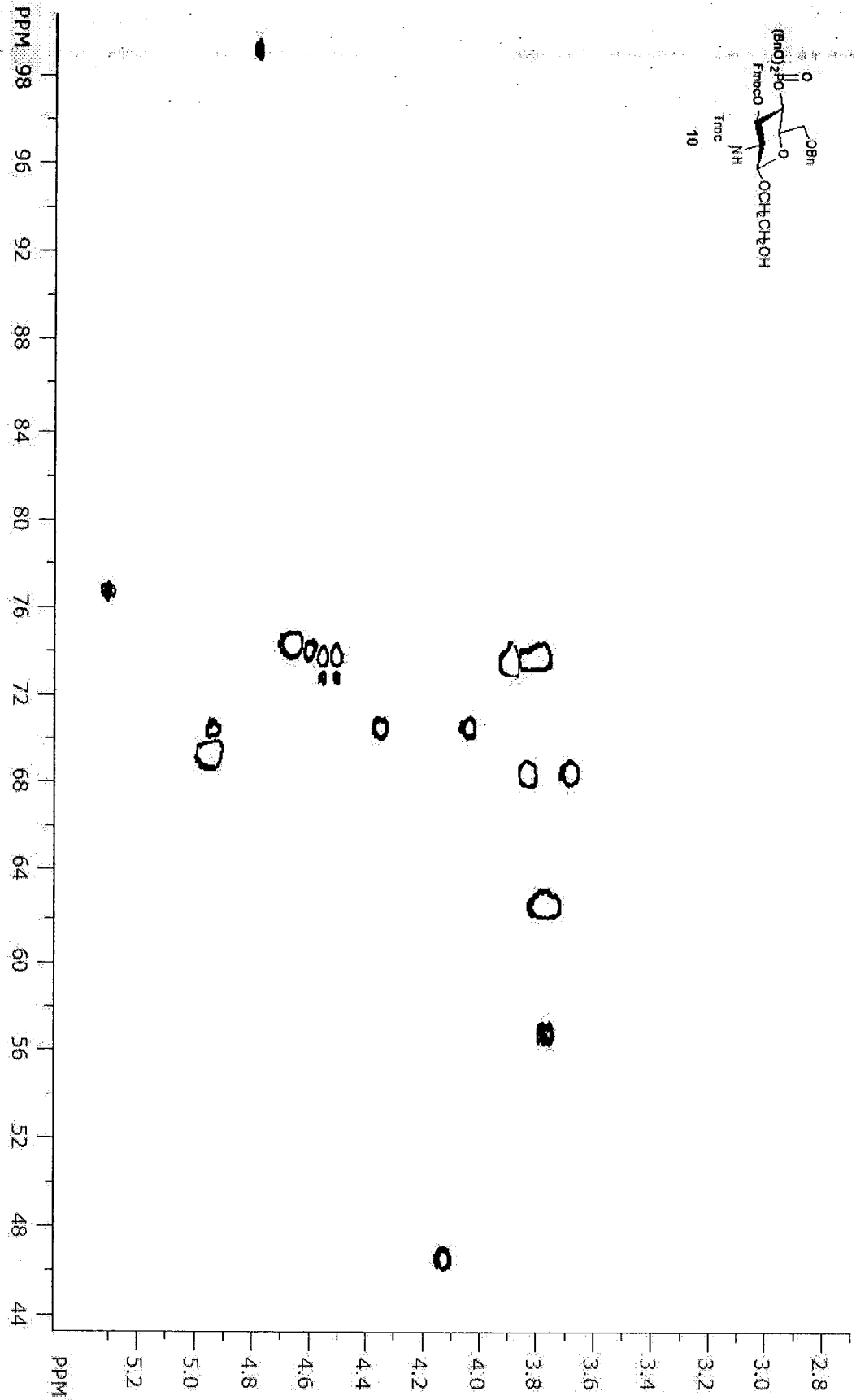
PPM
98
96
92
88
84
80
76
72
68
64
60
56
52
48
44
PPM
5.2
5.0
4.8
4.6
4.4
4.2
4.0
3.8
3.6
3.4
3.2
3.0
2.8
(BnO)2PO
FmocO
OBn
O
Troc
N
H
OCH2CH2OH
10

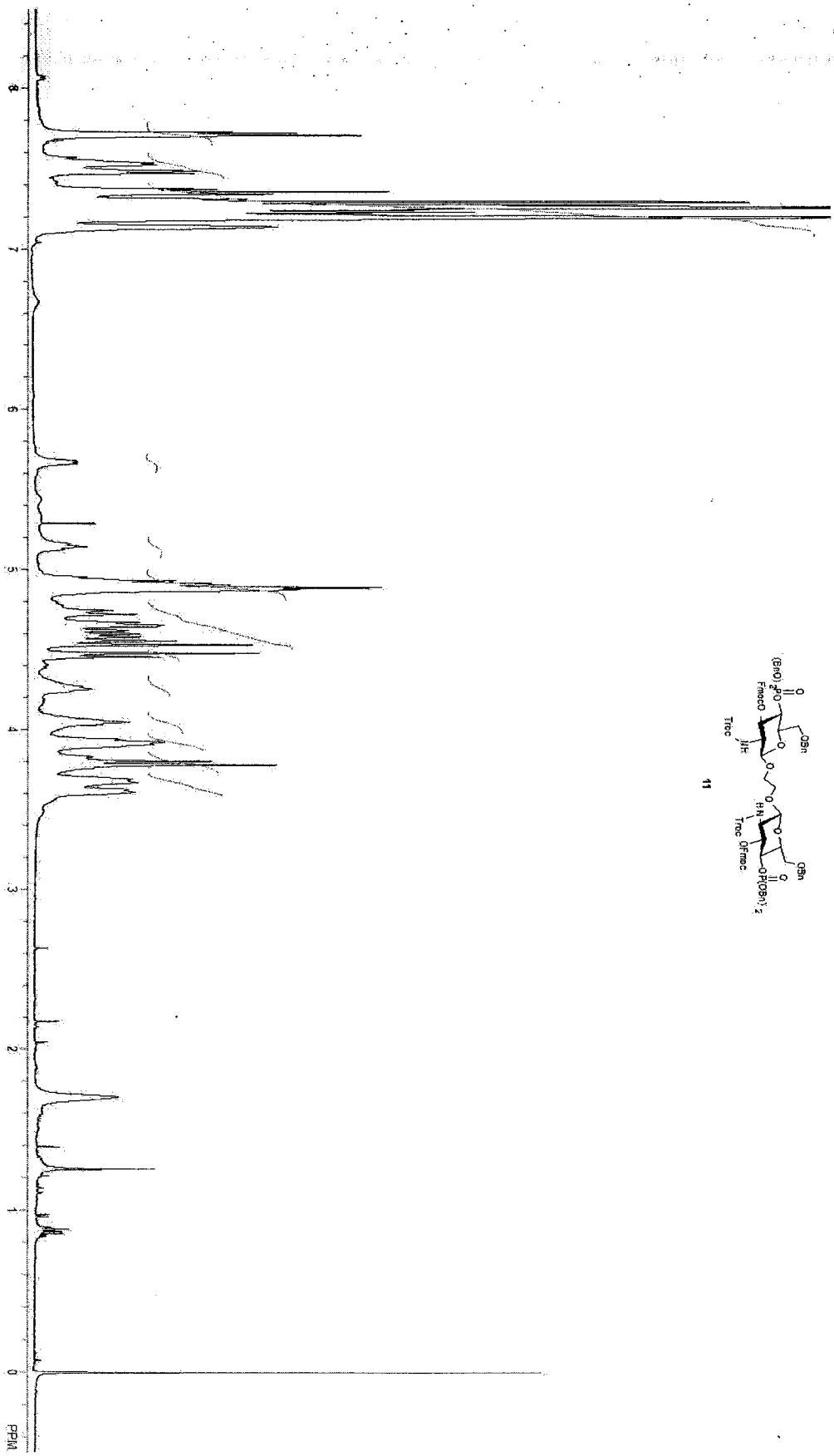

11

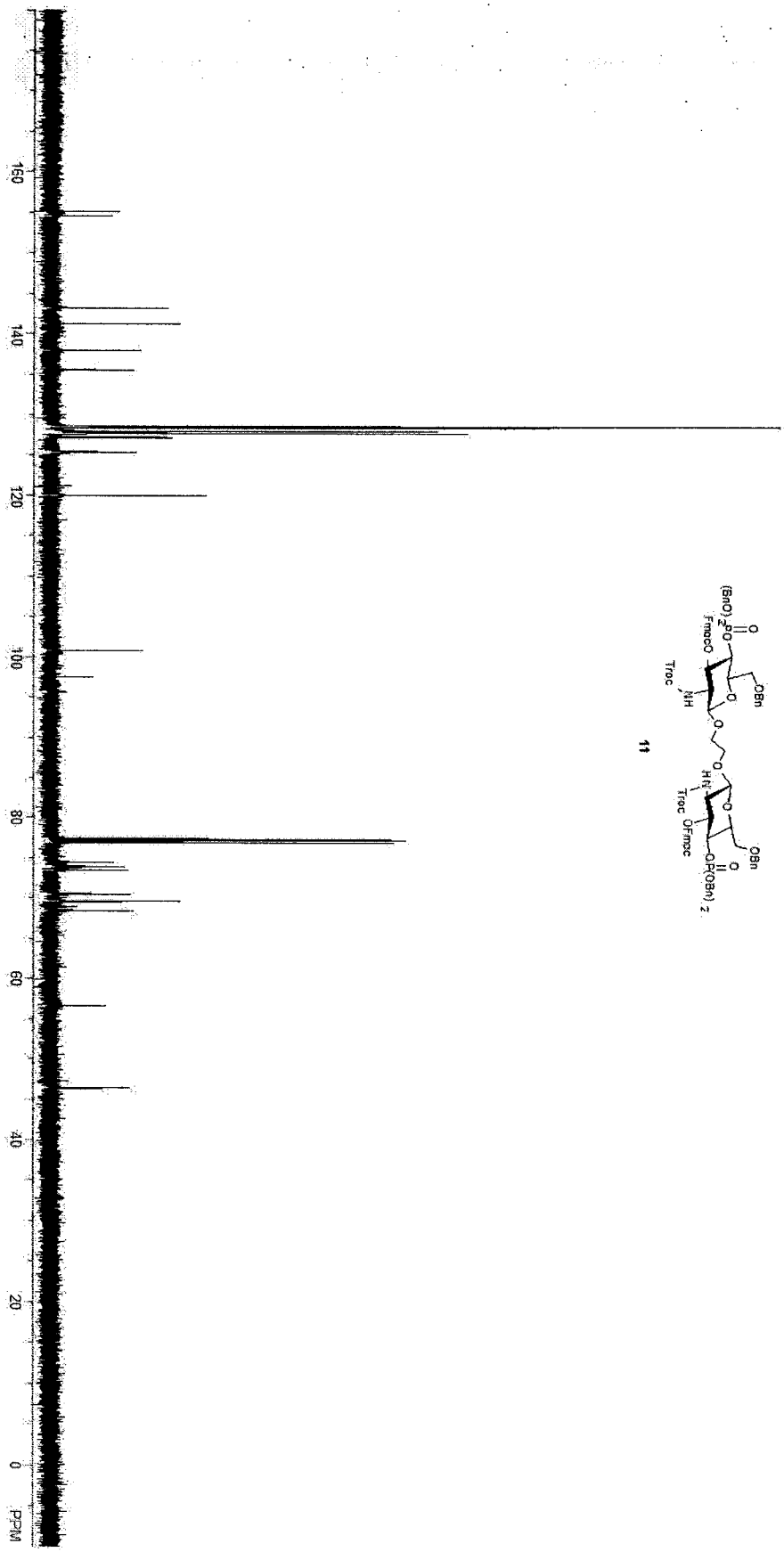
160
140
120
100
80
60
40
20
0
PPM
11
(BnO)2P
O
FmocO
Troc
NH
OBn
OFmoc
OP(OBn)2

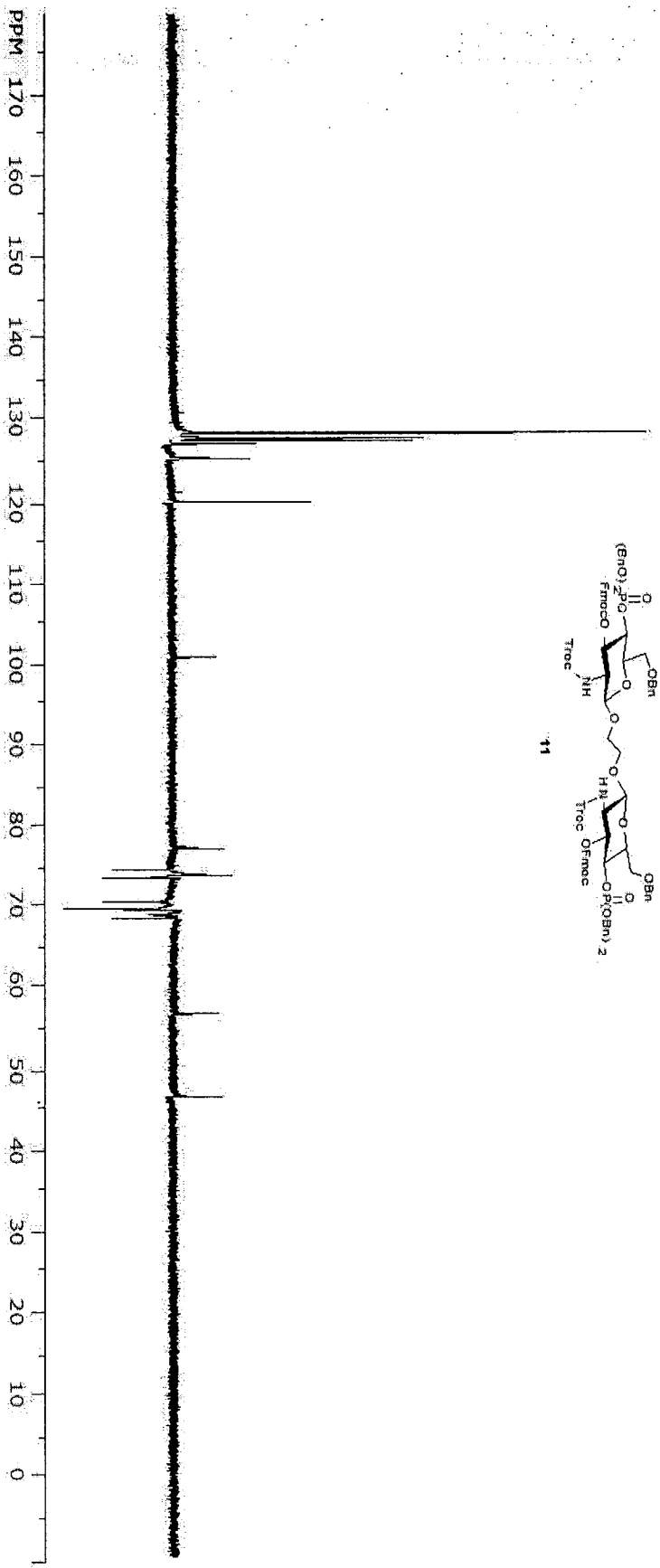
PPM
170
160
150
140
130
120
110
100
90
80
70
60
50
40
30
20
10
0
(BnO)2PO
FmocO
Troc
NH
OBn
O
O
O
O
H N
Troc
OFmoc
OBn
O
OP(OBn)2
11

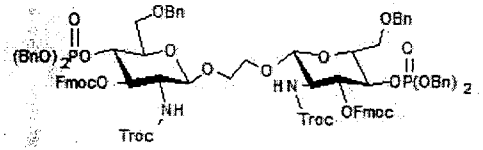
OBn
OBn
(BnO)2PO
FmocO
NH
Troc
HN
Troc
OFmoc
OP(OBn)2

11

3.0
3.2
3.4
3.6
3.8
4.0
4.2
4.4
4.6
4.8
5.0
5.2
5.4
5.6
5.8
PPM
PPM 5.8 5.6 5.4 5.2 5.0 4.8 4.6 4.4 4.2 4.0 3.8 3.6 3.4 3.2

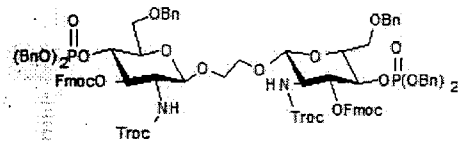
OBn
O
(BnO)2PO
FmocO
O
NH
Troc
O
HN
OBn
O
OP(OBn)2
Troc
OFmoc

11

3.4
3.6
3.8
4.0
4.2
4.4
4.6
4.8
5.0
5.2
PPM
PPM 98
96
92
88
84
80
76
72
68
64
60
56
52
48
44

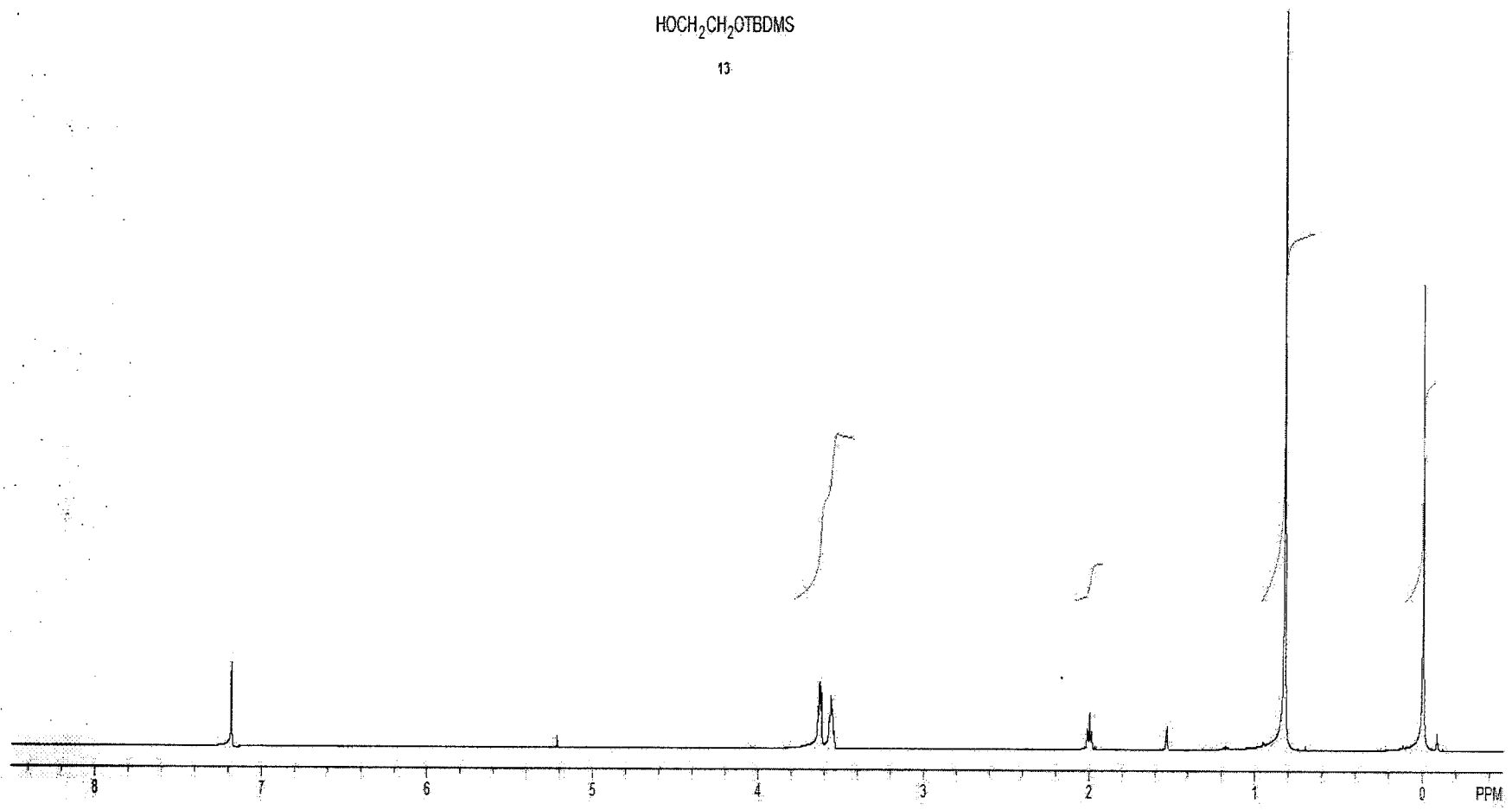
HOCH2CH2OTBDMS
13
8
7
6
5
4
3
2
1
0
PPM

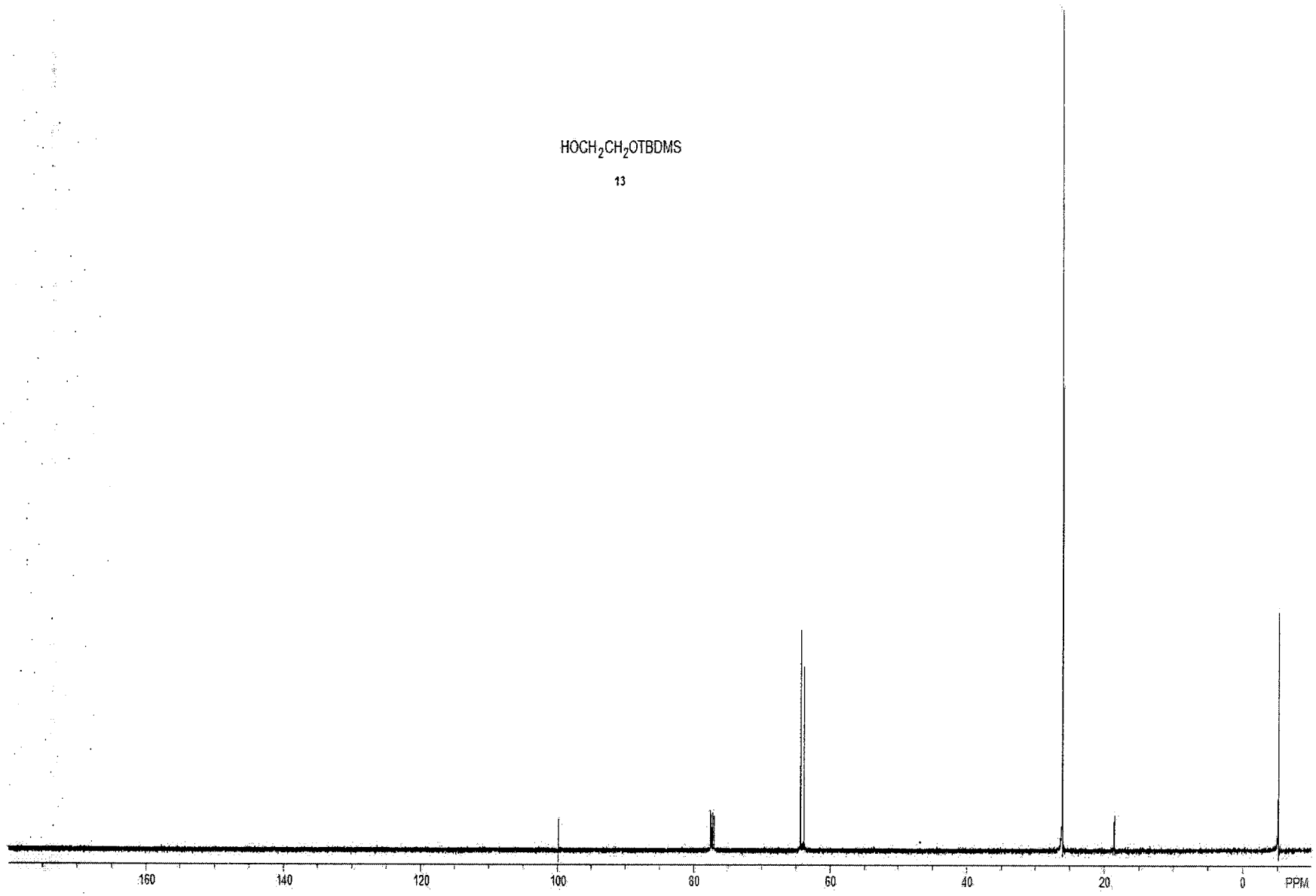
HOCH2CH2OTBDMS
13
160
140
120
100
80
60
40
20
0
PPM

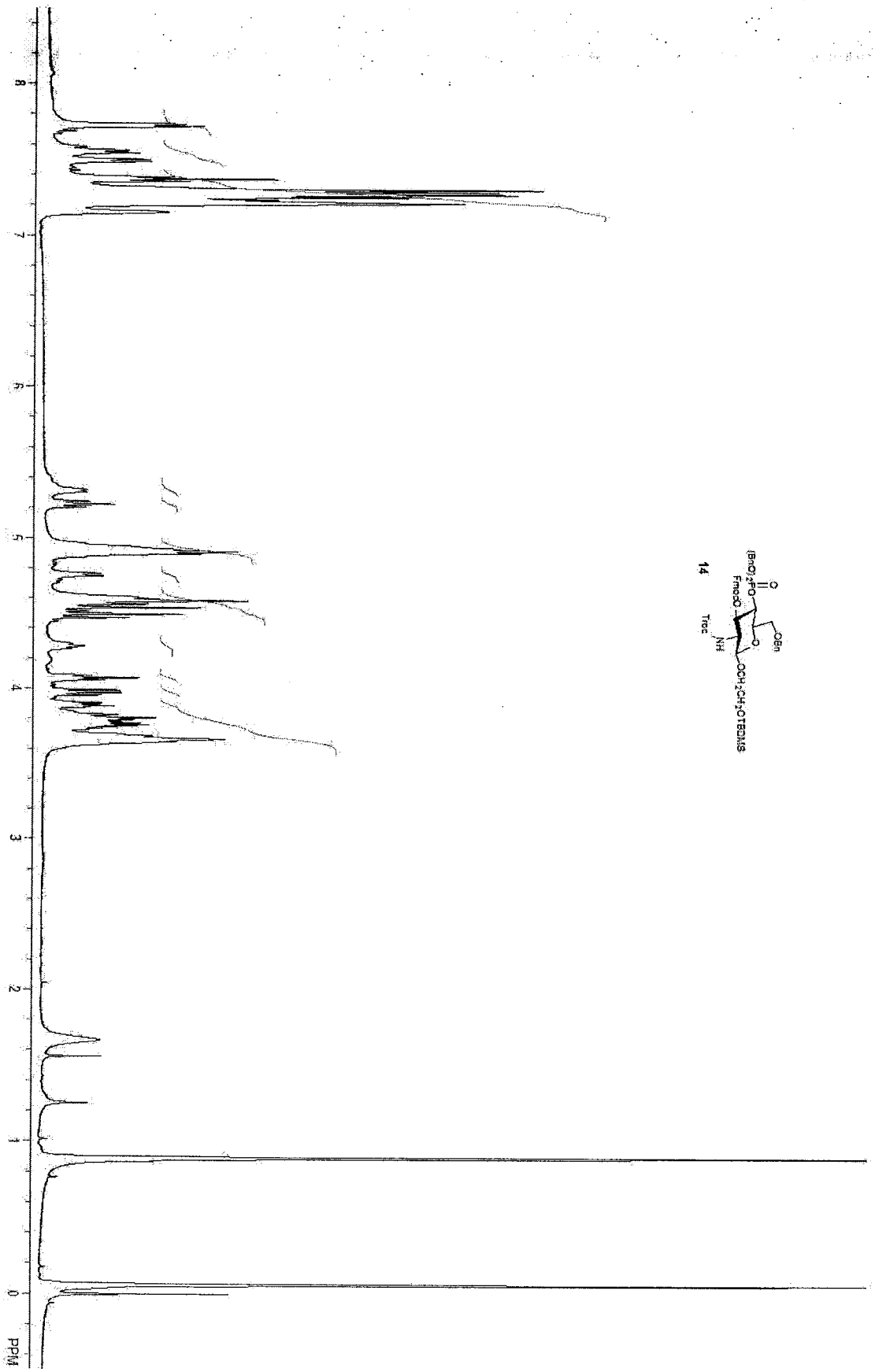
14
Troc
NH
OBn
PPM

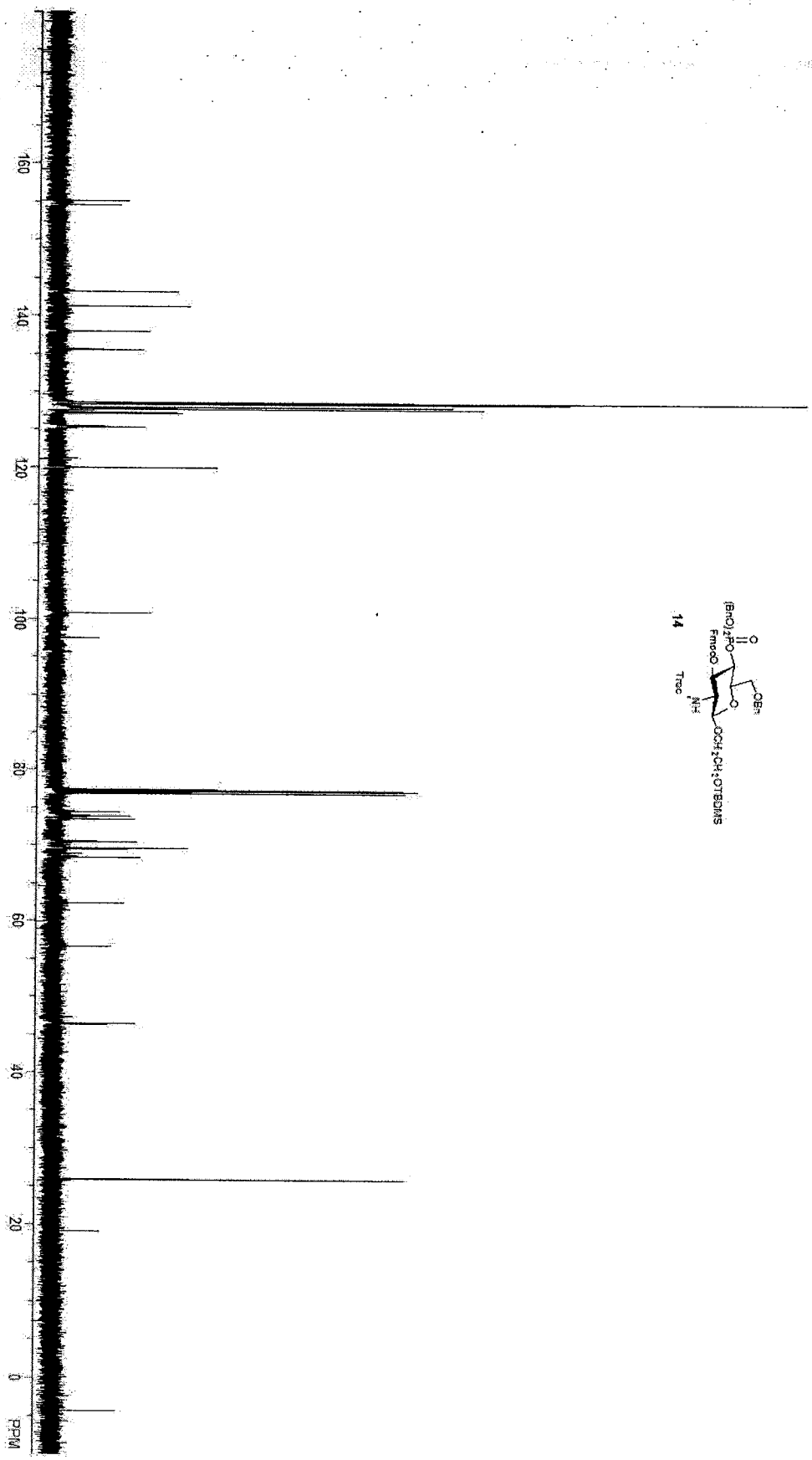
160
140
120
100
80
60
40
20
0
PPM

14
(BnO)2PO
FmocO
Troc
NH
OBn
OCH2CH2OTBSMS

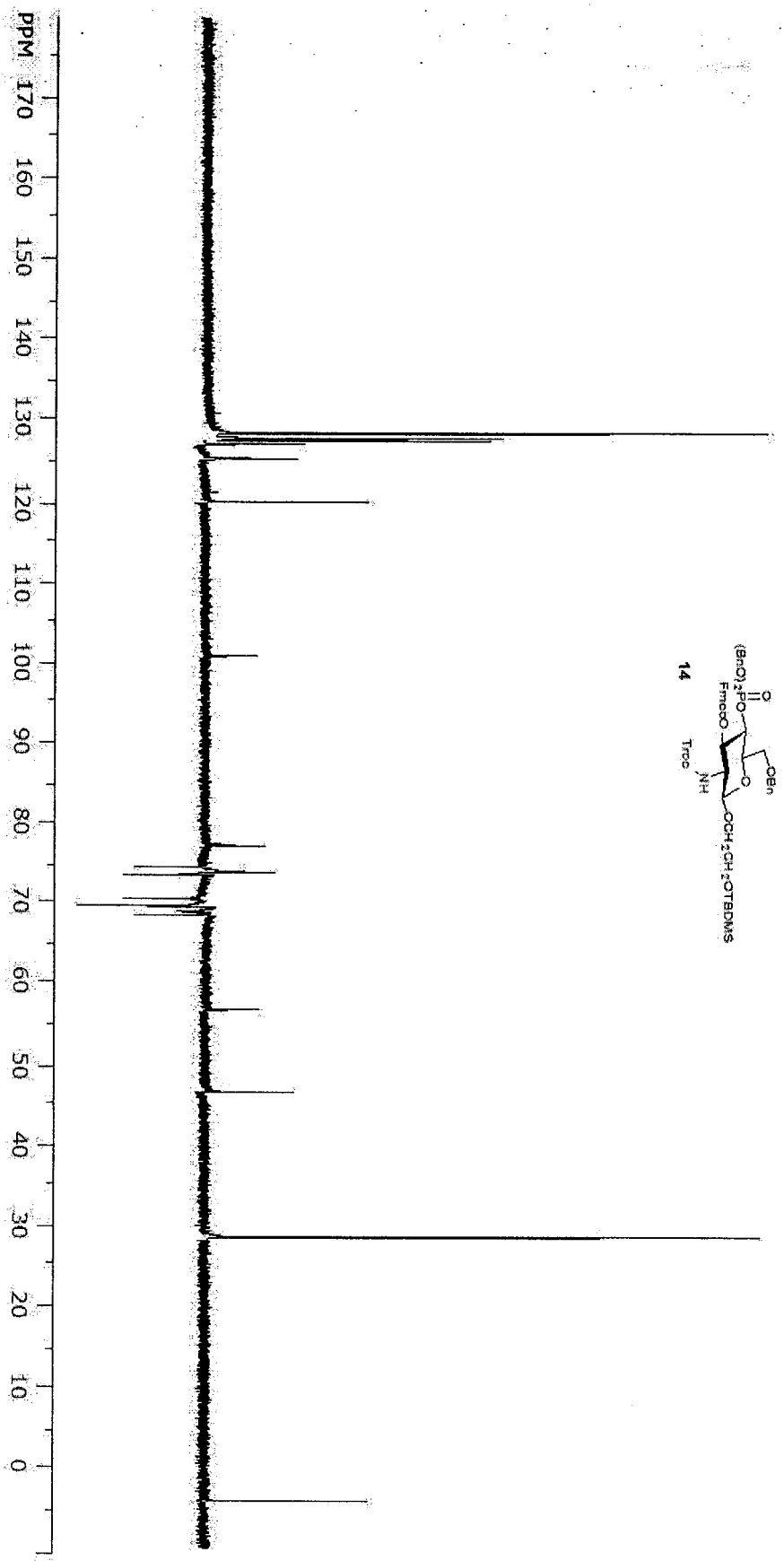
PPM
170
160
150
140
130
120
110
100
90
80
70
60
50
40
30
20
10
0
14
(BnO)2PO
FmocO
Troc
NH
OBn
OCH2CH2OTBDMS

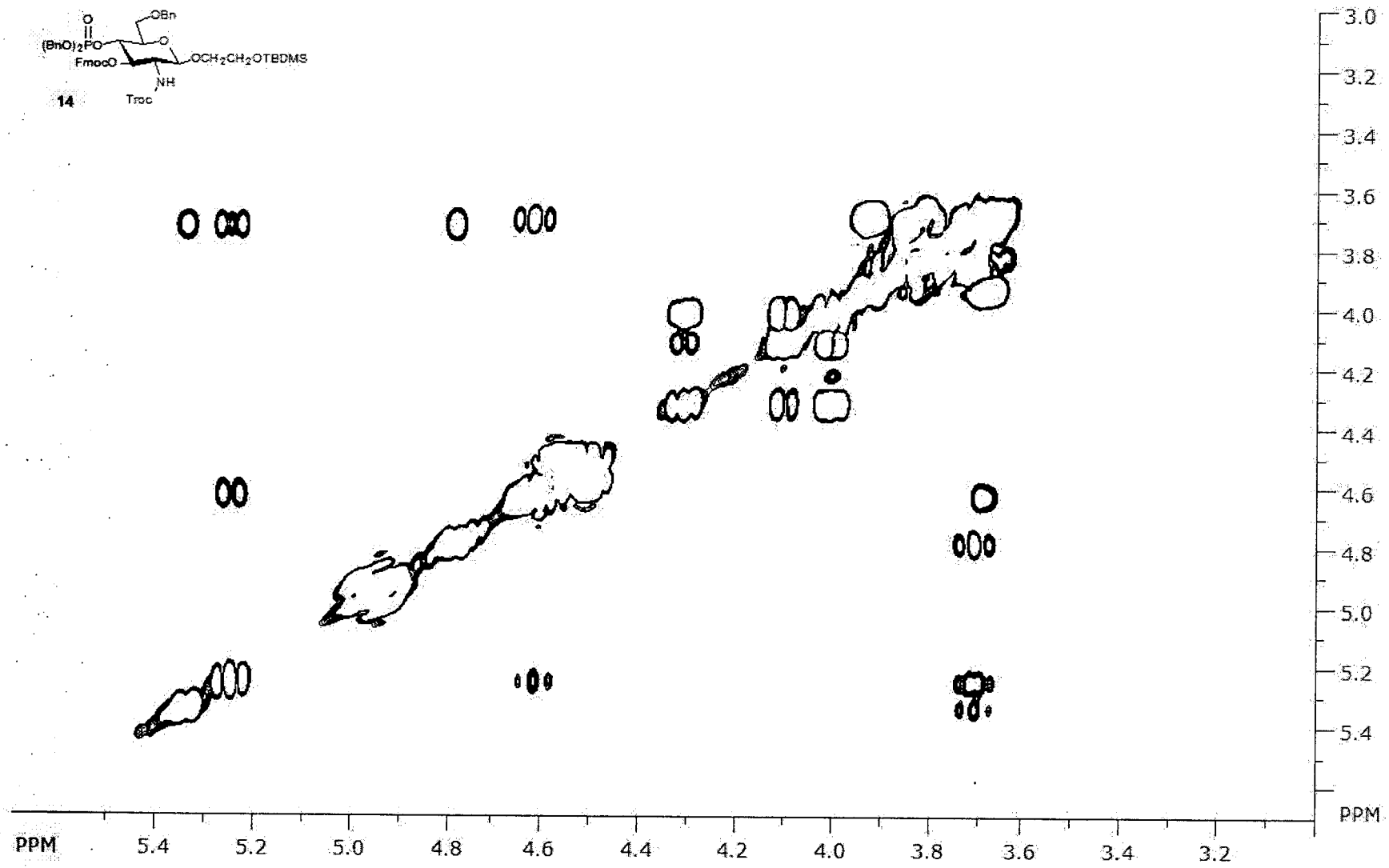
OBn
O
(BnO)2PO
O
FmocO
OCH2CH2OTBDMS
NH
Troc
14
3.0
3.2
3.4
3.6
3.8
4.0
4.2
4.4
4.6
4.8
5.0
5.2
5.4
PPM
PPM
5.4
5.2
5.0
4.8
4.6
4.4
4.2
4.0
3.8
3.6
3.4
3.2

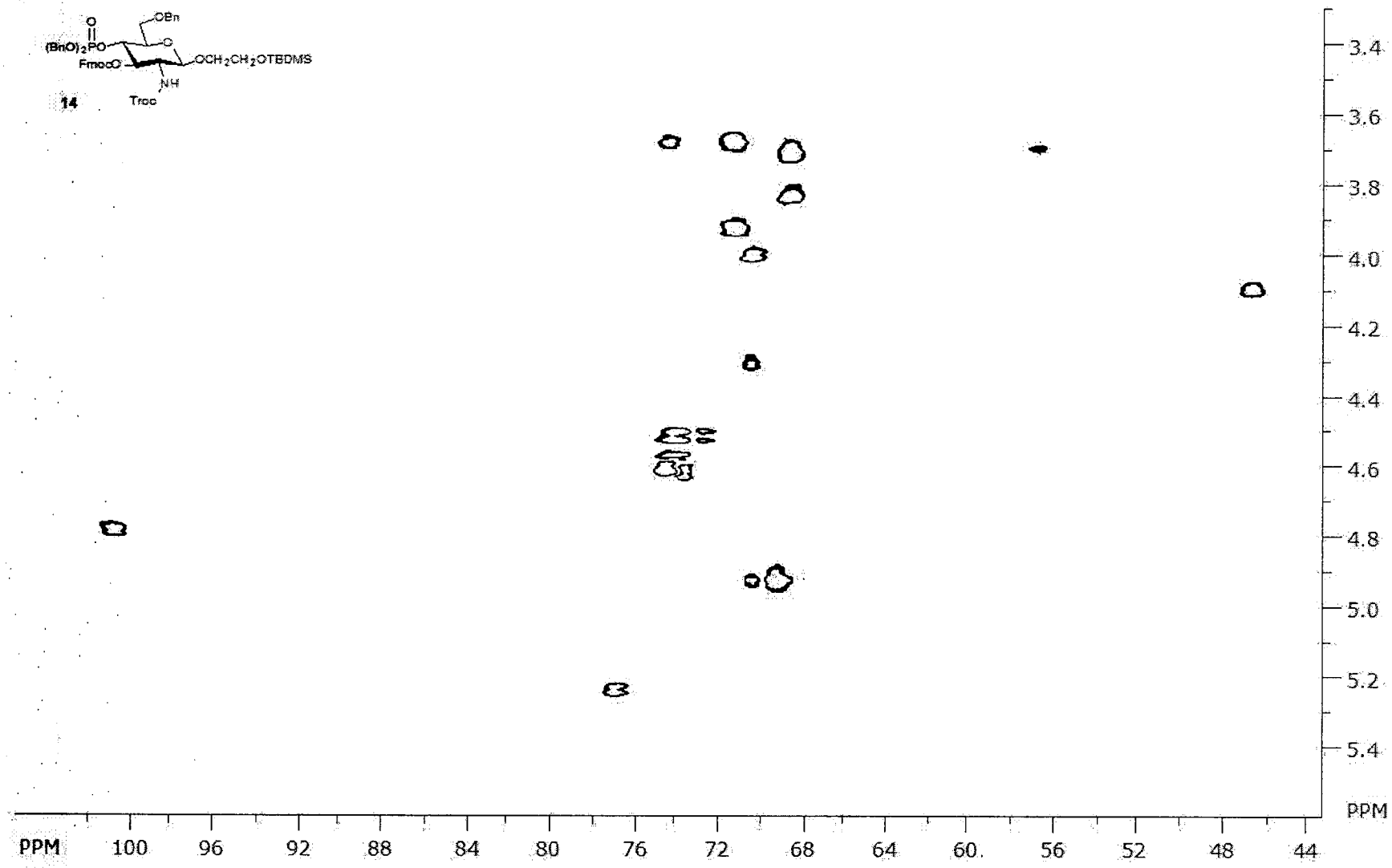
OBn
(BnO)2PO
FmocO
OCH2CH2OTBDMS
NH
Troc
14
3.4
3.6
3.8
4.0
4.2
4.4
4.6
4.8
5.0
5.2
5.4
PPM
PPM
100
96
92
88
84
80
76
72
68
64
60
56
52
48
44

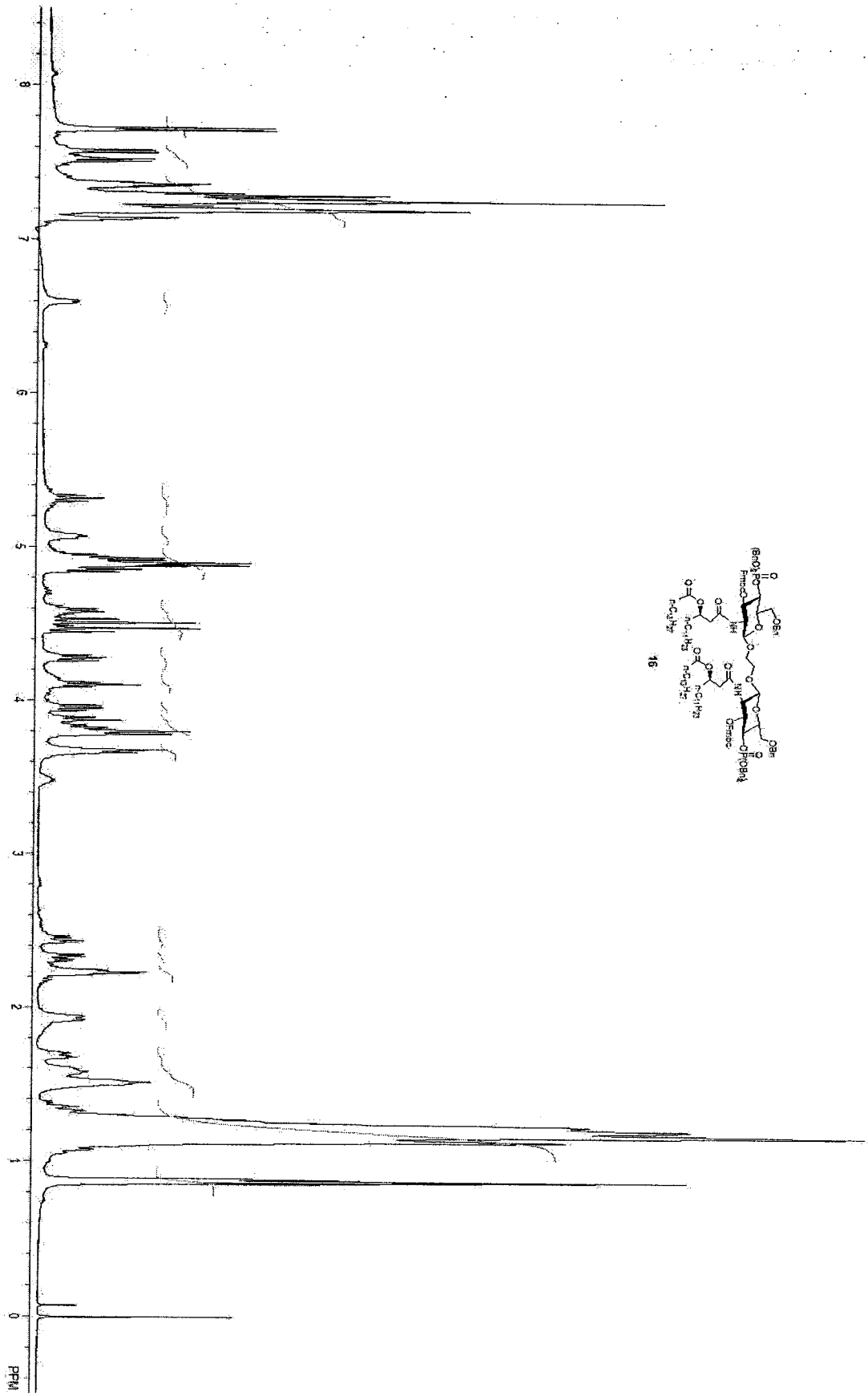

16

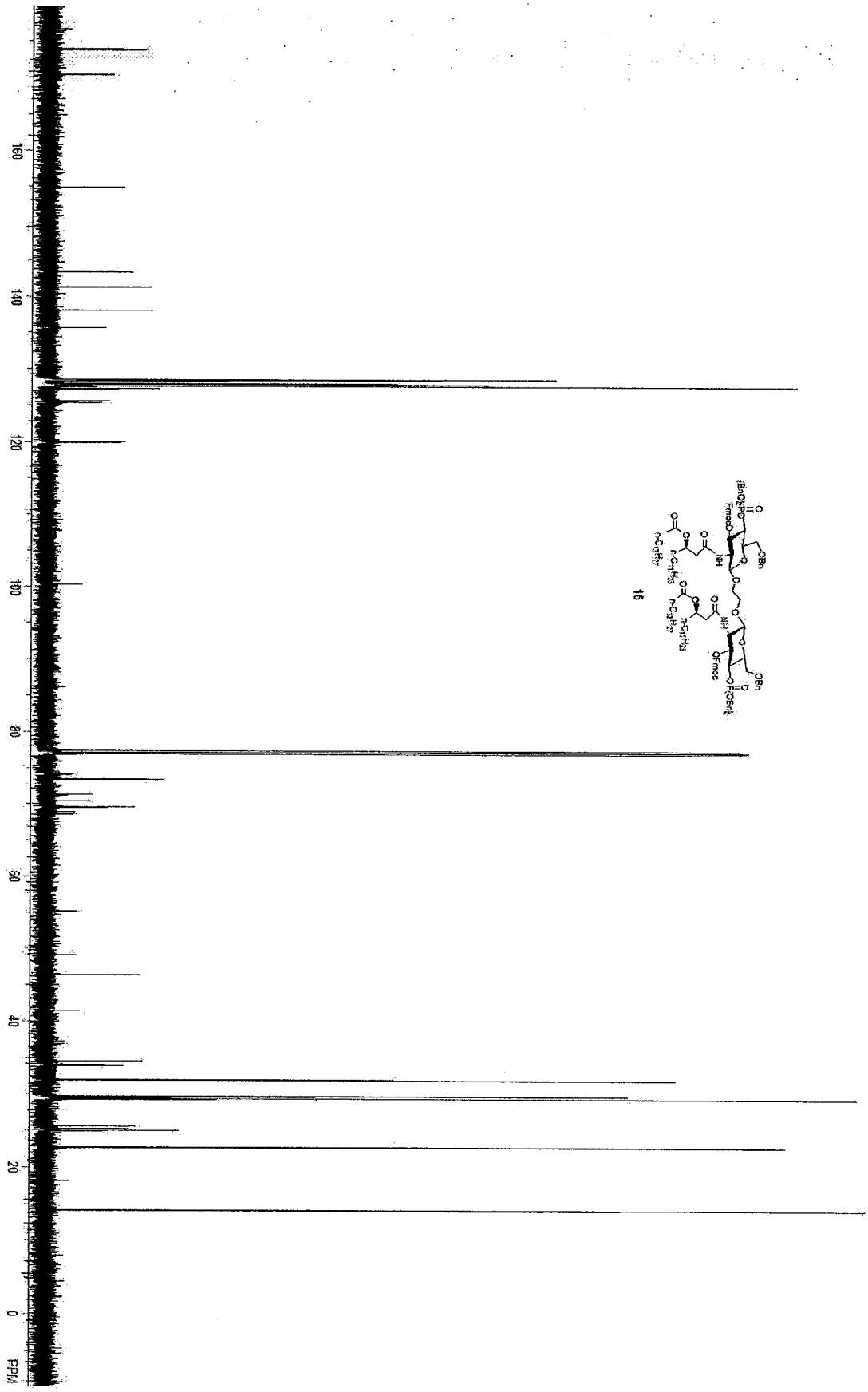

16

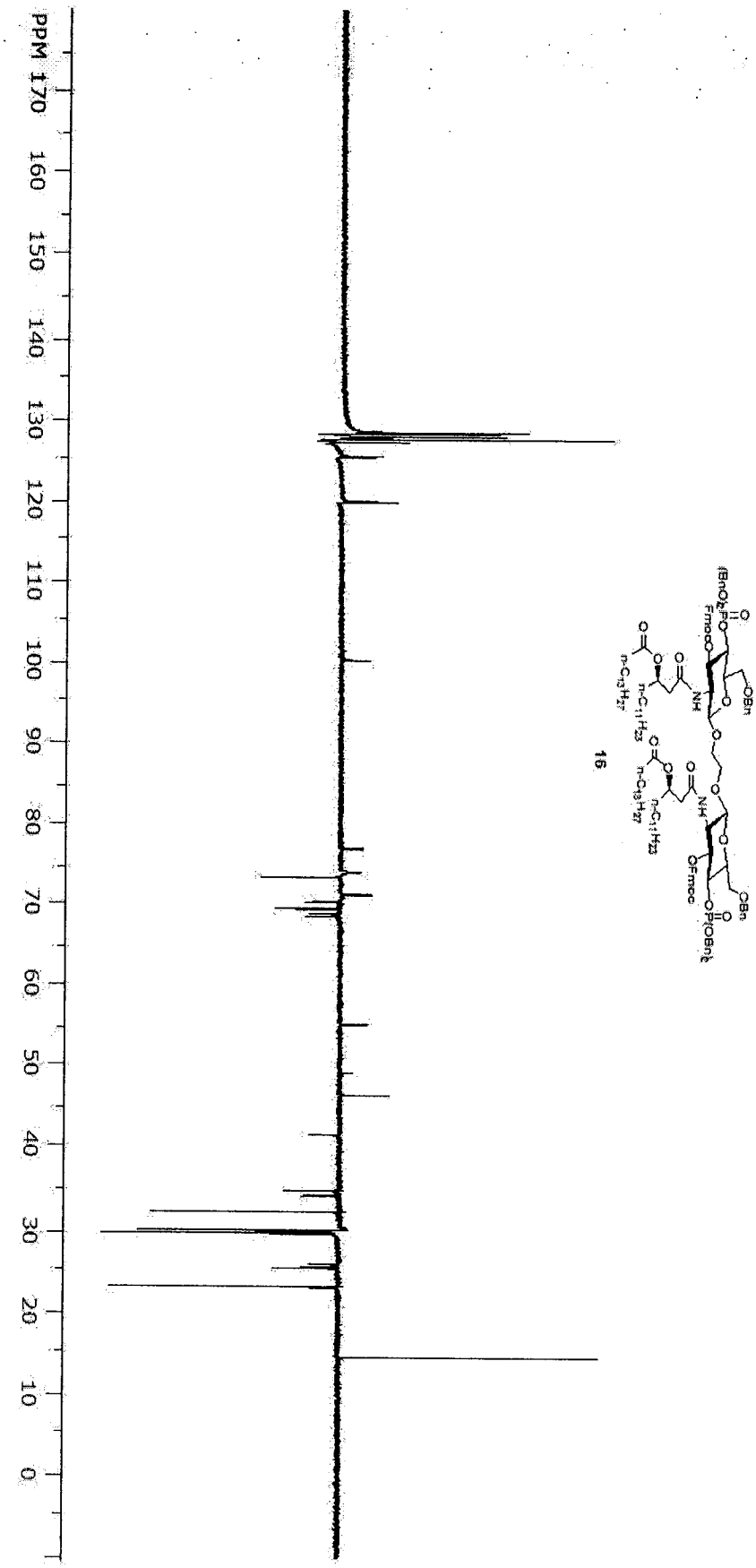

16

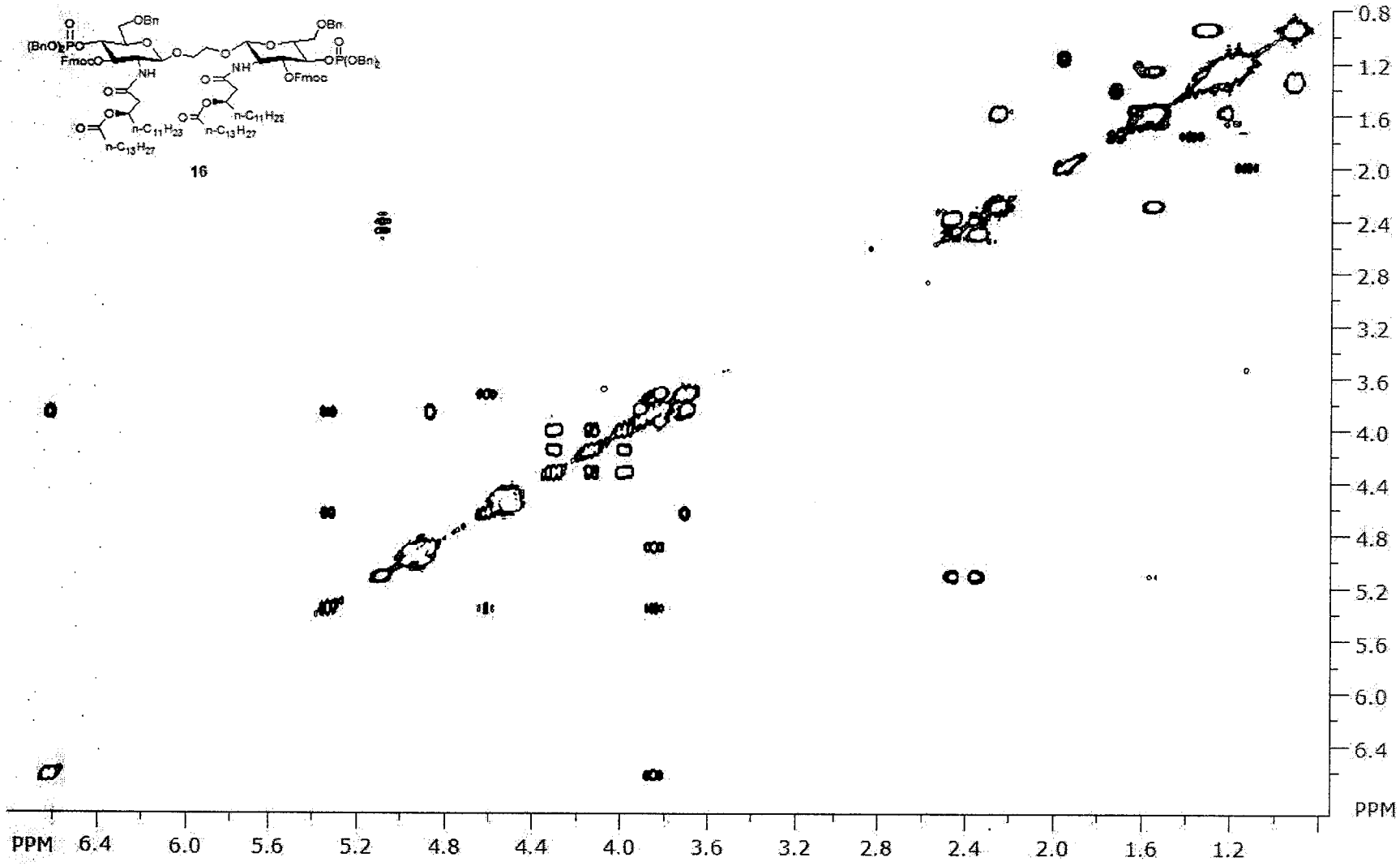
16
PPM
6.4
6.0
5.6
5.2
4.8
4.4
4.0
3.6
3.2
2.8
2.4
2.0
1.6
1.2
0.8

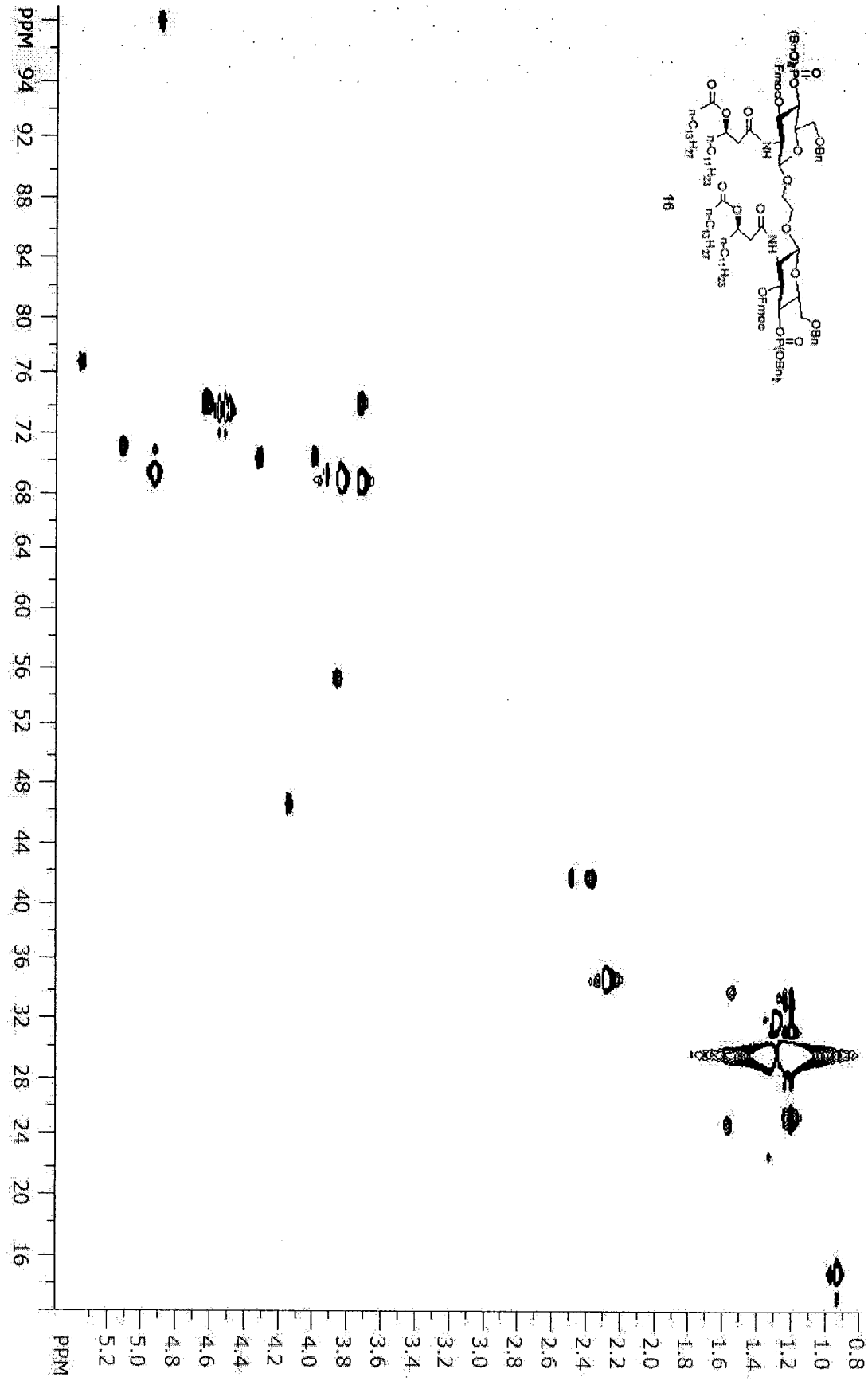
PPM
94
92
88
84
80
76
72
68
64
60
56
52
48
44
40
36
32
28
24
20
16
PPM
5.2
5.0
4.8
4.6
4.4
4.2
4.0
3.8
3.6
3.4
3.2
3.0
2.8
2.6
2.4
2.2
2.0
1.8
1.6
1.4
1.2
1.0
0.8

16

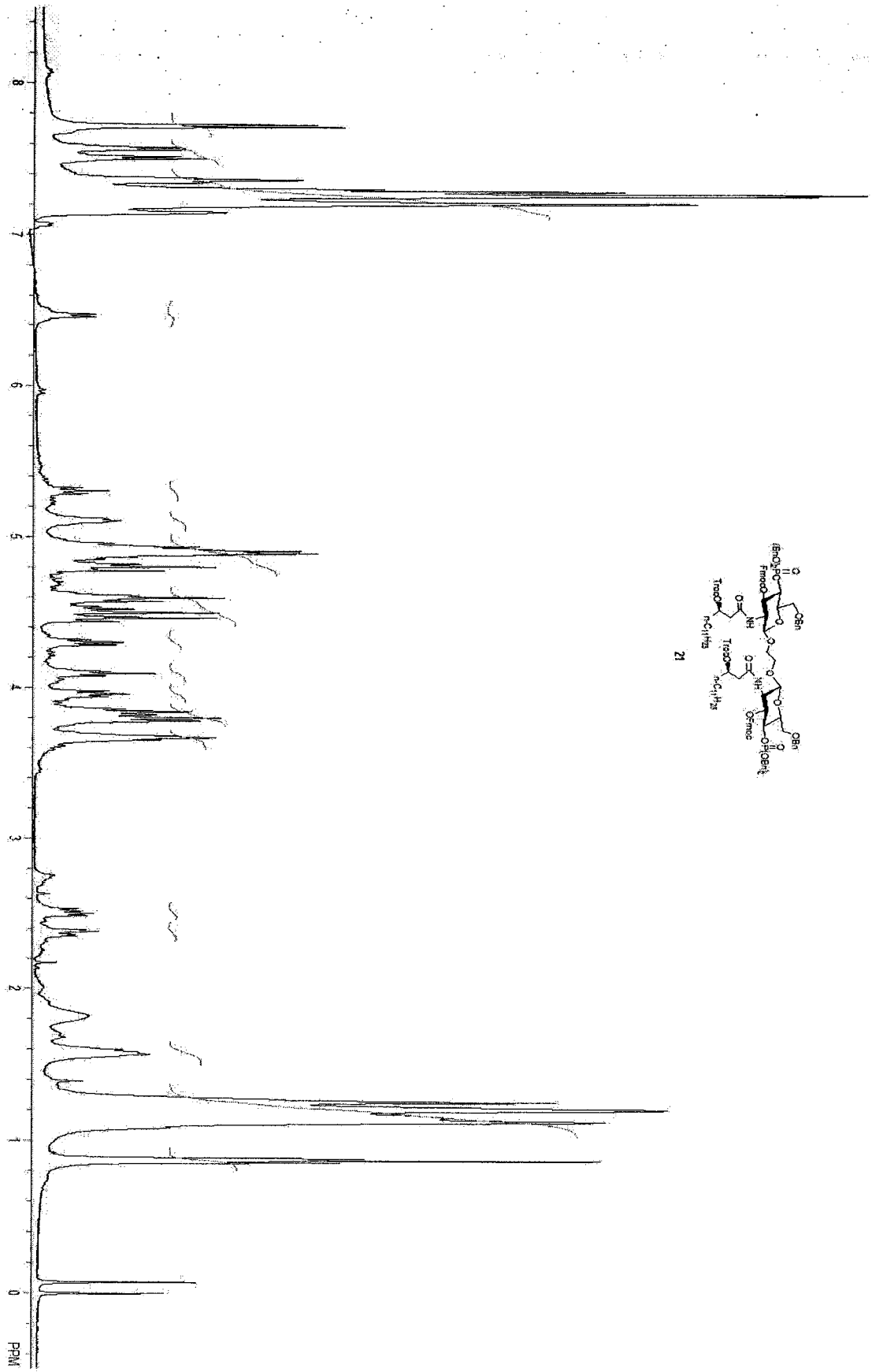

21

21

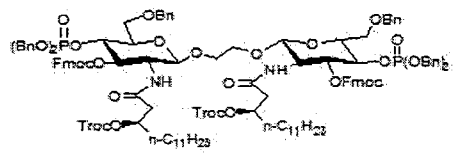

21

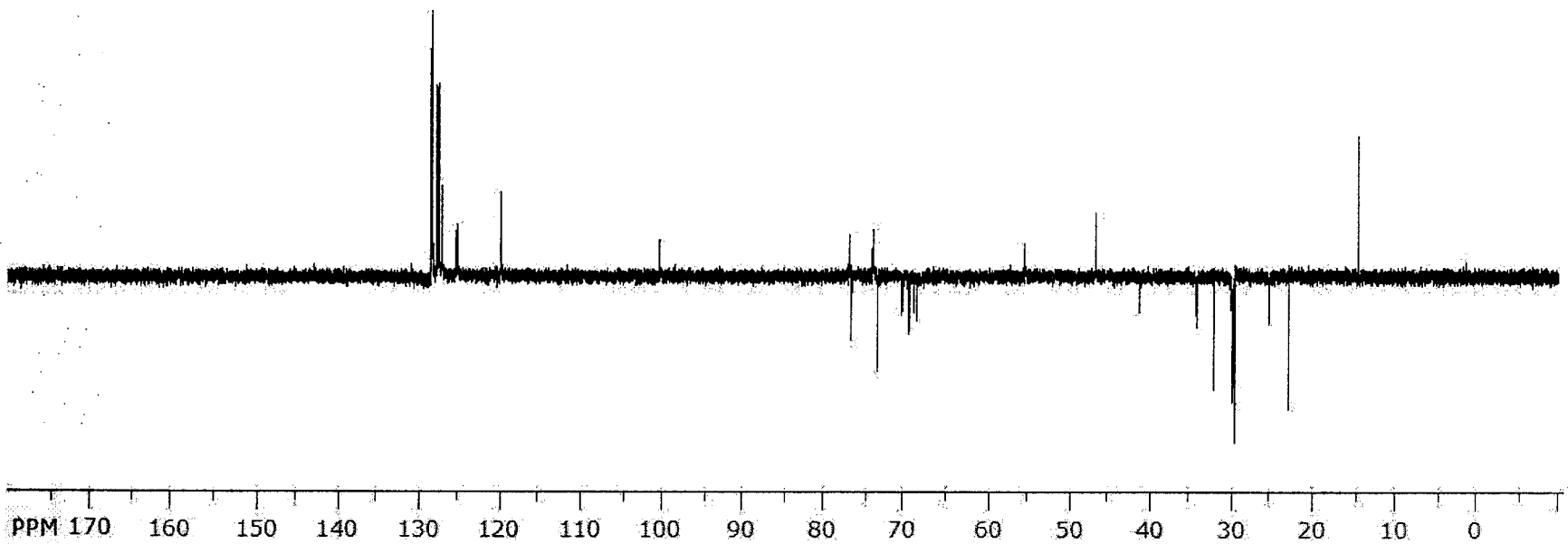

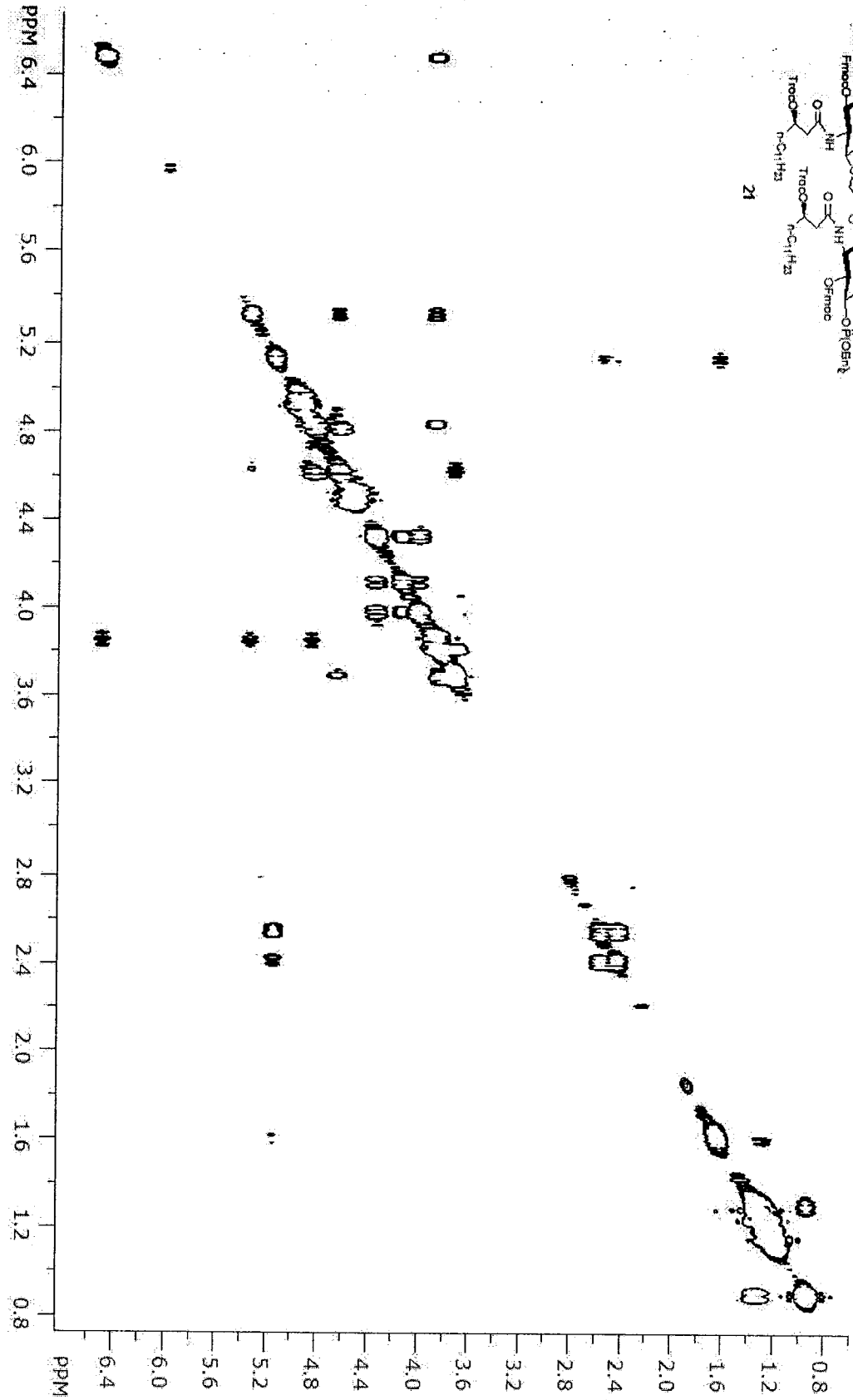
21
PPM 6.4
6.0
5.6
5.2
4.8
4.4
4.0
3.6
3.2
2.8
2.4
2.0
1.6
1.2
0.8
PPM

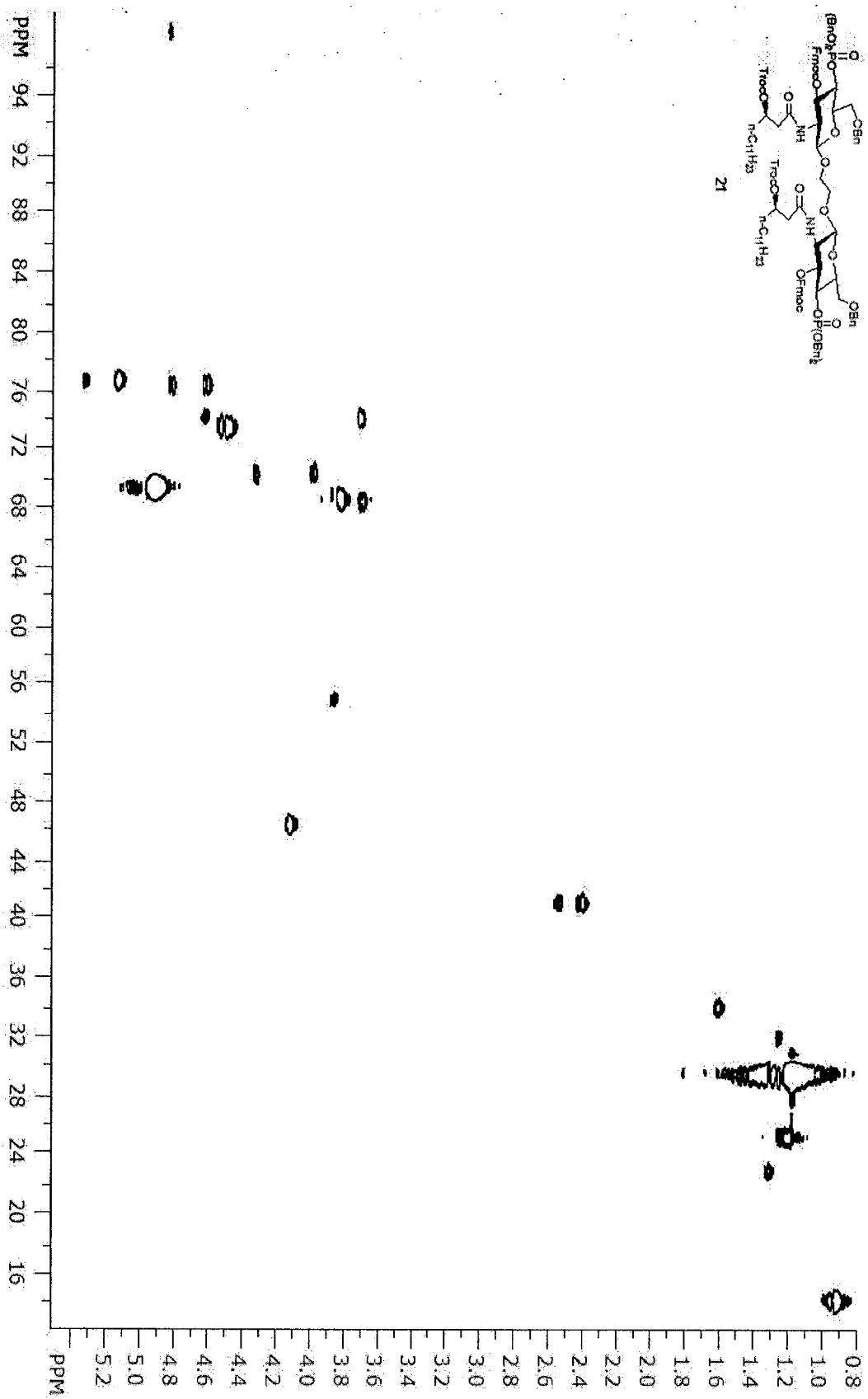
21
PPM
PPM

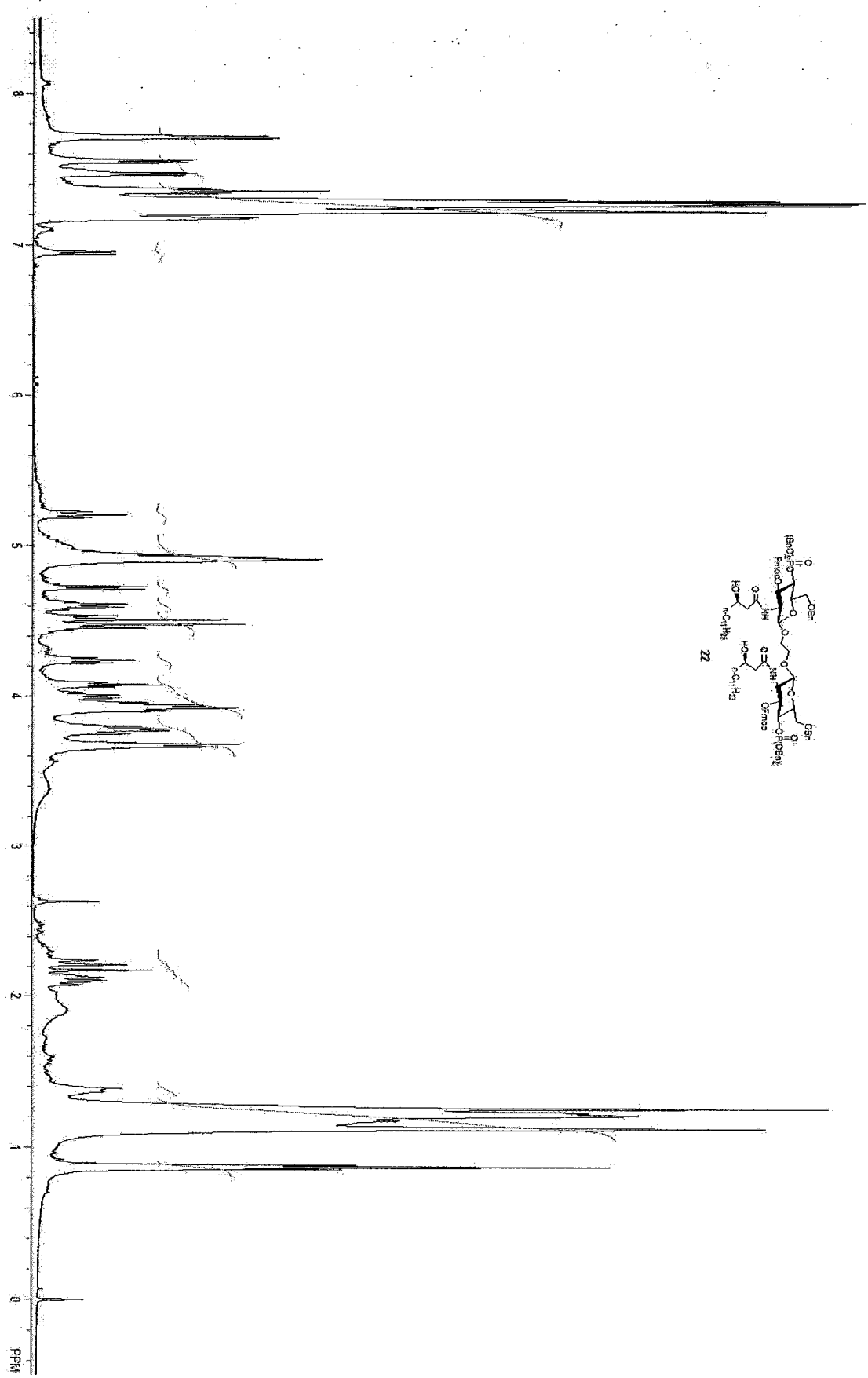

22

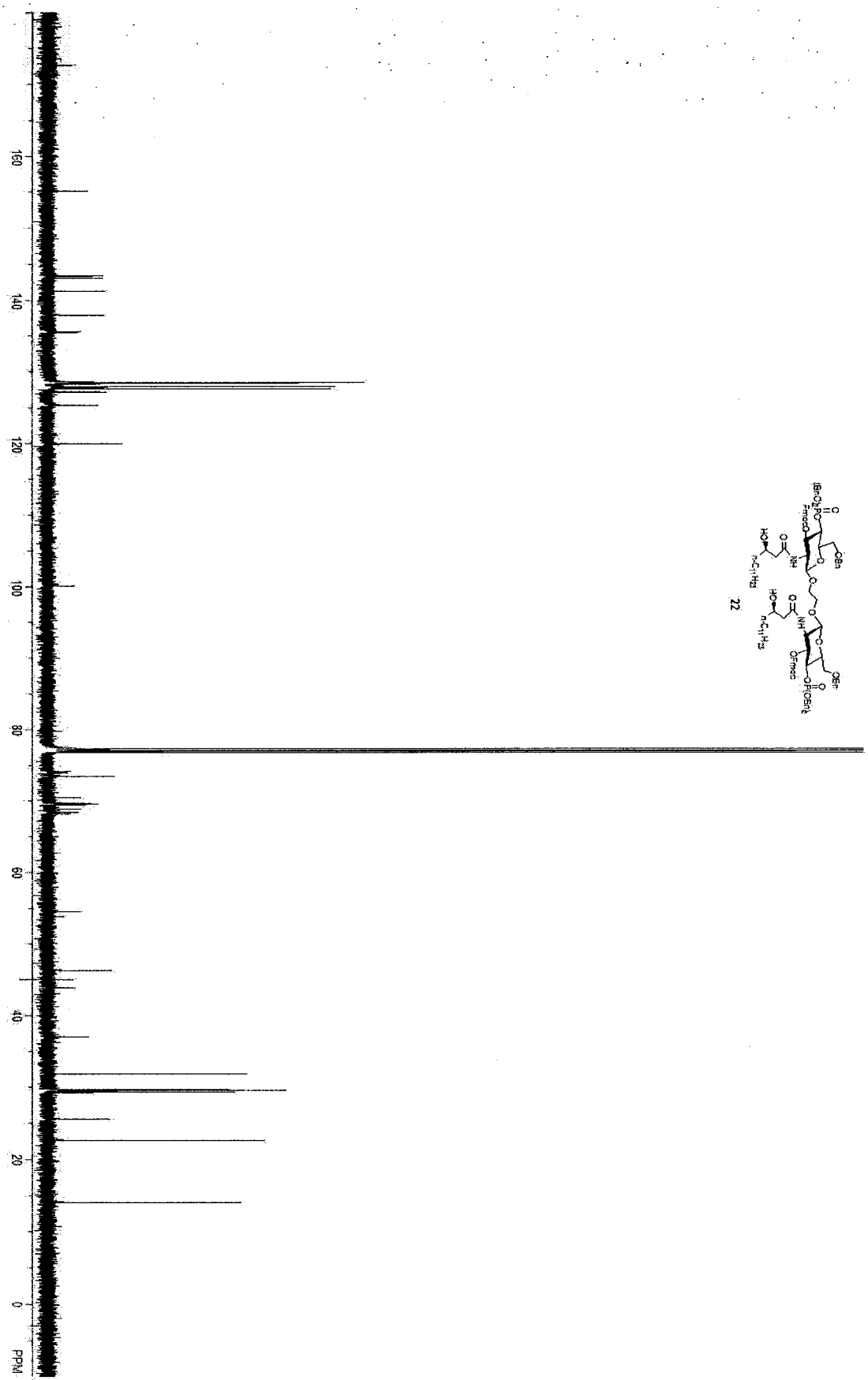
160
140
120
100
80
60
40
20
0
PPM

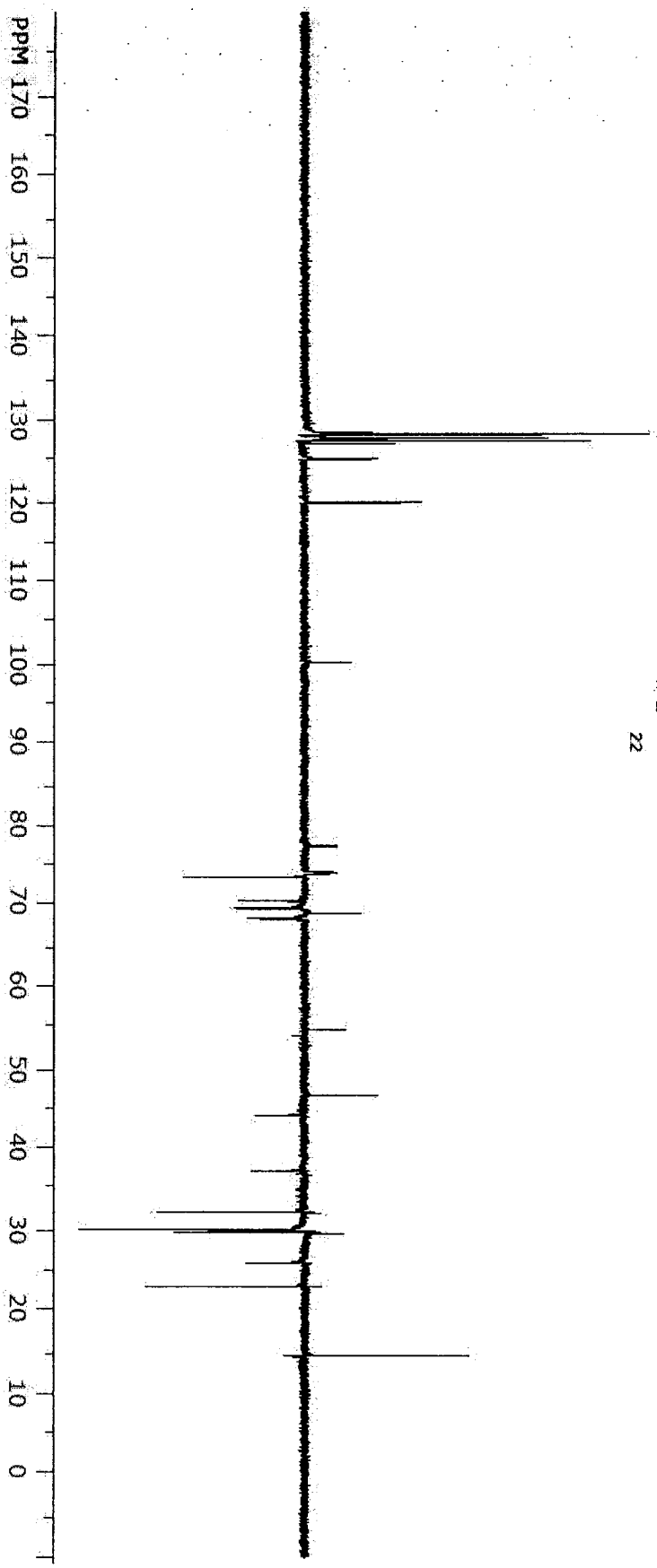

22

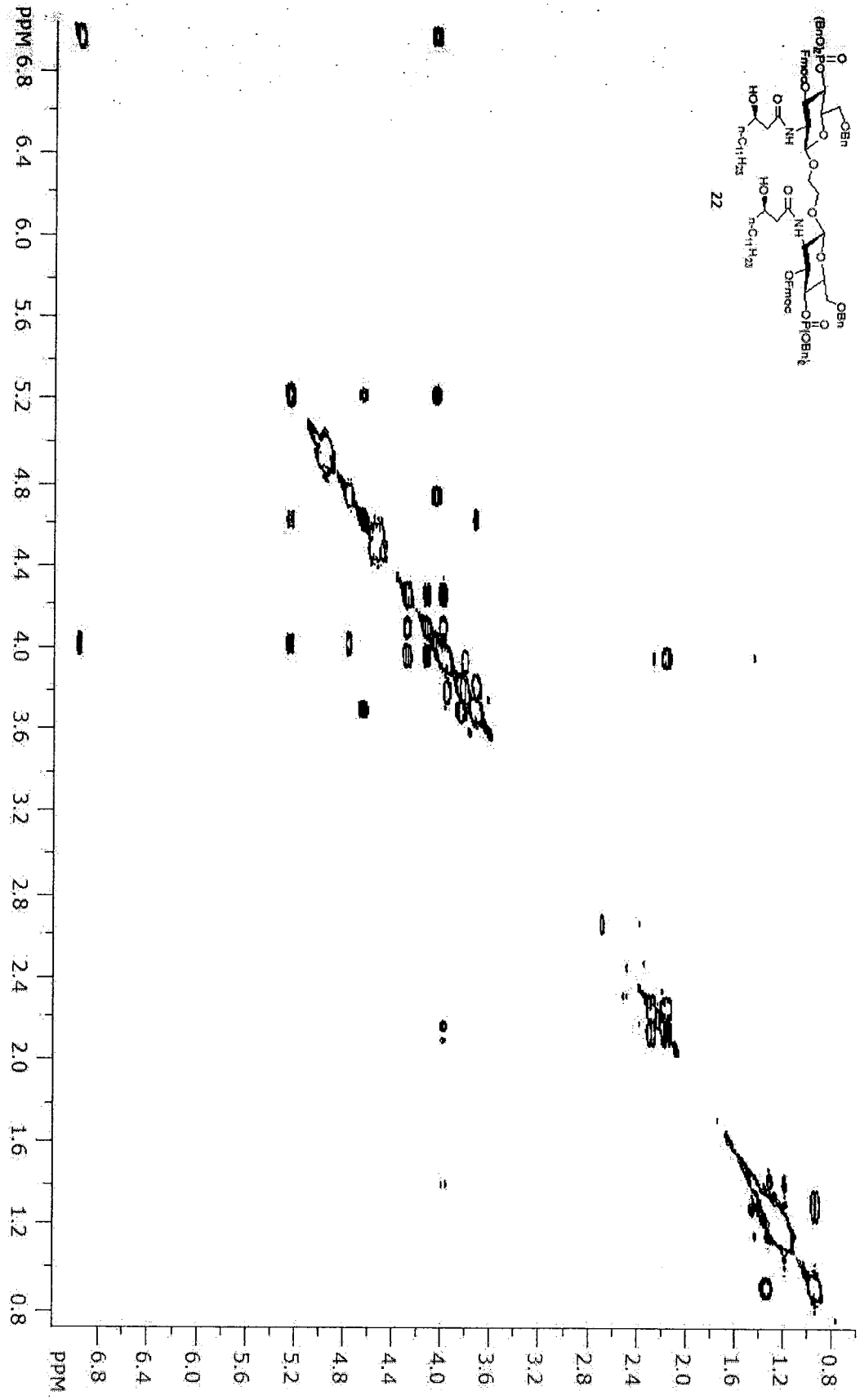
22
PPM 6.8 6.4 6.0 5.6 5.2 4.8 4.4 4.0 3.6 3.2 2.8 2.4 2.0 1.6 1.2 0.8
PPM 6.8 6.4 6.0 5.6 5.2 4.8 4.4 4.0 3.6 3.2 2.8 2.4 2.0 1.6 1.2 0.8

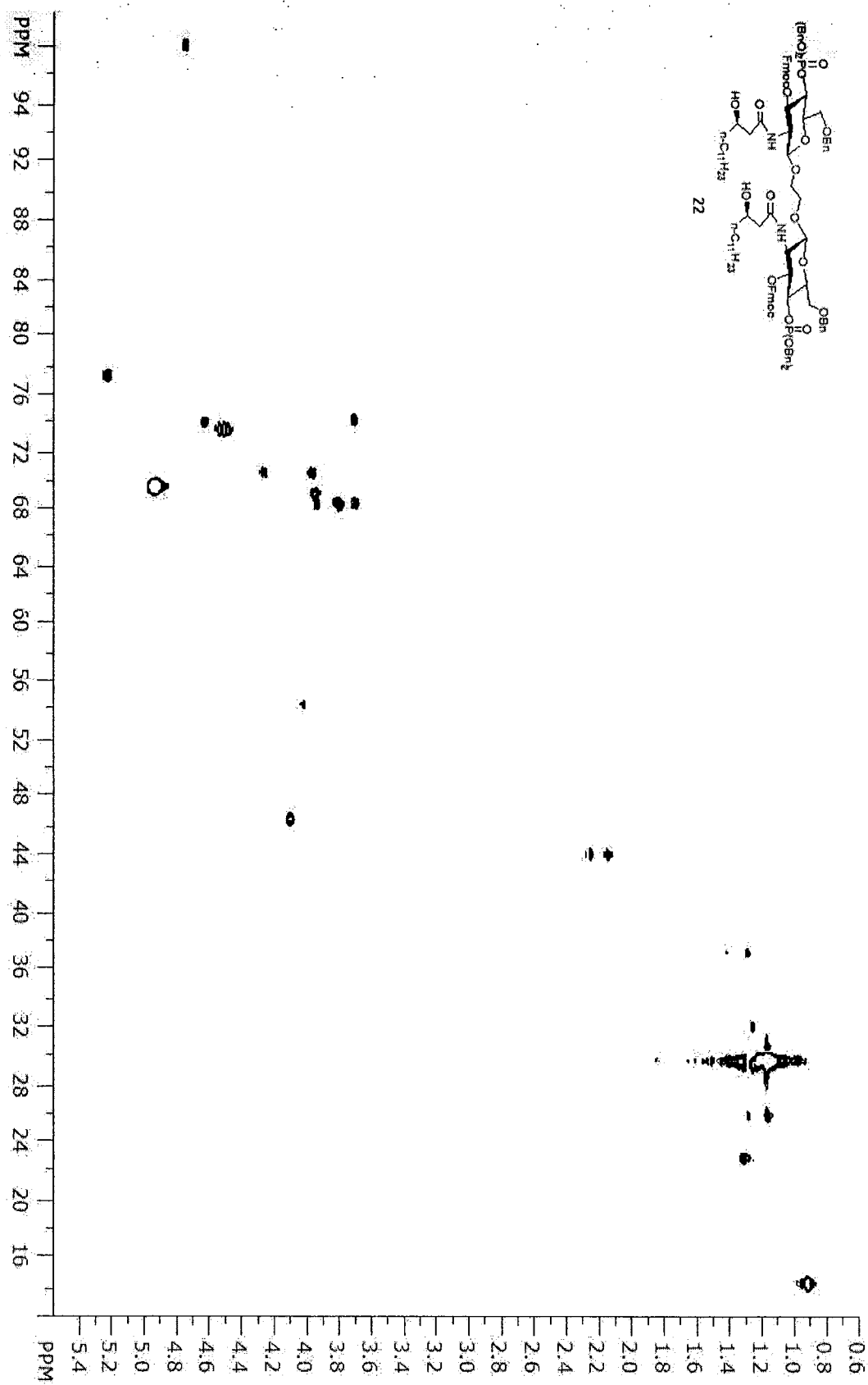
PPM
94
92
88
84
80
76
72
68
64
60
56
52
48
44
40
36
32
28
24
20
16
PPM
5.4
5.2
5.0
4.8
4.6
4.4
4.2
4.0
3.8
3.6
3.4
3.2
3.0
2.8
2.6
2.4
2.2
2.0
1.8
1.6
1.4
1.2
1.0
0.8
0.6

22

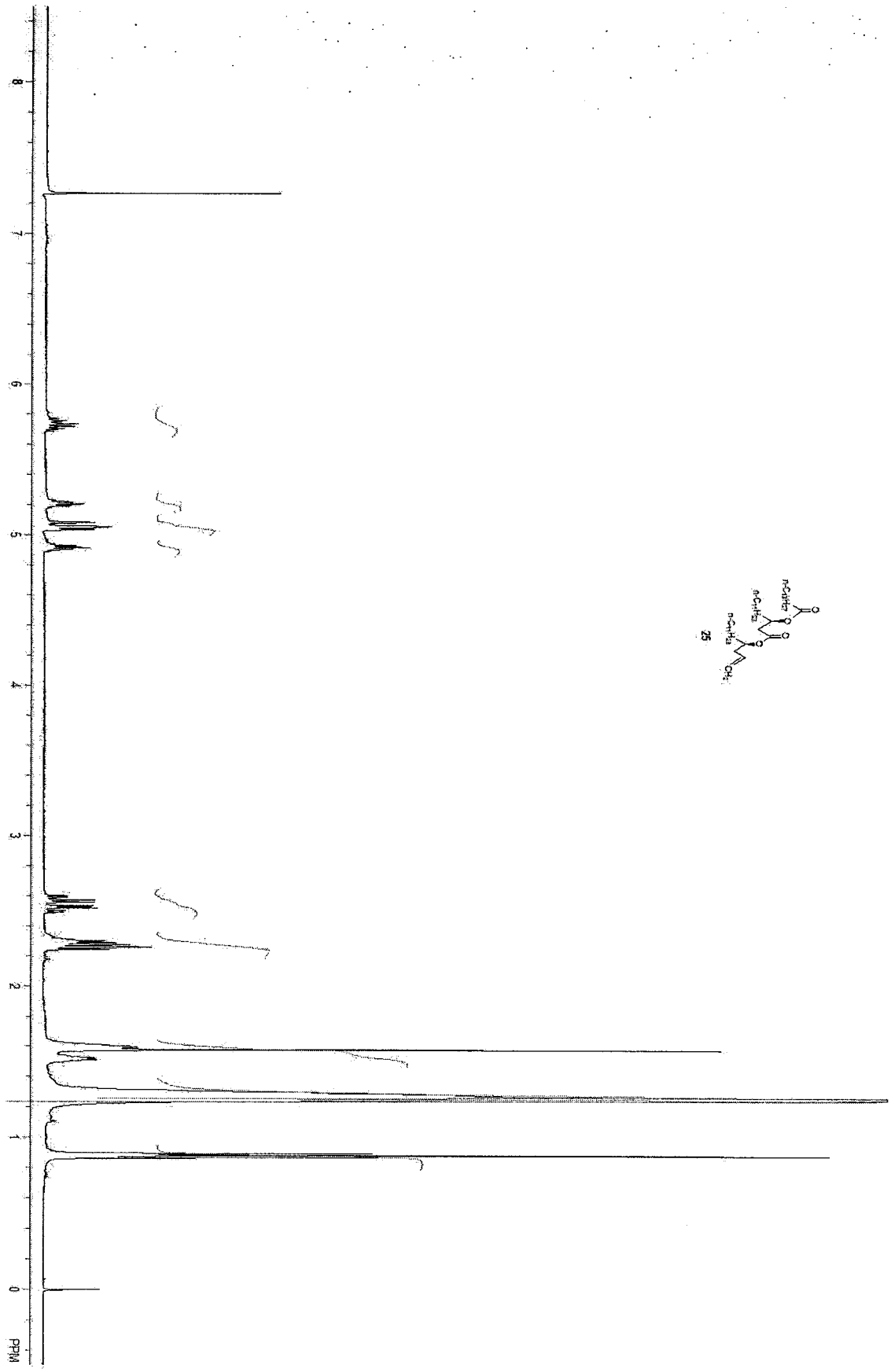
PPM
8
7
6
5
4
3
2
1
0

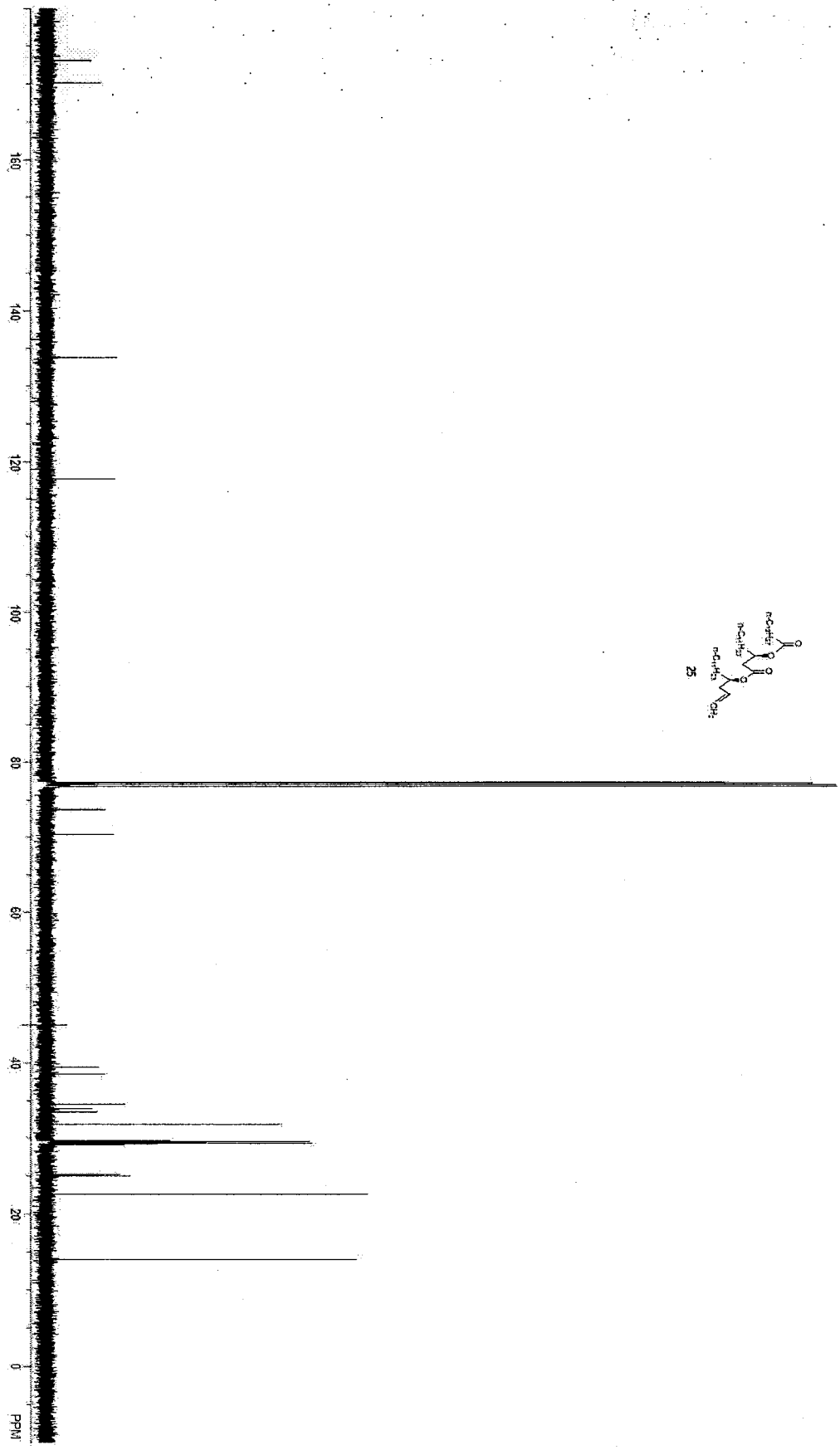

25

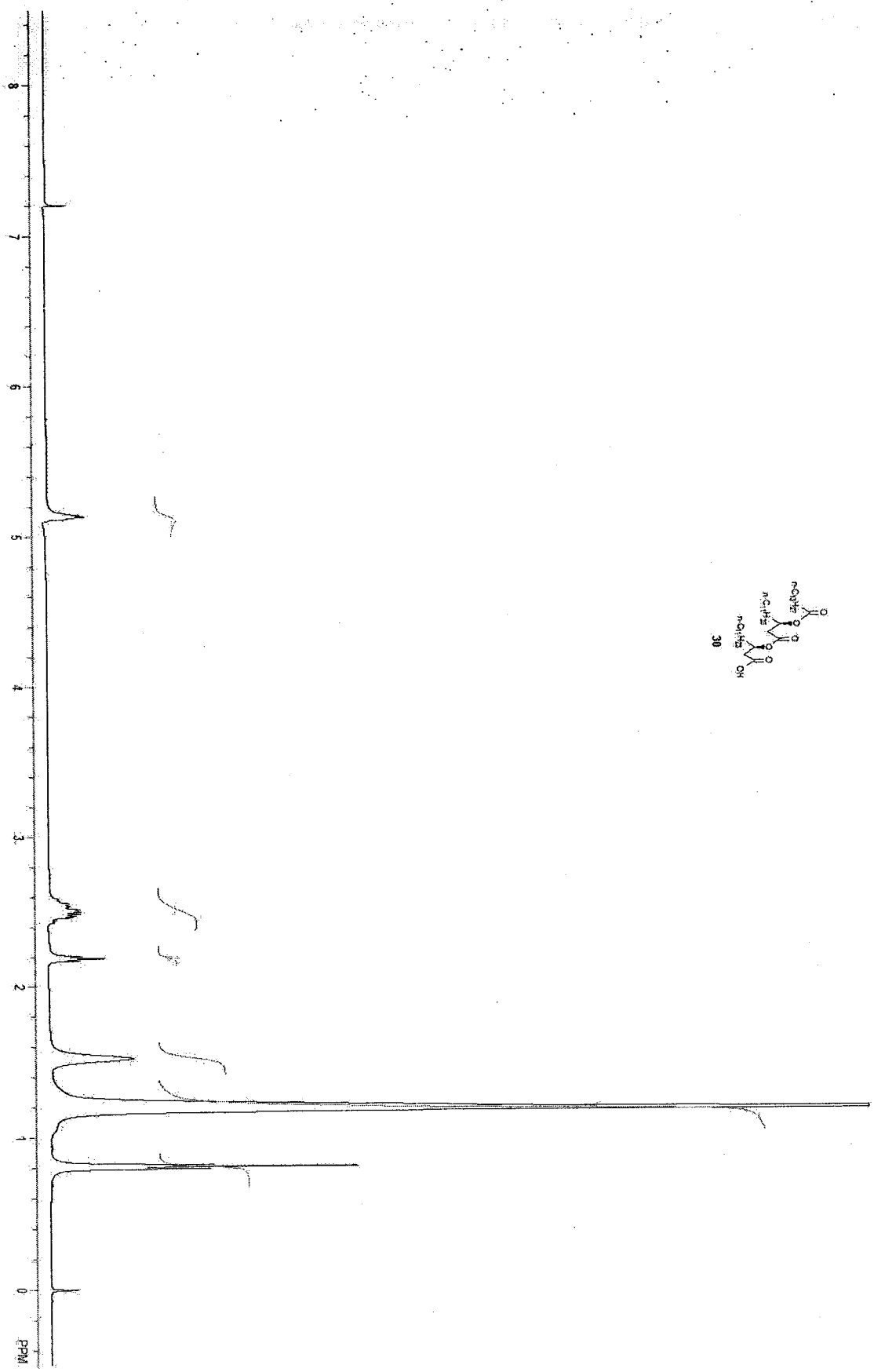
PPM
8
7
6
5
4
3
2
1
0
30

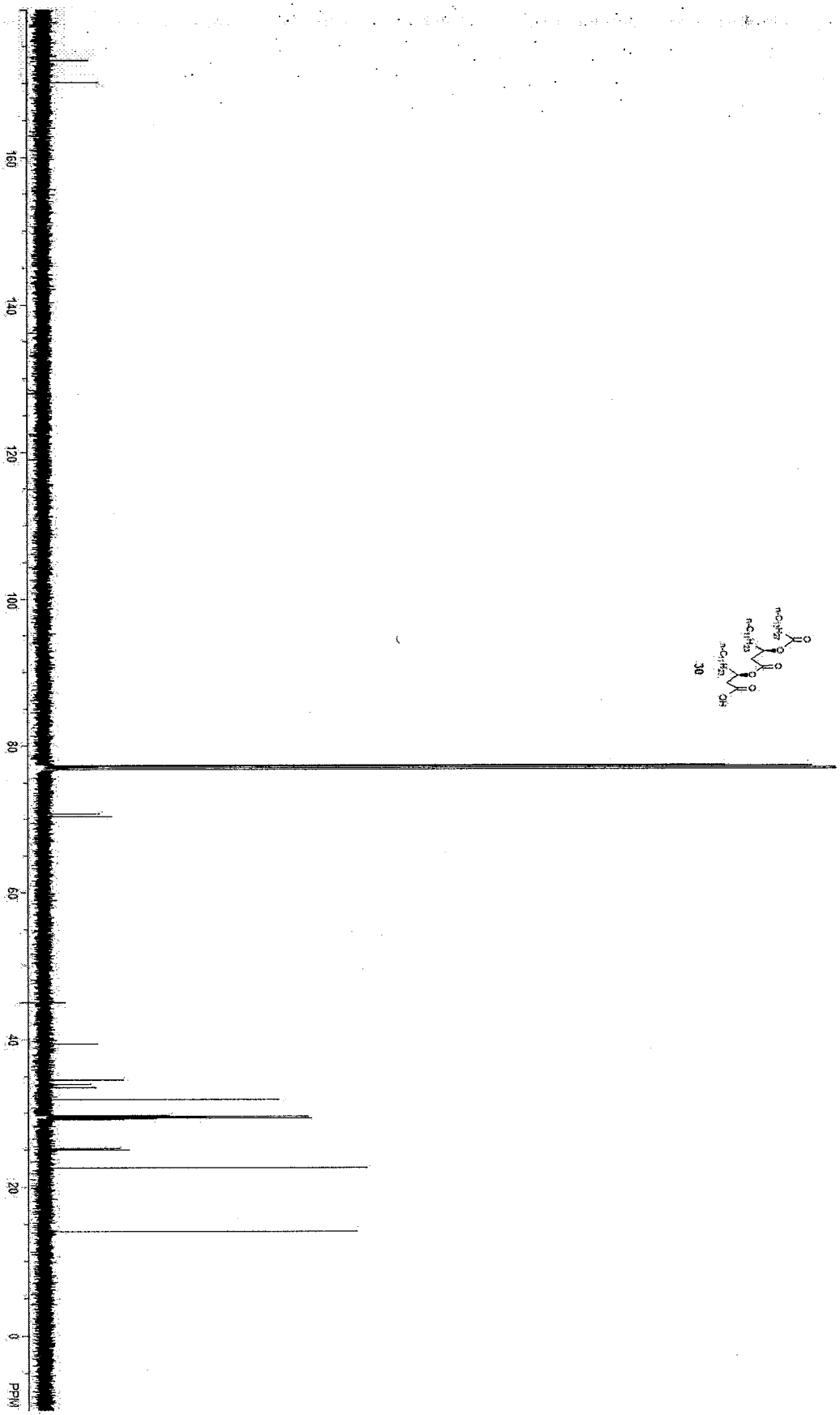
160
140
120
100
80
60
40
20
0
PPM

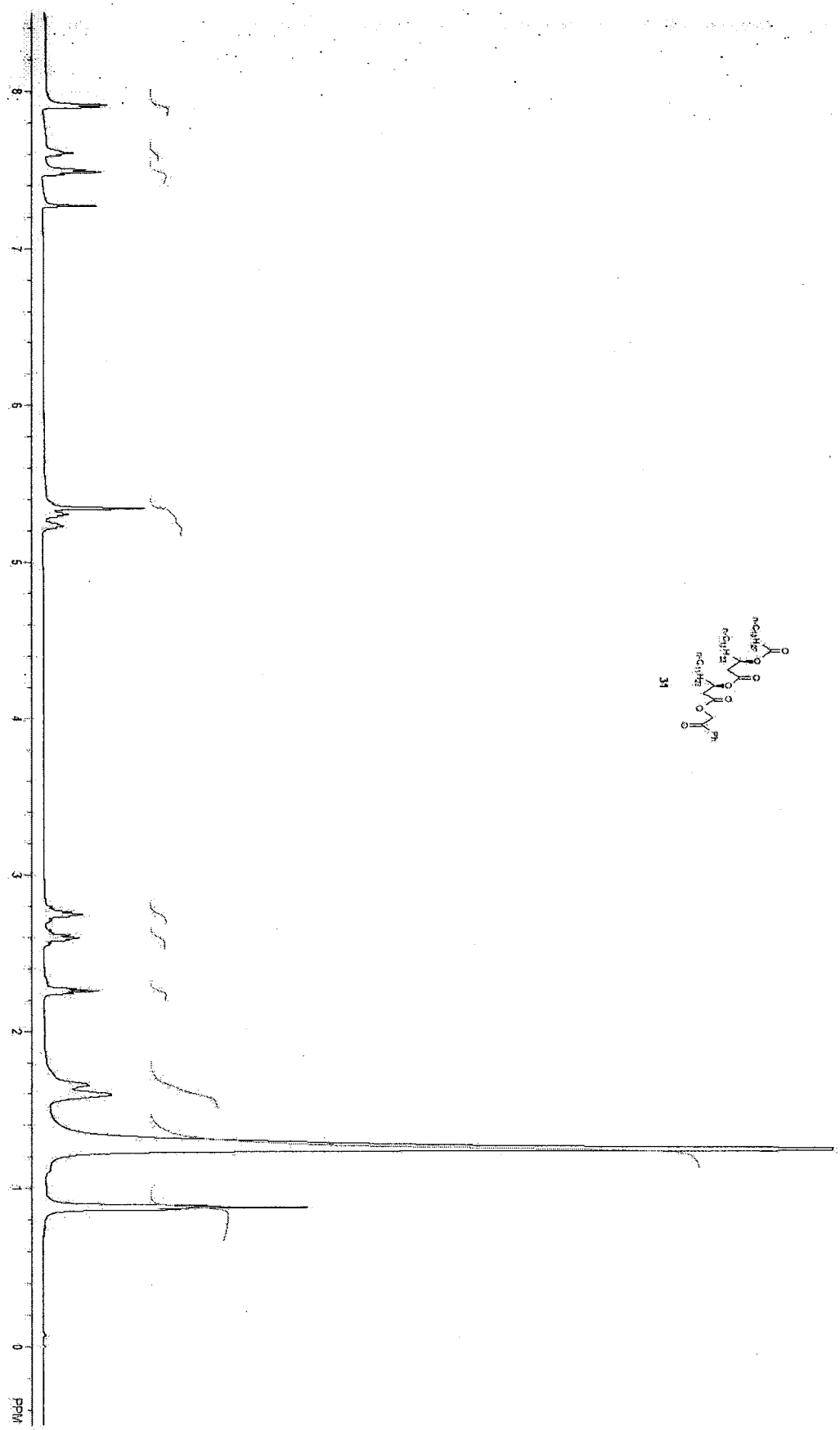

31

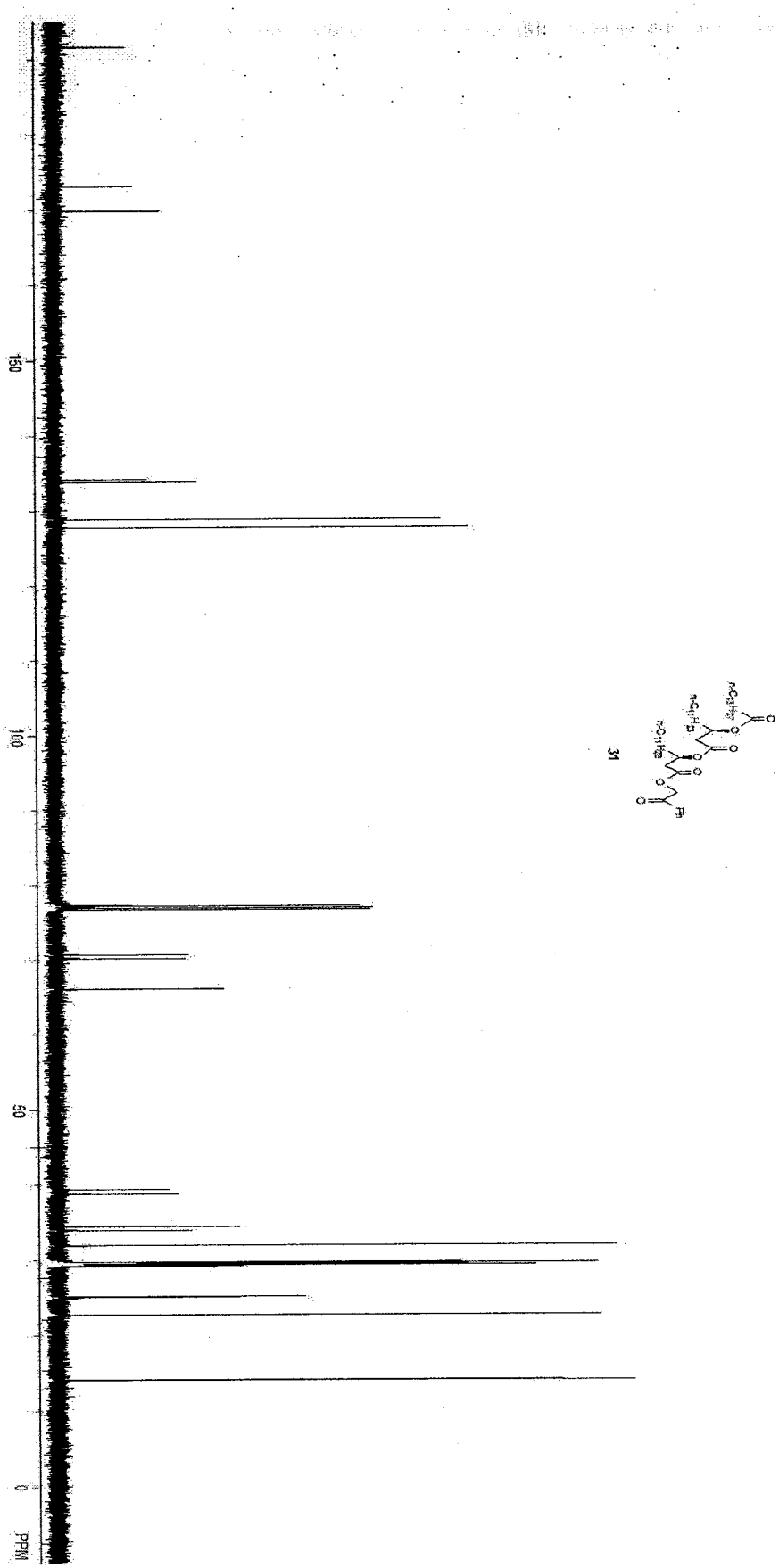

31

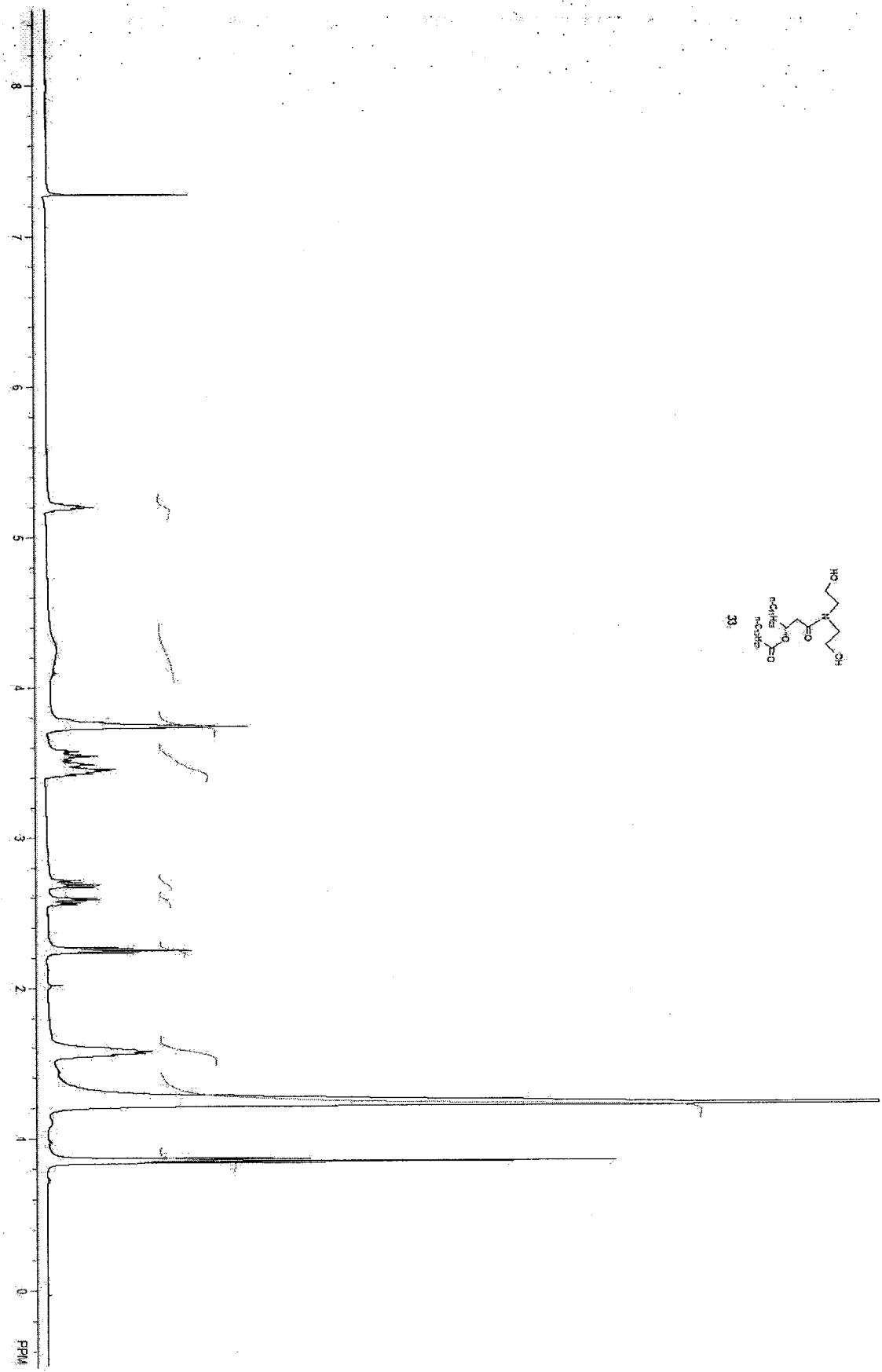
8
7
6
5
4
3
2
1
0
PPM

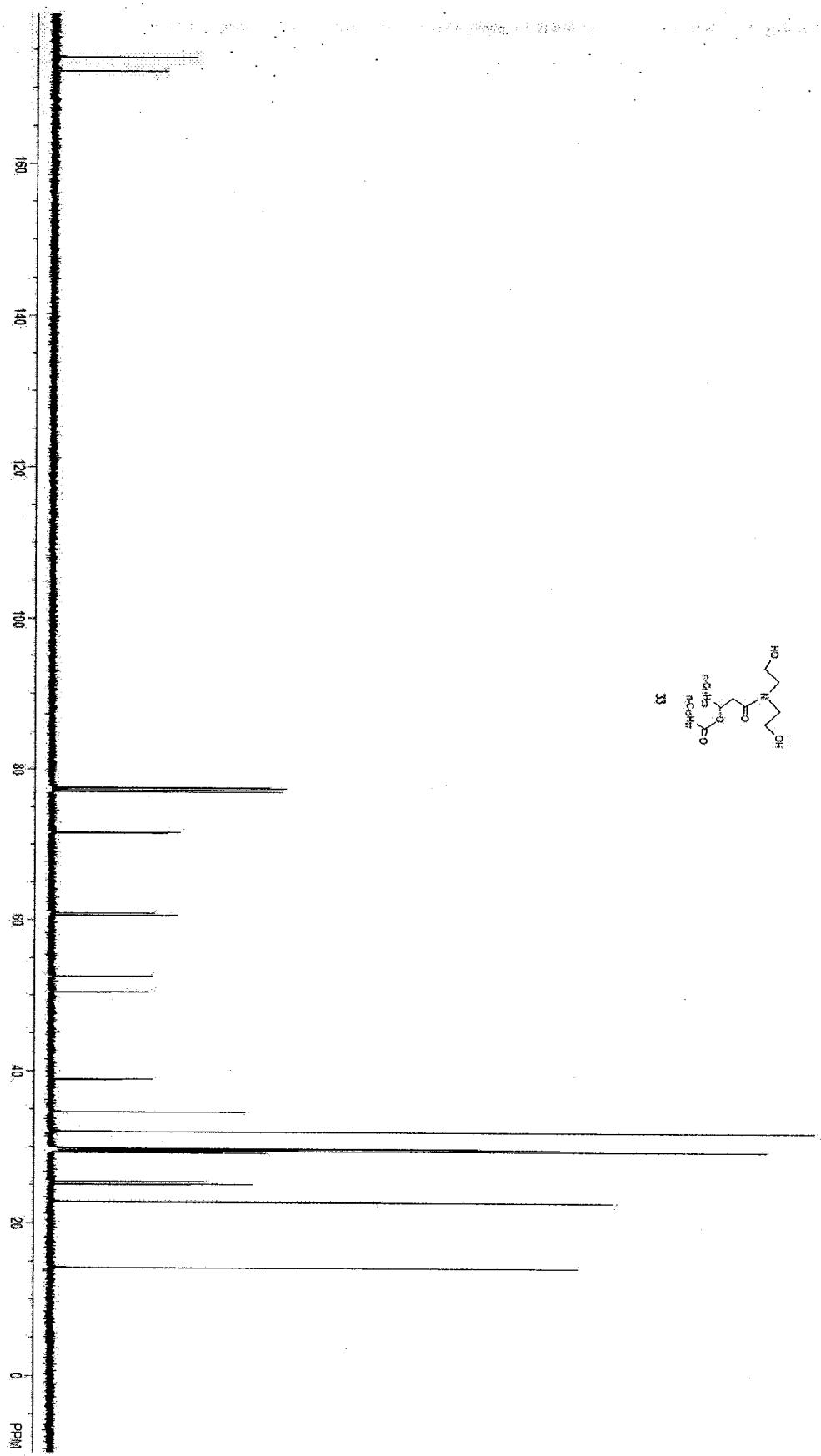

33

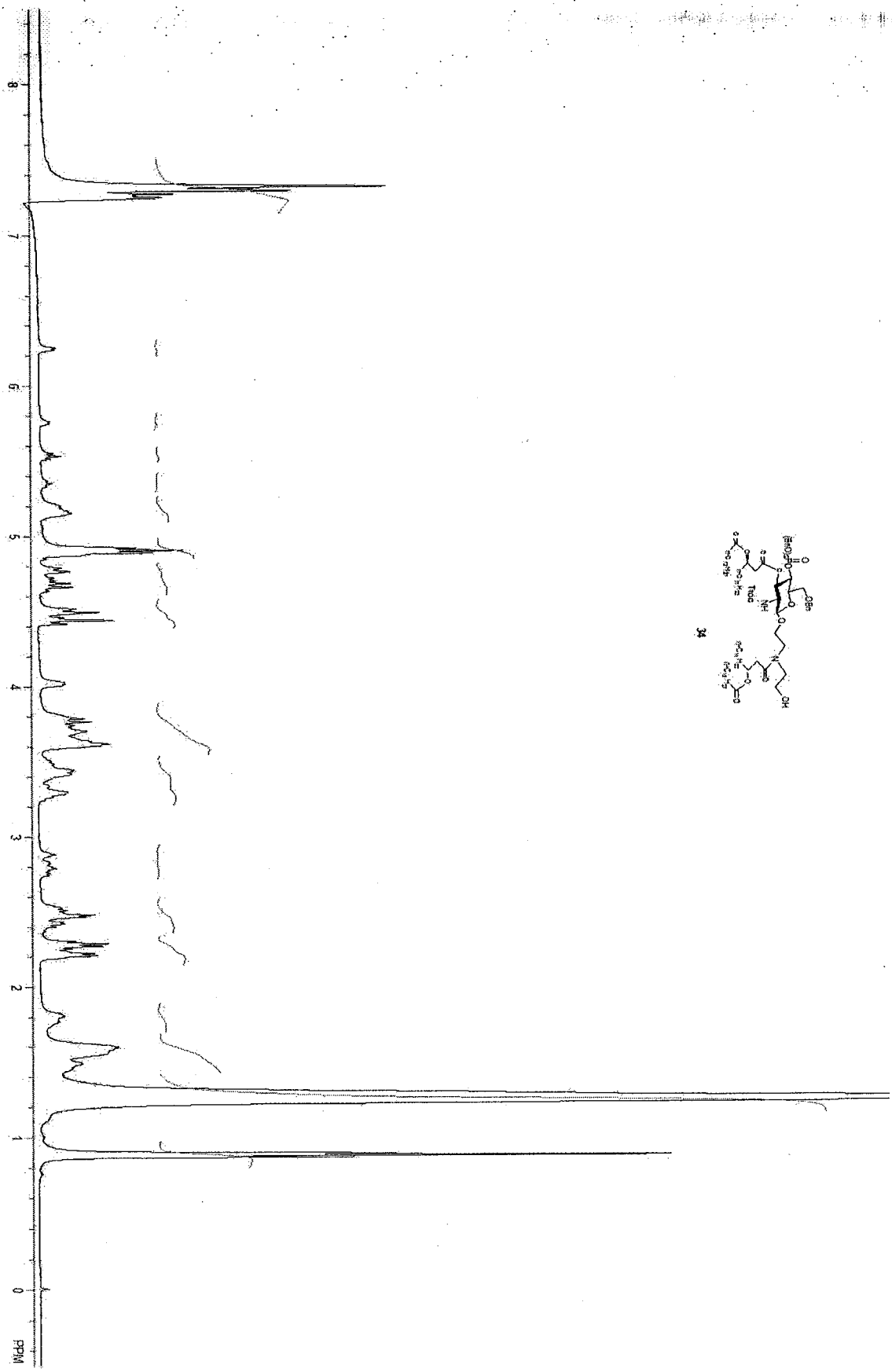

34

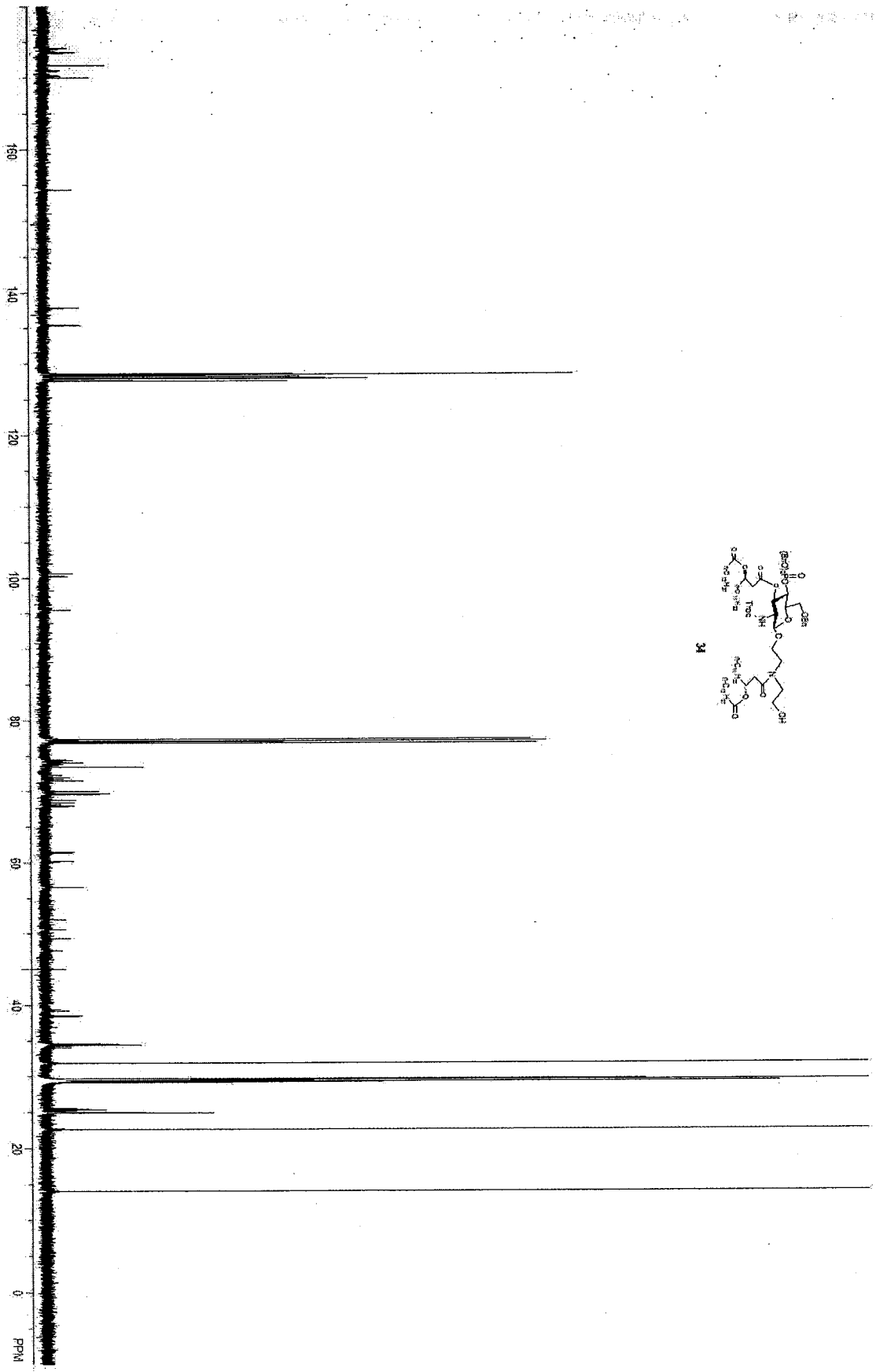

34

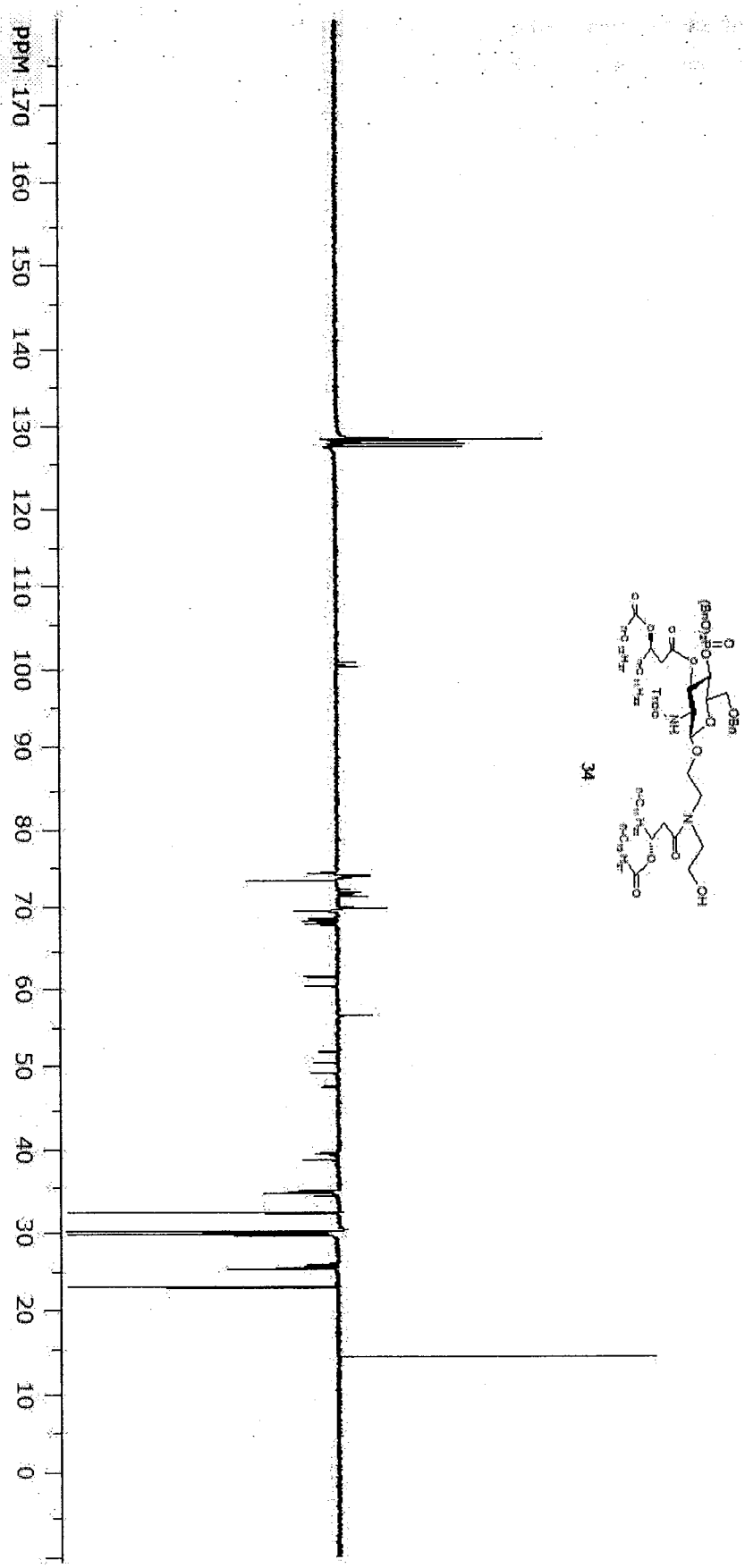

34

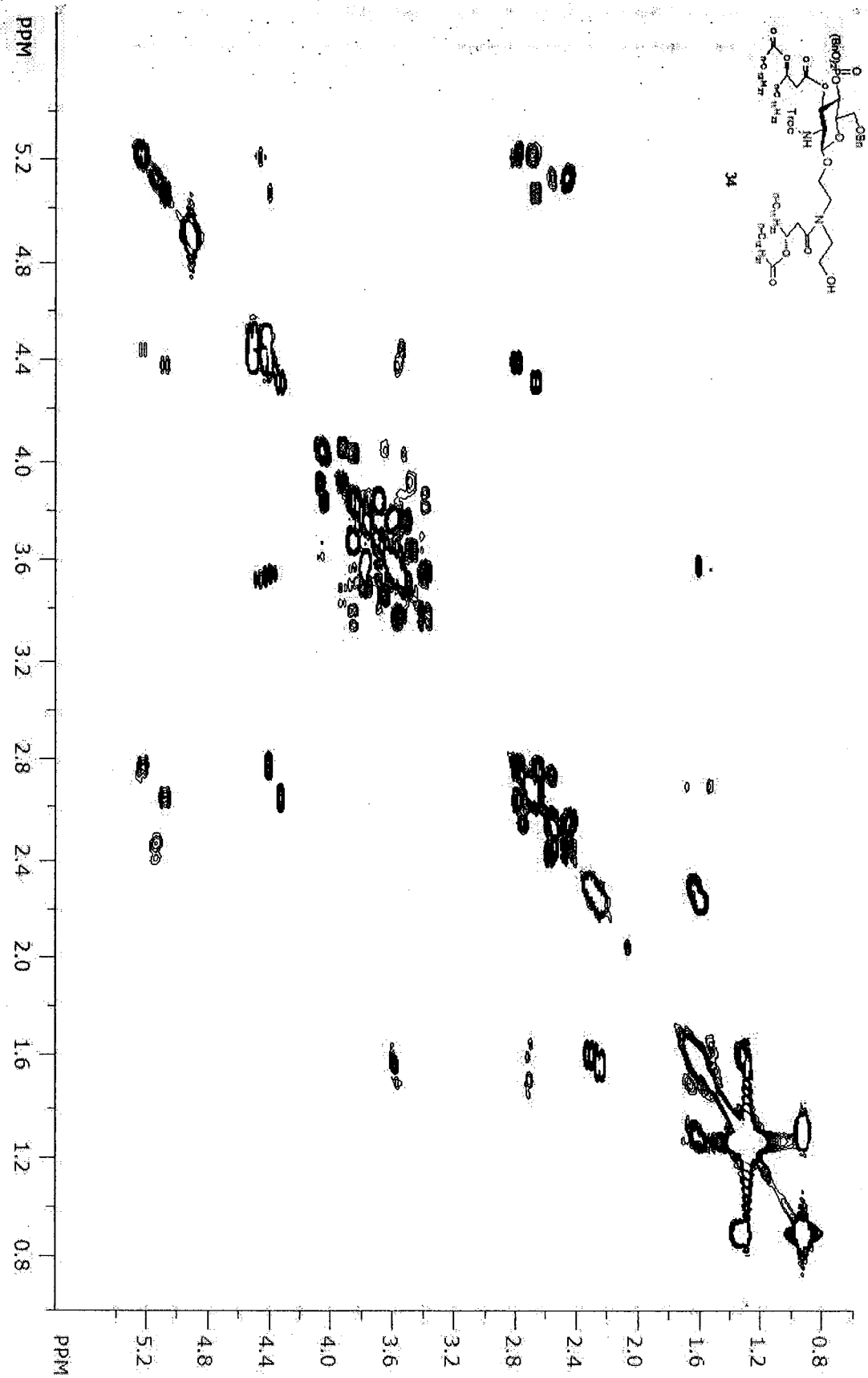
PPM
5.2
4.8
4.4
4.0
3.6
3.2
2.8
2.4
2.0
1.6
1.2
0.8
34

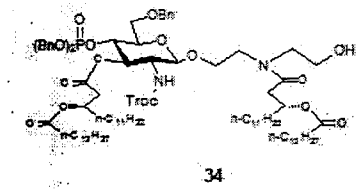

34

0.8
1.2
1.6
2.0
2.4
2.8
3.2
3.6
4.0
4.4
4.8
5.2
5.4
PPM
PPM 98 96 92 88 84 80 76 72 68 64 60 56 52 48 44 40 36 32 28 24 20 16 12

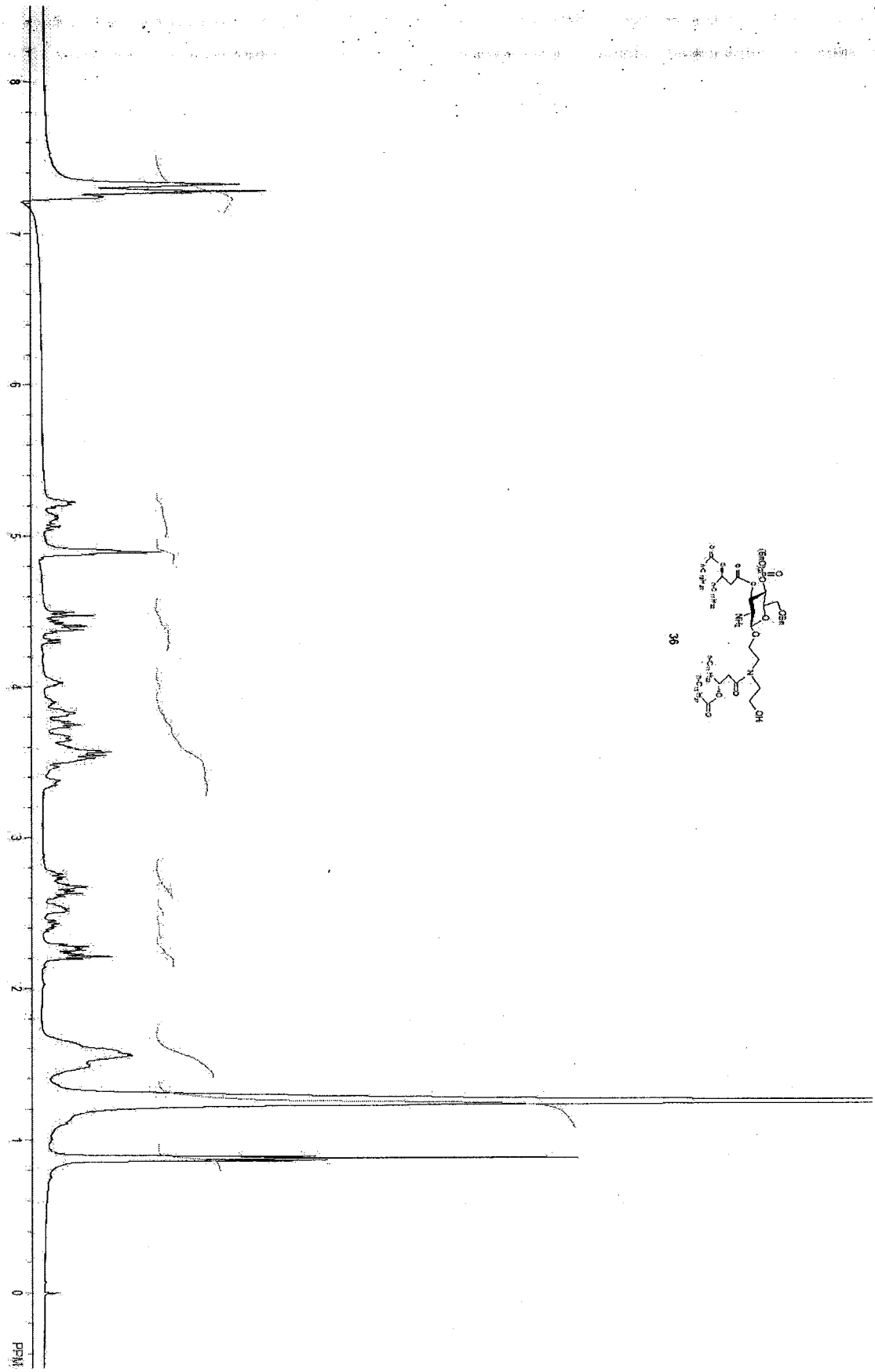

36

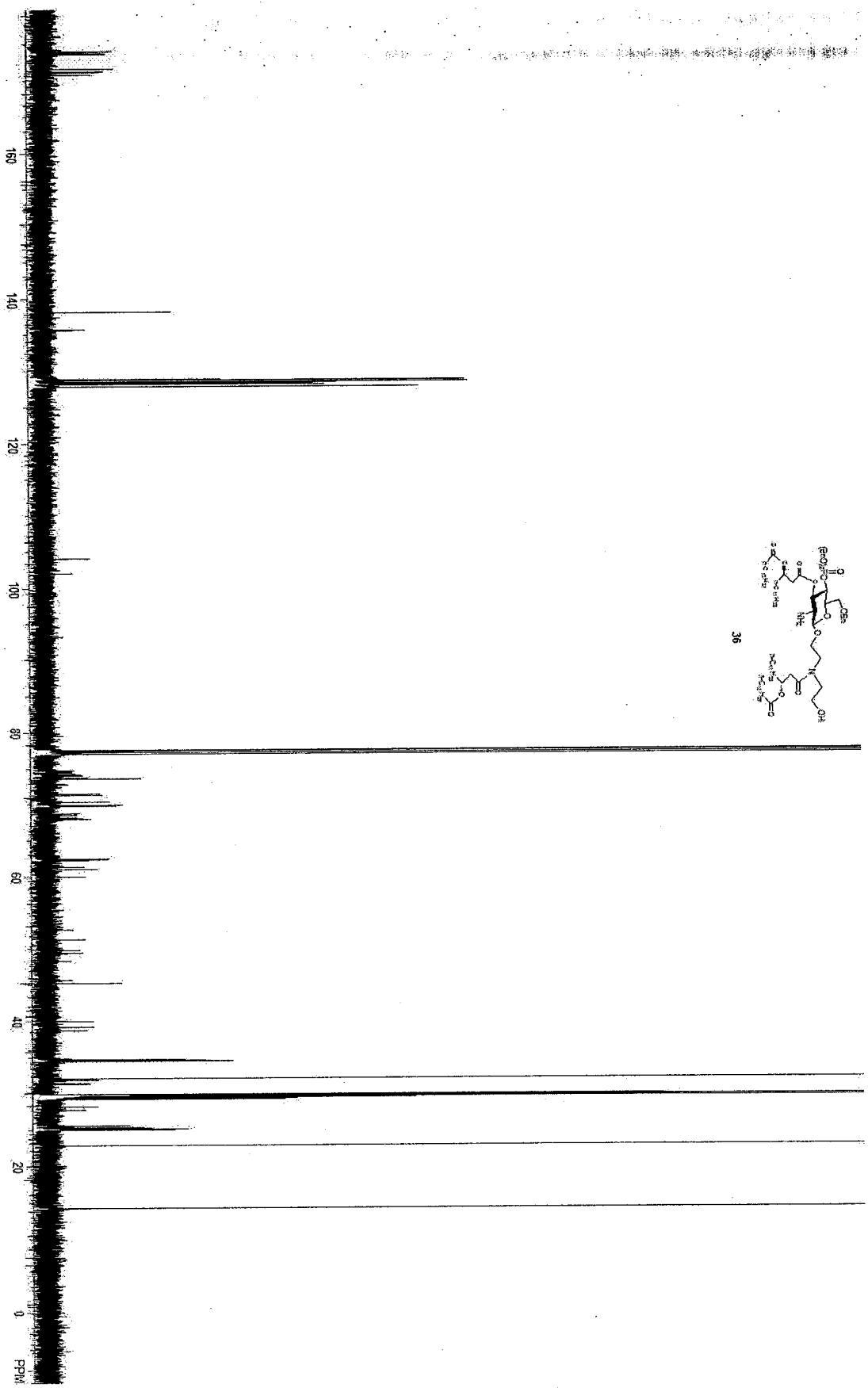

36

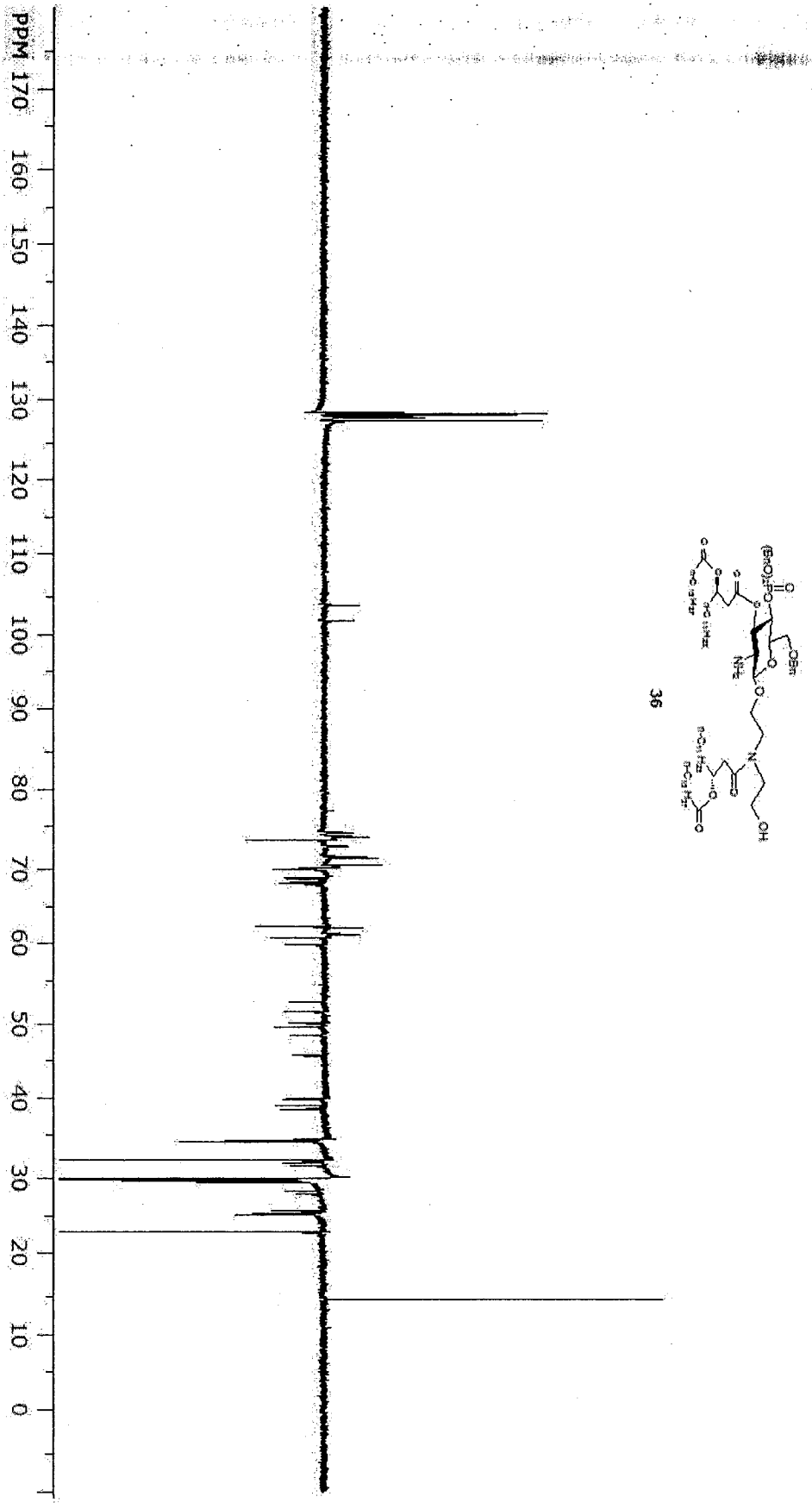

36

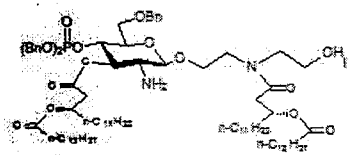

36

0.8
1.2
1.6
2.0
2.4
2.8
3.2
3.6
4.0
4.4
4.8
5.2
PPM
PPM
5.2
4.8
4.4
4.0
3.6
3.2
2.8
2.4
2.0
1.6
1.2
0.8

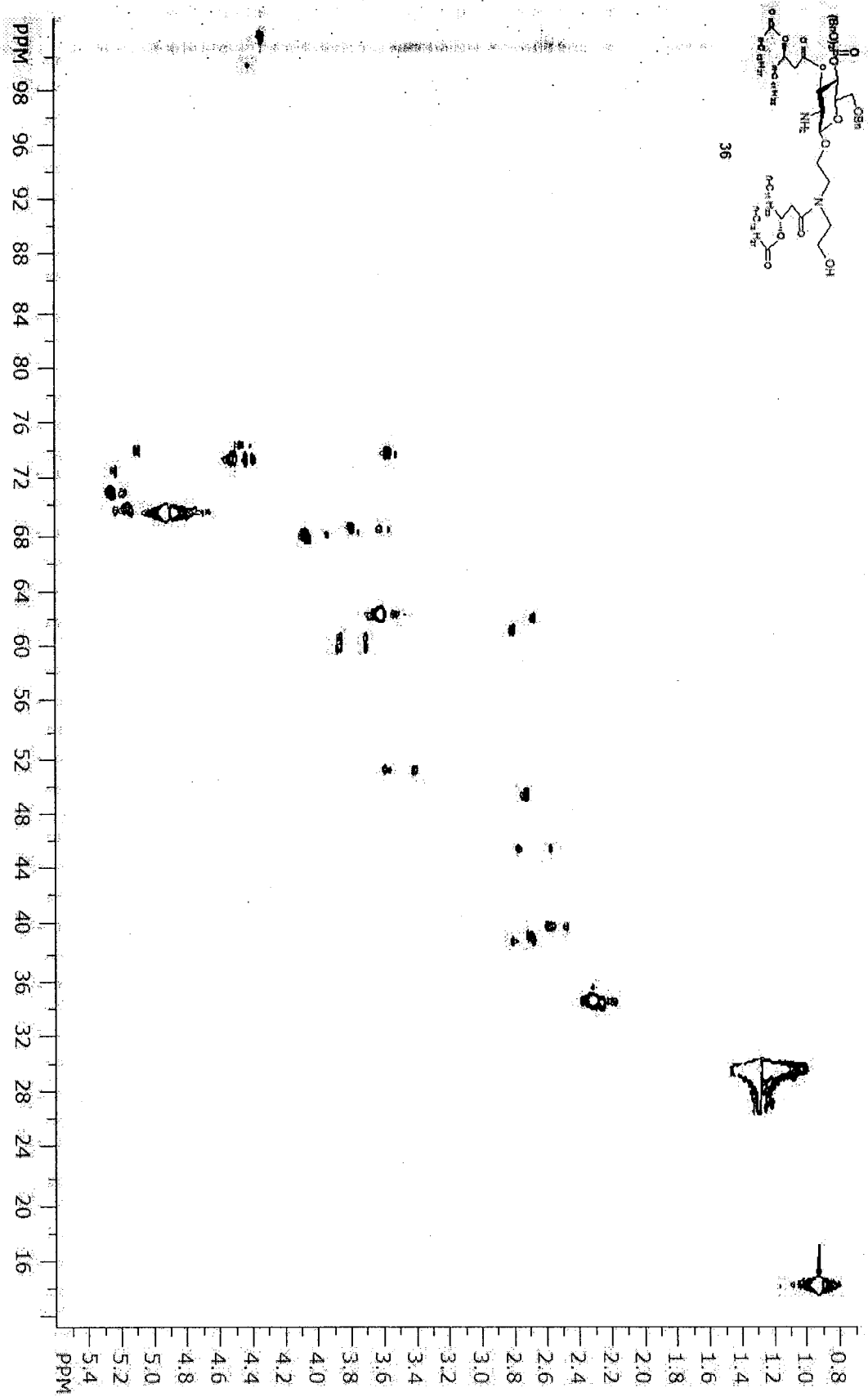
PPM
98
96
92
88
84
80
76
72
68
64
60
56
52
48
44
40
36
32
28
24
20
16
PPM
5.4
5.2
5.0
4.8
4.6
4.4
4.2
4.0
3.8
3.6
3.4
3.2
3.0
2.8
2.6
2.4
2.2
2.0
1.8
1.6
1.4
1.2
1.0
0.8
36

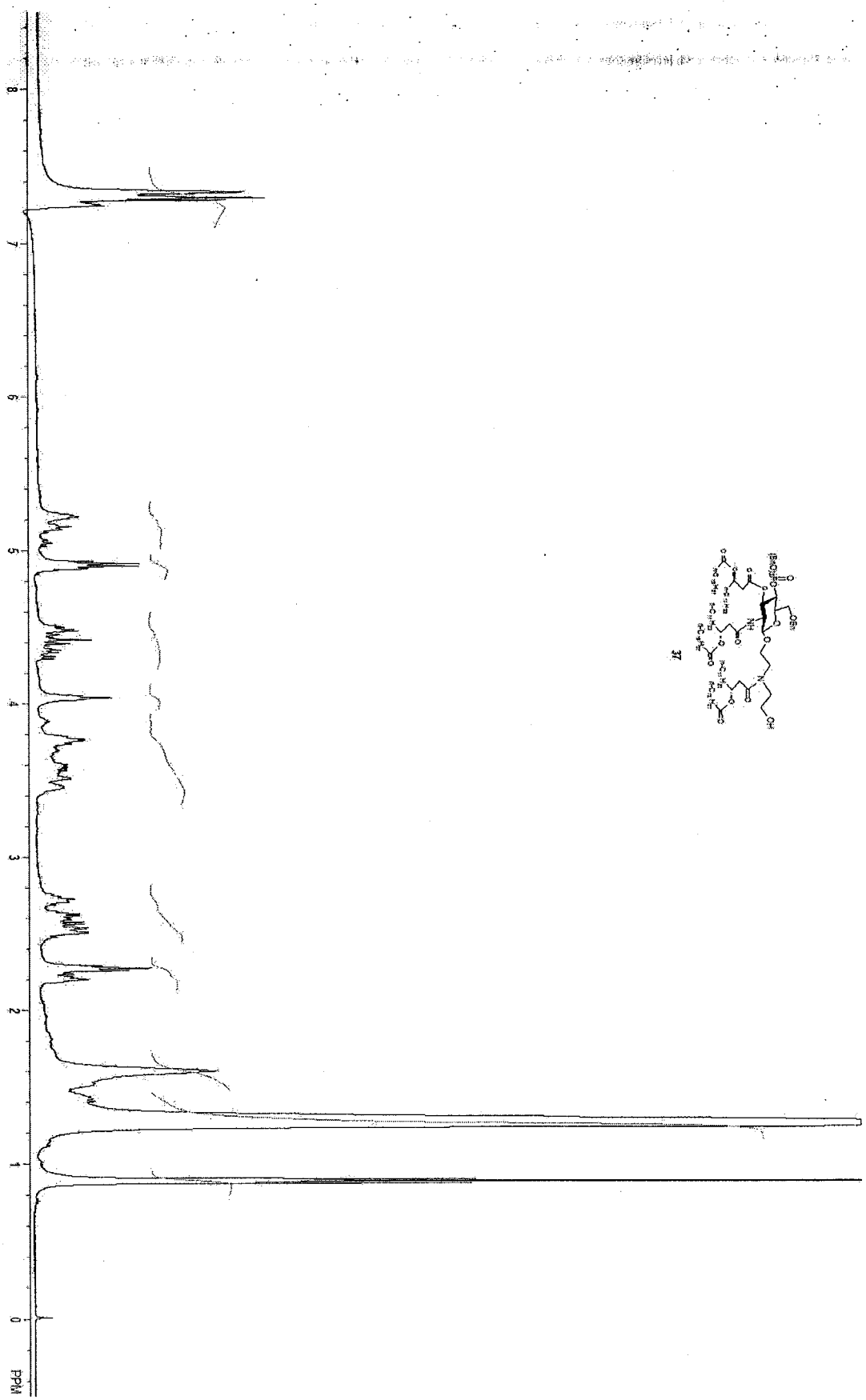

37

37

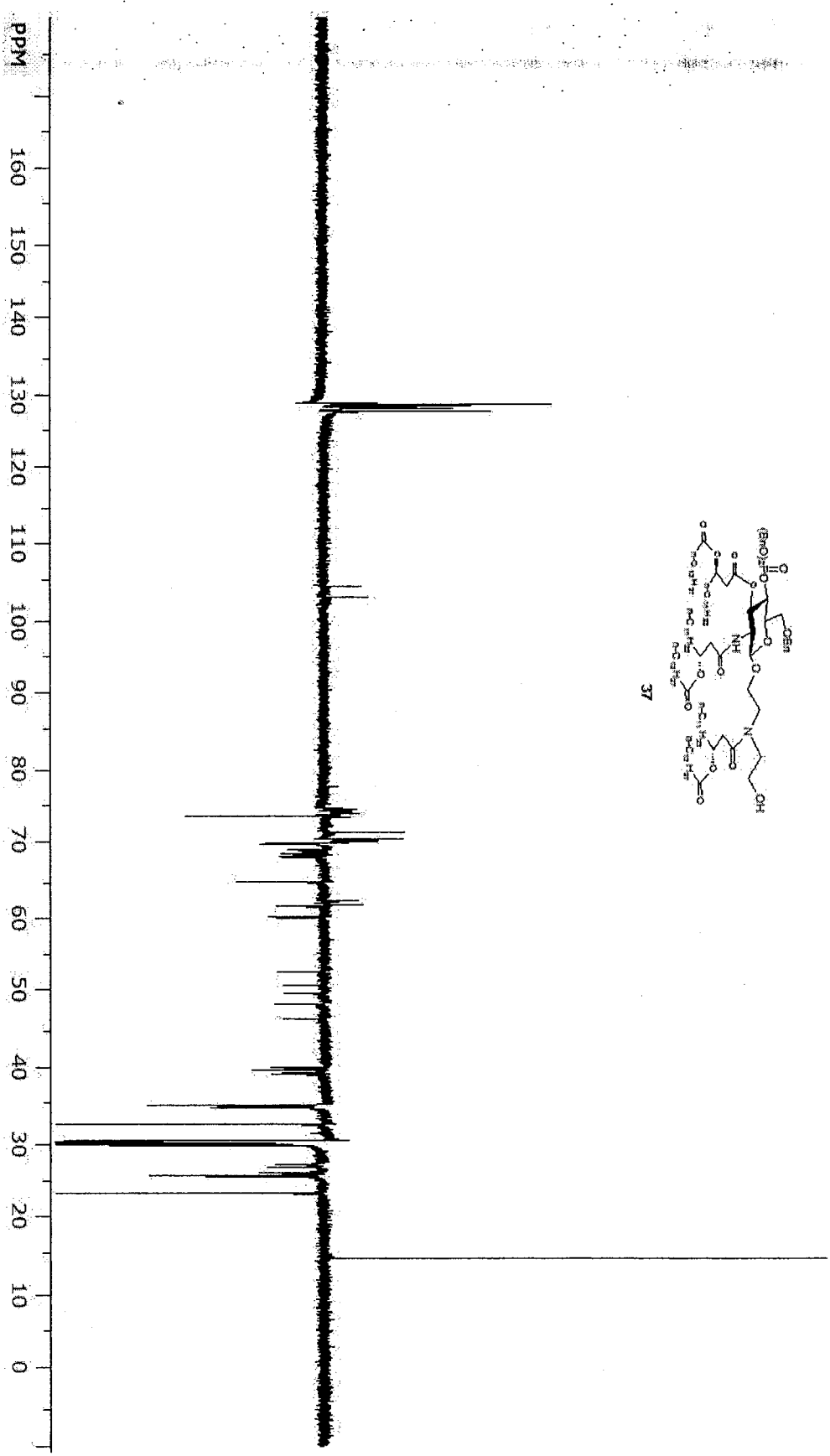

37

PPM
5.0 4.8 4.6 4.4 4.2 4.0 3.8 3.6 3.4 3.2 3.0 2.8 2.6 2.4 2.2 2.0 1.8 1.6 1.4 1.2 1.0 0.8
PPM
0.8 1.0 1.2 1.4 1.6 1.8 2.0 2.2 2.4 2.6 2.8 3.0 3.2 3.4 3.6 3.8 4.0 4.2 4.4 4.6 4.8 5.0 5.2

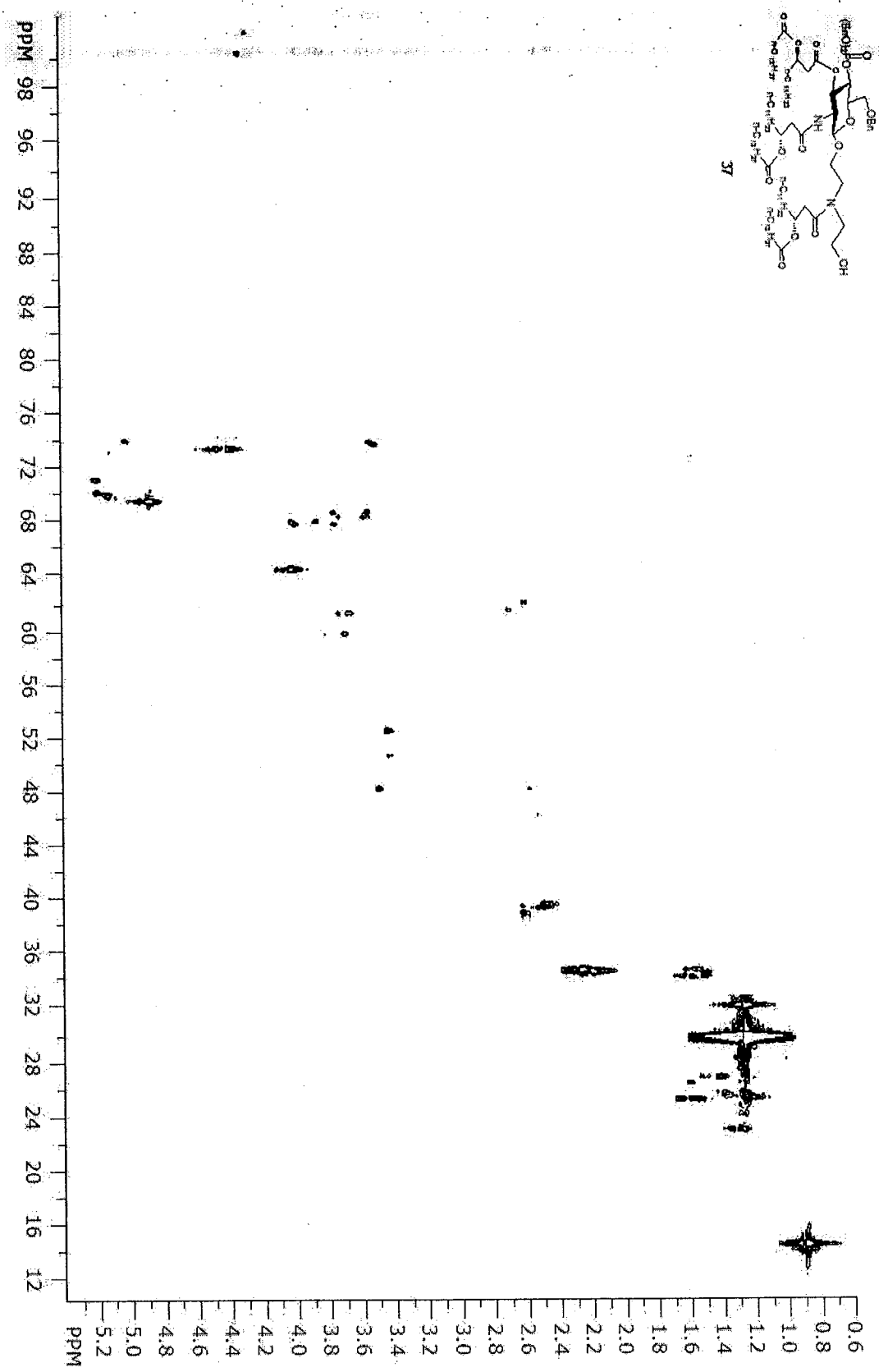
37
ppm
98
96
92
88
84
80
76
72
68
64
60
56
52
48
44
40
36
32
28
24
20
16
12
ppm
5.2
5.0
4.8
4.6
4.4
4.2
4.0
3.8
3.6
3.4
3.2
3.0
2.8
2.6
2.4
2.2
2.0
1.8
1.6
1.4
1.2
1.0
0.8
0.6

HRESI-MS (*m/z*) Calcd for $C_{47}H_{47}Cl_3NO_{13}PNa$ $[M + Na]^+$: 992.1751, found: 992.1743.

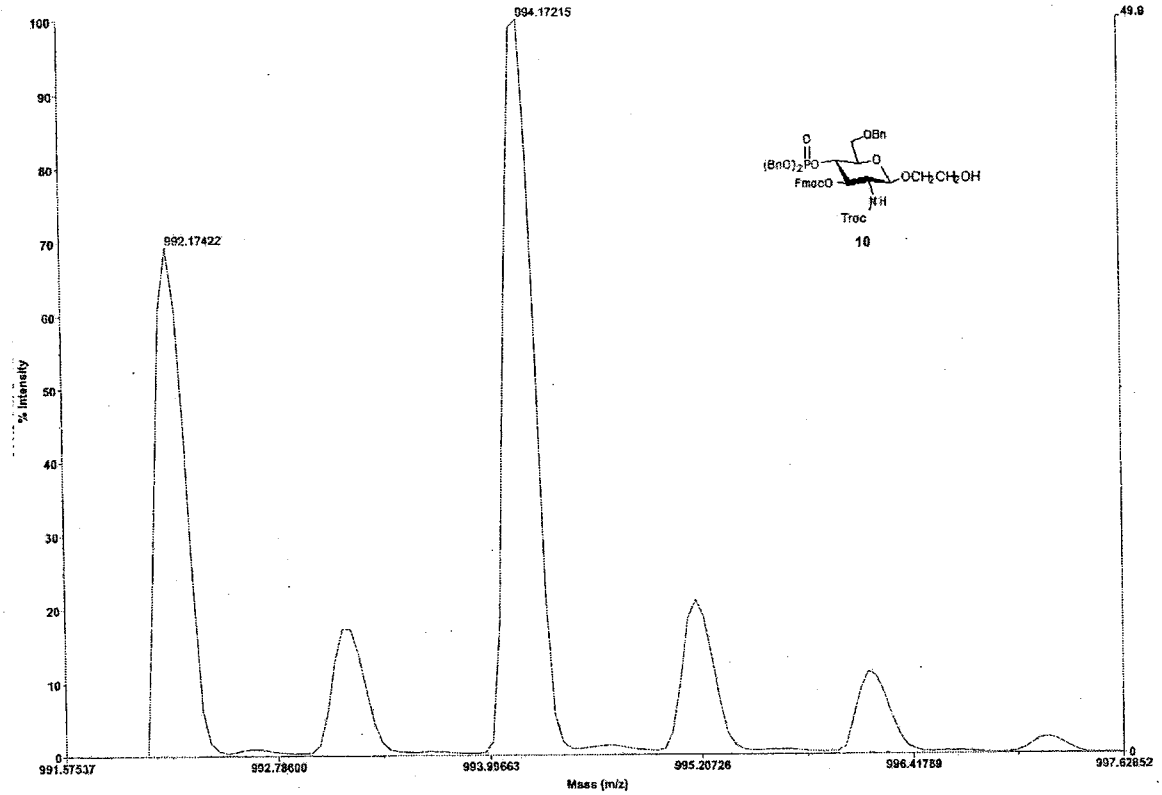

HRESI-MS (*m/z*) Calcd for $C_{92}H_{88}Cl_6N_2O_{24}P_2Na$ $[M + Na]^+$: 1899.3210, found: 1899.3232.

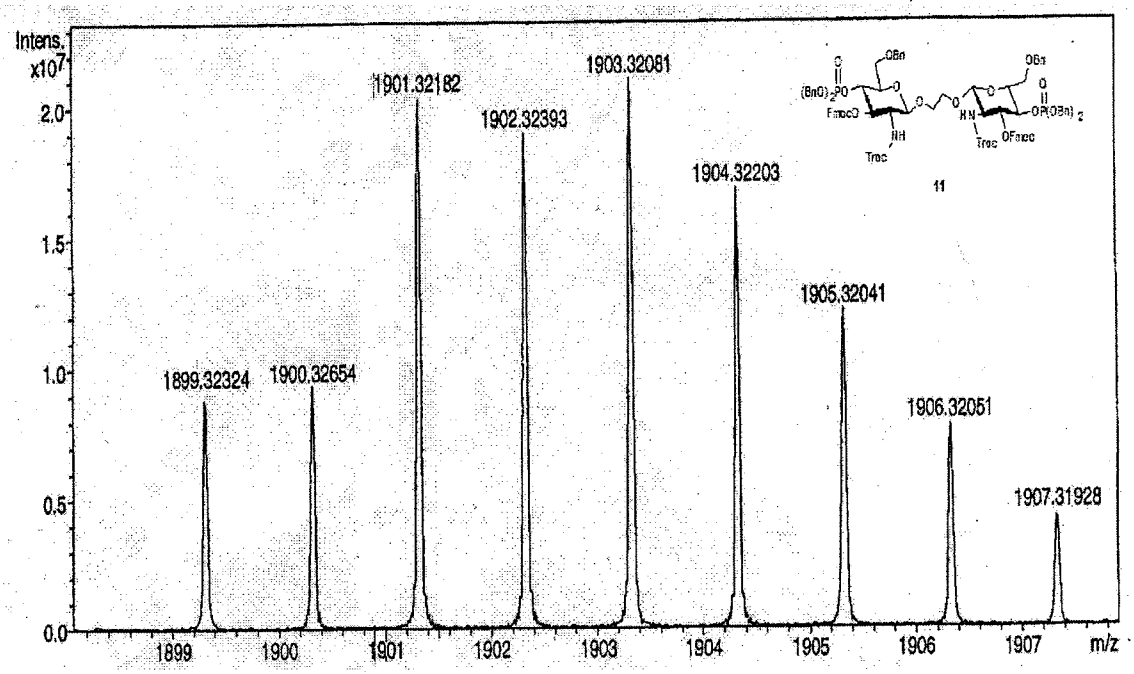

HRESI-MS (*m/z*) Calcd for $C_{142}H_{190}N_2O_{26}P_2Na$ $[M + Na]^+$: 2424.2931, found: 2424.2980 and 1223.6429 $[M + 2 Na]^{2+}$.

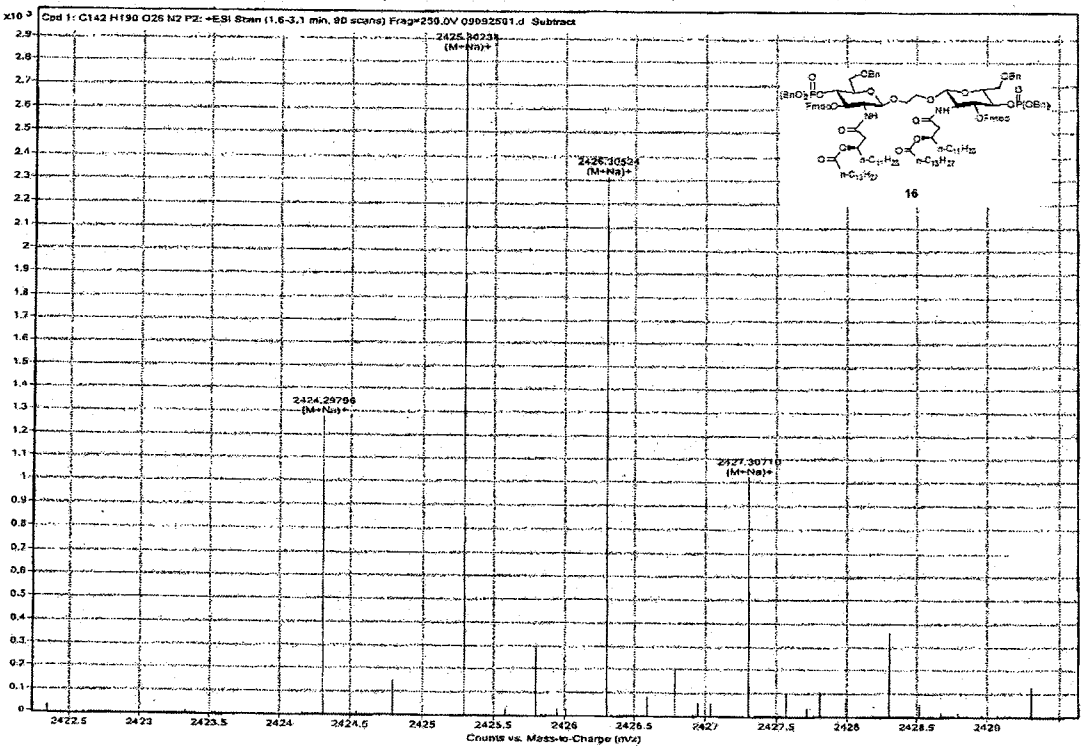

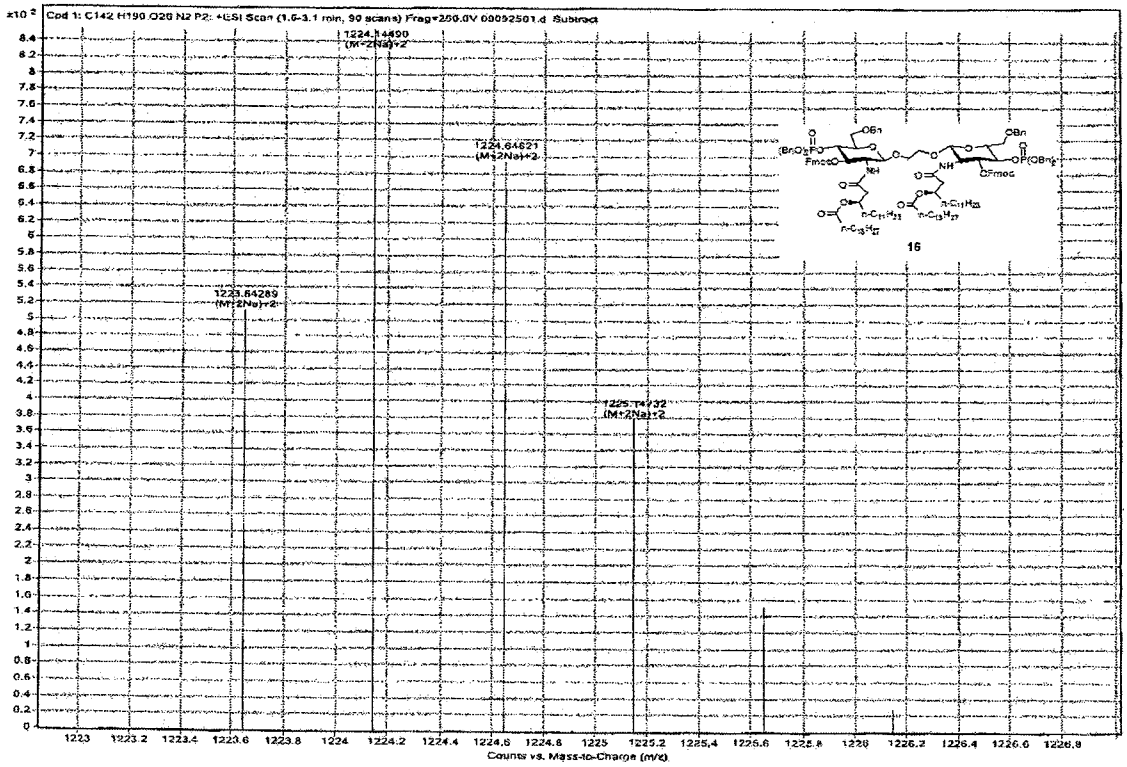

HRESI-MS (*m/z*) Calcd for $C_{70}H_{134}N_2O_{22}P_2$ $[M-2H]^{-2}$: 707.4379, found: 707.4373.

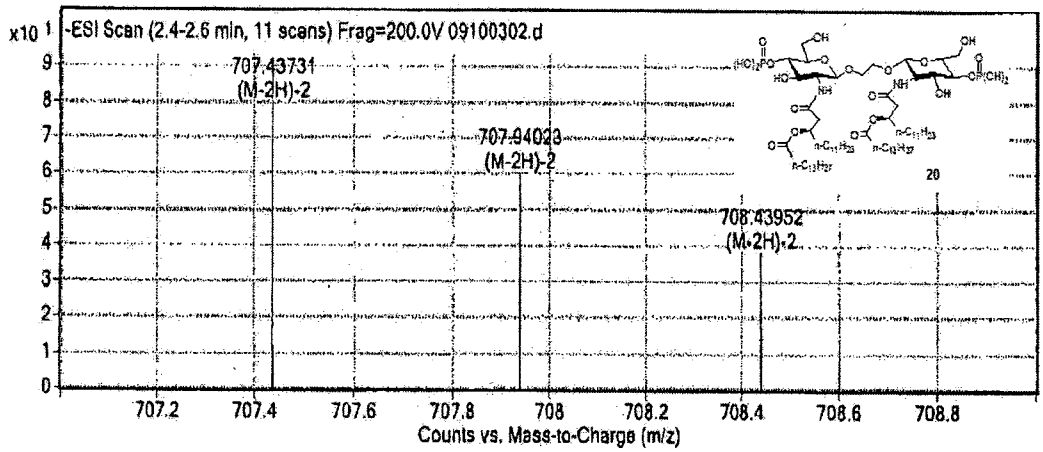

HRESI-MS (*m/z*) Calcd for $C_{120}H_{140}Cl_6N_2O_{28}P_2Na$ $[M + Na]^+$: 2351.6160, found: 2351.7104.

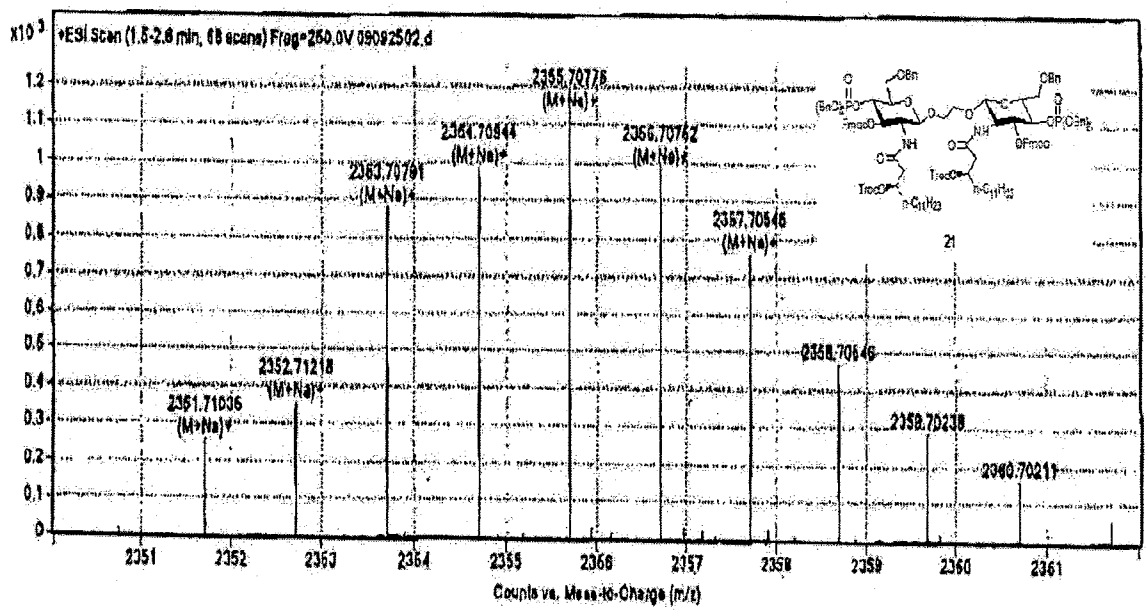

HRESI-MS (*m/z*) Calcd for $C_{114}H_{138}N_2O_{24}P_2Na$ $[M + Na]^+$: 2003.8076, found: 2003.8957 and 1013.4443 $[M + 2\ Na]^{2+}$.